Marshall University
Marshall Digital Scholar

Theses, Dissertations and Capstones

2004

Renal Basolateral Transport of Glucuronides and Other Organic Anions in Rat in Vitro Models

Sarah L. Miles

Follow this and additional works at: http://mds.marshall.edu/etd

Part of the Fluids and Secretions Commons, Life Sciences Commons, Nephrology Commons, and the Other Medical Sciences Commons

Recommended Citation

Miles, Sarah L., "Renal Basolateral Transport of Glucuronides and Other Organic Anions in Rat in Vitro Models" (2004). *Theses, Dissertations and Capstones.* Paper 759.

This Dissertation is brought to you for free and open access by Marshall Digital Scholar. It has been accepted for inclusion in Theses, Dissertations and Capstones by an authorized administrator of Marshall Digital Scholar. For more information, please contact zhangj@marshall.edu.

RENAL BASOLATERAL TRANSPORT OF GLUCURONIDES AND OTHER ORGANIC ANIONS IN RAT IN VITRO MODELS

by

Sarah L. Miles

Dissertation submitted to
the Graduate College
of
Marshall University
in partial fulfillment of the requirements
for the degree of

Doctor of Philosophy
in
Biomedical Sciences

Approved by

Gary O. Rankin, Ph.D. Committee Chairperson
Carl A. Gruetter, Ph.D.
Lawrence H. Lash, Ph.D.
Richard M. Niles, Ph.D.
Monica A. Valentovic, Ph.D.

Department of Pharmacology, Joan C. Edwards School of Medicine at Marshall University

APPROVAL OF EXAMINING COMMITTEE

Carl A. Gruetter, Ph.D.

Lawrence H. Lash, Ph.D.

Richard M. Niles, Ph.D.

Monica A. Valentovic, Ph.D.

Date

Gary O. Rankin, Ph.D., Advisor

Accepted by Graduate College

Leonard Deutsch, Ph.D., Dean

Date

ABSTRACT

RENAL BASOLATERAL TRANSPORT OF GLUCURONIDES AND OTHER ORGANIC ANIONS IN RAT IN VITRO MODELS

by Sarah L. Miles

Glucuronidation is a common Phase II biotransformation reaction that increases the hydrophilicity, and thus elimination, of toxins, xenobiotics, and endogenous compounds. Previous studies suggest that the kidney can secrete glucuronide conjugates, but the renal transport mechanisms for glucuronide secretion have not been determined. Based on the chemical nature of glucuronide metabolites, it is hypothesized that organic anion transporter (OAT) proteins along the basolateral membrane of the renal proximal tubule promote renal accumulation of glucuronide conjugates. The purpose of this study was to develop a rat renal proximal tubule model which demonstrates OAT activity and by which the contribution of OAT in the renal accumulation of glucuronide metabolites could be assessed. In the current study two in vitro models were established; freshly isolated renal proximal tubules (IRPTs), and renal cortical slices (RCSs) from the male Fischer 344 rat. These models demonstrate time-, temperature- and probenecid-sensitive uptake of prototypical OAT1 and OAT3 substrates fluorescein (FL) and ^{14}C-p-aminohippuric acid (PAH), and the prototypical OAT 3 selective substrate ^{3}H-estrone sulfate (ES). Accumulation of ^{14}C-4-acetamidophenyl-β-D-glucuronide (AG) was found to be time-dependent, but not temperature- or probenecid-sensitive in IRPTs. In the RCSs, AG uptake was time-dependent, but only minimally temperature- and probenecid-sensitive. Accumulation/inhibition studies with FL, PAH, ES and AG indicate very limited interaction between AG and OAT. PAH uptake was not affected by other glucuronides (i.e. testosterone glucuronide, methylumbelliferyl glucuronide) in IRPTs or RCSs. Studies using RCSs from Sprague-Dawley rats yielded comparable results to those found in Fischer 344 rat. In all models, accumulation of ^{14}C-AG was not inhibited by excess unlabeled AG. These results suggest that in these rat models, AG does not appear to be a substrate for renal basolateral membrane OAT proteins; that the contribution of OAT in the basolateral membrane transport of AG (and potentially other glucuronide metabolites) is minimal; and accumulation of AG does not appear to be a protein carrier-mediated process. Thus, rat renal proximal tubular cells do not appear to facilitate the accumulation of glucuronide conjugates, and thus do not appear to contribute to the renal secretion of glucuronide conjugates.

DEDICATION

I wish to dedicate this work to my family. To my husband, Dan, I am forever thankful for your friendship, love, continual support and endless patience through this long journey. To my father and mother for their years of support, encouragement and listening, I would not have finished this without you.

ACKNOWLEDGMENTS

I would like to express my sincerest gratitude to my mentor and advisor, Dr. Gary O. Rankin. His support, guidance, and optimism throughout this project have been the key to its completion. I am also grateful to Dr. Gruetter, Dr. Niles, and Dr. Valentovic who have been instrumental in helping to shape and mold this project as decisions about direction needed to be made. I would like to extend special thanks to Dr. Lawrence H. Lash who provided his expertise in the renal cortical cell isolation technique which was later adapted for use in this project. To Dr. Carlotta E. Groves, for providing her expertise in renal organic anion transport and aiding in data analysis, her assistance is deeply appreciated.

Special thanks to technicians John Ball, Dianne Anestis and Carla Cook for their training and support throughout this project.

I would also like to acknowledge and express my deepest appreciation to Dr. Eliza Robertson. Her friendship and moral support during these years have been a blessing. Thanks for everything.

TABLE OF CONTENTS

ABSTRACT iii

DEDICATION iv

ACKNOWLEDGMENTS v

TABLE OF CONTENTS vi

LIST OF FIGURES viii

LIST OF TABLES xii

LIST OF SYMBOLS / NOMENCLATURE xiii

CHAPTER I 1

INTRODUCTION 1
1.1 Glucuronides and renal organic anion transport 1
1.2 Hypothesis 2
1.3 Selection of animal species and in vitro models 2

CHAPTER II 4

REVIEW OF LITERATURE 4
2.1 Glucuronides 4
2.2 Role of the Kidney in Organic Anion Excretion 16
2.3 Organic Anion Transporter Proteins involved 26
in Renal Secretion of Organic Anions 26
2.4 Renal Transport of Prototypical Organic Anions 46
2.5 Summary 53

CHAPTER III 55

METHODS 55
3.1 Animals 55
3.2 Materials 55
3.3 Equipment 57
3.4 Isolation of Renal Proximal Tubules (IRPT) 58
3.5 Characterization of proximal tubules 60
3.6 Toxicity experiments in IRPTs 65
3.7 IRPT model characterization for organic anion transport (OAT) 67
3.8 ^{14}C-Acetamidophenyl-β-d-glucuronide (AG)
accumulation studies in IRPTs 76
3.9 Western blot analysis for OAT1 and OAT3 in IRPTs and HK2 cells 78

3.10 Accumulation studies with OAT substrates in renal cortical slices (RCS) 80
3.11 ^{14}C-acetamidophenyl-β-D-glucuronide (AG) accumulation studies in RCS 83
3.12 ^{14}C-AG accumulation studies in RCSs from male Sprague-Dawley rat 85
3.13 Statistics 86

CHAPTER IV 87

RESULTS 87
4.1 Studies Using Isolated Renal Proximal Tubules (IRPTs) 87
4.2 Studies in Renal Cortical Slices (RCS) 131

CHAPTER V 151

DISCUSSION 151
5.1 Characterization of IRPTs 151
5.2 Toxicity Studies 151
5.3 OAT1 and OAT3 studies in IRPTs 153
5.4 Acetamidophenyl glucuronide accumulation in IRPTs 155
5.5 OAT1 and OAT3 studies in RCSs 157
5.6 Acetamidophenyl glucuronide accumulation in RCSs 159
5.7 Interaction of glucuronide metabolites with OAT1 and OAT3 in IRPTs and RCSs 161
5.8 Conclusion 162
5.9 Future Directions 164

Bibliography 167

Appendix 185

Curriculum Vitae 202

LIST OF FIGURES

Figure 2.1 Mechanism of glucuronidation……..……p. 6

Figure 2.2 Formation of acetaminophen and diclofenac glucuronides……..…p. 8

Figure 2.3 Role of glucuronidation in the activation of xenobiotics to toxic metabolites…….p. 13

Figure 2.4 Structure of the renal nephron……..…….p. 20

Figure 2.5 A simplified overview of proximal tubular function……...…p. 21

Figure 2.6 Model of organic anion transporters in the renal proximal tubule…..p. 25

Figure 3.1 Schematic diagram of renal cortical tissue before and after Percoll density centrifugation……..p. 61

Figure 4.1 Freshly isolated renal proximal tubules from male Fischer 344 rat...p. 89

Figure 4.2 Percent LDH release from IRPTs treated with AG……..p. 91

Figure 4.3 Percent LDH release from IRPTs treated with APAP…….p. 92

Figure 4.4 Percent LDH release from IRPTs treated with DC……..p. 93

Figure 4.5 Effect of AG on nucleotide levels in IRPTs……p. 94

Figure 4.6 Effect of APAP on nucleotide levels in IRPTs……..p. 95

Figure 4.7 Effect of DC on nucleotide levels in IRPTs……...p. 96

Figure 4.8 Time-dependent accumulation of FL in IRPTs……...…p. 100

Figure 4.9 The effect of temperature on FL accumulation in IRPTs……..p. 101

Figure 4.10 The effect of probenecid on FL accumulation in IRPTs……..p. 102

Figure 4.11 IC_{50} determination of probenecid for FL uptake in IRPTs……...p. 103

Figure 4.12 The effect of ouabain on FL accumulation in IRPTs……...…p. 104

Figure 4.13 The effect of benzylpenicillin on FL accumulation in IRPTs…...…p. 105

Figure 4.14 The effect of dehydroepiandrosterone sulfate on FL accumulation in IRPTs……..p. 106

Figure 4.15 The effect of acetamidophenyl glucuronide on FL accumulation in IRPTs……..p. 107

Figure 4.16 The effect of probenecid on PAH accumulation in IRPTs……..p. 110

Figure 4.17 IC_{50} determination of probenecid for PAH uptake in IRPTs……p.111

Figure 4.18 The effect of acetamidophenyl glucuronide on PAH accumulation in IRPTs……..p. 112

Figure 4.19 The effect of testosterone glucuronide (TG), methylumbelliferyl glucuronide (MUG) and acetamidophenyl glucuronide (AG) on PAH accumulation in IRPTs…….p. 113

Figure 4.20 The effect of temperature on estrone sulfate accumulation in IRPTs……...p.116

Figure 4.21 The effect of probenecid on estrone sulfate accumulation in IRPTs…..…….p. 117

Figure 4.22 The effect of self-inhibition on estrone sulfate accumulation in IRPTs……..p. 118

Figure 4.23 The effect of acetamidophenyl glucuronide on estrone sulfate accumulation in IRPTs……p. 119

Figure 4.24 Time-dependent accumulation of acetamidophenyl glucuronide in IRPTs……..…..p.123

Figure 4.25 The effect of temperature on acetamidophenyl glucuronide accumulation in IRPTs……..p. 124

Figure 4.26 The effect of probenecid on acetamidophenyl glucuronide accumulation in IRPTs……..p. 125

Figure 4.27 The effect of self-inhibition on acetamidophenyl glucuronide accumulation in IRPTs……..p. 126

Figure 4.28 The effect of estrone sulfate on acetamidophenyl glucuronide accumulation in IRPTs……..p. 127

Figure 4.29 The effect of D-saccharic acid 1,4-lactone on acetamidophenyl glucuronide accumulation in IRPTs……..……p. 128

Figure 4.30 Western blot analyses for OAT1 and OAT3….....p. 130

Figure 4.31 Mannitol accumulation in RCSs…….p. 133

Figure 4.32 The effect of probenecid on PAH accumulation in RCSs……...p. 135

Figure 4.33 The effect of testosterone glucuronide (TG), methylumbelliferyl glucuronide (MUG) and acetamidophenyl glucuronide (AG) on PAH accumulation in RCSs……...p. 136

Figure 4.34 Time-dependent accumulation of ES in RCSs…….p. 138

Figure 4.35 The effect of probenecid and temperature on ES accumulation in RCSs……...…p. 139

Figure 4.36 Time-dependent accumulation of acetamidophenyl glucuronide in RCSs……...…p. 142

Figure 4.37 The effect of temperature and probenecid on AG accumulation in RCSs……...p. 143

Figure 4.38 The effect of p-aminohippuric acid and estrone sulfate on AG accumulation in RCSs…...……...p. 144

Figure 4.39 The effect of self-inhibition on AG accumulation in RCSs……..p. 145

Figure 4.40 The effect of temperature and probenecid on AG accumulation in RCSs from Sprague-Dawley rat…….……..…p. 148

Figure 4.41 The effect of p-aminohippuric acid on AG accumulation in RCSs from Sprague-Dawley rat……..p. 149

Figure 4.42 The effect of self-inhibition on AG accumulation in RCSs from Sprague-Dawley rat…….p. 150

LIST OF TABLES

Table 1. Types of glucuronides formed from various chemical substrates……p. 9

Table 2. Properties of basolateral OAT transporters in renal proximal tubules.....p. 28

Table 3. PAH substrate specificities for basolateral OAT transporters……p. 33

Table 4. Substrate specificity of various compounds in selected OAT isoforms…….p. 49

Table 5. Substrate specificity of probenecid in selected OAT isoforms……..…p. 52

Table 6. Biochemical characteristics of IRPTs from male F344 rat……..p. 89

LIST OF SYMBOLS / NOMENCLATURE

ACE – angiotensin-converting enzyme

ADP – adenosine diphosphate

AG – acetaminophen glucuronide/acetamidophenyl glucuronide

AMP – adenosine monophosphate

ANOVA- analysis of variance

AP – alkaline phosphatase

APAP- acetaminophen

ATP – adenosine triphosphate

AZT - azidothymidine

BLMV – basolateral membrane vesicle

BSP - bromosulfopthalein

BSA – bovine serum albumin

cAMP – cyclic adenosine monophosphate

cGMP – cyclic guanosine monophosphate

CHO cells – Chinese hamster ovary cells

CL_{CR}- creatinine clearance

CL_{REN} – renal clearance

COS7 -

DBSP – dibromosulophthalein

DEXA – dexamethasone

DHEAs- dehydroepiandrosterone sulfate

DC – diclofenac

DT – distal tubule

E2-17βG – β-estradiol 17β-D-glucuronide

EGF – epidermal growth factor

ERK – extracellular signal regulated kinase

ES – estrone sulfate

F344 – Fischer 344 rat

FL - fluoresceine

fu – unbound fraction of drug

GFR – glomerular filtration rate

GSH – glutathione

HB -

HeLa cells – immortal cell line derived from human cervical carcinoma

HEK293 cells – human embryonic kidney cell line

HK – hexokinase

HK2 – immortalized human kidney cell line

HX – hypophysectomized

IRPT(s)- isolated renal proximal tubule(s)

IC_{50} – inhibitory concentration (50% inhibition)

KH – Krebs Henseleit

LDH – lactate dehydrogenase

LLC-PK1 – Porcine kidney proximal tubule cell line

LSC – liquid scintillation counter

MAPK – mitogen activated protein kinase

MEK – mitogen activated extracellular-regulated kinase kinase

MN - mannitol

mRNA – messenger ribonucleic acid

MRP_2/cMOAT – multidrug resistance transporter

MUG – methylumbelliferyl glucuronide

NaDC – sodium dicarboxylate exchanger

NLT – novel liver transporter

NKT – novel kidney transporter

NPT – sodium dependent inorganic phosphate transporter

NSAID – nonsteroidal anti-inflammatory drug

OA – organic anion

OAT – organic anion transporter

OATP – organic anion transporting polypeptide

OK – opossum kidney

PAH – para-aminohippurate / para-aminohippuric acid

PB – probenecid

PG – benzylpenicillin, penicillin G

PGE_2 – prostaglandin E_2

$PGF_{2(\alpha)}$ – prostaglandin $F_{2(\alpha)}$

PKA – protein kinase A

PKC – protein kinase C

PMA – phorbol 12-myristate 13-acetate

PT – proximal tubule

RBF – renal blood flow

RCS – renal cortical slices

SD – Sprague-Dawley

SE – standard error

SL – D-saccharic acid 1,4-lactone

T_3 – Triiodothyronine

TEA - tetraethlyammonium

TG – testosterone glucuronide

UDP – uridine diphosphate

UDPG – UDP-glucose

UDPGA – UDP-glucuronic acid

UGT – UDP glucuronosyltransferase

URAT – urate transporter

UTP – uridine triphosphate

CHAPTER I

Introduction

1.1 Glucuronides and renal organic anion transport

Glucuronidation is a major Phase two biotransformation reaction that increases the hydrophilicity, and thus elimination of toxins, xenobiotics and endogenous compounds. While the liver is the primary site of glucuronidation, this reaction also takes place in other organs including the kidney. Until recently, glucuronidation has been considered a detoxification pathway. However, recent findings have shown that certain reactive glucuronide conjugates have the potential for covalent binding within tissues. Many drugs are metabolized to glucuronide conjugates with potential for inducing toxic reactions. Several analgesics (such as diclofenac, sulindac, and ibuprofen) which are metabolized to glucuronide conjugates have been shown to cause various forms of renal toxicity. However, the mechanism of nephrotoxicity for these metabolites has not been fully established.

Results from previous studies suggest that the renal proximal tubule (PT) has the ability to secrete glucuronide conjugates. Currently, the transport mechanisms within the kidney for glucuronide conjugate transport have not been established. Because of the anionic nature of the glucuronide metabolite, the primary transporters of interest are the organic anion transporter (OAT) proteins (specifically, OAT1 and OAT3). The major site of localization of these transporters in the kidney is along the basolateral membrane of the PT. While OAT transporters exist on the luminal membrane of the PT as well, the basolateral OATs are more likely to be of major importance in the role of glucuronide secretion by the kidney. These OAT proteins transport organic

anions (OAs) from the blood into the proximal tubular cells as the initial step in secretion. This initial transport step in secretion is of importance in determining how renal proximal tubular cells contribute to the accumulation of glucuronide metabolites within the kidney cells. The second step in glucuronide secretion involves efflux across the luminal membrane into the luminal fluid. The luminal membrane also contains numerous transporters, both from the OAT family, as well as others such as multidrug resistance transporters (MRP) which direct the efflux of compounds out of the cell and into the luminal fluid for removal from the kidney. With increased understanding of the role of the basolateral OATs to glucuronide accumulation, we may better understand the role of these metabolites in the potential renal toxicity of compounds which are metabolized to glucuronide conjugates.

1.2 Hypothesis

It is hypothesized that the first step of renal secretion of glucuronide conjugates involves organic anion transporters along the basolateral membrane of the PT.

1.3 Selection of animal species and in vitro models

The Fischer 344 rat was chosen as the primary animal model in this study due to the fact that the rat shares numerous similar anatomical and physiological characteristics similar to humans as well as metabolic pathway similarities, allowing for comparisons in absorption excretion and distribution of pharmacologic compounds (Kacew and Festing, 1996). Additionally, the Fischer 344 rat strain is an inbred strain which remains genetically consistent for many generations. This provides greater data uniformity. Sprague-Dawley (SD) rats were chosen as a secondary animal model for comparison to the Fischer 344 rat because the SD rat has been indicated to demonstrate renal secretion of

acetaminophen glucuronide (AG) (Galinsky and Levy, 1981). Freshly isolated renal proximal tubules (IRPTs) were chosen as a study model because this in vitro model provides an enriched population of PT segments where cells are able to maintain communication and metabolism. Access to the basolateral membrane of the PT and the contribution of this portion of the kidney to the secretion of compounds can be separated from other components of the kidney in this model. Most importantly, one can study the handling of molecules by the basolateral membrane of the PT without having to consider a significant contribution of the apical membrane. Isolation of PT fragments involves enzymatic collagenase digestion of the cortical tissue. Once separated from the cortical tissue, tubules collapse and access to the luminal membrane is not available. This is important because it enables the separation between secretion (basolateral) and reabsorption (luminal) processes of the PT. Renal cortical slices (RCSs) were chosen as a secondary in vitro model to assess glucuronide secretion. The use of RCSs also allows for access to the basolateral membrane without significant interference from the apical membrane since in this model, again, the lumens of the tubules collapse. The RCS model is useful in addition to the IRPT model in that it provides a heterogeneous cell population, the orientation of the cortical nephron is maintained, cellular communication and metabolism is maintained and no enzymatic digestion is required in the establishment of the model (all cellular proteins should be undamaged by any enzymatic digestion). Both IRPTs and RCSs have frequently been used as in vitro models to study renal transport of xenobiotics in various animal models.

CHAPTER II

Review of Literature

2.1 Glucuronides

2.1.1 Glucuronidation and its Role in Bioactivation

Glucuronidation is a major Phase II drug-metabolizing reaction. The glucuronidation pathway is catalyzed by UDP-glucuronosyltransferases (UGTs). Currently, there are approximately 20 distinct UGTs known in both humans and rats. This superfamily of UGT proteins is divided into 2 families (UGT1, UGT2) based on sequence homologies. UGTs, which catalyze the conversion of hydrophobic substrates to hydrophilic glucuronides are found in hepatic and extra hepatic tissues. This superfamily yields a range of isozymes, each possessing different physical and catalytic properties (Mulder et al., 1990). Most vertebrates are capable of generating UGT-directed glucuronides from a number of structurally divergent substances (Tukey and Strassburg, 2000). Conservation in exon/intron organization is maintained in rodents as several UGT2 genes have been characterized and shown to contain the same exon/intron branch points (Haque et al., 1991; Makenzie and Rodbourn, 1990). The human UGTs range from 529 to 534 amino acids in length, with several highly conserved domains that are important for membrane targeting and activity. UGT activity has also been shown to be inducible. Several xenobiotics cause the induction of UGT and are broken down into two major classes; (1) the polycyclic aromatic hydrocarbon induced UGT and (2) the Phenobarbital induced (PB) UGT (Mulder et al., 1990). These compounds result in an increase in UGT enzyme protein as a result of increased mRNA levels. Due to the overlapping substrate specificity of UGTs,

the glucuronidation of some aglycones may be induced by more than one inducer.

Glucuronidation involves the transfer of the glucuronic acid group from UDP-glucuronic acid (UDPGA) to an acceptor group on a substrate by the enzyme UGT (Fig. 2.1). UDPGA is a highly water-soluble compound. The formation of UDPGA involves a two step reaction in the cytosol. UDPGA is synthesized from the precursors glucose-1-phosphate and uridine triphosphate (UTP) to form UDP-glucose (UDPG). UDPG is oxidized by UDPG dehydrogenase to UDPGA. UDPGA must be synthesized in the cell where glucuronidation takes place since it is not likely to be taken up by intact cells (Mulder et al., 1990).

Glucuronidation is a microsomal reaction which takes place in the smooth endoplasmic reticulum and serves as an important step in converting lipophillic substrates into hydrophilic glucuronide metabolites. Glucuronide metabolites are then eliminated from the body through the bile and urine. The mechanism of glucuronidation is an S_N2 reaction, the acceptor group of the substrate attacking the C_1 carbon of the pyranose ring to which uridine diphosphate (UDP) is attached in an α-glycosidic bond (Fig. 2.2). The resulting glucuronide has the β-glycosidic configuration. Glucuronides can be formed through hydroxyl (alcoholic, phenolic), carboxyl, sulfuryl, carbonyl, and amino (primary, secondary, and tertiary) linkages (Mulder et al., 1990; Tukey and Strassburg, 2000). Examples of various chemical substrates (shown as functional groups) that undergo glucuronidation are shown in Table 1. The reactivity of a given substrate will depend on the structure, due to both electronic and steric factors (Mulder et al., 1990). In addition to structural requirements, substrates for glucuronidation must also be sufficiently lipid soluble. The thickness or bulkiness of the substrate molecule is important in determining which UDPGT forms will glucuronidate a given substrate (Mulder et al., 1990). Extensive analysis of specific catalytic activities attributed to recombinant UGT proteins has demonstrated broad overlap of substrates targeted for glucuronidation.

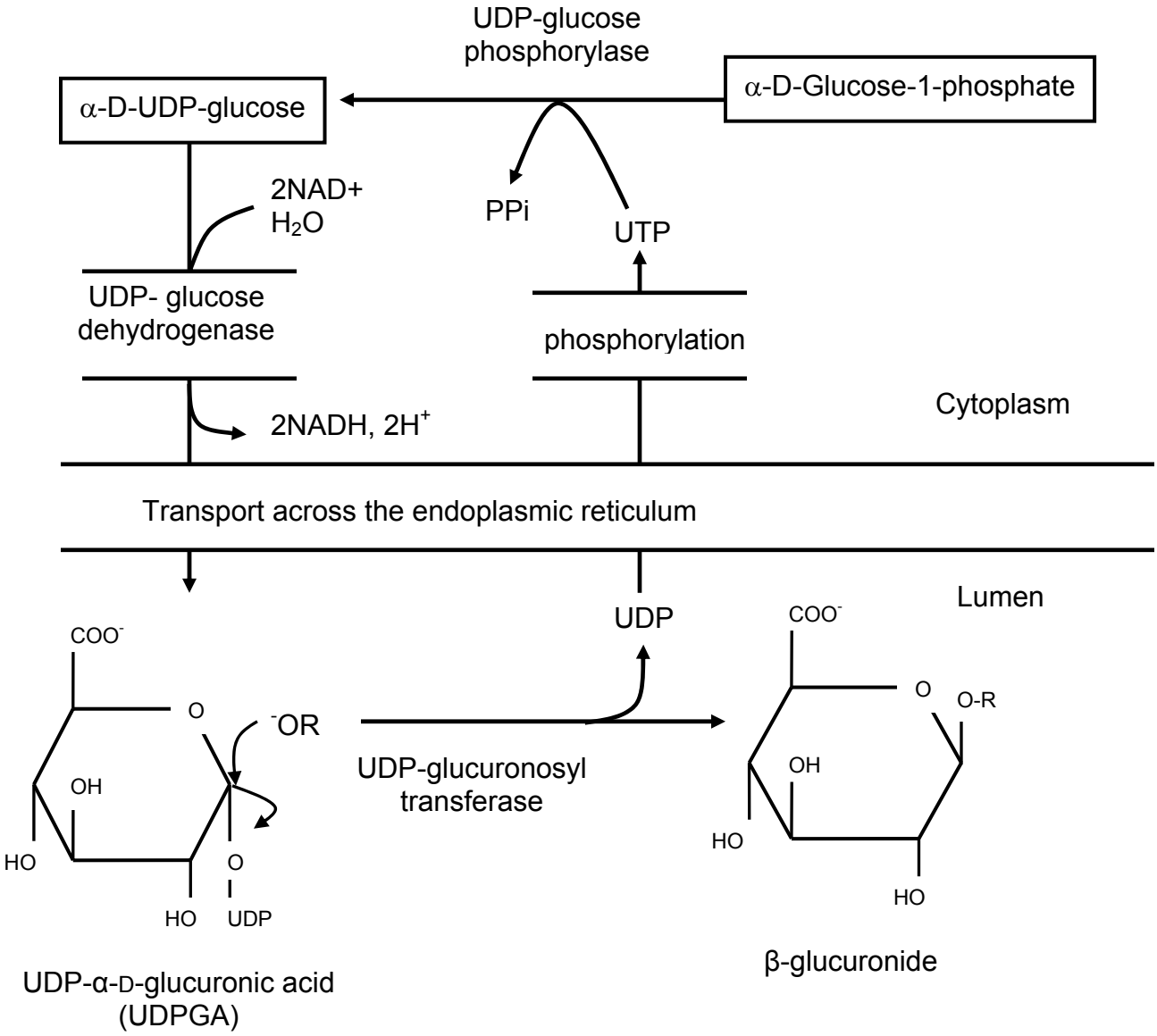

Figure 2.1 Mechanism of glucuronidation. Glucuronidation involves the transfer of the glucuronic acid group from UDP-glucuronic acid (UDPGA) to an acceptor group on a substrate by the enzyme UDP-glucuronosyltransferase. It is synthesized in the cytosol from the precursors glucose-1-phosphate and uridine triphosphate (UTP) to form UDP-glucose (UDPG). UDPG is oxidized by UDPG dehydrogenase to UDPGA and transported into the smooth endoplasmic reticulum. The mechanism of glucuronidation is a S_N2 reaction, the acceptor group of the substrate attacking the C_1 carbon of the pyranose ring to which UDP is attached in a α-glycosidic bond. The resulting glucuronide has the β-glycosidic configuration. Glucuronide metabolites are then eliminated from the body through the bile and urine

While the liver is one of the primary sites of glucuronidation based on UDPGT activity, UDPGT is also localized in the kidney, mainly in the proximal tubular cells (Mulder, 1990; Tukey and Strassburg, 2000). It has been reported that in the rat, the kidney lacks some of the major UDPGT activities present in the liver (Lucier and McDaniel, 1977), in particular testosterone (Lucier and McDaniel, 1977) and morphine (Rush et al., 1983). In humans, UDPGT activity is present in the kidney, where bile acids are readily conjugated (Matern et al., 1984; Parquet et al., 1985) High levels of glucuronidation also occur in the intestinal mucosa. In the rat intestine, the major UDPGT enzyme present is the planar phenol UDPGT, which is the major xenobiotics-metabolizing form (Hartiala, 1973; Koster et al., 1986). Most other organs and tissues also possess glucuronidation activity, although it may be very low (Mulder et al., 1990).

It is important to note that the kidney has the potential to come in contact with glucuronides formed at both extrarenal sources such as the liver and small intestine, as well as at intrarenal sources by conjugation of the parent xenobiotic within the PT cell. Until recently, glucuronidation has been accepted to be a detoxification reaction that terminated the biological activity of both endogenous compounds as well as xenobiotics. As opposed to the previously accepted detoxification mechanism, some glucuronides (particularly those of the acyl classification) are now understood to be potentially reactive intermediates (Smith et al., 1990; Van Breemen and Fenselau, 1986; Hyneck et al., 1988). Many of these reactive glucuronide metabolites have been shown to covalently bind to tissue and serum proteins, and will be discussed in greater detail in the next section.

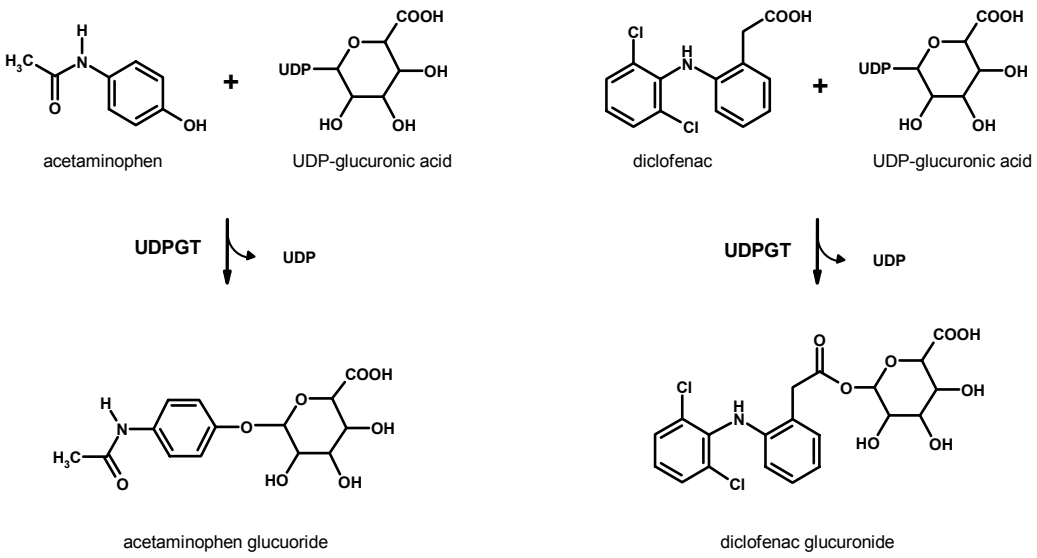

Figure 2.2. Formation of acetaminophen and diclofenac glucuronides.

Conjugation of acetaminophen with glucuronic acid leads to the formation of an ethereal glucuronide moiety, while conjugation of diclofenac with glucuronic acid leads to the formation of an acyl glucuronide moiety. Both conjugates are readily excreted in the urine.

Table 1. Types of glucuronides formed from various chemical substrates.

O-glucuronide substrates		
	phenols	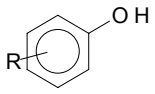
	alcohols	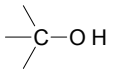
	carboxylic acids	
	hydroxylamines hydroxamic acids	
S-glucuronide substrates		
	thiophenols	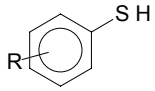
	thiols	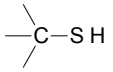
	carbamic acids	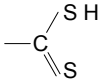
N-glucuronide substrates		
	aromatic amines hydroxylamines	
	tertiary amines	
	(thio)carbamate	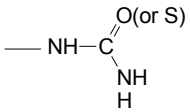
	sulfonamides	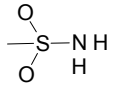
C-glucuronide substrates		
	1,3 dicarbonyl compounds	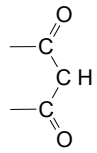

2.1.2 Toxicity Associated with Glucuronides

As shown in Fig 2.2, glucuronidation of a hydroxyl group results in an ether-type glucuronide while glucuronidation of a carboxy group results in an ester-type (acyl) glucuronide. While it has previously been accepted that glucuronidation was a detoxification mechanism, in the past several years, many published reports have indicated that some acyl glucuronides are potentially reactive intermediates that undergo not only hydrolysis and intramolecular acyl migration, but also bind reversibly to proteins in vivo and in vitro (Faed, 1984; van Breemen and Fenselau, 1985; Spahn-Langguth and Benet, 1992). Acyl glucuronides have been found to be electrophiles, reacting with sulfhydryl and hydroxyl groups resulting in covalent binding of the molecule to tissue and plasma proteins (Stogniew and Fenselau, 1982).

Covalent binding to protein can occur by two mechanisms, the first being nucleophillic displacement where a protein functional group reacts at the carboxylic (acyl) carbon of the acyl glucuronide leaving the protein irreversibly bound to the drug moiety and releasing glucuronic acid (Fig 2.3). The second mechanism is via an acyl migration by which the aglycone migrates from the 1-hydroxyl group of the glucuronic acid to the 2,3 and 4-hydroxyl groups of the glucuronic acid portion. The aldehyde group of the ring open tautomer then condenses with a lysine group on the protein to form an imine. At the completion of the reaction, the irreversibly bound product still contains a glucuronic acid which acts as a covalent link between protein and drug (Fig. 2.3). In spite of the presence of glucuronic acid in other types of glucuronides (N-, S-, C-, or ether glucuronides) they do not undergo acyl migration and therefore no ring opening and aldehyde formation are possible. Covalent binding to protein has been found for a number of compounds forming acyl-glucuronide metabolites. Studies have demonstrated that in vivo binding to plasma proteins of tolmentin (Hyneck et al., 1988), fenoprofen (Volland et al., 1991), diflunisal and probenecid (McKinnon and Dickinson, 1989) is correlated with exposure to the reactive acyl

glucuronide metabolites of these xenobiotics. Clofibric acid was also shown to irreversibly bind to rat liver tissue in vivo in a dose dependent manner (Sallustio et al., 1991). King and Dickinson (1993) have further demonstrated the covalent binding of difluinisal via its acyl glucuronide metabolite to plasma proteins, as well as kidney, small intestine and large intestine tissues of rat, with such binding increasing with the duration of dosing. Other studies have demonstrated irreversible covalent binding of suprofen to renal tissue of rat (Smith and Liu, 1995). This study by Smith and Liu (1995) further demonstrated that enhanced exposure of a particular organ to reactive acyl glucuronides due to excretion by or metabolism within the organ may result in enhanced covalent binding to tissues within that organ. McGurk et al. (1996) also demonstrated irreversible binding of mefenamic acid via its acyl glucuronide metabolite to human serum albumin as well as cellular proteins in culture. Mefenamic acid, a nonsteroidal anti-inflammatory drug (NSAID) commonly used to relieve pain, has been implicated in several cases of nephrotoxicity including acute renal failure and tubulointerstitial nephritis (Woods, 1981; Jenkins et al., 1988).

Covalent binding of reactive acyl glucuronide metabolites to cellular constituents can result in acute toxicity, hypersensitivity reactions, mutagenesis or carcinogenesis, although binding can occur without any harmful effects (Faed, 1984). From studies reported in the literature, there is evidence that antibodies occur in the blood of patients at low levels following administration of acetylsalicylic acid and valproic acid (Amos et al., 1971; Williams et al., 1992). An immunological mechanism may be the basis for anaphylactic reactions as well as organ toxicity, since covalent binding may be followed by antigen-antibody formation. Thus, acyl glucuronides may act as haptens, which upon binding to proteins become immunogens and induce antibody production (Zia-Amirhosseini, 1994).

It is important to note that an unacceptably high incidence of significant adverse drug reactions has been reported for NSAIDs of the aryl-alkyl acid class. Six of the 25 drugs removed from the U.S. and British market between 1964 and

1983 because of severe toxicity were acid compounds, five of which were NSAIDs (Spahn-Langguth and Benet, 1992). All six of these drugs (benoxaprofen, ticrynafen, ibufenac, zomepirac, indoprofen and aclofenac) are metabolized by humans to acyl glucuronides, i.e., reactive intermediates (Bakke et al., 1984). For zomepirac, the common NSAID toxicities of gastric irritation, nephritis, and acute renal failure were not a major factor in its withdrawl from the market. Removal was rather due to a high incidence of anaphylactic or anaphylactoid reactions (Corre and Rothstein, 1982; O'Brien and Bagby, 1984). Case reports have also described such reactions for tolmentin (Rossi and Knapp, 1982), sulindac, ketoprofen, acetylsalicylic acid and ibuprofen (O'Brien and Bagby, 1984). Additionally, in 1987, suprofen was withdrawn from the market due to cases of unexplained acute renal toxicity (Strom et al., 1989; Hart et al., 1987). Furthermore, disease states which compromise the excretion of acyl glucuronides may enhance exposure of the body to these reactive metabolites and lead to increased irreversible binding to tissue proteins. Whether such enhanced exposure with subsequent covalent binding is a causative factor observed in toxicity to that organ (where binding occurs) is still unknown.

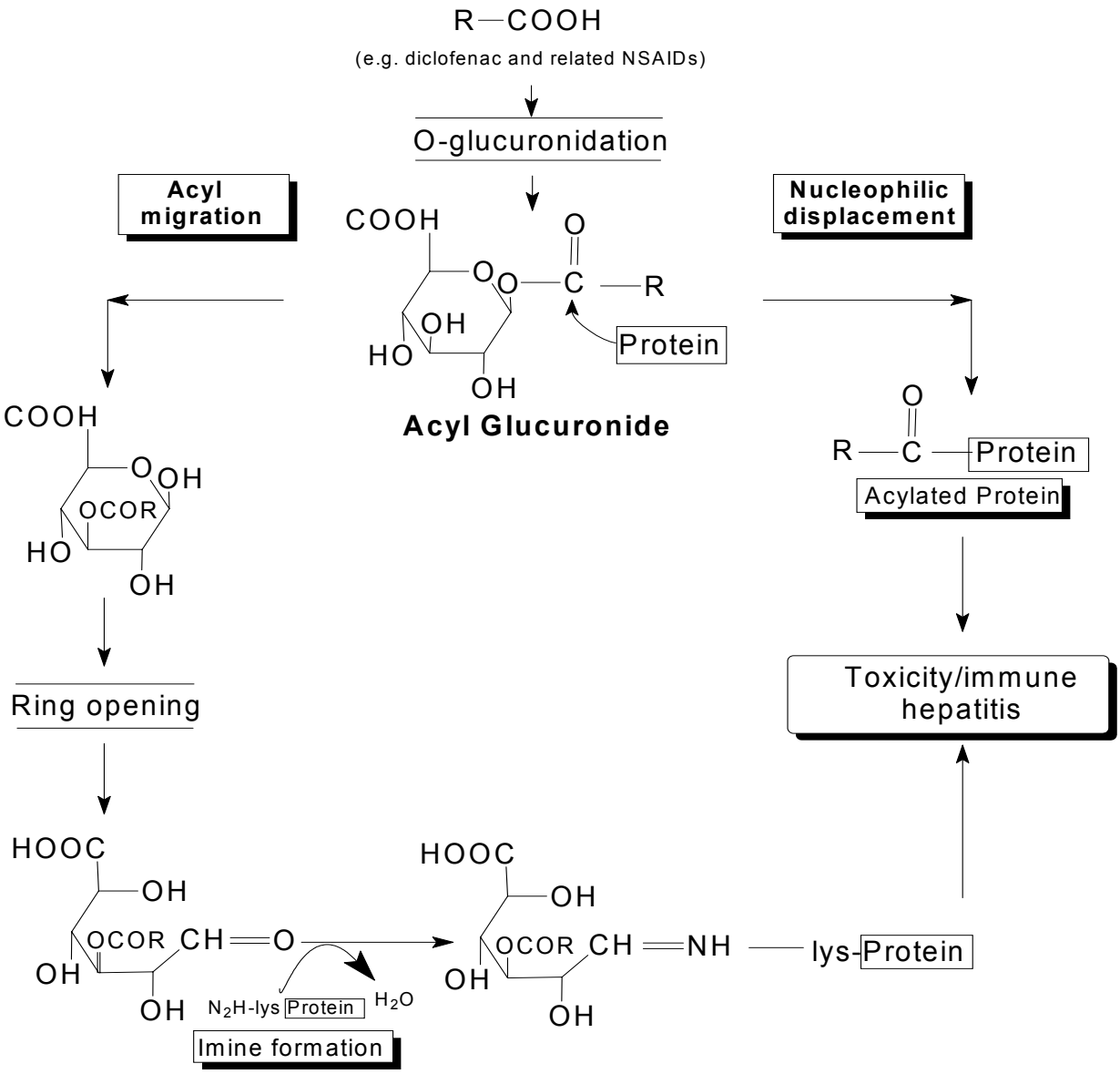

Figure 2.3. Role of glucuronidation in the activation of xenobiotics to toxic metabolites. Covalent binding to protein can occur by two mechanisms, the first being nucleophillic displacement where a protein functional group reacts at the carboxylic (acyl) carbon of the acyl glucuronide leaving the protein irreversibly bound to the drug moiety and releasing glucuronic acid. The second mechanism is via an acyl migration by which the aglycone migrates from the 1-hydroxyl group of the glucuronic acid to the 2,3 and 4-hydroxyl groups of the glucuronic acid portion. The aldehyde group of the ring open tautomer then condenses with a lysine group on the protein to form an imine. In this mechanism the glucuronic acid acts as a bridge between the acyl residue and the protein becoming part of the adduct.

2.1.3 Renal Formation of Glucuronide Conjugates

Immunohistochemical studies conducted in human and rat indicate that the highest concentration of renal UDPGTs is in the PT (Lock and Reed, 1998). Renal glucuronide formation has been confirmed in studies using perfused kidneys from both rats and humans for a number of phenols (4-dimethylaminophenol, p-nitrophenol, paracetamol) (Elbers et al., 1980; Diamond and Quebbemann, 1981; Emslie et al., 1981). Renal glucuronidation varies for different species and substrates. For example, in humans clearance of indomethacin occurs primarily by renal glucuronidation (Moolenaar et al., 1992). Vree and Van der Ven (1999) have shown that the acyl glucuronide metabolite of furosemide is also formed in part by the kidney tubules in humans. However, human renal synthesis of acetaminophen glucuronide from acetaminophen is negligible (Morris and Levy, 1984). In rat, it has been found that acetaminophen glucuronide is synthesized from acetaminophen by the kidney and secreted into the urine (Newton et al., 1982; Li et al., 2004). Li et al. (2004) demonstrated that 8.66 ± 2.99 % of the administered dose of acetaminophen appeared in the urine as the glucuronide conjugate. This is in close agreement with Hart et al. (1980), who demonstrated in isolated perfused rat kidney that 10% of paracetamol appeared in the urine as the glucuronide conjugate. It has also been demonstrated that estradiol-17β-D-glucuronide (E2-17βG) is also formed within the kidney and undergoes tubular secretion (Kanai et al., 1996). It can be seen that the kidney has the ability to contribute to the glucuronidation of numerous compounds. Thus total renal clearance of glucuronide conjugates must consider the renal contribution to glucuronide metabolites found in the urine. When the liver and the kidneys metabolize a drug into identical products and the kidney excretes these products in the urine, the differences in metabolic pathways are not detectable. Therefore, there is the potential for the resulting calculation of renal clearance (CL_{RE}) to be too high (Vree et al., 1992).

2.1.4 Renal Handling of Glucuronide Conjugates

It has been well established that the kidney has the ability to efficiently excrete glucuronide conjugates (Braun et al.,. 1957; Schachter and Manis, 1958: Yuan, 2002). While glucuronide conjugates can enter the proximal tubular filtrate via glomerular filtration, it has also been indicated that the kidney has the ability to secrete glucuronides (Duggin and Mudge, 1975; Galinsky and Levy, 1981; Watari et al., 1983; Somogyi et al., 1993; Van Crugten et al., 1991; Schachter and Manis, 1958). Since glucuronide conjugates in general are ionized at physiological pH and are highly polar chemical species, glucuronides are subject to a diffusional barrier in their movement across biological membranes (Evans, 1996). Glucuronide conjugates are generally acidic compounds and are generally more hydrophilic than their parent aglycones. Most glucuronide conjugates have pKa values of between 3-4, regardless of the pKa of the parent compound (Smith and Williams, 1966). Therefore, at physiological pH they are almost entirely ionized and are highly polar. Given their polarity, movement of glucuronide conjugates between the primary site of formation (hepatocytes), the systemic circulation, and target cells (renal proximal tubular cells in this discussion) may be restricted by their limited ability to passively diffuse across membrane barriers and may depend on carrier-mediated transport systems that are present in the cellular membranes. The movement of glucuronide conjugates across membranes has only recently begun to be investigated. Cellular transport of glucuronide conjugates has primarily been studied in the hepatocyte, the primary site of glucuronide formation (Sallusito et al., 2000). It has been shown that glucuronide metabolites are substrates for organic anion transporting polypeptide (oatp) transporters and multispecific organic anion transporter (OAT) proteins in the basolateral (sinusoidal) membrane of the hepatocyte (Sallusito et al., 2000). Sallusito et al. (2000) demonstrated that the sinusoidal uptake of gemfibrozil acyl glucuronide occurs against a 50 fold concentration gradient and is inhibited by the organic anion dibromosulophthalein (DBSP), a substrate for the oatp/OATP

transporter proteins. Additionally the uptake of bilirubin acyl glucuronide into rat hepatocyte sinusoidal membrane vesicles is saturable, temperature dependent, trans-stimulated, osomotically sensitive, electrogenic, Na+ independent and competitively inhibited by bromosulfopthalein (BSP), another substrate for oatp/OATP proteins (Adachi et al., 1990).

While the hepatic handling of glucuronide conjugates has begun to be investigated, currently very little is known about how the kidney secretes glucuronide conjugates, and more specifically, what transport protein(s) along the basolateral membrane of the PT cells are involved in transporting glucuronide conjugates from the blood across the basolateral membrane and into the PT cells. The kidney possesses several of the same OAT proteins as those found in hepatocytes (Kusuhara et al., 1999; Sekine et al., 1998). Isern et al. (2001) showed that Oatp1 expressed in *Xenopus* oocytes transports estradiol-17-β-glucuronide (Km ~ 5 μM). Multispecific organic anion transporter 3 (hOAT3), has also been shown to mediate the transport of estradiol-17-β-glucuronide (Cha et al., 2000). These and other OAT proteins in the kidney may potentially contribute to the renal secretion of glucuronide conjugates along the renal PT.

2.2 Role of the Kidney in Organic Anion Excretion

2.2.1 Renal Excretion

Maintenance of fluid and electrolyte homeostasis is a critical function of the kidney. The kidney also plays an important role in the elimination of numerous xenobiotics and endogenous compounds. Three processes are involved in the renal handling of drugs; glomerular filtration, tubular reabsorption and tubular secretion. The functional units of the kidney, the nephrons (Fig 2.4), determine the degree of renal elimination of compounds through a balance of filtration, reabsorption and secretion (Fig. 2.5).

Renal clearance (CL_{REN}) is defined as the hypothetical volume of plasma from which a substance is completely removed per unit of time (usually one min) in one pass through the kidney. Clearance of a compound depends on glomerular filtration rate (GFR), the rate of tubular secretion and the rate of tubular reabsorption of that compound.

Glomerular filtration is passive filtration of the blood as the blood flows through the glomeruli of the kidney. The extent to which a drug or drug metabolite is filtered depends on the molecular size and protein binding. GFR is determined or estimated by measuring the clearance of a filtered substance that is not reabsorbed, metabolized or secreted and is calculated as:

$$\text{Clearance} * \text{Plasma}_{\text{concentration}} = \text{Urine}_{\text{concentration}} * \text{Urine}_{\text{volume}}$$

$$\text{GFR} = \text{Urine}_{\text{concentration}} * \text{Urine}_{\text{volume}} / \text{Plasma}_{\text{concentration}}$$

If Cl_{REN} depends only on filtration,

$$Cl_{REN} = GFR * fu$$

where fu is the unbound fraction of drug and GFR is the glomerular filtration rate (normal human GFR = 125 ml/min). When this number is compared to renal blood flow (1200 ml/min) it can be seen that only ~25% of blood is filtered at the glomerulus.

The pores within the capillary endothelium and the ultrafiltration membrane of the glomerulus allow only small molecules (less than 400 – 600 A in diameter or about 5 kDa molecular weight) to be filtered into the tubular fluid. Large molecules such as most proteins, and therefore the drugs bound to them, cannot pass through the glomerulus, leaving only small, unbound compounds to be filtered at the glomerulus. General kidney function can also greatly affect glomerular filtration. Glomerular filtration is generally estimated by measuring creatinine clearance (CL_{CR}). Creatinine is an endogenous compound that is freely filtered at the glomerulus and is not protein bound (fu = 1). Therefore, for creatinine

$$Cl_{CR} = GFR$$

However, it is important to note that measures of renal drug clearance using CL_{CR} do not account for tubular secretion or reabsorption of drugs (Perri et al., 2003). An additional problem with using creatinine to estimate GFR is that, although freely filtered by the glomerulus, creatinine is also secreted in small amounts by the renal tubules. The extent of tubular secretion varies from one individual to another, as does renal function, which may introduce large errors in individuals with impaired renal function. Another more accurate measure of GFR can be obtained through the measurement of inulin clearance. Inulin is a polymer of fructose which is freely filtered at the glomerulus and is neither reabsorbed nor secreted by the renal tubules. It is metabolically inert and cleared only by the kidney.

Tubular reabsorption also affects the renal clearance of a compound. The tubular epithelium is the site of reabsorption of many substances, with molecules being reabsorbed (by transport or diffusion) across the luminal membrane of the tubules from the filtrate into the intracellular cytoplasm. From there, the molecules can pass across the basolateral membrane (by transport or diffusion) back into the plasma. As solutes are reabsorbed from the tubular lumen, water follows. While GFR is about 120 ml/min, reabsorption of solutes and water along the proximal, distal, and collecting ducts of the kidney is so extensive that only 1 – 2 ml/min of the filtered water is eliminated as urine. Reabsorption is important for many endogenous substances (e.g., glucose) as well as some xenobiotics. Compounds may be reabsorbed either by passive diffusion, if the compound is lipid soluble and nonionized, or by carrier-mediated transport if it is a charged molecule. It is important to note that the pH of the tubular lumen can also affect reabsorption by affecting the ratio of drug in non-ionized and ionized form. With tubular reabsorption, the clearance of a compound may then seem smaller than expected by glomerular filtration alone (Perri et al., 2003).

The third process of tubular function is secretion. Tubular secretion can effectively increase the renal clearance of a compound (as compared to glomerular filtration alone) by actively secreting a compound into the proximal

tubular lumen. Secretion involves transport of drugs against a concentration gradient, thereby concentrating the compound in the tubular lumen. This transport mechanism is energy dependent and involves carrier-mediated transport by way of cotransporter and/or counter transporter proteins along the tubular epithelia. The rate of tubular secretion depends solely on the protein transporters involved. Saturation of these transport mechanisms, and competition between compounds that use them, may affect the rate of drug elimination, and can thereby lead to drug interactions (Perri et al., 2003). While some drug interactions may be beneficial, acting to prolong the duration of action of a beneficial drug by decreasing its elimination via the kidney (e.g., probenecid treatment prevents the elimination of penicillin in the urine), this same mechanism can also lead to the accumulation of a toxic compound in the body.

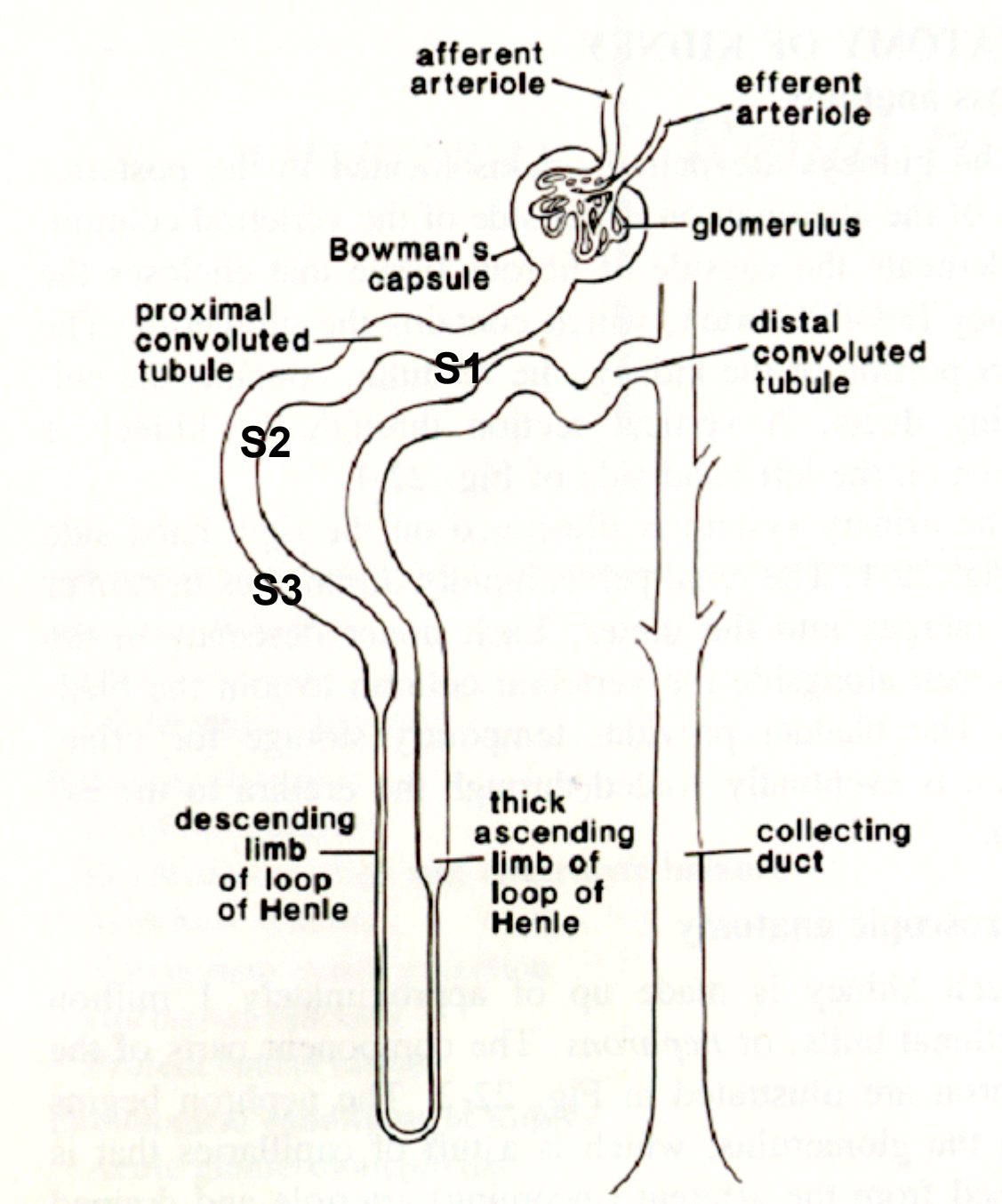

Figure 2.4. Structure of the renal nephron.

The proximal tubule is divided into three sections; S1 (proximal convoluted), S2 (proximal convoluted) and S3 (proximal straight). The S1 portion of the nephron is nearest the glomerulus, with the S3 segment nearest the Loop of Henle.

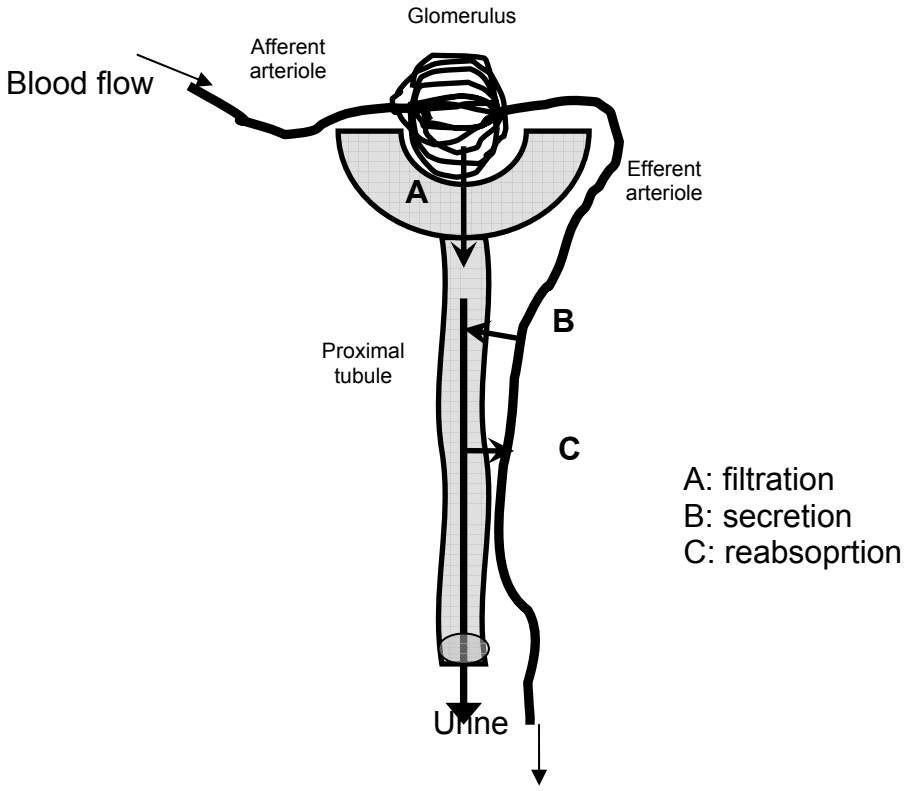

Figure 2.5. A simplified overview of proximal tubular function.

The proximal tubule plays an important role in the elimination of biotransformation products through a balance of filtration, secretion and reabsorption.

2.2.2 Drug Elimination by the Kidney

While all portions of the nephron can contribute to the elimination of compounds from the kidney, the PT is the portion of the nephron that plays the most significant role in drug elimination. To accomplish this elimination, the kidney possesses numerous transport proteins that are primarily localized to the proximal tubular epithelial cells of the nephron. Many of these transporters utilize adenosine triphosphate (ATP) or transmembrane ion gradients to drive movement of substrate compounds across the cell membrane in either a secretory or reabsorptive direction. The structural requirements for interaction of

drugs with renal transport mechanisms normally include either an electronegative (anionic) or an electropositive (cationic) charge, and a hydrophobic backbone. In the kidney, only a few uptake systems for organic anions have been proposed that interact with a variety of xenobiotics (Ullrich et al., 1997; Pritchard and Miller, 1993). These systems primarily include the multispecific organic anion transport proteins (OAT1 and OAT3). These and other systems will be discussed in greater detail in later sections. Despite the increasing knowledge of the molecular identity of individual transport proteins, and transporter substrate specificities, the overall knowledge regarding the role of these transporters in the renal handling of drugs and their metabolites is limited.

2.2.3 Tubular Secretion of Organic Anions

Tubular secretion of xenobiotics, especially organic anions, has been extensively studied (Pritchard and Miller, 1993; Moller and Sheikh, 1982; Brendayan, 1996). Organic anions are weakly acidic compounds that are ionized at physiological pH. A major system for net tubular secretion of hydrophobic organic anions exists in the PTs of almost all vertebrates. Mechanisms of organic anion transport in the kidney PTs have been studied over the past several decades. In addition to in vivo experiments, studies have also used tissue slices, isolated tubules, perfused tubules, cultured cells, membrane vesicles and peritubular capillary perfusion to study how the kidney handles various xenobiotics (Moller and Sheikh, 1982; Pritchard and Miller, 1993). The results of these studies indicate that the secretion of organic anions from the blood into the urine is accomplished sequentially. Tubular secretion involves a molecule (e.g., an organic anion) first passing from the blood into the interstitial fluid and then across the basolateral membrane into the renal tubular cells. Once inside the tubular epithelial cells, the molecule is then moved from the cell across the luminal membrane and into the tubular lumen for excretion in the urine. To accomplish secretion, two distinct transporters are required; one at the

basolateral membrane of the cell (to accept organic anions from the blood into the cell), and one at the apical membrane (luminal membrane) to excrete organic anions from the cell into the tubular fluid (urine).

When organic anion secretion was studied in isolated perfused renal PTs from various species, the steady-state concentration of organic anions (OA) in the tubule lumen was found to be greater than that in the peritubular bathing medium and the concentration in the cell was greater than in either the lumen or the peritubular bathing medium (Dantzler, 2002). Because the inside of the cell is negatively charged (-70 mV) as compared to the lumen (-3 mV), and the peritubular fluid (0 mV), and because OA are negatively charged at physiological pH and do not appear bound inside the cells, this pattern of OA accumulation is compatible with transport into the cells against an electrochemical gradient at the basolateral membrane, with movement from the cell into the lumen down an electrochemical gradient (Dantzler, 2002). Membrane permeability studies in various models have shown that (1) the permeability of the luminal membrane for efflux of OAs is greater than that of the basolateral membrane; (2) backflux of OAs across the epithelium from lumen to the peritubular fluid is small; and (3) any backflux that does occur crosses the cells from the luminal membrane across to the basolateral membrane (Dantzler, 2002). In the renal PT, the general direction of movement of OAs is in a secretory direction. This involves transporters along the basolateral membrane, as OAs must move against an electrochemical gradient to enter the cell. However, once inside the cell, OAs move easily across the luminal membrane for excretion in the urine. Any OAs that move back across the basolateral membrane (back flux) generally are those reabsorbed from the luminal fluid and are intended to be returned to the general circulation by crossing the basolateral membrane and reentering the blood.

2.2.4 Transport of organic anions across the basolateral membrane

The first step in tubular secretion of OAs is the uptake from blood across the basolateral membrane of epithelial cells in the PT. Transporter-mediated systems have been shown to play a significant role in endogenous and exogenous OA uptake in the PT. Entry of OAs along the basolateral membrane of proximal tubular cells is of primary importance because it leads to the entry of potentially reactive compounds into the proximal tubular (PT) cell. As these compounds accumulate within the cells, potentially toxic reactions can result. Several transporters from the OAT family have been localized to the basolateral membrane of renal PT cells (Fig 2.6). These transporters include the multispecific organic anion transport proteins 1, 2 and 3 (OAT1, OAT2 and OAT3). The model organic anion used for studying OAT transport is p-aminohippurate (PAH). PAH is nearly completely removed from the blood entering both kidneys and by calculating the rate of PAH clearance, can be used to approximate renal blood flow. PAH is extensively protein bound and must enter the luminal fluid via secretion. In general, transepithelial renal secretion of a wide range of hydrophobic OAs involves transport into the cell of the PTs against an electrochemical gradient at the basolateral membrane by countertransport for α-ketoglutarate moving down its electrochemical gradient (Fig 2.6). This step is the dominant rate limiting step in the secretory process. In the following sections, each transporter contributing to the basolateral uptake of OAs into the proximal tubular cells will be discussed in detail and is shown in Figure 2.6.

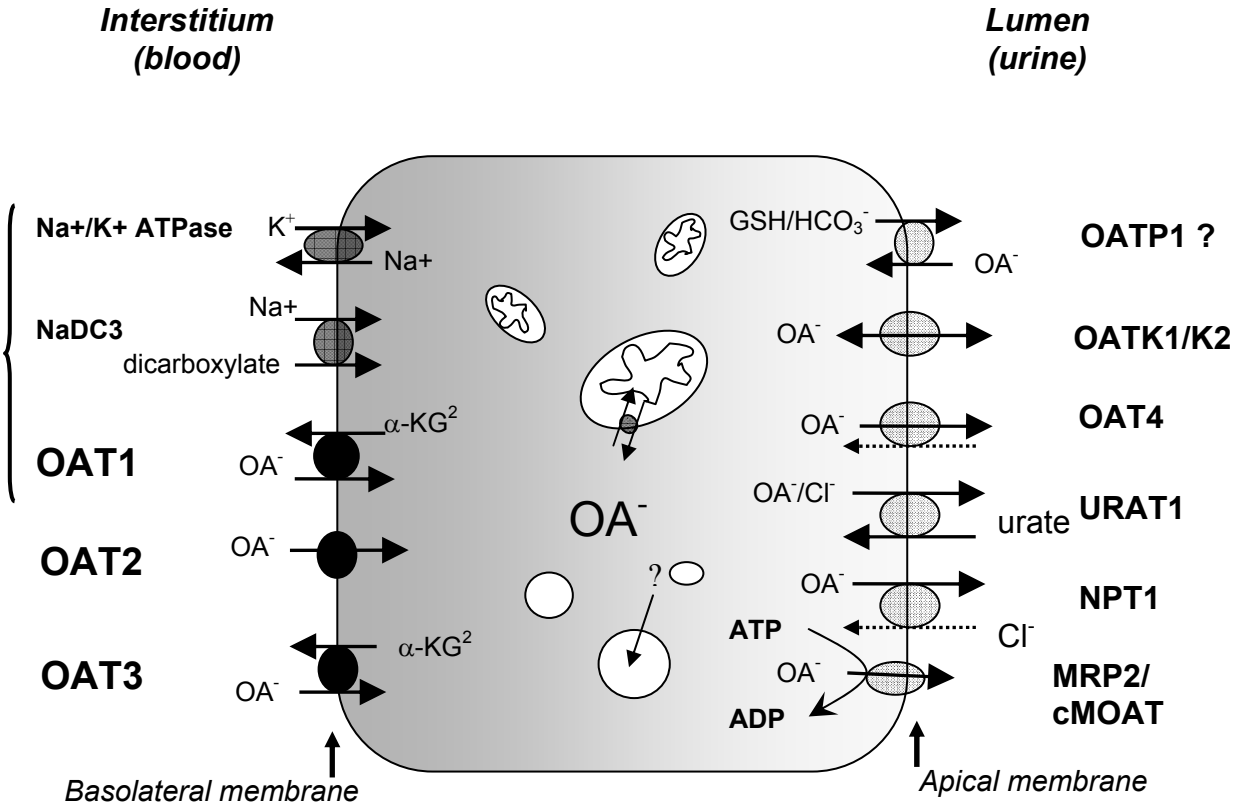

Figure 2.6 Model of organic anion transporters in the renal proximal tubule.

Uptake of organic anions (OA^-) across the basolateral membrane is mediated by the classic sodium-dependent organic anion transport system, which includes α-ketoglutarate (α-KG^{2-})/OA^- exchange via the multispecific organic anion transporter (OAT1) and sodium-ketoglutarate cotransport via the Na^+/dicarboxylate cotransporter (NaDC3). A second sodium-independent uptake system for OA^- has been identified only in human proximal tubules (OAT2) and is not a dicarboxylate exchanger. OAT3 has been shown to transport bulky OA^- and has recently been demonstrated to be a dicarboxylate exchanger. Intracellular accumulation of substrates of both transport systems has been demonstrated in both mitochondria as well as vesicles of unknown origin. The apical (brush-boarder) membrane contains various transport systems for efflux of OA- into the lumen or reabsorption from the lumen into the cell. The multidrug resistance transporter, MRP2, mediates primary active luminal secretion. The organic anion transporting polypeptide, OATP1, and the kidney-specific OAT-K2 and OAT-K1 might mediate facilitated OA- efflux but could also be involved in reabsorption via an exchange mechanism. URAT1 functions as an exchanger mediating reabsorption of uric acid, but can also transport OAs. OAT4 is present only in human kidney, and its mechanism is unknown. The human type I sodium-dependent inorganic phosphate transporter, NPT1, originally thought to function primarily in the reabsorption of phosphate from the glomerular filtrate, has since been determined to transport organic anions

2.3 Organic Anion Transporter Proteins involved in Renal Secretion of Organic Anions

2.3.1 Organic anion transporter 1 (OAT1)

Previously referred to as the PAH transporter (Lu et al., 1999), OAT1 is the first of 5 members of the OAT family. OAT1 through OAT5 are all members of the Slc22a (amphiphillic solute transporter) family, which is a subset of the major facilitator superfamily (Koepsell and Endou, 2004). Sequencing of various OAT1 clones reveals regions coding for 546 (mouse; Lopez-Nieto et al., 1997), 550 or 563 (hOAT1 short isoform; Hosoyamada et al., 1999; Race et al., 1999; long isoforms; Hosoyamada et al., 1999;), or 551 (rat; Sekine et al., 1997; Sweet et al., 1997; rabbit; Bahn et al., 2002) amino acids. Compared to hOAT1 (100%), homologies decrease in order in comparison to hOAT1; rabbit (91.3%)>rat (90.6%)>pig (89.6%)>mouse (87.9%)>>flounder (55.9%)>>*C. elegans* (28.1) (Burckhardt and Burckhardt, 2003). In the human, OAT1 appears in four splice variants; OAT1-1, OAT1-2, OAT1-3, and OAT1-4. Preliminary findings show no difference between OAT1-1 and OAT1-2 with respect to transport whereas OAT 1-3 and OAT 1-4 appear to be nonfunctional (Buttler et al., 2001). Membrane topology models of OAT1 predict 12 putative transmembrane domains. Four consensus sequences for N-glycosylation are present in the large extracellular loop between the first and second transmembrane domains and four protein kinase C phosphorylation sites are predicted in a large intracellular loop between the sixth and seventh transmembrane domains (Burckhardt and Burckhardt, 2003). Studies using mouse OAT1 demonstrate that a large portion of the protein remains in the intracellular compartment, suggesting that glycosylation of OAT1 is involved in the sorting of the OAT1 protein to the plasma membrane. Immunoblot analysis using polyclonal antibodies against hOAT1 shows a single protein band with molecular mass of 80-90 kD in human kidney cortex extract.

This size is decreased to 60 kD following deglycosylation (Cihlar et al., 1999). In the rat kidney a single 77 kD protein band is detected with rOAT1 antiserum (Nakajima et al., 2000). The predicted molecular weight of hOAT1 and rOAT1 from amino acid sequence is 60 kD. These heavier molecular weights suggest that OAT1 is a glycosylated protein (Sekine et al., 2000).

Physiologically, OAT1 mediates the first step in the renal excretion of many anionic drugs (e.g. antibiotics, anti-viral drugs, NSAIDs, diuretics, angiotensin converting enzyme (ACE) inhibitors, angiotensin II antagonists, anti-neoplastic agents, anti-epileptic agents) and endogenous anions (e.g. cyclic nucleotides, dicarboxylates, prostanoids, neurotransmitter metabolites) and acts in parallel with other OA transporting proteins along the basolateral membrane in the PT (Sekine et al, 2000). OAT1 is one of the primary transporters for OAs along the basolateral membrane of the renal PT. The contribution of OAT1 in OA secretion in numerous models has been thoroughly studied and characterized. Molecular properties of OAT1 are summarized in Table 2.

2.3.1.1 Cloning and Tissue Distribution

Molecular cloning of organic anion transport proteins from a number of species has greatly advanced the knowledge of organic anion transport. OAT1 (Slc22a6) was first identified by expression cloning from the kidneys of mouse and initially identified as NKT (novel kidney transporter, Lopez-Nieto et al., 1997). Later, OAT1 was identified in rat (OAT1, Sekine et al., 1997; ROAT, Sweet et al., 1997), and flounder (fOAT1, Wolff et al., 1997). The human ortholog was cloned in 1998 by Reid et al. (hOAT1, 1998) and later by four other laboratories (hOAT1, Hosoyamada et al.,1999; Race et al.,1999; Cihlar et al., 1999; PAHT, Lu et al., 1999). Additional orthologs of OAT1 have also been identified in rabbit (Bahn et al., 2002) and pig (Hagos et al., 2002). The term “OAT1” is used to refer to all orthologs, and the species from which the ortholog was derived is

Table 1. Characteristics of basolateral OAT transporters in renal proximal tubules

Transporter	Cloned from	Expression	Localization	Transport	Substrates	Regulation
OAT 1	human, pig, rabbit, rat, mouse, flounder, C.elgans	Kidneys>>brain	Human: proximal tubules, basolateral membrane. Rat: proximal tubules, segments S1~S2>S3; basolateral membrane	Exchange of organic anions against α-ketoglutarate	PAH, FL, α-KG, cAMP, cGMP, NSAIDs, methotrexate, β-lactam antibiotics, ochratoxin A, uric acid, PGE_2	Down regulation by protein kinase C (PKC); up-regulation by mitogen-activated kinase (MEK)/ extracellular regulated kinase (ERK)1/2
OAT 2	human, rat, mouse	human: liver>kidneys male rat: liver>kidneys female rat: kidneys>liver[a]	Human: Basolateral membrane of proximal tubule Rat: luminal membrane of collecting ducts cortical thick assending limb of Henle's loop	uniport of organic anions	PAH, α-KG, salicylate, acetylsalicylate, PGE2	not demonstrated
OAT 3	human, rat, mouse	human: kidneys>>skeletal muscle, brain rat: liver>>kidney> brain[b] or kidney>>liver> lungs>brain[a]	Human: basolateral membrane of proximal tubule Rat: proximal tubules, S1>S2=S3, basolateral membrane; thick ascending limb of Henle's loop, connecting tubule. colleting duct	Exchange of organic anions against α-ketoglutarate	PAH, FL, cimetidine, DHEA-S, estradiol glucuronide, estrone sulfate, methotrexate, ochratoxin A, PGE2, PGF2α, salicylate, benzylpenicillin, ($E_2 17\beta G$)	Down regulation by PKC

a. Buist et al. 2002
b. Kusuhara et al. 1999

generally indicated by a lower case letter designation preceding OAT1 (i.e. rOAT1 for rat OAT1) (Burckhardt and Burckhardt, 2003).

Northern blot analysis has revealed that OAT1 is highly expressed in the cortex of the kidney of the human (Cihlar et al., 1999; Hosoyamada et al., 1999; Lu et al., 1999; Race et al., 1999), rat (Buist et al., 2002; Kobayashi et al., 2002a; Sekine et al., 1997; Sweet et al., 1997), and mouse (Lopez-Nieto et al., 1997). Besides kidney, OAT1 has also been detected to some degree in brain, liver, skeletal muscle, and placenta and possibly retina (Burckhardt and Burckhardt, 2003). In SD rats, Buist et al. (2002) found that the amount of OAT1 mRNA in the kidney steadily increased after birth, reaching a maximum around 30 days. After 30 days, mRNA levels decreased in females but remained constant in males. This indicates that there is a gender difference in OAT1 expression in adult SD rats. Kobayashi et al. (2002a) however, did not find a gender difference in the expression of OAT1 in 35-day old Wistar rats. The potential for gender and species difference in OAT1 expression must therefore be considered when studying transport of organic anions and other compounds in various in vitro and in vivo systems from different rat strains.

Immunohistochemical analysis of OAT1 protein has shown that OAT1 is localized to the basolateral membrane of proximal tubular cells in humans (Hosoyamada et al., 1999; Motohashi et al., 2002) and rat (Kojima et al., 2002; Tojo et al., 1999). The proximal tubule, which is comprised of three sections (S1, S2, S3) shows varying amounts of OAT1 expression in each section. It has been demonstrated that, in rat, OAT1 is primarily expressed in the S2 portion of the proximal tubule (Tojo et al., 1999) with the S1 and S3 segments showing only weak expression of the OAT1 protein (Kojima et al., 2002). Protein labeling for the OAT1 protein in the human PT has shown varying results, either showing S1=S2=S3 (Motohashi et al., 2002) or labeling only in the S1 and S2 portions (Hosoyamada et al., 1999). Cerrutti et al. (2002) demonstrated, using Western blot studies, that OAT1 protein in basolateral membrane vesicles (BLMV) from female Wistar rats at 110-130 days of age was present at only 40% of the level

found in BLMV from male rats. Kobayashi et al. (2002a), however, did not find a gender difference in expression of OAT1 in male and female Wistar rats at 7 weeks of age. Protein analysis has revealed that the amount of OAT1 protein can potentially be different in male and female rats (possibly depending on age as well), and this may contribute to gender differences in the pharmacokinetics of anionic drugs.

2.3.1.2 OAT1 Substrates; Characterization and Specificity

Cloned OAT1 has been expressed in *Xenopus laevis* oocytes, COS7 cells, LLC-PK1 cells, HeLa cells, CHO cells, and in immortalized mouse PT cells. More than 150 substrates have been tested with the cloned and heterologously expressed OAT1 from human, rat, mouse, flounder and *C. elegans*, demonstrating a wide range of compounds that are substrates for OAT1 (Burckhardt and Burckhardt 2003).

OAT1 demonstrates wide substrate selectivity including endogenous substances such as cyclic nucleotides (cAMP, cGMP), prostaglandins (PGE2), and uric acid, and numerous structurally unrelated drugs such as NSAIDs (acetylsalicylate, indomethacin, salicylate), N-acetylcysteine conjugates, antiviral drugs (acyclovir, cidofovir, zidovudine), diuretics (acetazolamide, bumetanide, ethracrynic acid, furosemide), antibiotics (benzylpenicillin, cephaloridine, tetracycline), uricosuric drugs, antineoplastic drugs (methotrexate) and ochratoxin A. The prototypical substrate for OAT1 is PAH (Miller and Pritchard 1997). Fluorescein (FL) also shows the same transport properties as PAH and is thus used as a prototypical substrate for OAT1 as well (Dantzler, 2002). Numerous studies have been conducted using PAH as a marker substrate for OAT1 uptake. Studies using various classes of substrates tested on PAH transport have been used to establish the structural requirements for substrates interacting with the PAH transporter (Burckhardt and Burckhardt 2003). It has been determined that the structural requirements for OAT1 substrates include:

1. Substrates must have a hydrophobic domain of 4-10 Å
2. An increase in the strength of the negative charge (decrease in pK_a) favors the interaction with the PAH transporter.
3. A full ionic charge is not necessary (uncharged polarized molecules can interact with OAT provided they are hydrophobic enough)
4. Electron withdrawing side groups (Cl, Br, NO_2) increase affinity for OAT1 (Burckhardt and Burckhardt 2003)

Binding of substrates to the transporter most likely involves hydrophobic interactions and the formation of hydrogen bonds. The negatively charged molecules may bind to oppositely charged amino acid residues of OAT1. Because hydrogen bonds are relatively weak, release of substrates after translocation into the cell is easier. The formation of hydrogen bonds enables a transporter to interact with molecules from various chemical classes, indicating that hydrogen bonds may play a key role in polyspecific transporters (Burckhardt and Burckhardt, 2003). While OAT1 proteins from various species show similar function, it has been demonstrated that there are species differences in substrate specificity of the various isoforms. It has been shown that rOAT1 has the ability to transport the compound methotrexate (Sekine et al., 1997; Uwai et al., 2000) while hOAT1 does not (Lu et al., 1999). It is important to note also, that OAT1 transport is not strictly limited to OAs. While the prototypical organic cation tetraethylammonium (TEA) was not transported by rOAT1 (Uwai et al., 1998; Sekine et al., 1997; Sweet et al., 1997) and did not inhibit other isoforms of OAT (hOAT1: Cihlar et al., 1999; Islinger et al., 2001; fOAT1; Wolff et al., 1997), OAT1 has been shown to transport cimetidine, a weak base which forms a cation (fOAT1: hOAT1: Burckhardt et al., 2003). Cimetidine has also been shown to inhibit PAH accumulation in intact rat kidney (Ullrich et al., 1993).

OAT1 is thought to be the classic sodium-dependent organic anion transporter along the PT. Characterization of OAT1 transport has been carried out in various expression models using uptake experiments utilizing radiolabeled PAH. Summary of transport and Km values for PAH transport are listed in Table

3. Uptake of labeled PAH was found to be saturable, with Km values ranging from 3.9 to 430 μM (Burckhardt and Burckhardt, 2003). In rOAT1 expressing models, Km values for PAH uptake ranged from 11-85.1 μM where as in hOAT1 expressing models, Km for PAH uptake ranged from 3.9-22 μM (Table 3).

Transport by OAT1 involves transport against an electrochemical gradient in exchange for α-ketoglutarate (or other dicarboxylates such as glutarate) (Pritchard and Miller, 1996) (Fig. 2.5). OA exchange for dicarboxylate has been demonstrated in several OAT1 clone models (Lu et al., 1999; Apiwattanakul et al, 1999; Cihlar and Ho, 2000). The α-ketoglutarate concentration is maintained by metabolic production within the cell, and also by Na^+ coupled uptake of α-ketoglutarate into PT cells via the Na^+-dicarboxylate exchanger (NaDC3) (Fig. 2.5). This inside to outside concentration difference of Na^+ provides the driving force for the uptake of organic anions against negative membrane potential. Preloading cells with glutarate has been shown to increase the uptake of PAH by OAT 1 (human: Cihlar et al., 1999; Ho et al., 2000; Lu et al., 1999; Motojima et al., 2002; rat: Cihlar et al., 1999; Pombrio et al., 2001; Sekine et al., 1997; Sweet et al., 1997). Coexpression of OAT1 with the Na^+-dicarboxylate exchanger also demonstrated an increase in PAH uptake with dicarboxylate present outside of the cell (thus available as substrate for the dicarboxylate exchanger; Sekine et al., 1997; George et al., 1999). Sodium that is transported into the cell by the Na^+-dicarboxylate exchanger is removed by the membrane bound Na^+/K^+-ATPase to maintain the sodium gradient across the basolateral membrane, thus classifying OAT1 as a tertiary active transporter.

Table 3 PAH substrate specificities for basolateral OAT transporters

Transporter	Species	Expression system	Transport (+/-) or Km (μM)	References
hOAT1	Human	Oocyte	+	Race et al. 1999
			3.9	Islinger et al. 2001
			4.0	Cihlar et al. 1999
			9.3	Hosoyamada et al. 1999
		CHO cells	15.4	Cihlar and Ho, 2000
				Ho et al. 2000
		HeLa cells	5.0	Lu et al. 1999
		Mouse PTC	15.8	Takeda et al. 2000
			20.1	Takeda et al. 2001
		OK cells	22.0	Motojima et al. 2002
rOAT1	Rat	Oocyte	11.0	Pombrio et al. 2001
			14.3	Sekine et al. 1997
			31.0	Uwai et al. 2000
			70.0	Sweet et al. 1997
		LLC-PK1	47.0	Nagata et al. 2002
			59.5	Hasegawa et al. 2002
		Mouse PTC	43.2	Takeda et al. 1999
			85.1	Sugiyama et al. 2001
hOAT2	Human	EcR293	+	Sun et al. 2001
		LLC-PK1	+	Morita et al. 2001
rOAT2	Rat	Oocyte	+	Sekine et al. 1998
hOAT3	Human	Oocyte	87.2	Cha et al. 2001
rOAT3	Rat	Oocyte	64.7	Kusuhara et al. 1999
			278.0	Feng et al. 2001
		LLC-PK1	+	Hasegawa et al. 2002
			-	Nagata et al. 2002

2.3.1.3 Regulation

The mechanism responsible for the basolateral uptake of OAs is well understood. However, the cellular regulation of OA transporters has only recently begun to be studied. Physiological studies have established the regulation of organic anion transport by hormones, kinases, growth factors and even substrates (Terlouw et al., 2003). OAT1 proteins possess several potential phosphorylation sites for protein kinases, suggesting that phosphorylation of one or more of these sites may play a role in OAT1 regulation (Sekine et al., 2000). Studies carried out in various OAT expression models have all implicated that protein kinase C (PKC) may play a role in the regulation of this transport system (Shuprisha et al., 2000). Early studies on the activation of PKC by phorbol esters in isolated PTs from rabbit revealed conflicting data. Hohage et al. (1994) demonstrated that activation of PKC revealed a stimulation of PAH uptake, where Gekle et al. (1999) found that PKC activation by phorbol esters caused an inhibition of PAH uptake. Studies using stauorosporine, a PKC inhibitor, reversed the stimulation or inhibition by phorbol esters, indicating that PKC has the ability to regulate OAT activity. Stimulation of PKC by phorbol esters has also been shown to inhibit the uptake of FL in killifish tubules (Miller, 1998) and inhibit PAH transport across both the basolateral and luminal membranes in opossum kidney (OK) cells (Sauvant et al., 2001; Takano et al., 1996). PKC activation by parathyroid hormone has also been shown to cause an inhibition of PAH transport in OK cells (Nagai et al., 1997). These studies in conjunction with others indicate inhibition of OAT1 by activation of PKC (human: Lu et al., 1999; rat: Uwai et al., 1998; mouse: You et al., 2000). Thus, while the definitive role of PKC in activation or inactivation of OAT1 via phosphorylation remains to be fully elucidated, it is evident that PKC plays an important role in the regulation of OAT1 protein in the renal PT.

While studies have shown a relationship between PKC activation and inhibition of OAT1 transport, it has not been determined whether PKC regulation

involves a decrease in membrane expression by internalization of membrane transporters or by inhibition of recruitment of transporters to the membrane. In studies conducted on mouse OAT1, activation of PKC led to a decrease in V_{max} with no change in K_m, indicating internalization of active transporters (You et al., 2000). Interestingly, PKC was not shown to directly phosphorylate the mOAT1 protein, suggesting PKC may actually phosphorylate an OAT1 regulatory protein that is responsible for internalization/inhibition of OAT1. Wolff et al. (2003) has demonstrated that PKC-induced hOAT1 downregulation is achieved through carrier retrieval from the cell membrane and does not involve phosphorylation of the hOAT1 protein.

As described previously, OAT1 is a tertiary active transport carrier. Therefore, inhibition of uptake via OAT1 can also be accomplished through regulation of either the Na^+/K^+-ATPase or NaDC3. Treatment of flounder PTs with phorbol esters is thought to inhibit OA uptake via OAT1 by inhibition of Na^+,K^+-ATPase (Halpin and Renfro, 1996) because PKC activation has been shown to partially deactivate renal Na^+,K^+-ATPase (Bertorello and Aperia, 1989). Studies by Rover et al. (1998) indicate that PKC did not affect transport mediated by the basolateral NaDC3 in rabbit.

Of additional interest is regulation via epidermal growth factor (EGF). EGF is an endogenous compound that is important in normal tubulogenesis, and has been shown to enhance the basolateral uptake of OAs in opossum kidney (OK) cells (Sauvant et al., 2001). This activation is believed to be via the mitogen-activated protein kinase (MAPK) pathway because EGF stimulates both OA uptake and phosphorylation of extracellular signal-regulated kinase 1 and 2 (ERK1/2). Both OA uptake and ERK1/2 phosphorylation was prevented by inhibition of mitogen activated extracellular signal-regulated kinase kinase (MEK) (Sauvant et al., 2001) Sauvant et al. (2004) also showed in OK cells that EGF stimulates basolateral OA transport. They demonstrated that activation is through ERK1/2, arachidonic acid, phospholipase A2, and generation of prostaglandins. EGF activates adenylate cyclase and protein kinase A (PKA),

stimulating OA uptake. Thus, this demonstrates another cellular mechanism for regulation of OAT1 activity in the PT cell.

Triiodothyronine (T_3) or dexamethasone (DEXA) pretreatment in rats has been shown to increase renal PAH excretion (Bahn et al., 2003). Stimulation was accompanied by increased protein synthesis in the renal cortex in both cases. Increased OAT1 mRNA levels following T_3 or DEXA treatment indicate that OAT1 expression can also be regulated by T_3 and DEXA.

There are indications that a number of physiological factors help regulate basolateral organic anion transport in mammals. However, there are still many details regarding the pathways involved in OAT regulation that remain to be clarified, as well as questions about the actual physiological significance of regulation that remain unanswered.

2.3.2 Organic Anion Transporter 2 (OAT2)

In humans, OAT2 (SLC22A7) appears to participate in the renal handling of organic anions. OAT2 has been shown to share 42% amino acid sequence identity to OAT1. OAT2 is quite possibly only a minor contributor to organic anion secretion along the basolateral membrane of the PT, as it has only been localized to that membrane in the human kidney. However, since information on OAT2 is limited, its full contribution to OA handling has not been elucidated. Molecular properties of OAT2 are summarized in Table 2.

2.3.2.1 Cloning and Tissue Distribution

OAT2 was the first member of the OAT family to be cloned. In 1994, a gene product was cloned from rat liver and named novel liver transporter (NLT). It has sequence motifs similar to a major facilitator superfamily and was cloned but not characterized (Simonson et al., 1994). Later, it was recloned and identified as polyspecific organic anion transporter and renamed OAT2 (Sekine

et al. (1998a). Two splice variants of hOAT2 have been reported (hOAT2A and hOAT2B) but the sequences have not been determined (Sun et al., 2001). Studies of the OAT2 proteins have shown that rOAT2 is a protein of 535 amino acids (Simonson et al., 1994) and mOAT2 has 540 amino acids (Kobayashi et al., 2002b). The two splice variants of hOAT2 (2A and 2B) have 546 and 538 amino acids respectively (Sun et al., 2001). The protein structure has been predicted to contain 12 transmembrane spanning domains. The large first extracellular loop between the first and second transmembrane helix of rOAT2 and mOAT2 contains two potential sites for N-glycosylation. Two potential sites for phosphorylation by protein kinase A (PKA) and protein kinase C (PKC) have been reported for rOAT2 and six potential sites for PKC phosphorylation have been reported for mouse OAT2 (Burckhardt and Burckhardt, 2003).

Expression of mRNA of hOAT2 has been detected in the liver and kidney (liver>kidney) (Sekine et al., 1998a; Sun et al., 2001). Immunohistochemical analysis revealed that hOAT2 is localized to the basolateral side of the PT in kidney (Enomoto et al., 2002a; Khamdang et al., 2002). In male rats the OAT2 transcript was also found in the liver with little expression in the kidney (Sekine et al, 1998b; Simonson et al, 1994; Sun et al., 2001). Immunofluorescence localization by Kojima et al. (2002) demonstrated the presence of rOAT2 in the renal cortex and medulla. The expression level of rOAT2 was much lower compared to that of rOAT1 and rOAT3 (Kojima et al., 2002). rOAT2 has been shown to be localized on the apical side of the medullary thick ascending limbs of Henle's loop, and cortical and medullary collecting ducts, whereas rOAT2 was not detected in the proximal tubular cells (Kojima et al., 2002). Gender differences in OAT2 expression have also been shown (Buist et al., 2002; Kobayashi et al., 2002a). Female rats show a higher expression of OAT2 in the kidneys compared to male rats. This gender difference appears at the onset of estrogen production in female rats, suggesting that hormones may play a role in regulation of renal OAT2, but not hepatic OAT2 (Kobayashi et al., 2002a).

It is important to note that immunohistochemistry studies have yielded results that differ for human and rat, as well as gender differences in expression. Immunohistochemistry has shown that localization of OAT2 varies between humans and rats, and this must be taken into consideration when studying and comparing the effects of certain compounds that may be substrates for OAT2. With varying levels of expression of OAT2, different organs from different species may respond differently to therapeutic or toxic compounds. Gender differences present the same problems when studying the effects of certain xenobiotics, as males or females may be more or less susceptible to certain drug effects, thus confounding any comparison that might be made between males and females. Both of these points become additionally important in considering the contribution of OAT2 in the secretion of OA along the basolateral membrane of the renal PT. While studies in humans may show transport of a compound, studies in rats may yield significantly different results, and results in male study models may yield varying results from those found in females.

2.3.2.2 OAT2 Substrates; Characterization and Specificity

The substrate selectivity of OAT2 and OAT1 appear to be similar, however, the transport efficacy for each substrate is different. The transport of PAH by hOAT2 occurs at much lower levels than by hOAT1 (Sekine et al., 1997). When expressed in *Xenopus laevis* oocytes, hOAT2 demonstrated uptake of organic anions such as salicylate, acetylsalicylate, PGE_2, methotrexate, dicarboxylates and PAH (Sekine et al., 1998a). hOAT2 has been shown to transport $PGF_{2\alpha}$ in a time- and concentration-dependent manner (Enomoto et al., 2002a). Khamdang and colleagues (2002) have also documented transport of cephaloridine by hOAT2 and its contribution to the renal excretion of this antibiotic. Studies conducted with rat OAT2 have shown that rOAT2 mediates the transport of $PGF_{2\alpha}$ with an affinity similar to that of hOAT2 (Takeda et al., 2002).

In the kidney (as well as liver) rOAT2 mediates saturable uptake of salicylate from the blood in a sodium independent manner, like that of OAT1 (Sekine et al., 1998a). Salicylate uptake however, was not *trans*-stimulated by intracellular glutarate (Sekine et al., 1998a). When OAT2 was expressed in LLC-PK_1 cells, transport of α-ketoglutarate was not found (Morita et al., 2001). This indicates that OAT2 does not function as a dicarboxylate exchanger, exchanging an extracellular OA against intracellular α-ketoglutarate. PAH transport was also not inhibited by dicarboxylates further supporting this conclusion (Burckhardt and Burckhardt, 2003). Summary of transport and Km values for PAH transport are listed in Table 3. Wolff (unpublished results: Burckhardt and Burckhardt, 2003) has indicated that OAT2 shows low affinity for PAH, concluding that if OAT2 is present in the basolateral membrane of PT cells, it is unlikely to contribute much to organic anion secretion. Human OAT2 is also only weakly inhibited by probenecid, the prototypical inhibitor of the OAT proteins. Enomoto et al. (2002) have determined that the Ki value of probenecid for human-OAT2-mediated organic anion uptake is 766 μM. Khamdang et al. (2003) demonstrated this point by showing that cephaloridine induced nephrotoxicity was not reversible in human OAT2-expressing S2 cells when treated with 1mM probenecid, but nephrotoxicity could be reversed in S2 human-OAT1 and S2 human-OAT3 cells by treatment with probenecid.

2.3.2.3 Regulation

Hormonal regulation of rOAT2 has been studied. Findings have shown that there is an increase in OAT2 mRNA levels in male rat kidney following castration, with subsequent decrease in levels following post castration treatment with testosterone (Kudo et al., 2002; Kobayashi et al., 2002a). However, this increase is minimal and does not approach the levels seen in female kidney. Administration of estrogen to castrated males provided conflicting results in mRNA levels of OAT2 (increase: Kudo et al., 2002; decrease: Kobayashi et al.,

2002a). This indicates that sex steroids do not apper to be the primary mediator of the gender difference in OAT2 expression in rats. Buist et al. (2003) and Kobayashi et al. (2002a) were able to demonstrate in hypophysectomized (HX) rats, a marked decrease in OAT2 mRNA in female rats, while the levels of OAT2 in HX male rats was not altered. Continuous infusion of growth hormone (GH) (female pattern) significantly increased OAT2 mRNA in HX rats compared with untreated rats (Buist et al., 2003). This demonstrated that the female pattern of growth hormone secretion is at least partially responsible for the elevation of OAT2 in the female rat kidney compared with male kidney. Other mechanisms of regulation (e.g., PKC) have not been determined.

2.3.3 Organic Anion Transporter 3 (OAT3)

OAT3 (SLC22A8) has also been shown to participate in the renal excretion and reabsorption of anionic drugs. The OAT3 protein contains 536 amino acids for rOAT3, 537 for mOAT3, and either 543 or 568 for hOAT3. Rat OAT3 is 49% and 39% identical to rOAT1 and rOAT2, respectively. Human OAT3 is 51% and 36% identical to hOAT1 and hOAT2 respectively (Burckhardt and Burckhardt, 2003). The expressed OAT3 protein is predicted to have 12 transmembrane domains with a large, putatively extracellular loop located between the first and second transmembrane domain. The OAT3 protein contains four potential sites for N-glycosylation. Rat OAT3 contains three potential PKC phosphorylation sites, while hOAT3 contains eight potential phosphorylation sites (Burckhardt and Burckhardt, 2003). There is no experimental data available on the topological organization of OAT3 prevailing within the membrane.

Due to OAT3 presence in the basolateral membrane of the PT, it can play an important role in the renal excretion of organic anions. Physiologically, OAT3 also mediates the first step in the renal excretion of many anionic drugs and endogenous anions, acting in parallel with other OA transporting proteins along

the basolateral membrane in the PT. Molecular properties of OAT3 are summarized in Table 2.

2.3.3.1 Cloning and Tissue Distribution

OAT3 was first cloned from rat kidney (rOAT3: Kusuhara et al., 1999). The human homolog, hOAT3 was later cloned by Race et al. (1999). Cha et al. (2001) cloned the functional hOAT3 from human kidney based on sequences derived from rOAT3. OAT3 has also been cloned from rabbit (Dantzler and Wright, 2003).

Northern blot analysis showed that rOAT3 is actually most abundantly expressed in the liver, followed by the kidney, while hOAT3 transcripts are expressed abundantly in the kidney and at lower levels in the brain and skeletal muscle (Race et al., 1999; Kusuhara et al., 1999). Studies by Buist et al. (2002) however, have shown rOAT3 to be most abundant in the kidney, rather than the liver. Levels of renal OAT3 in rat have been shown to increase after birth and reach maximum levels by 14 days. Similar levels were detected in male and female animals (Buist et al., 2002). In human kidneys, it is important to note that mRNA levels for OAT3 are nearly three times higher than that for OAT1 (Motohashi et al., 2002). In rat kidney, OAT1 has been found to be more highly expressed in the kidney than OAT3, with OAT3 being expressed predominantly in the liver (Dresser et al., 2000; Kusuhara et al., 1999). This indicates that OAT3 may play a more significant role in OA transport in the human kidney than OAT1.

OAT3 has been localized to the basolateral membrane of the renal PT in both rat (Hasegawa et al., 2002) and human (Cha et al., 2001). Kojima et al. (2002) have shown that rOAT3 is present at the basolateral membrane in all sections of the PT (S1, S2, S3), as well as in the thick ascending limbs, the distal tubules, and the collecting ducts. Interestingly, in the human kidney, OAT3

appears to be confined to the basolateral membrane of the PTs where it is co-localized with OAT1 (Motohashi et al., 2002).

2.3.3.2 OAT3 Substrates; Characterization and Specificity

Characterization of OAT3 transport conducted in *Xenopus laevis* oocytes showed PAH uptake by rOAT3 (Cha et al., 2001; Kusuhara et al., 1999). Summary of transport and Km values for PAH transport for OAT3 are listed in Table 3. Results from additional studies have indicated that rOAT3 does not transport PAH, but rather suggest that the affinity of rOAT3 for PAH is lower than that of rOAT1 (Sugiyama et al., 2001; Nagata et al., 2002). This is apparently true for hOAT3 as well. Studies by Cha et al (2001) indicate a 4-10 fold higher Km for PAH transport by hOAT3 compared to hOAT1 (87.2 μM and 9 μM respectively). Rat OAT3 also demonstrated a higher Km for PAH transport than rOAT1 (65 μM and 14 μM respectively (Cha et al., 2001), suggesting that OAT1 and OAT3 transporters would have different contributions in tubular secretion.

Rat OAT3 has been shown to transport several other OAT substrates, including benzylpenicillin, cimetidine (cation), 17*β*-estradiol-D-17*β*-glucuronide ($E_2$17*β*G), estrone sulfate, indoxyl sulfate, ochratoxin A and pravastatin. hOAT3 has been shown to transport azidothymidine (AZT), cAMP, cimetidine, dehydroepiandrosterone sulfate (DHEA-S), estradiol glucuronide, estrone sulfate, methotrexate, ochratoxin A, PGE_2, $PGF_{2\alpha}$, salicylate, taurocholate, urate, and valacyclovir (Burckhardt and Burckhardt, 2003). OAT3 can be distinguished from OAT1 by its ability to transport sulfate and glucuronide conjugates of steroid hormones. For this reason an estrogen conjugate, estrone sulfate (ES), has been used as the prototypical OAT3 substrate. OAT3 also shows interaction with cimetidine (a cationic drug) whereas OAT1 does not (Cha et al., 2001, Feng et al., 2001). This indicates that OAT3 does not discriminate between organic anions and cations as sharply as OAT1 (Burckhardt and Burckhardt, 2003).

The mechanism of transport of OAT3 has recently been redefined. OAT3 was originally shown to function as a uniporter, and not as an anion exchanger in the manner of OAT1 transport (exchange of an OA for a dicarboxylate). Kusuhara et al. (1999) found that estrone sulfate (ES) transport by rOAT3 could not be *trans*-stimulated by unlabeled ES, PAH, or ochratoxin A. Cha et al. (2001) reported similar results for hOAT3. These findings lead to the conclusion that OAT3 did not function as an anion exchanger like OAT1. However, up to this point, no studies had been conducted to determine the contribution of internal α-ketoglutarate or glutarate to OAT3 transport. It has been demonstrated that hOAT3 has the ability to interact with glutarate (Cha et al., 2001), indicating the potential for OAT3 to interact with dicarboxylates. Recent findings however, have shown that OAT3 does function as a dicarboxylate exchanger in the same mechanism as OAT1. Sweet et al. (2003) demonstrated that ES transport by rOAT3 expressed in *Xenopus laevis* oocytes was significantly trans-stimulated by preloading cells with glutarate (a dicarboxylate). Additionally, it was shown that when OAT3 was coexpressed with the Na^+/dicarboxylate exchanger, ES transport was significantly inhibited by the presence of Li^+ or methylsuccinate, and by the exclusion of Na^+ from the preloading medium, all of which act to inhibit the Na^+/dicarboxylate exchanger. These results indicate that OAT3 functions as an OA/dicarboxylate exchanger that couples OA uptake indirectly to the sodium gradient. Similar results were also found in rat renal cortical slices (Sweet et al., 2003). Bakhiya et al. (2003) have also shown that hOAT3 functions as an OA/dicarboxylate exchanger similar to OAT1.

2.3.3.3 Regulation

Treatment of rOAT3 expressing mouse proximal tubular cells with the phorbol ester, phorbol 12-myristate 13-acetate(PMA), a PKC stimulator, inhibited the uptake of ES in a dose and time-dependent manner (Takeda et al., 2000b). Inhibition of PKC by chelerythrine chloride reversed the effects of PMA. These

results indicated that PKC activation downregulates rOAT3 mediated organic anion transport. Inhibition was determined to be due to the internalization of transporters, or to an inhibition of translocation of preformed transporters to the membrane.

Rat OAT3 also appears to undergo some regulation by testosterone. In male rats, OAT3 is much more highly expressed in the liver, than in female rats (renal expression is the same in males and females). Kobayashi et al. (2002a) demonstrated that after castration, OAT3 levels in the liver of male rats decrease, and testosterone treatment restored normal male levels. Additionally, HX increased OAT3 mRNA in female liver indicating a role for growth hormone in the female pattern of OAT3 expression as well (Kobayashi et al., 2002a; Buist et al., 2003).

2.3.4 Luminal Transport of Organic Anions

As mentioned previously, the secretion of OAs can be divided into two processes (1) uptake of OA across the basolateral membrane into PT cells and (2) efflux of the OA out of the cell into the tubule lumen across the luminal membrane. Far less is known about the mechanisms involved in OA transport into the tubular lumen than is known about basolateral transport of OAs. Movement of OAs across the luminal membrane during the transepithelial secretory process occurs down an electrochemical gradient. Since the luminal membrane appears to be highly permeable to substances with low lipid solubilities, this transport must be carrier-mediated. At the luminal membrane, the efflux carriers differ among various species.

Currently, several OA transporters have been identified at the luminal membrane of renal proximal tubular cells (Figure 2.6). The luminal membrane may contain organic anion uniporters or “channels” (Burckhardt and Pritchard, 2000). These luminal uniporters have been identified in several animal species including; flounder, rat, rabbit, and pig. A second type of transporter found at the

luminal membrane includes organic anion/Cl^- (OH^-, HCO_3^-) antiporters, found in dog and rat. A third type of transporter found in the luminal membrane is an organic anion/α-ketoglutarate antiporter (human, cow). A fourth type of OA transporter localized to the luminal membrane is an ATP-driven organic anion transporter (Burckhardt and Burckhardt, 2003). Several specific transporters have been identified in the luminal membrane of the PT. Human type I sodium-dependent inorganic phosphate transporter, NPT1, a sodium phosphate cotransporter, expressed in HEK293 cells by Uchino et al. (2000), was shown to facilitate secretion of PAH and urate. OAT4 was cloned from human cDNA (Cha et al., 2000) and shown to be localized at the luminal membrane (Babu et al., 2002). However, the contribution of OAT4 to the efflux of OAs across the basolateral membrane is uncertain, as it has not been show to transport PAH (Cha et al., 2000). URAT1 has also been cloned, based on its sequence homology to OAT4 (Enomoto et al., 2002a) and has been shown to function as an antiporter, exchanging urate against either chloride or certain monovalent organic anions. As with OAT4, PAH does not appear to be a substrate for URAT1 and thus does not contribute to PAH secretion. Multidrug resistance transporter 2 (MRP2) is mainly responsible for the ATP-dependent translocation of sulfated or glucuronidated compounds such as glutathione S-conjugates, bilirubin glucuronide, 17-β-glucuronosyl estradiol, and glutathione disulfide (Konig et al., 1999; Keppler et al., 1997). In human and rat, MRP2 has been located in the proximal tubular cell at the luminal membrane (Schaub et al., 1997, 1999), and has been shown to transport PAH (Van Aubel et al., 2000b). A kidney specific transporter, termed rOAT-K1 was also cloned from rat kidney (Saito et al., 1996) and has been shown to transport methotrexate, but not PAH. rOAT-K1 does not share any significant sequence identity with OAT isoforms and is therefore thought to belong to a different gene family. A second kidney specific transporter, rOAT-K2 was also identified from rat kidney (Masuda et al., 1999), and has been shown to transport methotrexate, folate, taurocholate and PGE_2. PAH has been shown to interact only weakly with rOAT-K2. Rat OAT-K1 and

OAT-K2 have been identified at the luminal membrane in the kidney (Masuda et al., 1997, 1999; Tojo et al., 1999; Hasegawa et al., 2002). OATP1 transporters have also been localized to the luminal membrane in the S3 segment of the renal PT (Bergwerk et al., 1996) where it meditates uptake of OAs from the luminal fluid into the proximal tubular cell. OATP3 is thought to be a multispecific anion transporter that accepts many types of organic anions including taurocholate and other bile acids as substrates (Echkardt et al., 1999; Burchkardt and Wolf, 2000). The driving force for OATP3 is considered to be reduced glutathione (Li et al., 1998). Isern et al. (2001) demonstrated that mouse OATP1 mediates sodium-independent uptake of the anionic steroid conjugates dehydroepiandrosterone sulfate (Km ~ 8 μM) and estradiol-17-glucuronide (Km ~ 5 μM). Rat OATP1 gene expression was much higher in the kidneys of male rats than female rats (Kato et al., 2002).

2.4 Renal Transport of Prototypical Organic Anions

2.4.1 Renal Transport of Para-aminohippuric Acid (PAH)

PAH is the prototypical substrate for OAT1 at the basolateral membrane of the renal PT cell (Km values presented for various systems in Table. 2). OAT3 has also been shown to transport PAH (Table 3). At the basolateral membrane, PAH uptake against its concentration gradient is coupled to dicarboxylate (most often α-ketoglutarate) exchange (Pritchard, 1988; Burckhardt and Wolf, 2000; Sekine et al, 2000) and is indirectly coupled to Na^+ uptake (Shimada et al., 1987; Pritchard 1988). PAH does not appear to interact with luminal transport proteins in the kidney including hOAT4 (Cha et al, 2000), urate transporter (URAT1; Enomoto et al., 2002a), rOATP1 or rOATP2 (Sugiyama et al., 2001). PAH shows only limited affinity for NPT1 (Uchino et al., 2000) and MRP2 (Leier et al., 2000). At the luminal membrane, PAH is transported by either an anion exchanger which transports many organic and inorganic anions such as urate, lactate, OH^-,

and Cl^- as substrates (Kahn et al., 1983; Kahn and Aronson, 1983; Guggio et al., 1983; Steffens et al., 1989; Ohoka et al., 1993) or a membrane potential sensitive system (Martinez et al., 1990; Werner et al., 1990; Ohoka et al., 1993). In dog and rat renal brush-border membrane vesicles, an anion antiporter exchanged PAH or urate against OH^-, HCO_3^- CL^-, lactate acetoacetate or monovalent succinate (Burckhardt et al., 2001). Studies conducted by Ulrich and Rumrich (1997) using PAH preloaded rat proximal tubular cells, demonstrated that luminal PAH transport in the rat PT in situ is insensitive to electrical potential and therefore may occur by anion exchange. The main driving force for luminal PAH influx in rat nephrons in situ may be the intracellular PAH concentration, as the electrical potential difference seems not to be important.

Currently, the molecular identity of the antiporters and/or uniporters involved in PAH secretion across the luminal membrane is unknown. Of the cloned OATP transporter proteins known to be located in the luminal membrane of the kidney PTs, oatp1 and OAT-K1 do not transport PAH. This excludes these transporters as candidates for PAH antiporters or uniporters. OAT-K2 was only weakly inhibited by PAH, but transport of labeled PAH has not been demonstrated. NPT1 had been shown to display low affinity uptake of labeled PAH (Km of 2.7 mM). MRP2 has been shown to be a luminal transporter of PAH; however there may be luminal PAH transporters that have not yet been identified.

2.4.2 Renal transport of Estrone-3-Sulfate (ES)

ES is the prototypical substrate for OAT3 (see Table 4 for Km values in various systems). Studies by Sweet et al. (2002) have indicated that OAT3 is not the only basolateral transport protein responsible for ES uptake. ES transport by OAT3 has not been shown to be trans-stimulated by unlabeled ES (Cha et al., 2001) Interaction of ES with other basolateral transporters has also been demonstrated. ES has been suggested to interact with URAT1, as ES cis-

stimulated uptake of urate by URAT1 (Enomoto et al., 2002). There has been conflicting results regarding the interaction of ES with MRP2. Sasaki et al. (2002) demonstrated that ES was not a substrate of MRP2, yet ES stimulated the transport of other substrates of MPR2. Of particular importance, Sweet et al. (2002) determined that ES did not interfere with PAH transport by OAT1, thus enabling the use of ES to determine the contribution of OAT3 in a system in comparison to the contribution of OAT1 to a substrate's transport by the OAT system. At the luminal membrane, in humans, ES appears to be transported by OAT4 (Cha et al., 2000), and stimulates efflux of substrates by the luminal transporters URAT1 and MRP2.

2.4.3 Renal Transport of Fluorescein (FL)

FL has been used in several studies as a model OAT substrate. FL accumulates in proximal tubular cells of the kidney (Terlouw et al., 2000). FL is thought to be transported into the cytoplasm of PTs by a basolateral mechanism similar to the classical organic anion system (Sullivan et al., 1990). In isolated non-perfused proximal S2 segments from rabbit, Sullivan et al. (1990) found a Km for FL transport of 10 μM. Masereeuw et al. (1994) determined that FL uptake in isolated proximal tubular cells from rat was concentration dependent, saturable and probenecid sensitive, with an apparent Km of 59 ± 15 μM. Dose dependent inhibition of FL uptake by PAH indicated that FL uptake is regulated by the PAH transport system, and therefore, FL is a suitable substrate for studying this system. It has also been demonstrated that FL transport in isolated S2 segments of rabbit PT is stimulated by increased intracellular α-ketoglutarate levels, suggesting FL transport is carried out in the same manner as PAH transport (Sullivan and Grantham, 1992; Nikiforov, 1995).

Table 4. Substrate specificity of various compounds in selected OAT isoforms

Compound	Transporter	Expression system	Transport (+/-) or Km (μM)	Inhibition (+/-) or IC_{50} (μM)	References
benzylpenicillin	hOAT1	Oocyte		+	Hosoyamada et al. 1999
				+	Islinger et al. 2001
		HeLa cells		-	Lu et al. 1999
		Mouse PTC		+	Jung et al. 2001
	rOAT1	Oocyte	+	1680.0	Jariyawat et al, 1999
				+	Islinger et al. 2001;
				+	Sekine et al. 1997
		LLC-PK1		418	Hasegawa et al. 2002
				800.0	Nagata et al. 2002
	rOAT2	LLC-PK1		+	Morita et al. 2001
	hOAT3	Oocyte		+	Cha et al. 2001
		Mouse PTC		+	Jung et al. 2001
	rOAT3	Oocyte		+	Deguchi et al. 2002
				+	Kusuhara et al. 1999
		LLC-PK1	82.6	82.6	Nagata et al. 2002
				52.8	Hasegawa et al. 2002
DHEA-S	hOAT2	EcR293	-		Sun et al. 2001
	hOAT3	Oocyte	+	+	Cha et al. 2001
Estrone Sulfate	hOAT3	Oocyte	3.1		Cha et al. 2001
		Mouse	2.2		Takeda et al. 2001
			7.5		Takeda et al. 2000
				+	Babu et al. 2002
	rOAT3	Oocyte	2.34		Kusuhara et al. 1999
			33		Feng et al. 2001
				+	Feng et al. 2001
					Deguchi et al. 2002
		Mouse PTC	618		Takeda et al. 2002
		LLC-PK1		9.1	Nagata et al. 2002
Fluorescein	hOAT1	Oocytes		+	Islinger et al. 2001
		CHO cells	+		Cihlar and Ho. 2000
		HeLa cells		+	Lu et al. 1999
	?	rabbit S2 segments	10		Sullivan et al. 1990
	?	rat isolated PT cells	59		Masereeuw et al. 1994
Paracetamol	rOAT1	Oocytes		2099	Apiwattanakul et al. 1999

FL transport in isolated S2 segments of rabbit PT is inhibited by probenecid and PAH (IC_{50} 6 μM and 141 μM respectively: Sullivan and Grantham, 1992). While specific transport proteins have not been identified in the efflux of FL into the luminal fluid, efflux at the luminal membrane of isolated perfused rabbit PTs has been found to be a saturable process and, therefore, suggested to be a carrier-mediated process (Shuprisha et al., 2000).

2.4.4 Inhibition of Renal Organic Anion Transport by Probenecid

Probenecid is a highly lipid soluble benzoic acid derivative. Probenecid has been used as the prototypical inhibitor of organic anion transport across epithelial barriers. This becomes extremely important in the renal PT where it inhibits the secretion of drugs and drug metabolites. Probenecid was used originally in medicine to prolong the action of penicillin and prevent its loss in the urine (Insel, 1996). Probenecid has been shown to function as an inhibitor of OAT1, OAT3, MRP, URAT1, NPT1, and OATP transporters (see Table 5 for inhibitory values and references). Probenecid inhibits renal secretion of the glucuronide conjugates of NSAIDs such as naproxen, ketoprofen, indomethacin and causes plasma concentrations of these compounds to increase (Insel, 1996). Macdonald et al. (1995) also demonstrated in humans that co-administration of probenecid with diflunisal greatly reduces the renal clearance of diflunisal glucuronides (both acyl and ether). Dickinson (1993) also found a 70% reduction in the renal clearance of both diflunisal glucuronide conjugates. Vree et al. (1993a) have suggested that probenecid may be glucuronidated in the kidney and that it may inhibit renal glucuronidation of such drugs as nalidixic acid (Vree et al., 1993b) and indomethacin (Vree et al., 1994). The role of probenecid, particularly in vivo, can be complicated as it can inhibit the secretion and formation of glucuronide conjugates, as well as the secretion of other organic anions.

2.4.5 Renal Secretion of Acetaminophen Glucuronide (AG)

Studies on renal tubular secretion of acetaminophen glucuronide have offered confounding results. The liver is the primary site of acetaminophen glucuronidation, however, extrahepatic glucuronidation has also been found (Li et al., 2004). It has been shown that serum protein binding of acetaminophen glucuronide in humans is less than 10% (Duggin and Mudge, 1975; Morris and Levy, 1984), and therefore, AG is readily available for glomerular filtration. Renal clearance of acetaminophen glucuronide in many instances was determined after administration of acetaminophen (Morris and Levy, 1984; Galinsky and Levy, 1981; Duggin and Mudge, 1975) and conjugate clearance values must then be considered as estimates of conjugate renal clearances. It has been demonstrated that the kidney has the ability to glucuronidate acetaminophen (Ross et al., 1980; Hart et al., 1980; Newton et al., 1982; Emslie et al., 1981; Li et al., 2004). When acetaminophen is administered, renal glucuronidation of acetaminophen to AG with subsequent efflux into the tubular lumen cannot be separated from secretion.

Several studies have been conducted to determine the renal secretion of acetaminophen glucuronide. In 1975, Duggin and Mudge found in dog, that AG at low plasma concentrations (~20 μg/ml), appears to undego tubular secretion via an active transport process. At higher plasma concentrations of AG (~90 μg/ml), it was found that AG appeared to be reabsorbed. It was also found that net tubular AG secretion was not probenecid sensitive, while secretion of the sulfate conjugate of acetaminophen was probenecid sensitive (Duggin and Mudge, 1975). Renal secretion of AG was also demonstrated in rat by Galinsky and Levy (Sprague-Dawley rats: 1981) and Watari et al. (Wistar rats: 1983).

Table 5. Substrate specificity of probenecid in selected OAT isoforms

Compound	Transporter	Expression system	Transport (+/-) or Km (μM)	Inhibition (+/-) or IC_{50} (μM)	References
Probenecid	hOAT1	Oocytes		+	Cihlar et al. 1999
				+	Hosoyamada et al. 1999
				+	Islinger et al. 2001
				+	Pombrio et al. 2001
				+	Race et al. 1999
		CHO cells		6.3	Cihlar et al. 1999
				6.5	Ho et al. 2000
				7.4	Mulato et al. 2000
		HeLa cells		+	Lu et al. 1999
		Mouse PTC (S_2)		4.29	Jung et al. 2001
				12.1	Takeda et al. 2001
		OK cells		+	Motojima et al. 2002
	rOAT1	Oocyte	-	+	Uwai et al. 1998
				+	Cihlar et al. 1999
				+	Mulato et al. 2000
				+	Pombrio et al. 2001
				+	Sekine et al. 1997
				+	Sweet et al. 1997
				+	Tsuda et al. 1999
				+	Uwai et al. 2000
				+	Wada et al. 2000
	hOAT2	Mouse PTC (S_2)		766	Enomoto et al. 2002b
	rOAT2	LLC-PK1		+	Morita et al. 2001
	hOAT3	Oocyte		+	Cha et al. 2001
		Mouse PTC (S_2)		4.9	Jung et al. 2001
				9	Takeda et al. 2001
	rOAT3	Oocyte		+	Feng et al. 2001
				+	Kusuhara et al. 1999
				1.68	Deguchi et al. 2002
		LLC-PK1		4.43	Nagata et al. 2002
				20	Sugiyama et al. 2001

In contrast to these findings, Morris and Levy (1984) found that on average, renal clearance of AG did not exceed creatinine clearance in human subjects, suggesting that AG does not undergo appreciable tubular secretion. This lack of secretion, however, may be due to a balance between secretion and reabsorption. It has also been suggested in studies in dog, that AG is completely filtered at the glomerulus and does not undergo secretion (Heckman et al., 1986).

There are many factors that determine renal secretion of AG. It has been reported that the kidney has the potential to secrete AG, and this secretion is most likely via the organic anion transport pathway. However, to date, all studies have been conducted in whole animals, or whole organ systems. Currently there is no information at the cellular level about the renal handling of AG, or other glucuronide conjugates.

2.5 Summary

Glucuronidation is an important biotransformation process that can lead to the formation of both inert and reactive metabolic metabolites. Toxicity associated with glucuronide conjugates has primarily been associated with the glucuronide metabolites of carboxylic acid containing compounds. Glucuronidation of carboxylic acids leads to the formation of acyl glucuronides which have been shown to be reactive intermediates. Acyl glucuronides have been shown to become covalently bound not only to serum proteins, but also within various tissues of the body. This covalent binding can lead to toxicity and hypersensitivity reactions. Currently, there is little knowledge about how the kidney handles glucuronide metabolites, and whether transport of reactive acyl glucuronide metabolites has any implications for the nephrotoxicity of certain compounds, particularly NSAIDs which have been shown to form acyl glucuronide metabolites. Glucuronide conjugates are organic anions, carrying a negative charge at physiological pH. The renal PT, which is the primary site of xenobiotic secretion in the kidney, possesses several organic anion transport

proteins along the basolateral membrane that facilitate uptake of organic anions from the blood into the proximal tublular cells. Table 2 provides a brief summary of the characteristics of these OAT transporters. The kidney has been shown to demonstrate transport of several organic anions including PAH, fluorescein, and estrone sulfate. Tables 4 and 5 provide a list of various OAT substrates with Km values. These OAT proteins (principally OAT1 and OAT3) may be responsible for the transport of glucuronide conjugates in the kidney. However, information on renal handling of glucuronide conjugates by basolateral OAT proteins in the kidney is currently lacking. Since information on renal glucuronide handling is extremely limited, this project was designed to investigate the transport of a prototypical glucuronide, acetamidophenyl glucuronide (AG). To study the transport of AG by the kidney, rat in vitro models were used to gain insight into how the kidney may secrete glucuronide metabolites with emphasis on the basolateral organic anion transport system.

CHAPTER III

Methods

3.1 Animals

Male Fischer 344(F344; 175-200 g) and Sprague-Dawley rats (SD; 200-250 g) were obtained from Hilltop Lab Animals, Inc. (Scottdale, PA) and were placed in standard plastic cages prior to use. Animals were maintained under controlled ambient temperature (21-23ºC), humidity (40-55%) and light cycle (lights on 0600-1800 h) with free access to food (Purina Rat Chow) and water at all times. Animals were allowed a minimum of 5 days to acclimatize to the animal facilities prior to tissue collection.

3.2 Materials

4-Acetamidophenyl-ring-UL^{14}C β-D-glucuronide sodium salt (AG; specific activity: 48.8 mCi/mmol), was purchased from Sigma Chemical Co. (Saint Louis MO) (Cat. no. A 1329). p-[Glycyl-^{14}C]-aminohippuric acid (PAH; specific activity: 52.7 mCi/mmol) (Cat no. NEC 563), D-[1-^{3}H(N)]-mannitol (MN; specific activity:17 Ci/mmol) and [6,7-^{3}H(N)]-estrone sulfate, ammonium salt (ES; specific activity: 46 Ci/mmol) (Cat no. NET 1012 and NET 203, respectively) were purchased from Perkin Elmer Life and Analytical Sciences (Boston, MA). All other chemicals not listed were purchased from Sigma Chemical Co (St. Louis, MO) or Fisher Scientific (Agawam, MA) and were of highest purity available.

4-Acetamidophenol (acetaminophen, APAP): Aldrich: A7302
p-Acetamidophenyl β-D-glucuronide: Sigma: A4438
Adenosine 5'-triphosphate: Sigma: A2383

Bovine Serum Albumin (BSA): Sigma: A4503

Brilliant Blue G250 (Coomassie blue): Fisher: BP100-25

Collagenase IV: Sigma: C9891

Dehydroepiandrosterone sulfate: Sigma: D5297

Deoxyribonuclease 1 (DNase 1): Sigma: DN 25

Diclofenac: Sigma: D6899

ECL™ Western Blotting Detection Reagents (Amersham Biosciences, RPN2106)†

Estrone-3-sulfate: Sigma: E 0251

Fluorescein: Sigma: F6377

Heparin: Sigma: H3393

HK-2 human kidney, PTCs, transformed (ATCC, CRL-2190)

Hyperfilm™ ECL high performance chemiluminescence film (Amersham Biosciences, RPN2114K) †

Methylumbelliferyl glucuronide: Sigma: M9103

Nicotinamide adenine dinucleotide phosphate: Sigma: N0505

OAT1 antibodies, affinity pure (Alpha Diagnostic International, OAT11-A)

OAT3 antibodies, affinity pure (Alpha Diagnostic International, OAT31-A)

Ouabain: Sigma: O3125

p-aminohippuric acid: Sigma: A1422

Pentobarbital: Sigma: P3761

Penicillin G (Benzylpenicillin): Sigma: P3020

Percoll ®: Sigma: P1644

Probenecid: Sigma: P8761

D-Saccharic acid 1,4-lactone: Sigma: S0375

Scintiverse II: Fisher: SX12-4

Soy bean trypsin inhibitor: Sigma: T9003

Testosterone glucuronide: Sigma: T8157

Triton X-100: Fisher: BP151

Endo H (endoglycosidase H) (New England Biolabs, P0702S)

3.3 Equipment

Located in VA Research Building:

Masterflex peristaltic pump

Osmette S osmometer

Mettler analytical balance

Corning pH meter

Dubnoff metabolic shaking incubators

Sorvall® Microspin 12 Centrifuge

Common facilities VA Research Building:

Beckman J6 MI refrigerated centrifuge

Beckman Avanti J25 ultracentrifuge

Beckman Optimal XL-100K Ultracentrifuge, Rotor SW 60 Ti

Beckman Avanti centrifuge, rotor J14

Phase contrast microscope

Beckman UV/Vis spectrophotometer

Perkin Elmer HTS 7000 bioassay reader-fluorescent microplate reader

Wallac 1409 liquid scintillation counter

Forma Scientific BioFreezer (-80)

IEC Centra CL2 Centrifuge

Medical Education Building:

Sorvall® RC 5B Refrigerated Superspeed Centrifuge, SS-34 rotor

Sorvall® MC5B Centrifuge

Beckman 126 HPLC

Trans-Blot Electrophoretic Transfer Cell (BioRad)†

Micromax RF Centrifuge, International Equipment Company

† All reagents and equipment for Western blot analysis were kindly provided by Dr. Kelley Kiningham.

3.4 Isolation of Renal Proximal Tubules (IRPT)

Male F344 rats were anestisized (pentobarbital sodium, 50mg/kg, i.p.) and renal proximal tubule (IRPT) fragments were isolated following the procedure described by Gesek et al. (1987) and modified by Aleo et al. (1991). Additional modifications were made, initiating renal retrograde perfusion by the procedure of Jones et al. (1979). The level of anesthesia was assessed using the toe pinch and corneal reflex methods. The peritoneal cavity was opened by a midline incision and 0.2 ml heparin (0.2% w/v in 0.9% saline) injected into the femoral vein. Ligatures were placed under the lower abdominal aorta (below the renal arteries), the coeliac and superior mesenteric arteries, and the upper abdominal aorta (as high in the abdominal cavity as possible). The ligature was then tied around the upper aorta, and the rat was sacrificed by bilateral pneumpthorax exsanguination. The celiac, mesenteric and lower abdominal arteries were then ligated. A small incision was made in the lower abdominal aorta above the ligature and a cannula (blunted 19 x 7/8 butterfly infusion set) inserted and tied in place. Retrograde perfusion was then initiated with the kidneys *in situ* with 75 ml of oxygenated (95% O_2 /5% CO_2) Perfusion buffer A (see appendix for buffer composition) at 12 ml/min for 3 min at 37ºC. The kidneys were transferred to a beaker containing continuously oxygenated Perfusion buffer A from which the buffer was being withdrawn to provide a recirculating system. After initial perfusion, cannulated kidneys were transferred to Perfusion buffer B (see appendix for buffer composition) for an additional 3 min (also continuously oxygenated). Following perfusion, kidneys were removed from the perfusion apparatus, decapsulated, and cortical tissue dissected away from the medulla, minced, and placed in a 50 ml plastic beaker with 25 ml of oxygenated

collagenase containing Incubation buffer (see appendix for composition). Digestion of cortical tissue was initiated at 37ºC in a shaking water bath (60 rpm) with continuous oxygenation. After 15 min, solid kidney tissue was allowed to settle in the beaker and freed PTs (PTs) remaining in suspension in the incubation buffer were removed by transfer pipette and placed in a 50 ml centrifuge tube. The suspension was centrifuged at 50 x g for 2 min at 4º C in a Beckman J6MI centrifuge (JS 4.2 rotor). The supernatant was removed and reserved for further cortical tissue digestion and the pellet was resuspended in oxygenated ice cold 1x Krebs-Henseleit (KH) buffer (see appendix for composition) and kept on ice. The remaining tissue was digested with an additional 25 ml of Incubation buffer for additional 5 min intervals until cortical tissue was completely digested. Total incubation time was typically 25 min. PTs were removed at the end of each 5 min interval, centrifuged as described and combined. The total pellet was then rinsed three times by resuspension in 25 ml ice cold 1x KH buffer and centrifugation at 50 x g for 2 min. The final PT pellet was then resuspended in 10 ml 1x KH buffer. This suspension of PT tubules was then divided in half and each 5 ml resuspended in polycarbonate round bottom centrifuge tubes each containing 30 ml oxygenated 45% Percoll solution (see appendix for compositon). A 5 ml 100% Percoll cushion was then injected into the bottom of each tube using a transfer pipette (Fig. 3.1A). PTs were then centrifuged at 17,000 x g for 10 min at 4º C in either a Beckman Avanti ™ Ultracentrifuge (JA 14 rotor) or a Sorvall® RC 5B superspeed centrifuge (SS 34 rotor) (allowed stopping without brake). Following centrifugation PTs formed a uniform layer above the cushion layer (Fig. 3.1B). This layer was removed using a transfer pipette, and rinsed three times in 1x KH buffer at 500 x g for 5 min at 4º C in a Beckman J6MI centrifuge (JS 4.2 rotor). PTs were then resuspended in oxygenated Transport buffer #1 (see appendix for composition) at a concentration of 1.0 mg protein/ml for all assays. Protein content was determined by the Bradford (1976) method using BSA as the standard and expressed in mg protein/ml.

3.5 Characterization of proximal tubules

Following isolation of PTs, biochemical and visual characterization of the isolated PTs was done to determine the purity of the isolated material. Analysis was conducted immediately following tubule isolation from the renal cortical tissue (pool sample), and again following Percoll density gradient enrichment (PT sample). Tubules were analyzed for alkaline phosphatase (AP), a brush border enzyme found only in the proximal tubular segment of the nephron and for hexokinase (HK), a cytosolic enzyme present in highest concentrations in the distal portion of the nephron. In addition to enzymatic characterization, lactate dehydrogenase (LDH) release was analyzed to determine the viability of tubules both before (pool sample) and after Percoll enrichment (PT sample). LDH is a cytosolic enzyme that is released due to cell death or damage.

3.5.2 Biochemical characterization of proximal tubules

Alkaline phosphatase (AP): AP activity was measured spectrophotometrically using Sigma Diagnostics Kit 104, based on the procedure of Bessey et al (1946). This assay is a quantitative colorimetric determination of AP and absorbance was measured on a Beckman DU® 530 Life Science UV/Vis spectrophotometer at 410 nm (10 mm cuvet). This procedure depends on the hydrolysis of p-nitrophenyl phosphate by the alkaline phosphatase enzyme yielding p-nitrophenol and inorganic phosphate. When made alkaline, p-nitrophenol is converted to a yellow complex that is readily measured at 400-420 nm. The intensity of the color is proportional to the phosphatase activity. For comparison purposes, AP activity was expressed in nmol p-nitrophenol liberated/min/mg protein.

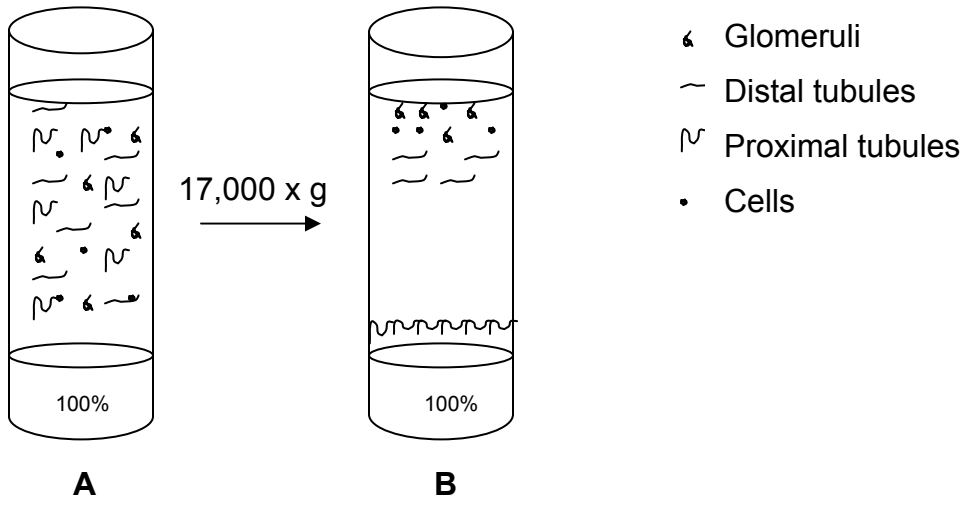

Figure 3.1. Schematic diagram of renal cortical tissue before and after Percoll density centrifugation. (A) Renal cortical tissue was resuspended in 30 ml of 45% Percoll solution with a 5 ml 100% Percoll cushion injected into the bottom of the tube. Before separation, all digested cortical tissue was equally distributed in the 45% Percoll solution. (B) Following centrifugation at 17,000 x g for 10 min. PTs formed a uniform layer above the 100% Percoll cushion. This layer was then removed by transfer pipette and represents the purified PTs used in uptake studies. Glomeruli, distal tubule (DT) fragments and individual cells were primarily found at the top of the Percoll gradient. The PT layer has minimal contamination by short DT fragments and individual cells as determined by enzymatic and visual characterization.

To determine AP content, 50 µl of sample or water (blank) was added to a tube containing 0.5 ml 221 alkaline buffer solution and 0.5 ml stock substrate solution (warmed to 37 º C) (see appendix for buffer and substrate composition), mixed and incubated for 5 min at 37 º C. After 5 min, 10 ml 0.05 N NaOH was added to each tube and mixed. Absorbance of the sample vs. blank was then read at 410 nm and AP units determined from a calibration curve. Four drops of concentrated HCl were then added to each tube (both sample and blank) and absorbance of sample vs. blank read at 410 nm and AP activity determined from the calibration curve. To determine the final value for AP activity, the AP activity value following HCl treatment was subtracted from the original AP activity value for each sample, yielding the corrected AP activity for each sample. This final

value was then multiplied 3x to account for using only a 5 min incubation rather than a 15 min incubation as directed by the assay protocol. This decreased incubation time was used because tubules had such high concentrations of AP.

Calibration curve for alkaline phosphatase:

1	2	3	4
Tube No.	Diluted p-Nitrophenol solution (mL)	NaOH 0.02 N (mL)	Alkaline Phosphatase Activity Sigma Units/mL
1	1.0	10.0	1.0
2	2.0	9.0	2.0
3	4.0	7.0	4.0
4	6.0	5.0	6.0
5	8.0	3.0	8.0
6	10.0	1.0	10.0

To create the calibration curve, the solutions indicated in columns 2 and 3 were pipetted into numbered tubes, and absorbance of each read immediately at 410 nm using 0.02 N NaOH as reference. The calibration curve was constructed by plotting absorbance vs. units in column 4.

Hexokinase (HK): Hexokinase activity was measured by the method of Joshi and Jagannathan (1966). This is a spectrophotometric kinetic assay measured at 340 nm. To determine the HK activity in IRPT samples, 0.1 ml of a 1 mg protein/ml IRPT suspension was mixed with 0.01 ml 10 % (v/v) Triton-X 100, 0.5 ml substrate solution, 0.5 ml NADP+, 2.88 µl G6PDH (at 600 units/ml), 7.12 µl H_2O, and 0.5 ml ATP in 10 mm pathlength 4.5 ml polystyrene disposable cuvette (see appendix for composition of all substrates and chemicals). The total reacting volume (1.62 ml) was then mixed and the change in absorbance was measured immediately for 3 min. The hexokinase assay is based on the following reactions:

$$\text{Glucose + ATP + } H_2O \longrightarrow \text{Glucose-6-phosphate + ADP + Pi}$$

$$\text{Glucose 6-phosphate + } NADP^+ \longrightarrow \text{6-phosphoglucose + NADPH + } H^+$$

Hexokinase activity was calculated as follows:

HK activity = A340 min^{-1}/ [6.22 x 10^3 $mol^{-1}L$)(10^3 ml^{-1})]x 10^9 nmol mol^{-1} x 16.2)

= 2604.5 nmol x Δ ABS/min

For comparison purposes activity was expressed in nmol $NADP^+$ reduced/min/mg protein.

Visual characterization*:* Visual appearance of isolated material was determined using a Nikon inverted Diaphot-TMD phase contrast microscope, with 100x magnification. Using a transfer pipette, a small amount of PT suspension was placed on a microscope slide and visualized for PT content following Percoll separation.

3.5.2 Protein content analysis- Bradford method

Protein content was measured by the Bradford (1976) method using bovine serum albumin (BSA) as the standard. To determine the amount of protein in initial IRPT isolates from Percoll separation, a 100 µl aliquot was removed and diluted in 400 µl H_2O in a glass Wheaton Tissuemizer. The PT suspension was homogenized and 25 µl of PT homogenate was analyzed for total protein content and calculated from a standard curve. Each 25 µl aliquot was placed in a 13x100 mm tube to which 25 µl of H_2O was added for a total reacting volume of 50 µl. Bradford reagent (2.5 ml) was then added to each tube, mixed on a vortex and allowed to incubate at room temperature. The remaining IRPT isolate from the Percoll separation was then diluted to a 1 mg protein/ml concentration with the appropriate amount of transport buffer for toxicity and uptake studies. The protein content in toxicity and uptake study samples was determined by analyzing either a 10 or 25 µl aliquot of IRPT

suspension from each flask and the amount of protein calculated from a standard curve, following a freeze thaw cycle of each sample to rupture the cell membranes. Each sample aliquot was brought to a final reacting volume of 50 µl with the appropriate amount of H_2O before the addition of Bradford reagent. The concentration curve was made using 1 and 2 mg protein/ml stock solutions of BSA. A 2 mg protein/ml solution of BSA was made by diluting 20 mg BSA/ 10 ml distilled H_2O and a 1 mg protein/ml solution was made by making a 1:1 dilution of a portion of the 2 mg protein /ml solution. Protein standards for the assay were prepared as described below (in duplicate) in 13x100 mm tubes:

Protein Stock	Volume stock	Volume water	Amount of Protein
2 mg/ml	30 µl	20 µl	60 µg
2 mg/ml	25 µl	25 µl	50 µg
2 mg/ml	20 µl	30 µl	40 µg
1 mg/ml	30 µl	20 µl	30 µg
1 mg/ml	20 µl	30 µl	20 µg
1 mg/ml	10 µl	40 µl	10 µg
1 mg/ml	5 µl	45 µl	5 µg

Bradford dye reagent (2.5 ml; see appendix for composition) was then added to each tube, mixed on a vortex and absorbance read at 595 nm using a Stasar III spectrophotometer (once mixed on a vortex, tubes were allowed to sit at room temperature for a minimum of 2 min, maximum of 1 hour). The absorbance of sample aliquots was measured in the same manner.

3.5.3 Lactate dehydrogenase (LDH) assay

LDH release was analyzed by a spectrophotometric kinetic assay (Sigma Diagnostics® Lactate dehydrogenase (LD-L) kit (procedure No. 228-UV) measured at 340 nm. This assay is based on the reaction:

$$\text{Lactate} + NAD^+ \underset{}{\overset{\text{LDH}}{\rightleftharpoons}} \text{Pyruvate} + NADH + H^+$$

Formation of NADH results in an increase in absorbance at 340 nm. The rate of increase in absorbance is directly proportional to LDH activity in the sample.

LDH release was assayed upon completion of enzymatic isolation of renal cortical tissue (pool sample), Percoll enrichment of cortical tissue (PT sample) or following incubation of IRPTs with a test compound. At this time, a 0.5 ml PT sample was taken and centrifuged to separate the "media" from "tissue" portion of the sample. The supernatant was decanted and reserved as the *media* sample. The remaining pellet (*tissue* sample) was homogenized in 1.0 ml of 10% Triton-X 100 to release intracellular LDH. The amount of LDH activity was then determined for both the tissue and media portions of the sample and LDH release into the media was expressed as percent of total.

3.6 Toxicity experiments in IRPTs

All toxicity experiments were conducted by placing 3-4 ml of tubule suspension in 25 ml polycarbonate Erlenmeyer flasks. Flasks were then placed in a shaking water bath incubator at 37ºC and sealed with a serum bottle stopper with an inlet and outlet for gas flow (95% O_2/5% CO_2). The atmosphere was equilibrated with shaking for 20 min in initial experiments but was shortened to 5 min in later experiments as shorter preincubations appeared to decrease variability between treatments. All assays were run in duplicate or triplicate depending on yield of tubule material.

3.6.1 Toxicity studies with acetaminophen (APAP), acetamidophenyl-β-D-glucuronide (AG), and diclofenac (DC)

Assays were run in duplicate for each treatment and time point. Toxicity was assessed by both increased lactate dehydrogenase (LDH) release and

alterations nucleotide levels (ATP, ADP, AMP). After preincubation, flasks containing 3.0 ml of PT suspension were treated with 30.0 µL distilled H_2O (control), 20 or 50mM APAP, AG or DC for a final concentration of 200 or 500 µM APAP, AG or DC. After addition of compound, oxygenation stoppers were replaced and shaking resumed at 100 rpm for 15, 30, or 60 min. At the end of each time point, 1.0 ml was removed for nucleotide analysis, and 0.5 ml removed and placed in a second 1.5 ml centrifuge tube for LDH analysis (as described in section 3.5.3).

3.6.2 Nucleotide (ATP, ADP, AMP) isolation

Following incubation with control (H_2O) or test compound 1.0 ml from each flask was removed and placed in a labeled 1.5 ml centrifuge tube and centrifuged for 10 min at maximum speed in a tabletop Sorvall Microspin centrifuge. The supernatant was discarded, and 300 µl 0.9% saline added to each pellet. Each pellet was mixed on a vortex to resuspend PTs and 50 µl removed for protein analysis. Perchloric acid (3M, 125 µl) was added to the remaining 250 µl of PTs in each sample tube and mixed on a vortex to precipitate proteins. Following addition of perchloric acid, sample tubes were kept on ice for 5 min, mixed on a vortex and centrifuged for 10 min at maximum speed. A 300 µl aliquot of supernatant was then removed from each sample tube, placed on ice in a clean, labeled 1.5 ml centrifuge tube, and the pH adjusted to approximately 7.0 with 6N KOH (volume of KOH recorded). All sample tubes were kept on ice for the duration of nucleotide isolation. Following pH adjustment the tubes were centrifuged for 10 min at 2000 x g in a Sorval MC12V centrifuge. The supernatant was prepared for HPLC analysis by filtration (Millipore HV .45 µm syringe filter) of 200 µl of supernatant, 200 µl distilled H_2O, and air pushed through the filter into a clean labeled 1.5 ml centrifuge tube. Each filtered sample was frozen at -80º C until analyzed.

Levels of ATP, ADP and AMP were determined using an HPLC method adapted from Lash et al. (1995). A 100 µl aliquot of extracted nucleotide sample was injected into a Beckman 126 model HPLC with a 100 µl injection loop. The mobile phase was a gradient of two solutions: Solvent A: 100 mM potassium phosphate, pH 6.0, and Solvent B: methanol. The gradient was 7.5 min at 100% A; 7.5 min linear gradient to 90% A; 15 min linear gradient to 75% A; 0.5 min linear gradient to 100% A and a 10 min re-equilibration at initial conditions. The flow rate of the mobile phase was 1.3 ml/min. The column was a Radial-Pak C18 cartridge (8 mm x 10 mm) (Waters Inc.; Milford, MA). The wavelength for detection was 254 nm. Adenine nucleotide concentrations were calculated from standard curves of ATP, ADP and AMP (0.94 - 9.4 nM), and expressed as nmol/mg protein.

Preparation of nucleotide standards:

Each standard sample for ATP, ADP and AMP was prepared in 1 ml of H_2O.

2.07 mg ATP (3.75 mM)

1.60 mg ADP (3.75 mM)

1.30 mg AMP (3.75 mM)

Each standard was diluted 1:10 for a final concentration of 0.376 mM. A final 1.0 ml standard of each was made by adding 250 µl of 1:10 dilution to yield a final standard concentration of 0.094 µmol/ml.

3.7 IRPT model characterization for organic anion transport (OAT)

Currently, there is limited quantitative information on the ability of the F344 rat kidney to transport classical organic anion transport (OAT) substrates. To verify that this model carried out organic anion transport, tubules were treated with various compounds that have been shown to be transported by the organic anion transporting proteins in the proximal tubular basolateral membrane in the kidney in other animal models. For these studies, the compounds selected to characterize this model were fluorescein (FL) (OAT 1 and 3), p-aminohippuric

acid (PAH) (OAT 1 and 3), and estrone sulfate (ES) (OAT 3). Both uptake and inhibition studies were conducted to show the presence and function of OAT in this system.

All uptake experiments were conducted by placing 3 ml (FL uptake experiments) or 4 ml (radioisotope experiments) of tubule suspension in 25 ml polycarbonate Erlenmeyer flasks. Flasks were then placed in a shaking water bath incubator at 37ºC and sealed with a serum bottle stopper with an inlet and outlet for gas flow (95% O_2/5% CO_2). The atmosphere was equilibrated with shaking for 20 min in initial FL experiments but was shortened to 5 min in later FL experiments as the longer time appeared to decrease variability between treatments. Preincubation for all radioisotope studies was carried out for 5 min. FL assays were conducted in duplicate or triplicate depending on tubule yield, and all radioisotope experiments were conducted in duplicate.

3.7.1 Accumulation and quantification of FL in IRPTs

Uptake and accumulation of 4 µM fluorescein (FL) in IRPTs was used to assess the presence and function of OAT transport in this model. Each experiment is described in detail following this section. This section primarily describes the quantification of FL content from each PT suspension sample following treatment.

In the experiments described in this section, to determine the amount of FL accumulation in IRPTs, 1.0 ml of PT suspension was removed from each flask at the end of the given time point and placed on ice in 5.0 ml ice cold Transport buffer #1 in a 15 ml centrifuge tube to stop FL uptake. PT suspension samples were immediately centrifuged at 2500 x g for 2 min. The supernatant from each sample tube was discarded and PT pellets were then rinsed again in 5 ml ice cold buffer and pellets frozen in an inverted position to allow excess buffer to drain from the PT material. PT pellets were ruptured either by freeze/thaw (frozen at – 20 º C for approximately 12 hours with subsequent addition of 1.5 ml

distilled water), or by homogenization with a Techmar Tissuemizer to release intracellular (cytosolic) FL. After disruption, material was centrifuged at 2500 x g for 5 min to pellet cellular debris. Cytosolic FL content in the supernatant was determined using a Perkin Elmer HTS 7000 bioassay fluorescence microplate reader (485 nm excitation, 538 nm emission). Triplicate 100 µl aliquots were taken from each sample and placed in a 96 well plate. To determine the FL content of each sample, samples were compared against standards of 4.0, 3.2, 2.4, 1.6, 0.8, 0.4, 0.2, and 0.0 µM FL and corrected for background untreated PT fluorescence. FL values were then converted to nmol/mg protein. An additional 1.0 ml was removed from each flask for protein determination using the Bradford (1976) method.

3.7.1.1 Time-dependent accumulation of FL in IRPTs

Time-dependent accumulation of FL was measured to assess the temporal aspects of OAT transport function in this model, and also to determine the best time points for subsequent assays. Following preincubation as previously described in section 3.6, 30 µl of 400 µM FL was added to each flask containing 3 ml of PT suspension for a final concentration of 4 µM FL. Tubules were then incubated at 37ºC in a shaking water bath (100 rpm) for 15, 30, 45, 60, and 120 seconds. At the end of each time point, samples were assayed for FL content as described in section 3.7.1.

3.7.1.2 The effect of temperature on FL accumulation in IRPTs

Temperature dependent accumulation of FL by IRPTs was used as a marker for active, carrier protein-mediated uptake along the tubular basolateral membrane in this model. Cellular transport of molecules requires temperatures closer to physiological levels (37ºC); accumulation of FL at cold temperatures (4ºC) will allow the distinction between basolateral protein-mediated transport,

and non-specific binding to tubular proteins or passive diffusion. Tubules were preincubated at either 4ºC or 37ºC. Following preincubation, 4 µM FL was added to each flask and incubated as previously described at 4ºC or 37ºC for 2 min. At the end of the 2 min incubation period, samples were assayed for FL content as described in section 3.7.1.

3.7.1.3 The effect of probenecid on FL accumulation in IPRTs and determination of the IC_{50} for probenecid accumulation in IRPTs

Probenecid is used as the typical inhibitor of organic anion transport (both OAT 1 and OAT 3) (Insel, 1996). To determine the effect of probenecid (and thus the contribution of OAT) on FL accumulation in this model, 3 ml of IRPTs at 1 mg protein/ml were incubated for 2 min at 37ºC in a shaking water bath (100 rpm) with 4 µM FL alone or co-incubated with 4 µM FL and 1 mM probenecid. At the end of the 2 min incubation period, samples were assayed for FL content as described in section 3.7.1.

To determine the inhibitory concentration that provides half maximal inhibition ($IC_{50)}$ for probenecid on FL accumulation in this model, 3 ml of IRPTs at 1 mg protein/ml were incubated for 2 min at 37ºC in a shaking water bath (100 rpm) in the presence of increasing concentrations of probenecid (5-250 µM). At the end of the 2 min incubation period, samples were assayed for FL content as described in section 3.7.1.

3.7.1.4 The effect of ouabain on FL accumulation in IRPTs

Ouabain is an inhibitor of the sodium/potassium ATPase, the energy driving force for OAT 1 transport along the basolateral membrane in renal PTs. To determine the effect of ouabain, and thus the contribution of OAT 1 to FL accumulation in this model, 3 ml of IRPTs at 1 mg protein/ml were incubated for 2 min at 37ºC in a shaking water bath (100 rpm) with 4 µM FL alone or in the

presence of 100 μM ouabain. Ouabain was added to tubules 10 min prior to the addition of FL to insure adequate inactivation of sodium/potassium ATPase. Due to the light sensitivity of ouabain, all incubations were conducted in the dark. At the end of the 2 min incubation period, samples were assayed for FL content as described in section 3.7.1.

3.7.1.5 The effect of benzylpenicillin (PG) on FL accumulation in IRPTs

PG has been shown to be a relatively selective inhibitor of rOAT3 (Hasegawa et al. 2002). To determine the contribution of OAT 3 in the accumulation of FL in this model, 3 ml of IRPTs at 1 mg protein/ml were incubated for 2 min at 37ºC in a shaking water bath (100 rpm) with 4 μM FL alone or in the presence of 1 mM PG. At the end of the 2 min incubation period, samples were assayed for FL content as described in section 3.7.1.

3.7.1.6 The effect of dehydroepiandrosterone sulfate (DHEAs) on FL accumulation in IRPTs

DHEAs has been demonstrated to be a substrate of OAT3 (Cha et al, 2001). To determine the contribution of OAT3 in the accumulation of FL in this model, 3 ml of IRPTs at 1 mg protein/ml were incubated for 2 min at 37ºC in a shaking water bath (100 rpm) with 4 μM FL alone or in the presence of 1 mM DHEAs. At the end of the 2 min incubation period, samples were assayed for FL content as described in section 3.7.1.

3.7.1.7 The effect of 4-acetamidophenyl-β-D-glucuronide (AG) on FL accumulation in IPRTs

To determine the ability of AG to interact at the site of FL transport in this model (presumably OAT1 and/or OAT3), 3 ml of IRPTs at 1 mg protein/ml were

incubated for 2 min at 37ºC in a shaking water bath (100 rpm) with 4 µM FL alone or in the presence of 500 µM AG. At the end of the 2 min incubation period, samples were assayed for FL content as described in section 3.7.1.

3.7.2 Accumulation and quantification of radioisotopes (^{14}C and ^{3}H) in IRPTs

To further characterize the uptake of typical OAT substrates in IPRTs, ^{14}C and ^{3}H radiolabeled substrates were used. The general method of test compound incubation and determination of isotope content of IRPTs following treatment is discussed in this section. Specific details of each uptake experiment are given in subsequent sections, but all analysis of radioisotope accumulation follow the same method as described in this section. Briefly, 25 ml polycarbonate flasks with 4 ml of 1 mg protein/ml PT suspension were preincubated for 5 min. A 1 ml aliquot was then removed for protein determination before addition of isotope. ^{14}C-*p*-Aminohippuric acid (PAH), ^{3}H-estrone-3-sulfate (ES), or ^{14}C-acetamidophenyl-β-D-glucuronide (AG), (approximately 0.1 - 0.2 µCi/ml) was added to each flask containing 3.0 ml of 1mg protein/ml IRPT suspension (see appendix for composition of stock and working solutions of radioisotopes). In each individual experiment, isotope concentrations vary slightly due to variation in the mixing of new working isotope solutions. Each working solution was made from stock isotope solutions and counted for radioactivity, and concentration calculated before use in each experiment. Tubules were incubated at 37º C in a shaking water bath (180 rpm) (specific time points given in experiment description). At the end of each time point, 5.0 ml ice cold transport buffer was added to each flask to stop uptake. Flasks were decanted into 15 ml centrifuge tubes and each flask was rinsed with an additional 5 ml cold buffer, and this rinse was added to initial 8.0 ml before centrifugation. PT suspensions were then centrifuged for 1 min at 7500 rpm in a IEC Centra CL2 Centrifuge. Tubule pellets were rinsed 2x in 5 ml ice cold transport buffer, resuspended in 1.0 ml of distilled H_2O and homogenized with a Teckmar Tissuemizer. Radioactivity of the total 1

ml IRPT homogenate (in two 0.5 ml aliquots) was then determined by liquid scintillation counting on a Wallac 1409 Liquid Scintillation Counter (LSC). Each 0.5 ml aliquot was placed in a 5 ml plastic scintillation vial, to which 5 ml of Scintiverse II were added. Each vial was labeled and mixed on a vortex before being analyzed. Untreated tubules were used to correct for background activity. Untreated tubules were prepared in the same manner as those treated with radioisotopes. Untreated tubules (1 ml) were homogenized and two 0.5 ml aliquots were used for "blank" measurements on the LSC for each experiment.

3.7.2.1 The effect of probenecid on PAH accumulation and the determination of the IC_{50} for probenecid on PAH accumulation in IRPTs

Accumulation of ^{14}C-PAH by IRPTs was used as a marker for basolateral OAT1 and OAT3 uptake in this model. Three milliliters of tubule suspension were incubated at 37ºC for 2 min with 73.8 µM ^{14}C-PAH (0.2 µCi/ml) alone, or in the presence of 1 mM probenecid. IRPT samples were then prepared and analyzed for ^{14}C-PAH content as described in section 3.7.2.

To determine the IC_{50} value for probenecid inhibition of PAH in this model, 3 ml of tubule suspension were incubated at 37ºC for 2 min with 4.5 µM ^{14}C-PAH (0.24 µCi/ml) in the presence of increasing concentrations of probenecid; 25, 50, 100, 150, and 250 uM. IRPT samples were then prepared and analyzed for ^{14}C-PAH content as described in section 3.7.2

3.7.2.2 The effect of AG on PAH accumulation in IRPTs

Inhibition of ^{14}C-PAH accumulation by AG was evaluated to assess the interaction of AG at the site of basolateral PAH transport (OAT1 and OAT3) in this model. Three milliliters of tubule suspension were incubated for 30 seconds with 2.5 µM ^{14}C-PAH (0.13 µCi/ml) alone, or in the presence of 1 mM AG. The concentration of PAH used in this experiment was minimized to maximize the

potential for reaction at the transport site for PAH. Since PAH is such a good substrate for OAT1 and OAT3, to determine whether AG could interfere with PAH at the site of transport, the minimum amount of PAH was used so as to maximize the effect of AG in competing for potential transport sites. IRPT samples were then prepared and analyzed for ^{14}C-PAH content as described in section 3.7.2.

3.7.2.3 The effect of testosterone glucuronide (TG) and methylumbelliferyl glucuronide (MUG) and AG on PAH accumulation in IRPTs

Inhibition of ^{14}C-PAH accumulation in IRPTs by TG and MUG was investigated to evaluate the interaction of additional glucuronide metabolites at the site of basolateral PAH transport (OAT 1 and 3) in this model. The effect of AG on^{14}C-PAH accumulation was also determined in this experiment as an additional control for the effects of TG and MUG (i.e. do all three glucuronides appear to have the same or different effects on PAH accumulation). Tubule suspensions (3 ml at 1 mg protein/ml) were incubated at 37ºC for 30 seconds with 4.4 µM ^{14}C-PAH (0.23 µCi/ml) alone, or in the presence of 500 µM TC, MUG or AG. A higher concentration of PAH was used in this experiment to assure consistant counting results on the LSC. Lower concenterations used in previous experiments often resulted in less consistant LSC results. IRPT samples were prepared and analyzed for ^{14}C-PAH content as described in section 3.7.2.

3.7.2.4 The effect of temperature on ES accumulation in IRPTs

Temperature dependent accumulation of ^{3}H-ES by IRPTs was used as a marker for active, protein-mediated OAT3 uptake in this model (Sweet et al., 2003). Cellular transport of molecules requires temperatures closer to physiological levels (37ºC); accumulation of ES at cold temperatures (4ºC) will allow distinction between basolateral protein-mediated transport, and non specific binding to tubular proteins or passive diffusion. Three milliliters of tubule

suspension were incubated at 4ºC or 37ºC for 60 seconds with 4 pM ^{3}H-ES (0.2 µCi/ml). IRPT samples were then prepared and analyzed for ^{3}H-ES content as described in section 3.7.2.

3.7.2.5 The effect of probenecid on ES accumulation in IRPTs

Accumulation of ^{3}H-ES by IRPTs was used as a marker for OAT 3 uptake along the basolateral membrane in this model. Three milliliters of tubule suspension were incubated at 37ºC for 30 seconds with 4 pM ^{3}H-ES (0.18 µCi/ml) alone or in the presence of 1mM probenecid. IRPT samples were then prepared and analyzed for ^{3}H-ES content as described in section 3.7.2

3.7.2.6 The effect of self-inhibition on ES accumulation in IRPTs

Inhibition of ^{3}H-ES accumulation by unlabeled (cold) ES was examined to assess whether basolateral uptake was a carrier protein-mediated transport process in this model, versus passive diffusion or other means of cellular accumulation. Ability of a compound to “self inhibit” accumulation indicates that the compound is taken into the tubules by carrier-mediated transport mechanisms. Three milliliters tubule suspension were incubated at 37ºC for 60 seconds with 4 pM ^{3}H-ES (0.2 µCi/ml) alone, or in the presence of 500 µM ES. IRPT samples were then prepared and analyzed for ^{3}H-ES content as described in section 3.7.2

3.7.2.7 The effect of AG on ES accumulation in IRPTs

Inhibition of ^{3}H-ES accumulation by AG was explored to assess the interaction of AG at the site of ES transport (OAT3) in this model. Three milliliters of tubule suspension were incubated at 37ºC for 60 seconds with 4 pM ^{3}H-ES (0.18 µCi/ml) alone or in the presence of 1 mM AG. The concentration of

ES used in this experiment was minimized to maximize the potential for reacting at the transport site for ES. IRPT samples were then prepared and analyzed for ^{3}H-ES content as described in section 3.7.2.

3.8 ^{14}C-Acetamidophenyl-β-d-glucuronide (AG) accumulation studies in IRPTs

AG was selected as a model glucuronide to determine whether IRPTs demonstrated accumulation of glucuronide metabolites. Due to its commercial availability, and because it was available in a radiolabeled form, AG was selected as a model glucuronide. To determine whether IRPTs facilitate glucuronide accumulation, various experiments, as described in subsequent sections, were conducted to determine the role of the basolateral membrane in the renal secretion of AG. Experiments were designed to determine whether the basolateral membrane demonstrated carrier protein-mediated transport of AG, and more importantly, whether AG interacts with OAT proteins along the basolateral membrane.

3.8.1 Time-dependent accumulation of AG in IRPTs

To determine if there was a temporal factor for the accumulation of ^{14}C-AG in this model, 3 ml of tubule suspension were incubated at 37ºC for 15, 30, 45, 60, 120 or 300 seconds with 4.5 µM ^{14}C-AG (0.22 µCi/ml). IRPT samples were then prepared and analyzed for ^{14}C-AG content as described in section 3.7.2. Temporal studies also allowed for the determination of the best time points for further uptake and inhibition studies to be conducted using ^{14}C-AG.

3.8.2 The effect of temperature on AG accumulation in IRPTs

Temperature dependent accumulation of ^{14}C-AG was used as a marker for active, carrier protein-mediated uptake of AG along the tubular basolateral membrane in this model. Accumulation of ^{14}C-AG at cold temperatures (4ºC) will allow distinction between basolateral carrier protein-mediated transport, and non-specific binding to tubular proteins or passive diffusion. Three milliliters of tubule suspension were incubated at 4ºC or 37ºC for 30 seconds with 2 µM ^{14}C-AG (0.1 µCi/ml). IRPT samples were then prepared and analyzed for ^{14}C-AG content as described in section 3.7.2.

3.8.3 The effect of probenecid on AG accumulation on IRPTs

To determine whether basolateral OAT proteins played a role in AG accumulation in this model, probenecid, the classical OAT inhibitor, was used to determine whether accumulation of AG could be inhibited. Three milliliters of tubule suspension were incubated for 30 seconds with 2 µM ^{14}C-AG (0.1 µCi/ml) (30 µl of ^{14}C-AG at 10 µCi/ml) alone or in the presence of 1mM probenecid. Probenecid was added at the same time as AG, or added 5 min prior to the addition of AG. IRPT samples were then prepared and analyzed for ^{14}C-AG content as described in section 3.7.2.

3.8.4 The effect of self-inhibition on AG accumulation in IRPTs

To determine whether basolateral carrier-mediated transport mechanisms played a role in ^{14}C-AG accumulation in this model, self-inhibition studies were conducted to determine whether unlabeled (cold) AG could inhibit the uptake of ^{14}C-AG by IRPTs. Three milliliters of tubule suspension were incubated for 30 seconds with 4.5 µM ^{14}C-AG (0.22 µCi/ml) alone, or in the presence of 5 mM AG. IRPT samples were then prepared and analyzed for ^{14}C-AG content as described in section 3.7.2

3.8.5 The effect of ES on AG accumulation in IRPTs

Inhibition of ^{14}C-AG accumulation by ES in this model was examined to determine whether a known substrate of OAT3 could effectively act as an inhibitor of AG accumulation in this model. This study was used to elucidate the role of OAT3 in AG uptake in this model. Three milliliters of tubule suspension were incubated for 30 seconds with 4.5 μM ^{14}C-AG (0.22 μCi/ml) alone, or in the presence of 100 μM ES. IRPT samples were then prepared and analyzed for ^{14}C-AG content as described in section 3.7.2.

3.8.6 The effect of D-saccharic acid 1,4-lactone on AG accumulation in IRPTs

Since IRPTs still have metabolic capabilities, including the deconjugation of glucuronide metabolites by β-glucuronidase, it was important to determine whether accumulation of ^{14}C-AG was being affected by the presence of β-glucuronidase in the tubule preparation. To assure that accumulation of AG was due to the conjugate, D-saccharic acid 1,4-lactone (SL) was used as an inhibitor of β-glucuronidase activity. Three milliliters of tubule suspension were incubated for 2 min with 4.5 μM ^{14}C-AG (0.21 μCi/ml) alone, or in the presence of 10 or 20 mM SL. Tubules were pre-incubated with SL for 5 min prior to the addition of ^{14}C-AG. IRPT samples were then prepared and analyzed for ^{14}C-AG content as described in section 3.7.2.

3.9 Western blot analysis for OAT1 and OAT3 in IRPTs and HK2 cells

3.9.1 Cell Fractionation

Plasma membrane fractions of immortalized human kidney (HK-2) cells were prepared from 7 day old monolayers scraped from T75 flasks or from Transwell membranes, pelleted at 270 x g and frozen. Cell pellets (HK-2 and F344 rat PTC)

were resuspended in homogenization buffer (HB; see appendix for composition), homogenized (15 slow strokes) and centrifuged (100 x g, 2 min) to remove intact cells. To separate membrane from cytosolic fractions, three different methods were used. The supernatants (whole cell lystes) were centrifuged at 100,000 x g for 1 hour at 4^{o}C (procedure provided by Dr. Mary Vore) to isolate crude membrane fractions or at 15,000 x g for 30 minute at 4^{o}C (Kikuchi et al., 2003) to isolate plasma membrane fractions. Proteins from the membrane pellets were extracted in HB containing 1% Triton-X 100 by frequent mixing on a vortex for 1 hour then tumbling overnight at 4^{o}C. The extracts were centrifuged for 30 minutes at 14,000 x g at 4^{o}C and the supernatants (membrane proteins) were assayed for protein content.

3.9.2 SDS-PAGE and Western Blot Procedure

Each sample was solubilized in loading buffer (4% sodium dodecyl sulfate, 62.6 mM Tris, 10% glycerol) with or without 5% 2-mercaptoethanol, loaded at 200-250 µg HK-2 protein/lane and 100 µg F344 rat or human protein/lane and separated by polyacrylamide gel electrophoresis on a 12.5% or 8% gel overnight at 4^{o}C (12.5% gel for 15 hours at 70 V; 8% gel for 15 hours at 74V). Proteins were transferred onto a nitrocellulose membrane, blocked with 5% nonfat dry milk in Tris-buffered saline containing 0.3% Tween 20 for 1 hour at 25^{o}C and incubated overnight at 4^{o}C with anti-ratOAT1 or OAT3 antibodies reported by the manufacturer to be specific for respective OATs and cross-reactive with the respective human orthologues (1:333, Alpha Diagnostics International). The bound antibody was detected on x-ray film by enhanced chemiluminescence with horseradish peroxidase-conjugated anti-rabbit IgG antibody. Buffer and gel formulations are recorded in the appendix.

3.10 Accumulation studies with OAT substrates in renal cortical slices (RCS)

Since IRPT isolation involves enzymatic digestion to release the tubules from the cortical tissue, there is the potential that this digestion could also damage the transport proteins along the basolateral membrane of the tubules. To determine whether enzymatic digestion had any consequence in the ability of IRPTs to demonstrate transport of both known OAT substrates and AG, renal cortical slices were used to study the accumulation of PAH, ES, and AG. Transport of these compounds was then compared to the findings in IRPTs to determine whether accumulation results were altered by enzymatic digestion of the basolateral membrane of the IRPTs.

3.10.1 Preparation of RCSs.

Rats were anesthetized with diethyl ether and tested for surgical anesthesia with toe pinch and corneal reflex. The abdomen was opened with a midline incision and the animal exsanguinated by rupturing the diaphragm and cutting the vena cava. The kidneys were removed, decapsulated and cut into quarters. Each quartered kidney was then placed in a 30 ml beaker containing 10 ml ice cold oxygenated Transport buffer #2 (see appendix for composition). The kidneys were kept on ice for the remainder of the slice preparation. Renal cortical slices were prepared free hand as previously described (Valentovic *et. al*. 1992) and placed in a clean 30 ml beaker containing 10 ml ice cold Transport buffer #2. To conduct uptake studies, slices were transferred with forceps into a 12 well cell culture plate in a shaking water bath incubator. Each well contained 3-4 slices (30-60 mg) in 1.0 ml of oxygenated Transport buffer #2 at 37ºC. Slices were allowed 5 min to equilibrate at 37º C at 100 rpm before the addition of test compound. Assays were conducted in duplicate at each concentration and time point.

3.10.2 Accumulation and quantification of radioisotopes (^{14}C and ^{3}H) in RCSs

This section describes the general method for analyzing uptake of radiolabeled substrates in RCSs. Details of specific experiments (time points and isotope concentrations) are provided in subsequent sections. This section also describes the method used in all experiments to determine the isotope content of treated slices.

At the end of each incubation period with a selected radioisotope, slices were removed from each assay well with forceps and placed in 2.0 ml of ice cold Transport buffer #2 in the corresponding well of a clean 12 well cell culture plate. This was done to both stop uptake of the radioisotope and to rinse excess radioisotope from the slices. After all slices were removed from the assay wells and transferred to rinse wells, the slices from each rinse well were removed and placed on a disk of heavy filter paper. Excess buffer was then removed from the slices by pressing slices between several discs of filter paper. The slices were removed from the filter paper and then weighed. Following weight determination the slices were transferred to labeled 13 x 100 mm glass tubes containing 1 ml H_2O and homogenized using a Teckmar Tissuemizer. Homogenates were divided into two 0.5 ml aliquots in 5 ml scintillation vials to count the total slice sample for each assay. Five milliliters of scintillation fluid (Scintiverse II) were added to each vial, mixed and analyzed for radioisotope content using a Wallac 1409 Liquid Scintillation Counter.

3.10.2.1 Time-dependent ^{3}H-Mannitol accumulation in RCS

Mannitol (MN) is not actively transported by any portion of the renal cortical slice. Thus, MN accumulation can be used to assess the amount of diffusion into interstitial spaces in the RCSs. Slices (30-60 mg) were incubated

at 37ºC for 10, 15, 30 or 60 min in the presence of 176 pM MN (0.3 µCi/ml). Slices were then prepared and analyzed for ^{3}H-MN content as described in section 3.10.2.

3.10.2.2 The effect of probenecid on PAH accumulation in RCSs

Inhibition of PAH accumulation by probenecid was studied to characterize the ability of this model to transport a classical OAT substrate, with inhibition by a the classical OAT transport inhibitor. Slices (30-60 mg) were incubated at 37ºC for 30 min with 4.7 µM ^{14}C-PAH (0.25 µCi/ml) alone or in the presence of 1 mM probenecid. Slices were then prepared and analyzed for ^{14}C-PAH content as described in section 3.10.2.

3.10.2.3 The effect of testosterone glucuronide (TG), methylumbelliferyl glucuronide (MUG) and acetaminophen glucuronide (AG) on PAH accumulation in RCSs

The ability of TG, MUG and AG to inhibit the accumulation of ^{14}C-PAH in renal cortical slices was evaluated to explore the interaction of glucuronide metabolites at the site of basolateral PAH transport (OAT1 and 3) in this model. Slices (30-60 mg in 1 ml Transport buffer #2) were incubated for 30 min with 4.7 µM ^{14}C-PAH (0.25 µCi/ml) alone or in the presence of 500 µM TG, MUG or AG. Slices were then prepared and analyzed for ^{14}C-PAH content as described in section 3.10.2.

3.10.2.4 Time-dependent accumulation of ES in RCSs

To determine the presence and function of OAT3 along the basolateral membrane of PTs in RCS, ES was chosen as the substrate for transport (Sweet et al, 2003). Time-dependent accumulation also allowed for assessment of OAT

transport function over time to determine the best time points for subsequent assays. Slices (30-60 mg) were incubated at 37ºC for 5, 10, 15, 30 and 60 min in the presence of 4 pM ^{3}H-ES (0.2 µCi/ml). Slices were then prepared and analyzed for ^{3}H-ES content as described in section 3.10.2.

3.10.2.5 The effect of temperature on ES accumulation in RCSs

To demonstrate that accumulation of ES in RCSs is via a carrier protein-mediated mechanism, temperature-dependent accumulation of ^{3}H-ES was assessed. Slices (30-60 mg) were incubated at 4ºC or 37ºC for 10 min with 4 pM ^{3}H-ES (0.2 µCi/ml). Slices were then prepared and analyzed for ^{3}H-ES content as described in section 3.10.2.

3.10.2.6 The effect of probenecid on ES accumulation in RCSs

Inhibition of ^{3}H-ES accumulation in RCS by probenecid was used to evaluate further the function of basolateral OAT3 transport in this model. Slices (30-60 mg) were incubated at 37ºC for 10 min with 4 pM ^{3}H-ES (0.2 µCi/ml) alone or in the presence of 1 mM probenecid. Slices were then prepared and analyzed for ^{3}H-ES content as described in section 3.10.2.

3.11 ^{14}C-acetamidophenyl-β-D-glucuronide (AG) accumulation studies in RCS

3.11.1 Time-dependent accumulation of AG in RCSs

To determine if there was a temporal factor for the accumulation of ^{14}C-AG in this model, slices (30-60 mg) were incubated at 37ºC for 2.5, 5, 15, 30, 45 or 60 min with 4.7 µM ^{14}C-AG (0.23 µCi/ml). Slices were then prepared and analyzed for ^{14}C-AG content as described in section 3.10.2.

3.11.2 The effect of temperature on AG accumulation in RCSs

Temperature-dependent accumulation of ^{14}C-AG was used as an indicator for active, protein-mediated uptake of AG along the tubular basolateral membrane in this model. Accumulation of ^{14}C-AG at cold temperatures (4ºC) will allow distinction between basolateral protein-mediated transport, and non-specific binding to tissue or passive diffusion. Slices (30-60 mg) were incubated at 4ºC or 37ºC for 30 min with 4.7 µM ^{14}C-AG (0.23 µCi/ml). Slices were then prepared and analyzed for ^{14}C-AG content as described in section 3.10.2.

3.11.3 The effect of probenecid on AG accumulation in RCSs

To determine whether OAT proteins along the basolateral membrane of RCS played a role in AG accumulation in this model, probenecid was used to determine whether accumulation of AG could be inhibited by a classical OAT inhibitor. Slices (30-60 mg) were incubated at 37ºC for 30 min with 4.7 µM ^{14}C-AG (0.23 µCi/ml) alone or in the presence of 1 mM probenecid. Slices were then prepared and analyzed for ^{14}C-AG content as described in section 3.10.2.

3.11.4 The effect of self-inhibition on AG accumulation in RCSs

To determine whether basolateral transport mechanisms played a role in ^{14}C-AG accumulation in this model, self-inhibition studies were conducted to determine whether unlabeled (cold) AG could inhibit the uptake of ^{14}C-AG. Slices (30-60 mg) were incubated at 37ºC for 30 min with 4.7 µM ^{14}C-AG (0.23 µCi/ml) alone or in the presence of 500 µM AG. Slices were then prepared and analyzed for ^{14}C-AG content as described in section 3.10.2.

3.11.5 The effect of PAH and ES on AG accumulation in RCSs

To explore further whether OAT plays a role in the accumulation of AG along the basolateral membrane of the PT in this model, known organic anion substrates of OAT1 and OAT3 were used as potential inhibitors of AG accumulation. Slices (30-60 mg) were incubated at 37ºC for 30 min with 4.7 µM ^{14}C-AG (0.23 µCi/ml) alone or in the presence of 1mM PAH or 500 µM ES. Slices were then prepared and analyzed for ^{14}C-AG content as described in section 3.10.2.

3.12 14C-AG accumulation studies in RCSs from male Sprague-Dawley rat

Several studies have reported contradicting results regarding the ability of the kidney to secrete glucuronide conjugates, namely AG (Duggin and Mudge, 1975, Galinsky and Levy, 1981, Watari et al, 1983, Morris and Levy, 1984 Heckman et al. 1986). Since these studies have been conducted in different animal models and strains, it was important to determine whether genetic strain had any influence in the ability to show basolateral transport of AG by the renal PT. The renal cortical slice model was chosen to assess renal transport of AG in the male SD rat. SD rats were chosen as an alternate rat strain because it was demonstrated by Galinsky and Levy (1981) that the SD strain appears to renally secrete AG.

The following studies were conducted and carried out as previously described for the corresponding studies conducted in RCSs from F344 rat at 4.3 µM ^{14}C-AG (0.21 µCi/ml):

3.12.1 The effect of temperature on AG accumulation in RCSs from SD rat (see section 3.11.2 for details on assay methods)

3.12.2 The effect of probenecid on AG accumulation in RCSs from SD rat (see section 3.11.3 for details on assay methods)

3.12.3 The effect of self-inhibition on AG accumulation in RCSs from S-D rat (see section 3.11.4 for details on assay methods)

3.12.4 The effect of PAH on AG accumulation in RCSs from S-D rat (see section 3.11.5 for details on assay methods)

3.13 Statistics

Values are expressed as the mean ± SE for 3-4 experiments. Values from each rat represent n=1. Data were analyzed using Non-linear Regression Analysis, Student t-test or One-Way Repeated Measures Analysis of Variance (ANOVA) followed by a Dunnett or Student-Newman-Keuls analysis. All statistical tests were run at 95% confidence interval, significance at $P<0.05$. Statistics were analyzed using Sigma Stat ® 2.03 statistical software (SPSS Inc., 1992-1997).

CHAPTER IV

Results

4.1 Studies Using Isolated Renal Proximal Tubules (IRPTs)

4.1.1 Characterization of Isolated Proximal Tubules

Since the renal PT is the primary site of drug transport and metabolism in the kidney, the first step of this study was to isolate renal PT segments from male F344 rats. Before the initiation of any toxicity or transport studies, it was necessary to characterize the isolated renal material to ensure that the tissue population that was isolated consisted primarily of PT fragments. Characterization of the PT fraction was carried out through enzymatic analysis and visual assessment. HK activity, AP activity, protein content and LDH release assays were conducted on the initial sample of digested cortical tissue containing tubules (pool sample) and on the enriched sample of tubules collected after Percoll separation (PT sample). HK and AP enzyme assays were used to assess the enrichment of the tubule sample. AP, which is a brush-border enzyme, was used as a marker for PT content. HK, a cytosolic enzyme with greatest activity in distal tubular cells was used as a marker for distal tubule contamination. Lash and Tokarz (1989) have reported PT fractions to have AP and HK activities of 403 $\pm$ 113 and 111 $\pm$ 48 nmol/min/mg protein respectively. Based on this information and assay results it was determined that the enriched proximal tubule (PT) samples isolated in these studies are of proximal tubular origin (Table 6). Viability was evaluated by measuring lactate dehydrogenase (LDH) release into the media and reported as a percent of total. LDH is a cytosolic enzyme and leakage from cells into the media can be correlated to sample viability (as percent LDH release increases, percent viability decreases).

Tubule viability for samples following Percoll separation was found to be approximately 89%, reported by percent LDH release in the range of 11.73 ± 0.91 (Table 6). These results indicated that the Percoll isolation procedure did not cause excessive damage to the tubule segments and they are adequate for toxicity and uptake studies. While it did not appear that the enzyme values changed significantly, the Percoll separation did effectively separate out any glomeruli and blood vessel tissue present in the pooled sample. Percoll density centrifugation provided a final PT sample that consisted primarily of proximal tubules with minimal distal tubule contamination. PT content was also observed microscopically as PTs were identified by their large diameter and unbranched morphology (Fig. 4.1). Based on morphological examination, there were a few distal tubules or collecting ducts (thin, straighter tubule segments) present in the sample and the major portion of the sample appeared to consist of PTs. Tubules appeared largely undamaged, although segments were shorter following Percoll separation and rinsing. No glomerular contamination was present in the PT sample based on microscopic examination.

Table 6. Biochemical characteristics of IRPTs from male F344 rat[a].

Parameter	Pool Sample	PT Sample
Protein content (mg protein/ml)	7.80 ± 0.23	7.62 ± 0.39
Cell viability		
LDH release (%)	4.84 ± 0.63	11.7 ± 0.91
Enzymes[b]		
Alkaline Phosphatase	521 ± 30.9	542 ± 26.9
Hexokinase	24.8 ± 1.94	22.6 ± 1.91

Note: a. All values are means ± SE of measurements from 8 rat preparations.

b. Enzyme results are total activity in nmol product per min, per mg protein.

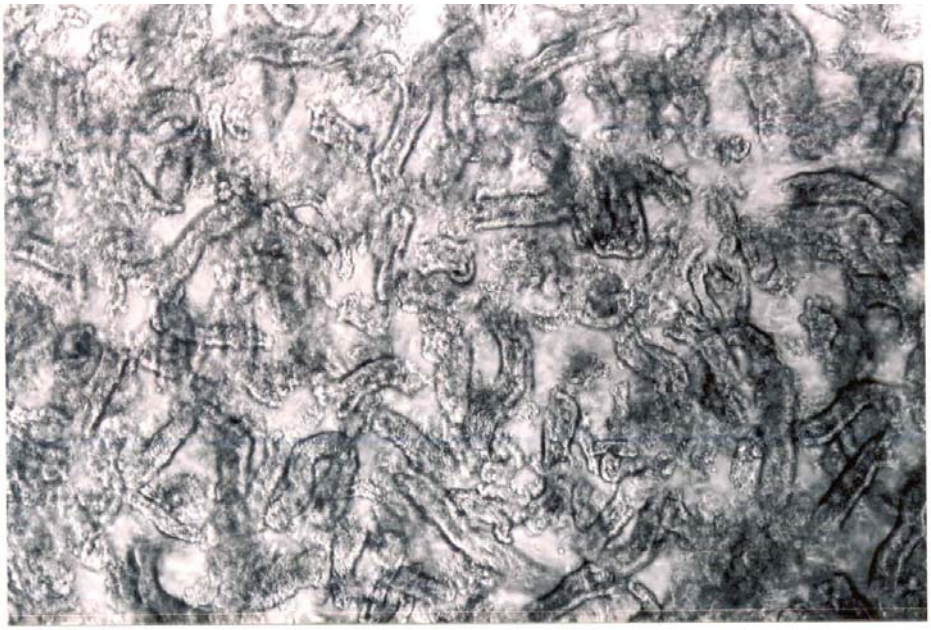

Figure 4.1. Freshly isolated renal proximal tubules from Fischer 344 rat. Tubules were isolated by collagenase digestion and enriched through Percoll density gradient centrifugation. The resulting isolated material consisted primarily of PT fragments as noted by their large diameter and unbranched morphology. Distal tubular contamination was minimal and no glomerular contamination was noted. Magnification 100x, Nikon inverted Diaphot-TMD phase contrast microscope.

4.1.2 Toxicity studies

Prior to conducting uptake studies it was necessary to ensure that the model compound (AG) was not toxic in this study system (IRPTs). Acetaminophen (APAP), the parent compound of AG, and diclofenac (DC) were also studied for toxicity since both of these compounds have been associated with nephrotoxicity. Additionally, DC is known to form an acyl-glucuronide metabolite. Toxicity was measured by LDH release from tubules incubated with 200 or 500 μM AG (Fig. 4.2), APAP (Fig 4.3) or DC (Fig 4.4). Incubations were carried out for 30 and 60 min for AG and APAP. DC studies were carried out for 15 and 30 min, as toxicity was already noted (by LDH release) by 30 min. These studies indicate that AG and APAP are not toxic at these concentrations or time points, and are therefore suitable for use in uptake studies in IRPTs. Since DC was found to be slightly toxic by 30 min it was not used in any future studies.

In addition to LDH release, nucleotide levels were also used to assess toxicity of AG, APAP and DC. Nucleotide levels were measured to determine whether tubules were not showing signs of toxicity at an earlier stage than could be detected by LDH release. Treatment with some chemicals may not trigger LDH release, but they may have a profound effect on the ability of a cell to produce energy in the form of ATP. To determine whether AG, APAP or DC had any intracellular toxic effects, following incubation of 3 ml of tubule suspension with 200 or 500 μM AG (Fig 4.5), and APAP (Fig. 4.6) for 30 or 60 min, or DC (Fig. 4.7) for 15 or 30 min, 1 ml of the tubule suspension was assayed for ATP, ADP, and AMP content. These studies indicate that AG and APAP do not show any early, toxic events at these concentrations or time points (i.e., no depressed production of nucleotides), and are therefore suitable for using in uptake studies in IRPTs. DC, however, was again found to be slightly toxic by 30 min as seen by depressed nucleotide levels. Toxicity studies at 15 min were also conducted with DC to determine whether depression of nucleotide levels might occur on an

earlier time frame than LDH release. Studies at 15 min demonstrate that while LDH release is not at significantly different levels than control, by this time point, ATP levels are already significantly decreased below control. This finding indicates that DC toxicity includes early cellular effects that occur before significant LDH release.

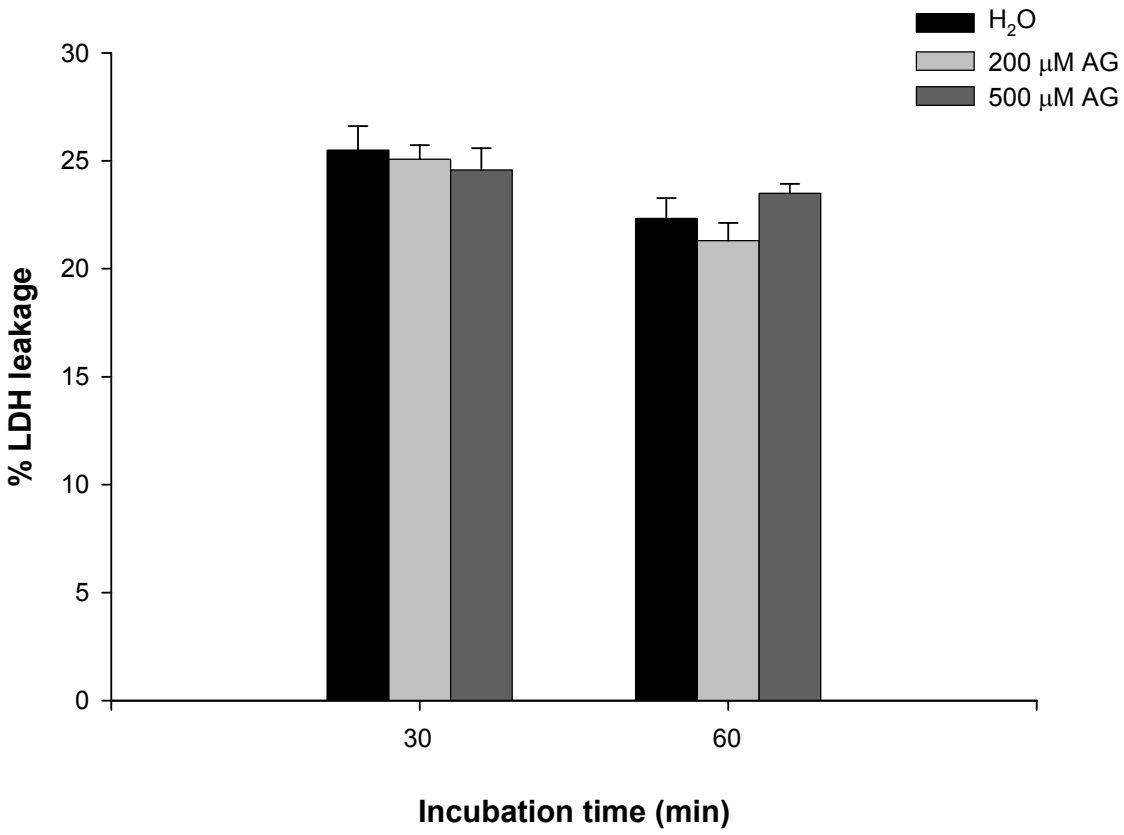

Figure 4.2. Percent LDH release from IRPTs treated with AG. To determine the toxicity of AG in IRPTs, 3 ml of tubule suspension (at 1 mg protein/ml) were incubated in the absence or presence of either 200 or 500 μM AG for 30 or 60 min. Separate flasks were used for each time point, and each concentration/time point was determined in duplicate. At the end of each time point, 1 ml of PT suspension was removed and assayed for LDH content. Each bar represents LDH release from the tubules into the incubation medium, and expressed as percent of total LDH ± SE for n=4. Percent LDH release by tubules treated with 200 or 500 μM AG was not significantly different from water treated tubules at either time point. LDH release was also not significantly different between time points for each concentration. Data were analyzed by Repeated Measures ANOVA.

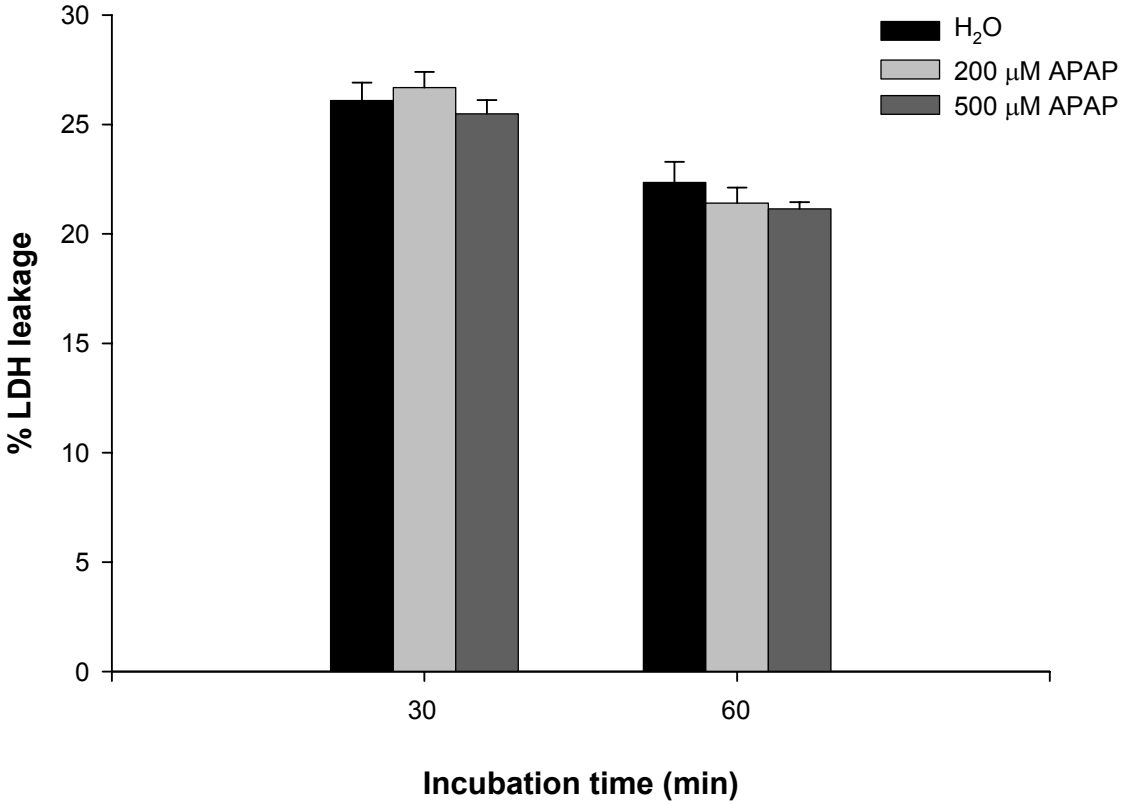

Figure 4.3. Percent LDH release from IRPTs treated with APAP. To determine the toxicity of APAP in IRPTs, 3 ml of tubule suspension (at 1 mg protein/ml) were incubated in the absence or presence of either 200 or 500 μM APAP for 30 or 60 min. Separate flasks were used for each time point, and each concentration/time point was determined in duplicate. At the end of each time point, 1 ml of PT suspension was removed and assayed for LDH content. Each bar represents LDH release from the tubules into the incubation medium, and expressed as percent of total LDH ± SE for n=4. Percent LDH release by tubules treated with 200 or 500 μM AG was not significantly different from water treated tubules at either time point. LDH release was also not significantly different between time points for each concentration. Data were analyzed by Repeated Measures ANOVA.

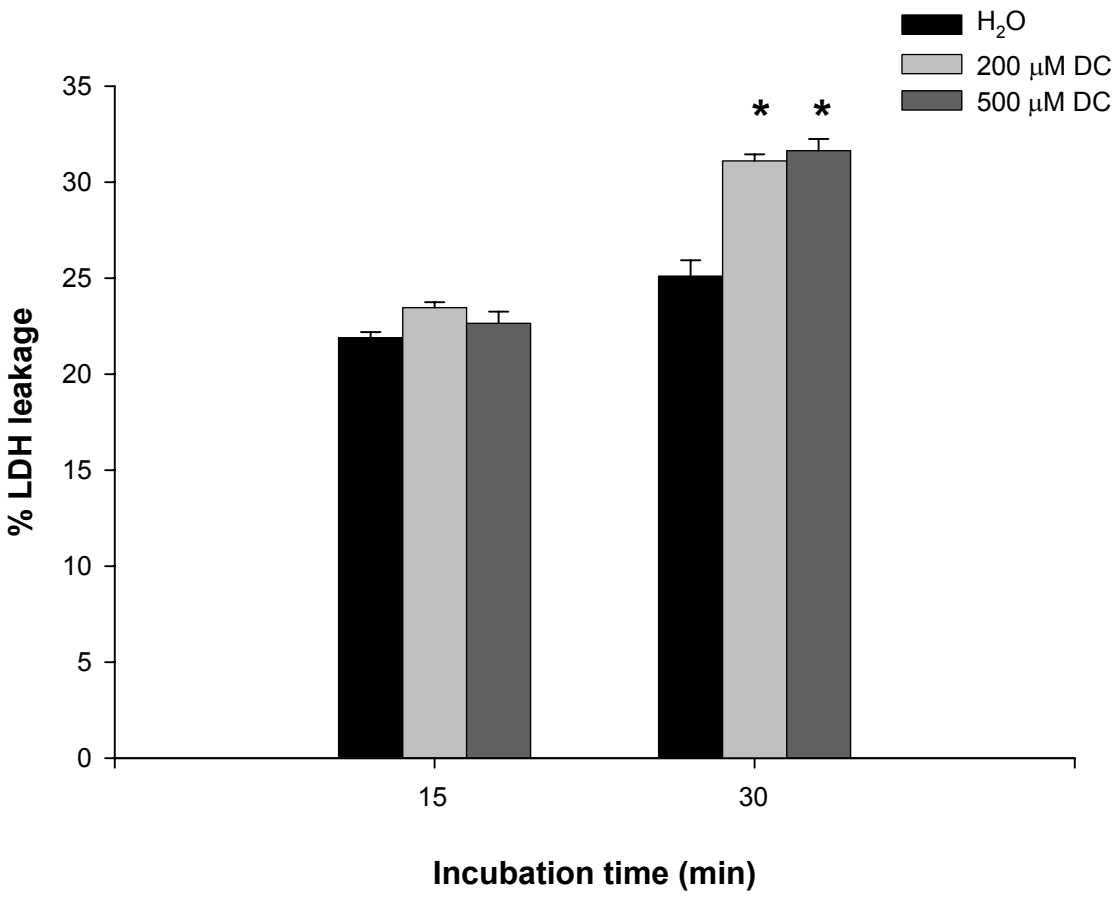

Figure 4.4. Percent LDH release from IRPTs treated with DC. To determine the toxicity of DC in IRPTs, 3 ml of tubule suspension (at 1 mg protein/ml) were incubated in the absence or presence of either 200 or 500 μM DC for 15 and 30 min. Separate flasks were used for each time point, and each concentration/time point was determined in duplicate. At the end of each time point, 1 ml of PT suspension was removed and assayed for LDH content. Each bar represents LDH release from the tubules into the incubation medium, and is expressed as percent of total LDH release ± SE for n=4 or 5. (* Percent LDH release significantly different from the appropriate control value ($P<0.05$)). Percent LDH release was significantly higher following DC treatment at 30 min. There was not a significant difference in LDH release between 200 and 500 μM DC at either time point. Data were analyzed by Repeated Measures ANOVA followed by Dunnett's analysis with a 95% confidence interval.

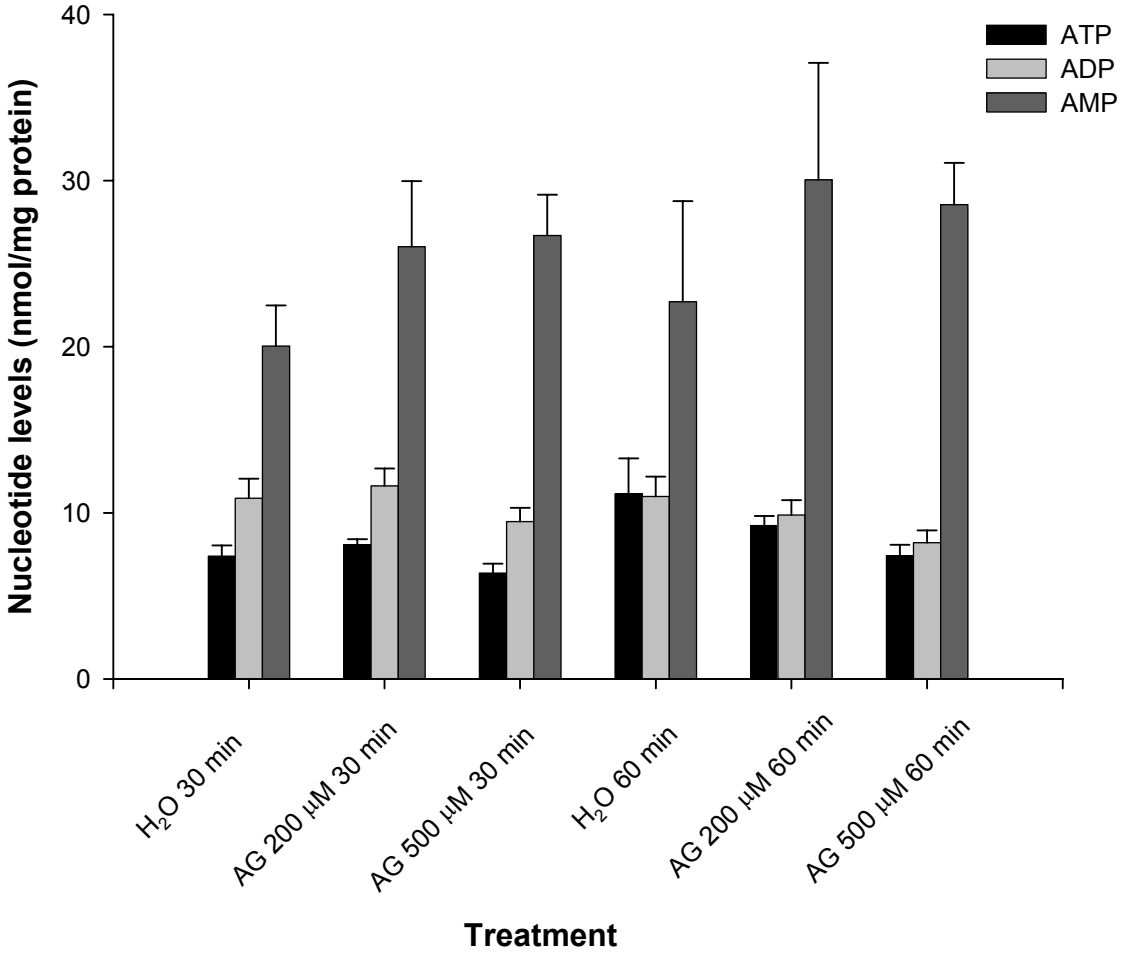

Figure 4.5. Effect of AG on nucleotide levels in IRPTs. To determine whether there may be earlier toxic events than LDH release associated with treatment of IRPTs with AG, nucleotide levels were determined after 30 and 60 min and used as a marker for tubular sensitivity to AG. Tubules (3 ml at 1 mg protein/ml) were treated in the absence or presence of 200 or 500 μM AG for 30 or 60 min. Separate flasks were use for each time point and each concentration/time point was measured in duplicate. At the end of each time point, each flask was sampled and ATP, ADP and AMP levels determined by HPLC for each sample. Each bar represents the mean nucleotide level (nmol/mg protein) ± SE for n=10 (30 min H_2O treatment), n=4 (60 min H_2O treatment) and n=4 (30 and 60 min AG treatments). No significant difference in nucleotide levels was determined for any AG concentration or time point for ATP, ADP or AMP as compared to control values. Data were analyzed by Repeated Measures ANOVA.

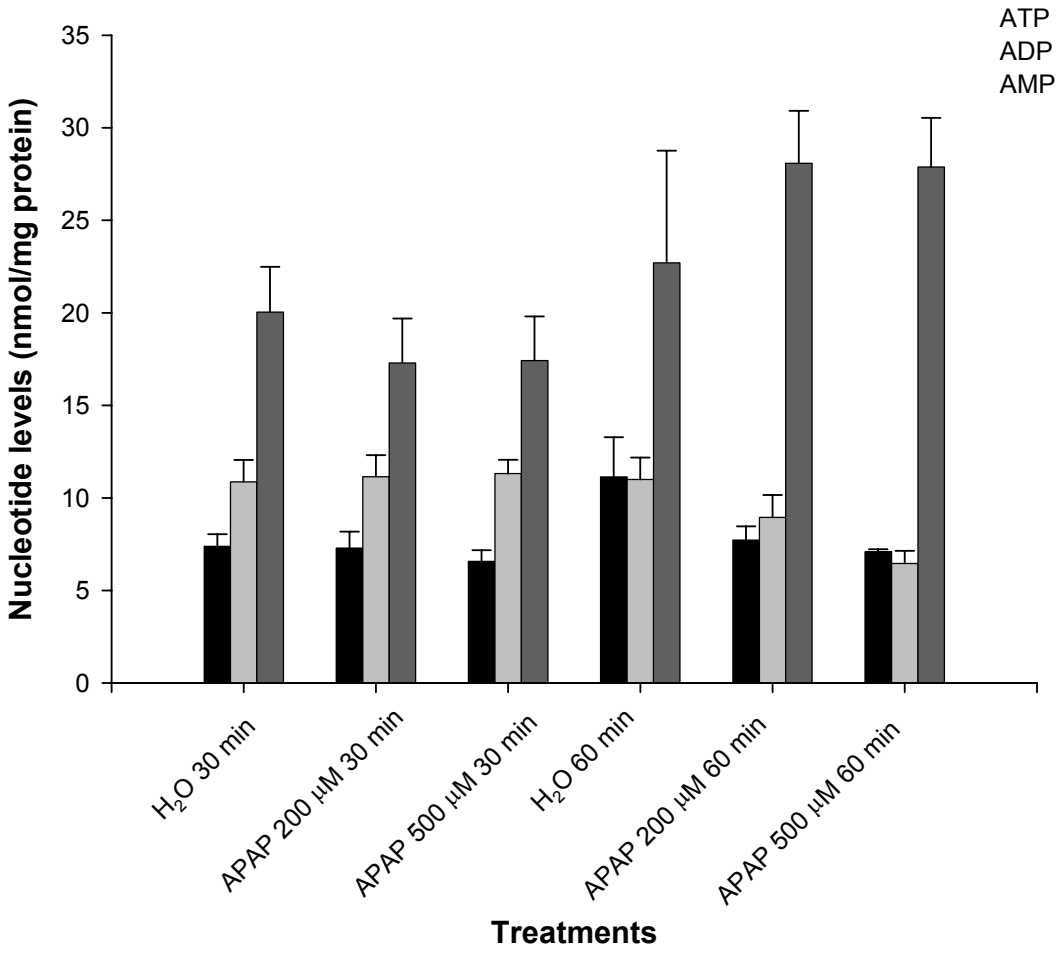

Figure 4.6. Effect of APAP on nucleotide levels in IRPTs. To determine whether there may be earlier toxic events than LDH release associated with treatment of IRPTs with APAP, nucleotide levels were determined after 30 and 60 min and used as a marker for tubular sensitivity to AG. Tubules (3 ml at 1 mg protein/ml) were treated in the absence or presence of 200 or 500 μM APAP for 30 or 60 min. Separate flasks were use for each time point and each concentration/time point was determined in duplicate. At the end of each time point, each flask was sampled and ATP, ADP and AMP levels determined by HPLC for each sample. Each bar represents the mean nucleotide level (nmol/mg protein) ± SE for n=10 (30 min H_2O treatment), n=4 (60 min H_2O treatment) and n=4 (30 and 60 min APAP treatments). No significant difference in nucleotide levels was determined for any APAP concentration or time point for ATP, ADP or AMP as compared to control values. Data were analyzed by Repeated Measures ANOVA.

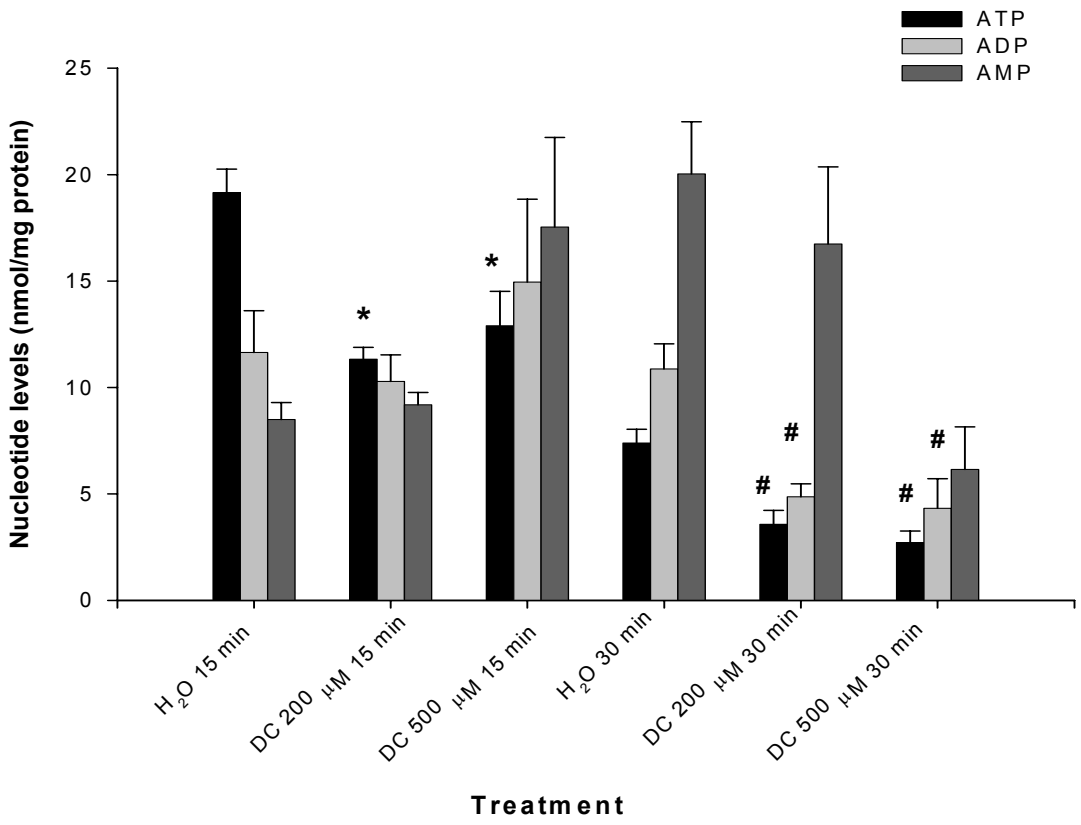

Figure 4.7. Effect of DC on nucleotide levels in IRPTs. To determine whether there may be earlier toxic events than LDH release associated with treatment of IRPTs with DC, nucleotide levels were determined after 15 and 30 min and used as a marker for tubular sensitivity to DC. Tubules (3 ml at 1 mg protein/ml) were treated in the absence or presence of 200 or 500 μM DC for 15 or 30 min. Separate flasks were use for each time point and each concentration/time point was determined in duplicate. At the end of each time point, each flask was sampled and ATP, ADP and AMP levels determined by HPLC analysis. Each bar represents the mean nucleotide level (nmol/mg protein) ± SE for n=4 (all 15 min treatments) n=10 (30 min H_2O treatment), and n=3 or 4 (30 min DC treatment). (* Significantly different from 15 min control (H_2O) levels $P< 0.05$)). ATP levels following DC treatment for 15 min were significantly lower than control ATP levels. ADP and AMP levels did not show a significant difference between control and DC treatment at 15 min. (# Signifncantly different from 30 min control (H_2O) levels ($P<0.05$)). ADP and ATP levels were both significantly lower than control levels following 30 min treatment with DC. AMP levels are not significantly different between control and DC treated. Data were analyzed by Repeated Measures ANOVA, followed by Dunnett's analysis with a 95% confidence interval.

4.1.3 Uptake studies

4.1.3.1 Fluorescein accumulation in IRPTs

Transport of organic anions by renal PTs of F344 rats has not been previously characterized. FL, a typical OAT1 and OAT3 substrate, has been used in numerous studies to assess the function of OAT transporters in various models. Thus, FL was used to study OAT function along the basolateral membrane of freshly isolated renal PTs from F344 rats. Based on studies conducted by Groves and Morales (1999) in suspensions of rabbit renal PTs, 4 μM was selected as the concentration of FL for uptake studies in this rat IRPT model. Temporal studies using IRPTs in the presence of 4μM FL revealed that FL is accumulated in IRPTs in a time-dependent manner (Fig. 4.8). Accumulation of FL appears steady up to 120 seconds. Time-dependent uptake, however, does not solely indicate uptake of FL by OAT proteins along the basolateral membrane. To characterize further OAT function in this model, various inhibition studies were conducted to determine whether accumulation of FL was a protein carrier-mediated process, and to further elucidate the contribution of OAT1 and OAT3 to FL accumulation.

To determine whether accumulation of FL along the basolateral membrane was via a protein carrier-mediated process, temperature dependent transport of FL was assessed. IRPTs were incubated with 4 μM FL at either 37ºC to allow protein-mediated transport, or at 4ºC to minimize protein-mediated transport. Tubules incubated with FL for 2 min revealed that at 4ºC, accumulation of FL was significantly lower than at 37ºC by approximately 93 % (Fig. 4.9). This reduction in basolateral uptake at 4ºC is consistent with transport mediated by a protein such as an organic anion transporter.

To characterize further the contribution of OAT along the basolateral membrane in IRPTs, inhibition of FL accumulation by probenecid was assessed.

Probenecid is the prototypical inhibitor of renal OAT (Insel, 1996), and should therefore inhibit FL uptake into IRPTs. To study the effect of probenecid on FL accumulation, tubules were incubated with 4μM FL in the presence or absence of 1 mM probenecid for 2 min (Fig. 4.10). Probenecid significantly inhibited FL accumulation along the basolateral membrane of IPRTs by approximately 86%. This reduction in basolateral uptake in the presence of probenecid is consistent with transport mediated by OAT proteins. To determine the IC_{50} value of probenecid for FL transport in the IRPT model, tubules were incubated with 4 μM FL for 2 min in the presence of increasing concentrations of probenecid (Fig. 4.11). The IC_{50} value was calculated from the non-linear regression equation to be approximately 67 μM in this model, with 250 μM probenecid yielding nearly maximal inhibition of FL accumulation (approximately 80%) in IRPTs.

Additional studies were conducted to further characterize FL accumulation in the F344 IRPT model. To help elucidate the role of OAT1 vs. OAT3 in FL accumulation along the basolateral membrane, various inhibitors were used that were selective for either OAT1 or OAT3. The first inhibitor used was the cardiac glycoside, ouabain. Ouabain directly inhibits the Na^+/K^+ ATPase which is known to drive OAT1 transport (Kelly and Smith, 1996). Tubules were incubated with 4 μM FL alone, or preincubated in the dark for 10 min with 100 μM ouabain, and then coincubated for 2 min with 4 μM FL, (Fig. 4.12). Ouabain significantly inhibited the basolateral accumulation of FL in IRPTs by approximately 51% suggesting a role for OAT1 in FL accumulation.

The effect of benzylpenicillin (penicillin G, PG) on FL accumulation along the basolateral membrane was assessed to elucidate the role of OAT3 in FL accumulation. PG is an OAT3-selective substrate for rOAT3 (Hasegawa et al., 2002). Tubules were incubated for 2 min with 4 μM FL in the presence or absence of 1mM PG (Fig. 4.13). PG significantly inhibited basolateral FL

accumulation in IRPTs by approximately 40%. The effect of PG on FL accumulation indicates that OAT3 also plays a role in FL transport in this model.

The effect of dehydroepiandrosterone sulfate (DHEAs) on FL accumulation along the basolateral membrane was also used to assess the potential role of OAT3 in FL accumulation. DHEAs is a substrate of OAT3 (Cha et al., 2000) and has been used in many models to study the function of OAT3 transport. To assess its value as a potential OAT3 inhibitor in this model, tubules were incubated with 4 μM FL in the presence or absence of 1 mM DHEAs (Fig. 4.14). DHEAs significantly inhibited basolateral FL accumulation in IRPTs by approximately 82%. The effect of DHEAs at this concentration indicates interaction with OAT1 and OAT3 as inhibition is comparable to that found for probenecid (86%).

To determine whether glucuronide metabolites interact with OAT transporters along the basolateral membrane of IRPTs, acetamidophenyl glucuronide (AG) was selected as a model glucuronide metabolite to assess whether it interacted with OAT proteins in this model. To determine whether AG interacted with OAT1 and OAT3, AG was used as a potential inhibitor of FL accumulation. If AG interacts with OAT proteins, it would cause inhibition of FL uptake by competition for the site of transport. Tubules were incubated for 2 min with 4 μM FL in the presence or absence of 1 mM AG (Fig. 4.15). AG did not cause significant inhibition (< 7%) of basolateral FL accumulation. This result indicates that AG does not appear to undergo transport via the same mechanisms (OAT1 and OAT3) as FL in this model. It may also indicate that AG is such a weak substrate for OAT that it does not have the ability to displace FL from the transporter protein (competitively inhibit FL binding).

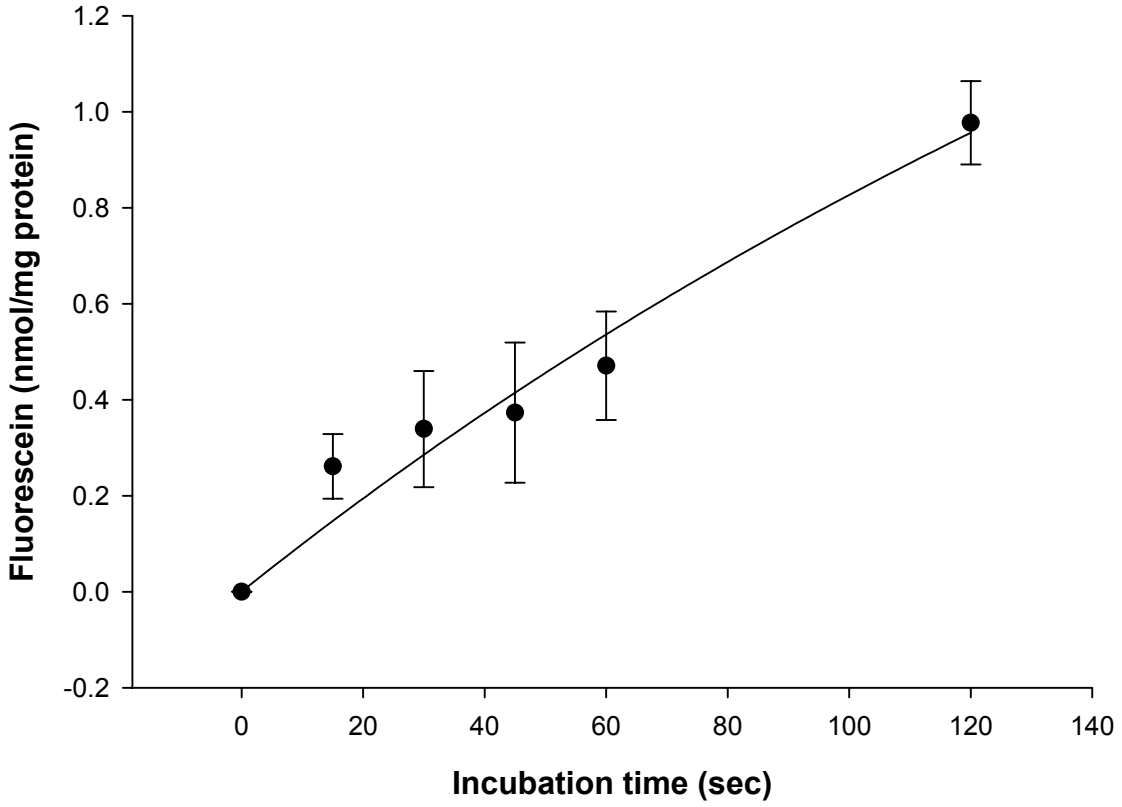

Figure 4.8. Time-dependent accumulation of FL in IRPTs. IRPTs were incubated at 1mg protein/ml in the presence of 4μM FL for 15, 30, 45, 60 and 120 sec. FL was added to each flask containing 3ml of tubule suspension (at 1 mg protein/ml) and incubated at 37ºC in a shaking water bath (100 rpm) under 95% O_2/5% CO_2. At the end of each assay, 1 ml of tubule suspension was removed from each flask and analyzed for tubular FL accumulation. Each point represents mean FL accumulation in nmol FL/mg protein ± SE for n=4. Data were analyzed by Nonlinear Regression analysis [(f=a*x/(b*x) ; a= 4.44, b= 436.73; r^2=0.96].

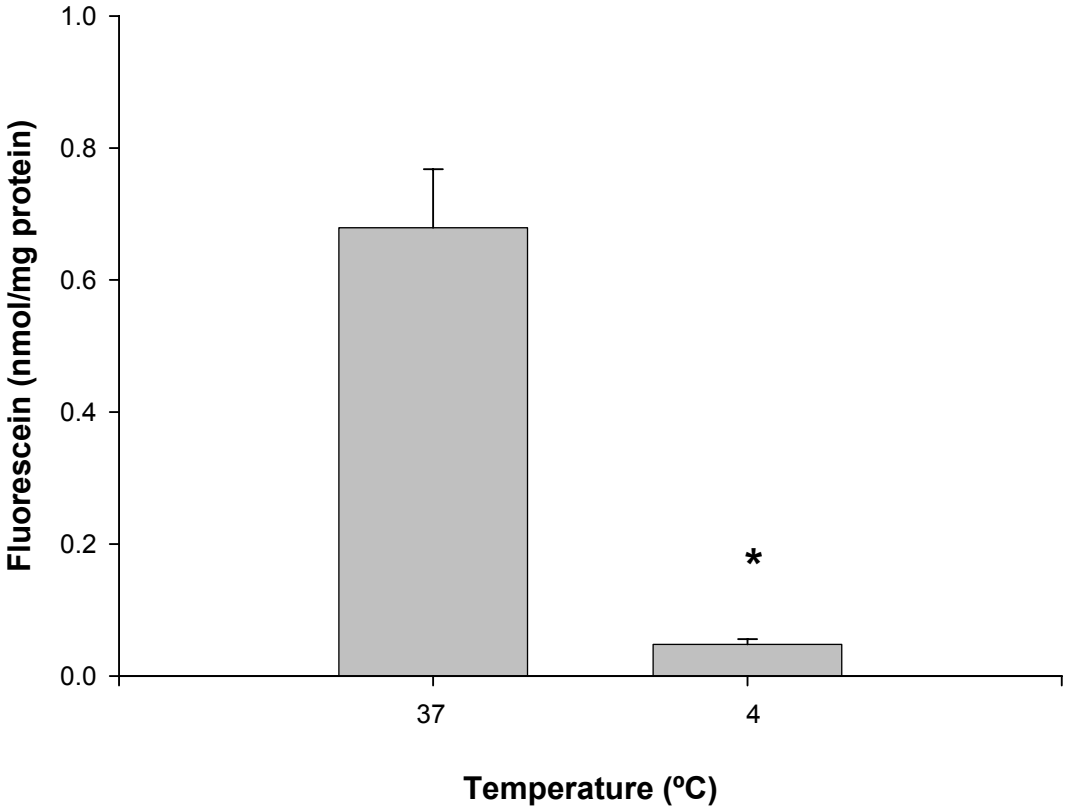

Figure 4.9. The effect of temperature on FL accumulation in IRPTs. To determine the effect of temperature on FL uptake in IPRTs, 3 ml of tubules (at 1 mg protein/ml) were incubated at 37ºC and 4ºC in the presence of 4 μM FL. FL was added to each flask of IRPT suspension and incubated for 2 min in a shaking water bath (100 rpm) under 95% O_2/5% CO_2. At the end of the assay, 1 ml of tubular suspension was removed from each flask and tubular FL accumulation determined. Each assay was run in triplicate. Bars represent mean FL content (nmol/mg protein) ± SE for n=4. (* Significantly different from control (37ºC) value). FL accumulation was significantly inhibited by incubation at 4ºC ($P<0.001$). Data were analyzed by Student's t-test, with a 95% confidence interval.

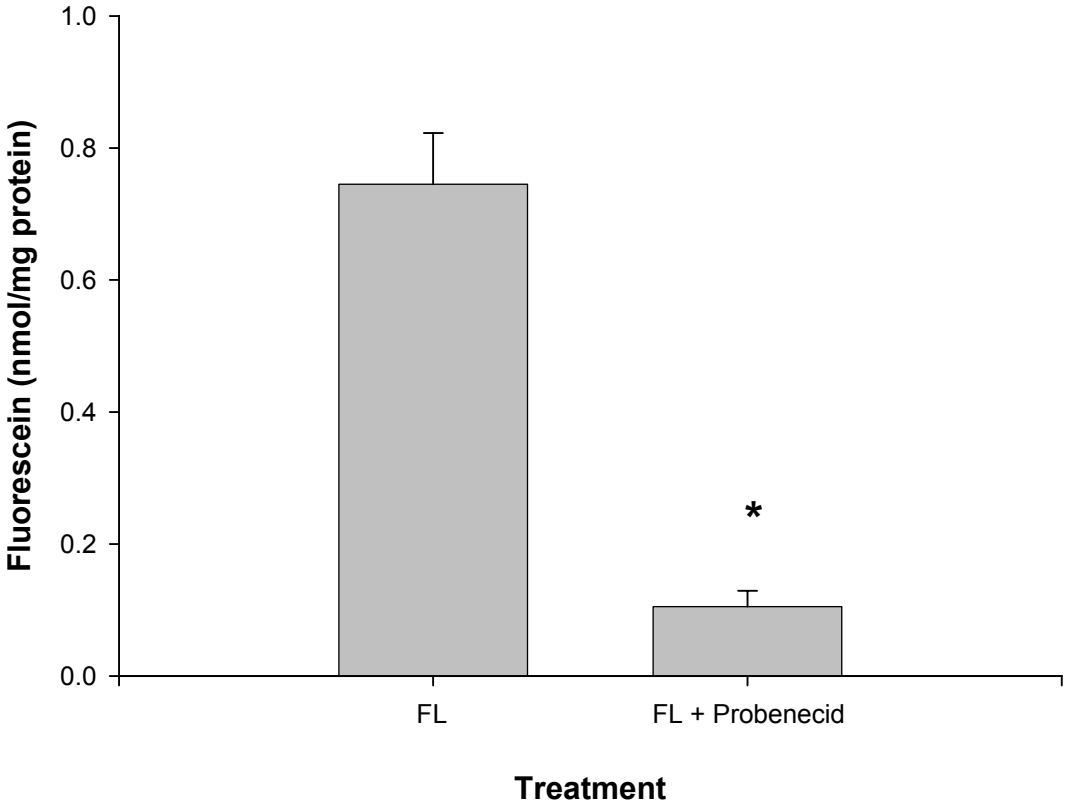

Figure 4.10. The effect of probenecid on FL accumulation in IRPTs. To determine the effect of probenecid on FL uptake in IPRTs, 3 ml of tubules (at 1 mg protein/ml) were incubated at 37ºC with 4 μM FL in the presence or absence of 1mM probenecid. Each flask containing IRPT suspension was incubated for 2 min in a shaking water bath (100 rpm) under 95% O_2/5% CO_2. At the end of the assay, 1 ml of tubular suspension was removed from each flask and tubular FL accumulation determined. Each assay was run in triplicate. Bars represent mean FL content (nmol/mg protein) ± SE for n=4. (* Significantly different from control (FL alone) treatment). FL accumulation in IRPTs was significantly inhibited by probenecid ($P<0.001$). Data were analyzed by Student's t-test, with a 95% confidence interval

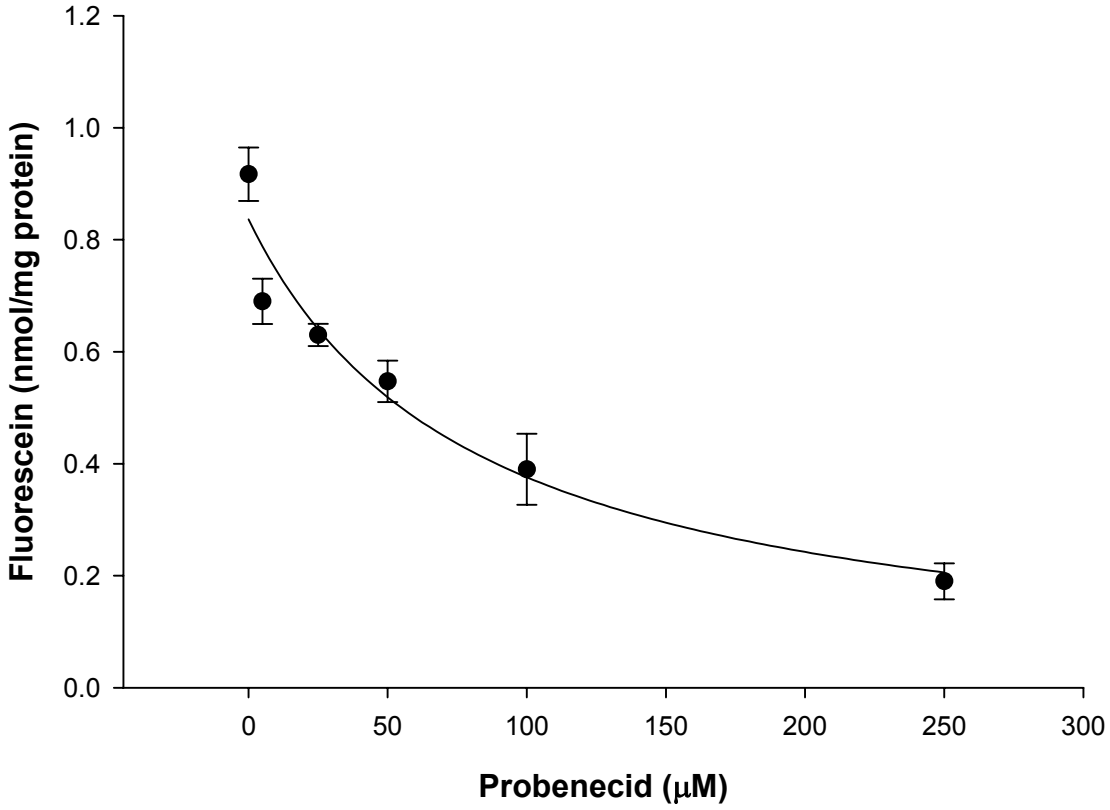

Figure 4.11. IC_{50} determination of probenecid for FL uptake in IRPTs. To determine the IC_{50} value of probenecid for FL uptake in IRPTs, 3 ml tubules (at 1 mg protein/ml) were incubated with 4 μM FL in the presence of increasing concentrations of probenecid. Each flask was incubated at 37 º C for 2 min in a shaking water bath (100 rpm). All assays were run in duplicate. At the end of each assay, 1 ml of tubular suspension was removed from each flask, and tubular FL accumulation determined. Probenecid concentrations used were 5, 25, 50, 100 or 250 μM. Each point represents mean FL content (nmol/mg protein) ± SE for n=3. Data were analyzed by Nonlinear Regression analysis. The IC_{50} value of probenecid for FL uptake in IPRTs was calculated from the nonlinear regression equation [(f=a*x/(b*x); r2=0.94] to be 67.4 μM.

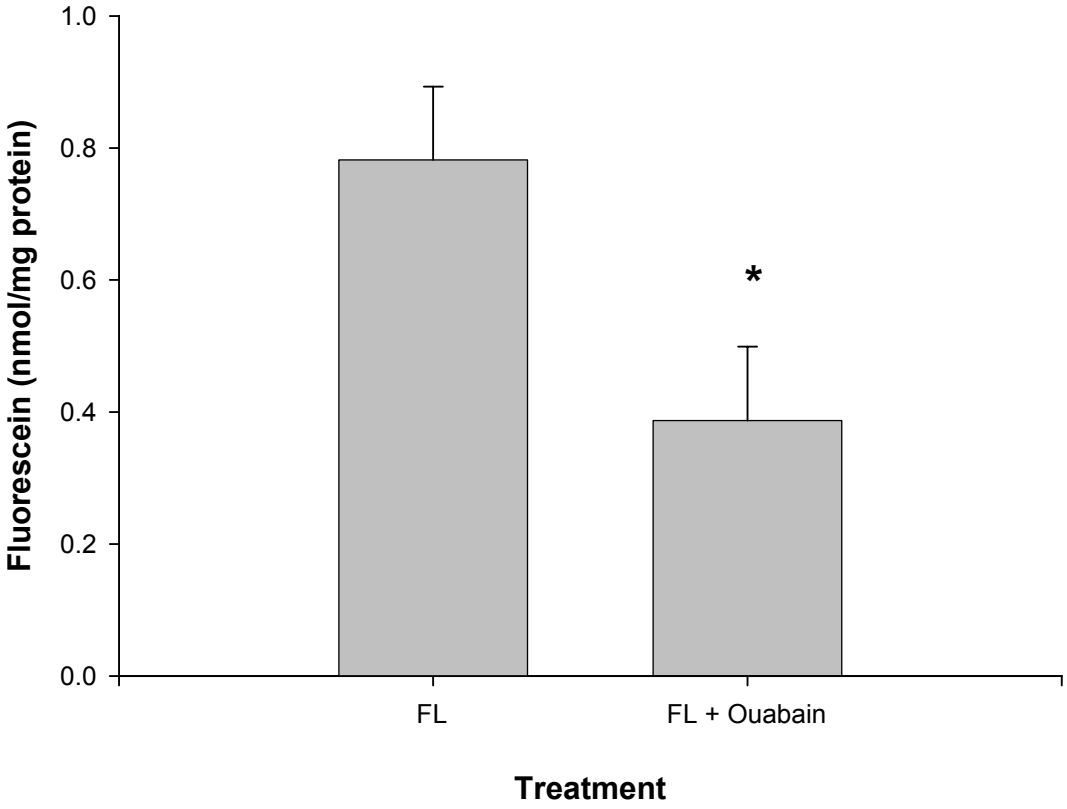

Figure 4.12. The effect of ouabain on FL accumulation in IRPTs. To determine the effect of ouabain on FL uptake in IPRTs, 3 ml of tubules (at 1 mg protein/ml) were incubated at 37ºC with 4 μM FL in the presence or absence of 100 μM ouabain. Each flask containing IRPT suspension was incubated for 2 min in a shaking water bath (100 rpm) under 95% O_2/5% CO_2. At the end of the assay, 1 ml of tubule suspension was removed from each flask and tubular FL accumulation determined. Each assay was run in triplicate. Bars represent mean FL content (nmol/mg protein) ± SE for n=4. (* Significantly different from control (FL alone) value). FL accumulation in IPRTs was significantly inhibited by ouabain ($P<0.05$). Data were analyzed by Student's t-test, with a 95% confidence interval.

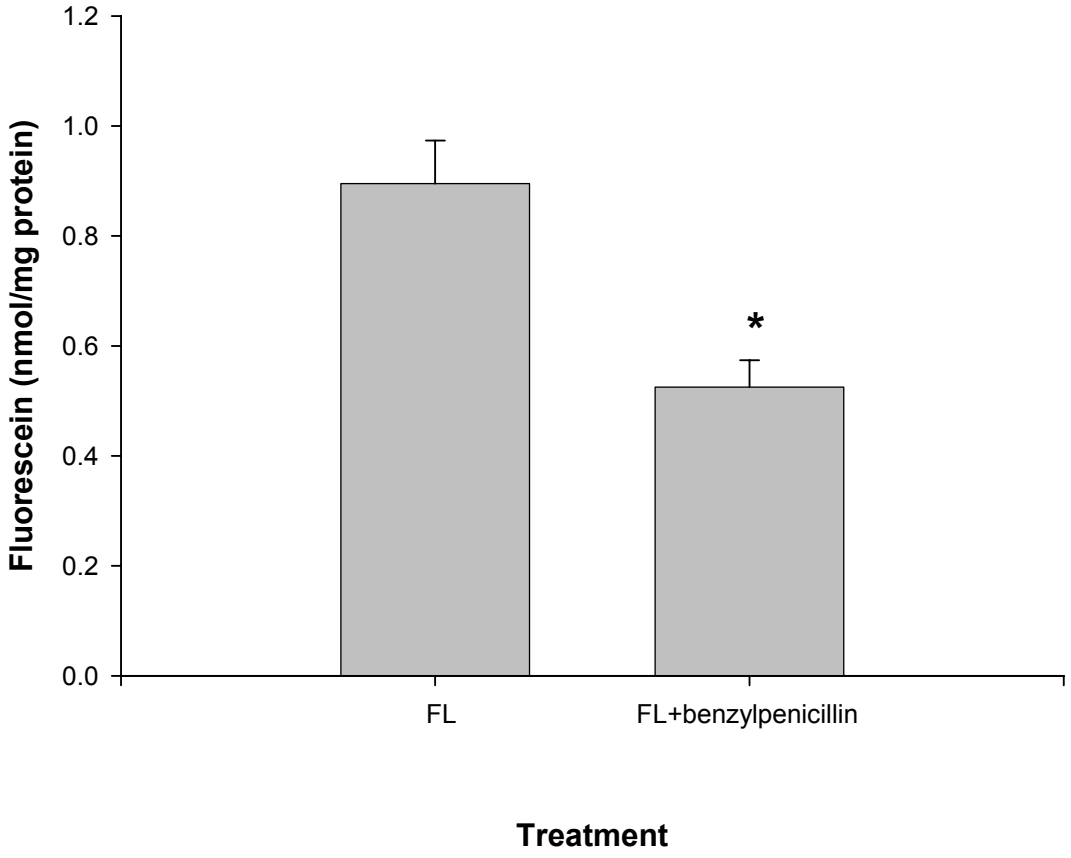

Figure 4.13. The effect of benzylpenicilin on FL accumulation in IRPTs. To determine the effect of benzylpenicillin on FL uptake in IPRTs, 3 ml of tubules (at 1 mg protein/ml) were incubated at 37ºC with 4 μM FL in the presence or absence of 1 mM benzylpenicillin. Each flask containing IRPT suspension was incubated for 2 min in a shaking water bath (100 rpm). At the end of the assay, 1 ml of tubule suspension was removed from each flask and tubular FL accumulation determined. Each assay was run in triplicate. Bars represent mean FL content (nmol/mg protein) ± SE. n=4. (* Significantly different form control (FL alone) values). FL accumulation in IPRTs was significantly inhibited by benzylpenicillin ($P<0.05$). Data were analyzed by Student's t-test, with a 95% confidence interval.

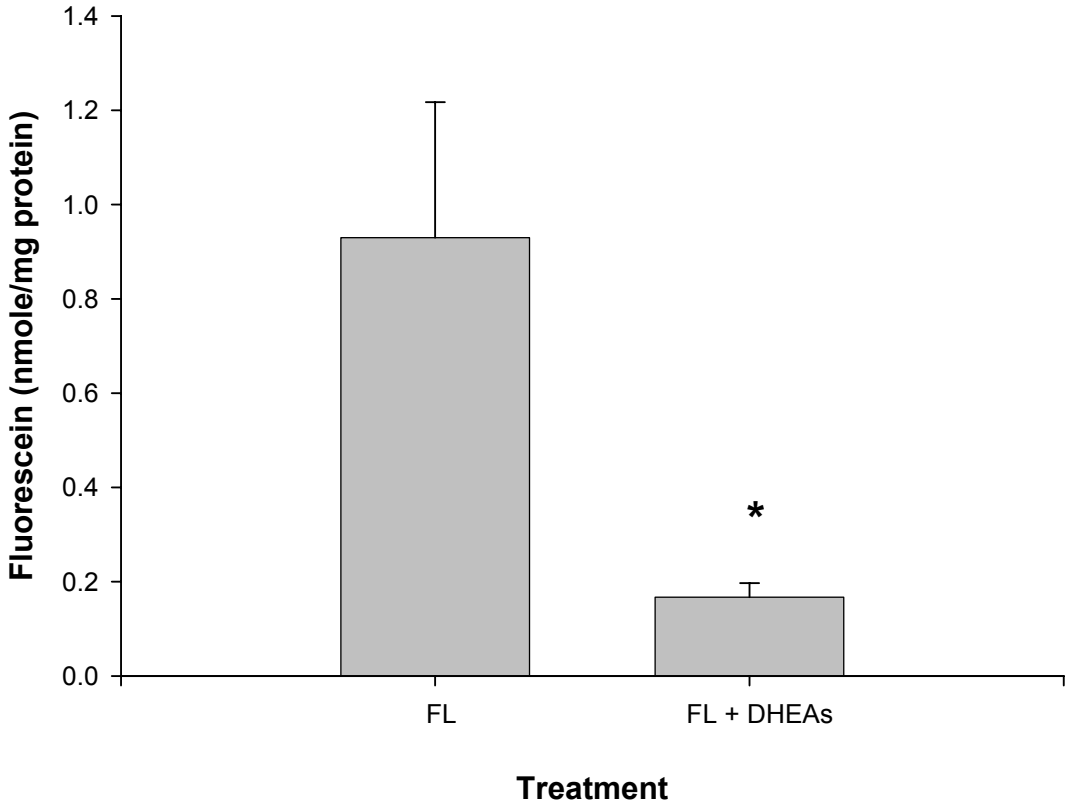

Figure 4.14. The effect of dehydroepiandrosterone sulfate on FL accumulation in IRPTs. To determine the effect of DHEAs on FL uptake in IPRTs, 3 ml of tubules (at 1 mg protein/ml) were incubated at 37ºC with 4 μM FL in the presence or absence of 1 mM DHEAs. Each flask containing IRPT suspension was incubated for 2 min in a shaking water bath (100 rpm) under 95% O_2/5% CO_2. At the end of the assay, 1 ml of tubule suspension was removed from each flask and tubular FL accumulation determined. Each assay was run in triplicate. Bars represent mean FL content (nmol/mg protein) ± SE for n=4. (* Significantly different from control (FL alone) values). FL accumulation in IPRTs was significantly inhibited by DHEAs ($P<0.05$). Data were analyzed by Student's t-test, with a 95% confidence interval.

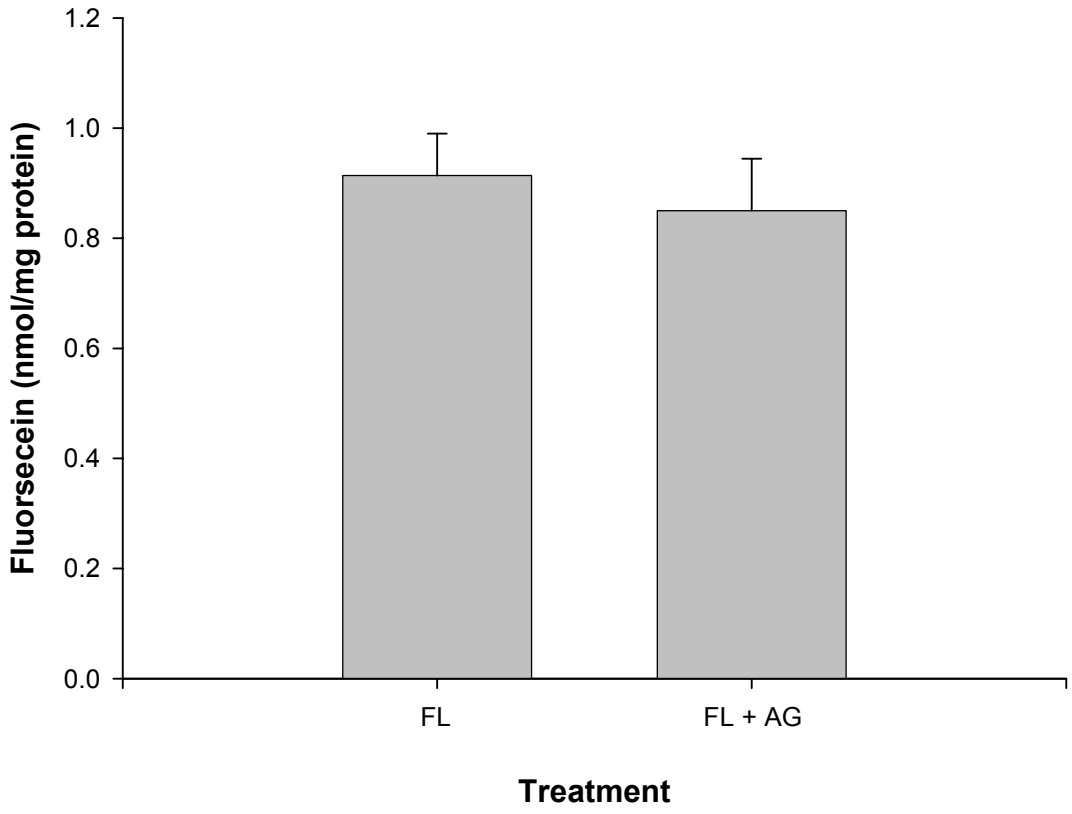

Figure 4.15. The effect of acetamidophenyl glucuronide on FL accumulation in IRPTs. To determine the effect of AG on FL uptake in IPRTs, 3 ml of tubules (at 1 mg protein/ml) were incubated at 37ºC with 4 µM FL in the presence or absence of 1 mM AG. Each flask containing IRPT suspension was incubated for 2 min in a shaking water bath (100 rpm) under 95% O_2/5% CO_2. At the end of the assay, 1 ml of tubule suspension was removed from each flask and tubular FL accumulation determined. All assays were run in triplicate. Bars represent mean FL content (nmol/mg protein) ± SE for n=4. FL accumulation was not significantly inhibited by incubation with AG. Data were analyzed by Student's t-test, with a 95% confidence interval.

4.1.3.2 PAH accumulation in IRPTs

PAH, a typical substrate of OAT1 and OAT3 proteins, has been used widely to study OAT uptake in various renal models. ^{14}C-PAH was used to further study and characterize the presence of OAT transporters along the basolateral membrane of the PT of F344 rats. Since PAH is readily available radiolabeled, and there is great deal of information available about this OAT substrate, PAH is useful for assessing OAT function in this model. Since PAH is a substrate for both OAT1 and OAT3, it provides an indication of OAT function in this model.

To determine first whether PAH uptake in this model was due to OAT transport across the basolateral membrane, the effect of probenecid on PAH uptake was assessed. Since probenecid is the typical inhibitor of OAT transport, and PAH is the typical OAT substrate, treatment with probenecid should block PAH uptake in this system if PAH uptake is OAT-mediated. To study the effects of probenecid on PAH accumulation, IRPTs (1mg protein/ml) were incubated with 73.8 μM PAH in the absence or presence of 1mM probenecid for 2 min (Fig. 4.16). This concentration of PAH was originally selected as the value that provided the Km concentration of PAH at 0.2 μCi/ml (Sweet et al., 1997; Kushara et al., 1999) Probenecid significantly inhibited PAH uptake in IPRTs by approximately 87%. This reduction in basolateral uptake in the presence of probenecid is consistent with transport mediated by OAT proteins. To determine the IC_{50} value of probenecid for PAH transport in the IRPT model, tubules were incubated with 4.5 μM PAH for 2 min in the presence of increasing concentrations of probenecid (Fig. 4.17). The IC_{50} value was calculated from the nonlinear regression equation to be approximately 106 μM in this model, with 250 μM probenecid yielding approximately 73% inhibition of PAH accumulation in IRPTs.

To assess further the contribution of OAT in glucuronide metabolite transport, AG was again used as a potential inhibitor of uptake of a known substrate of OATs. To determine the effect of AG on OAT protein transport, PAH was used as the known substrate, since PAH was shown to interact with OAT proteins in this IRPT model. In this study, IRPTs (1mg protein/ml) were incubated with 2.5 μM PAH in the absence or presence of 1 mM AG for 30 seconds (Fig. 4.18). This concentration of PAH is equivalent to .13 uCi/ml, and was used to try to minimize the amount of PAH in the incubation, thus maximizing the potential for interaction of AG with OAT. Incubation with AG did not significantly inhibit PAH uptake (approximately 9%), indicating either that AG does not interact with the same transporters responsible for PAH accumulation in this model or that AG is such a weak substrate for OAT (very low affinity for OAT) that it does not have the ability to displace PAH from the transport (OAT) proteins.

To determine whether other glucuronide metabolites may interact with PAH transport in this model, testosterone glucuronide (TG) and methylumbelliferyl glucuronide (MUG) were used as alternate potential inhibitors of PAH accumulation in IRPTs. AG inhibition was also studied again as a second control for TG and MUG inhibition. If inhibition with TG and MUG produced different results than inhibition with AG, it would indicate that various glucuronides may have different substrate specificities for basolateral OAT transporters. To study the effects of TG and MUG on renal OAT, IPRTs were incubated with 4.4 μM PAH in the absence or presence of 500 μM TG, MUG, or AG for 30 seconds (Fig. 4.19). Due to increased variability in the results obtained in the previous experiment, the concentration of PAH was increased to 0.25 μCi/ml to minimize the variability in ^{14}C-PAH counting. Significant inhibition of PAH accumulation was not seen in the presence of TG, MUG or AG. These results suggest that these glucuronide metabolites do not interact strongly with PAH transporters (OATs) along the basolateral membrane of IRPTs or again, TG

and MUG also have such weak affinity for the PAH transporter that they cannot displace PAH and thus inhibit PAH transport.

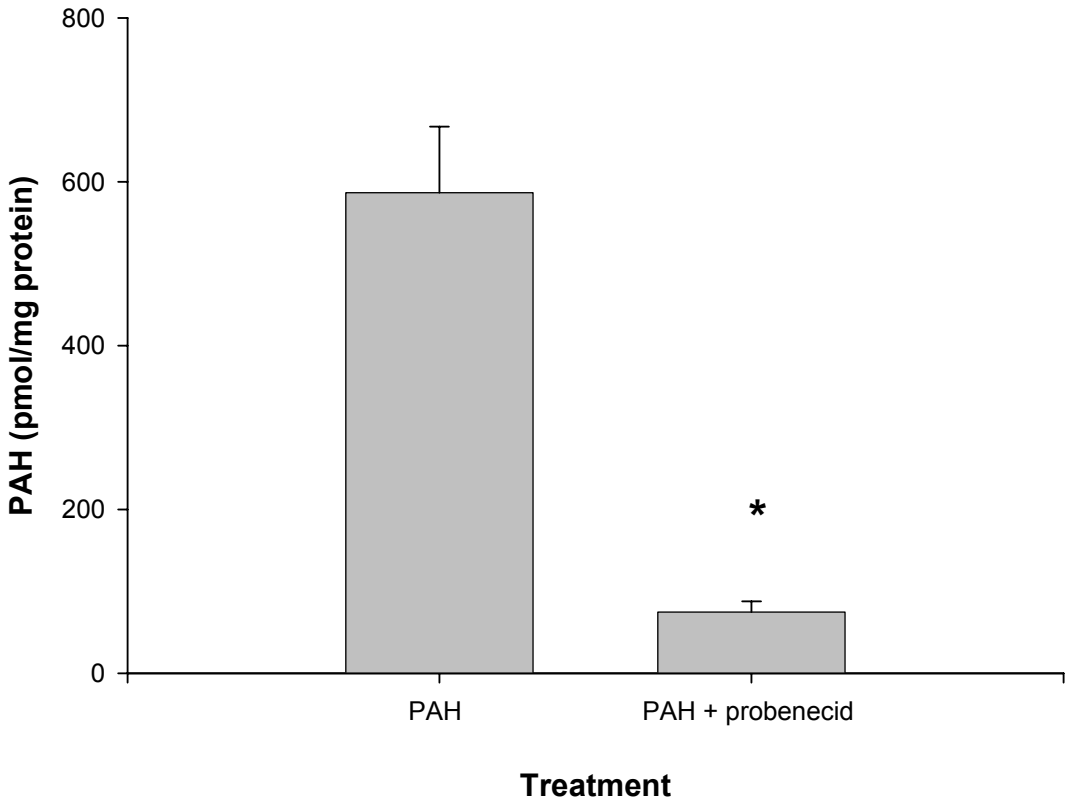

Figure 4.16. The effect of probenecid on PAH accumulation in IRPTs.

To determine the effect of probenecid on PAH accumulation in IRPTs, 3 ml of tubules (at 1 mg protein/ml) were incubated for 2 min with 73.8 μM ^{14}C-PAH in the absence or presence of 1 mM probenecid. Each flask was incubated at 37ºC in a shaking water bath (180rpm) under 95% O_2/5% CO_2. At the end of two min the total IRPT sample in each flask was analyzed for tubular PAH accumulation. All assays were run in duplicate. Bars represent mean PAH content (pmol/mg protein) ± SE for n=3. (*Significantly different from control (PAH alone) values). Probenecid significantly inhibited PAH accumulation in IRPTs from Fischer 344 rat ($P<0.05$). Data were analyzed by Student's t-test, with a 95% confidence interval.

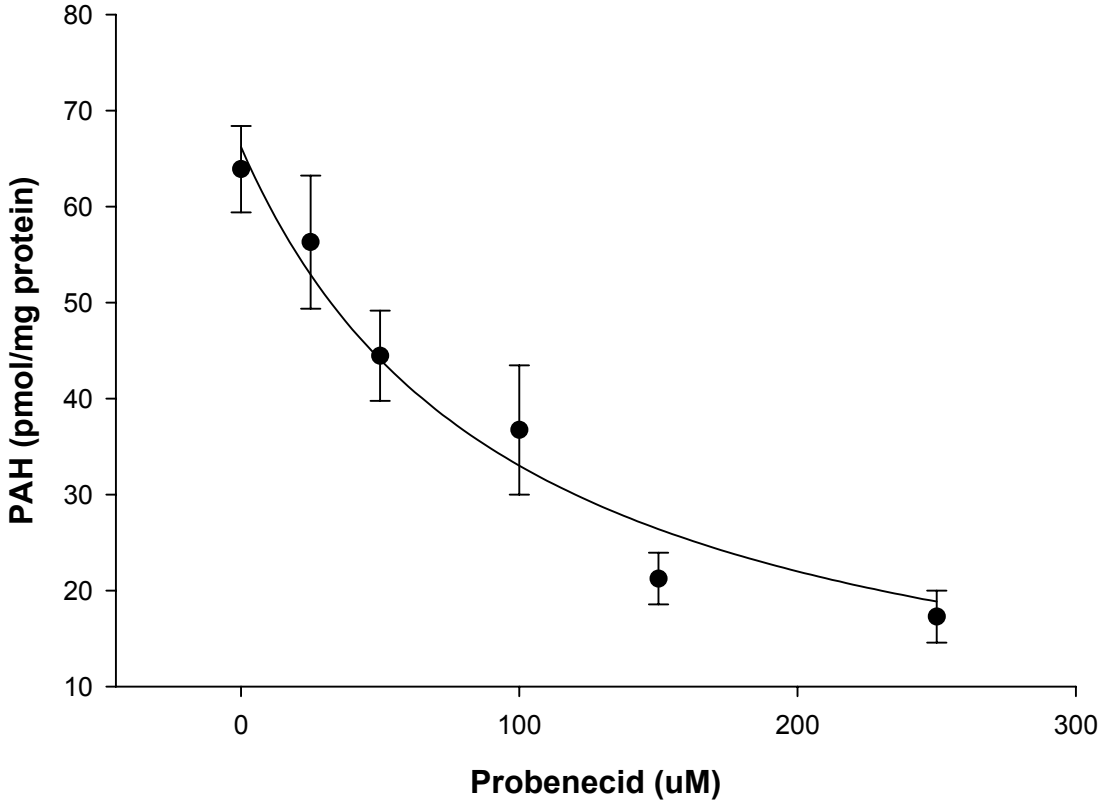

Figure 4.17. IC_{50} determination of probenecid for PAH uptake in IRPTs.

To determine the IC50 value of probenecid for ^{14}C-PAH uptake in IRPTs, 3 ml tubules (at 1 mg protein/ml) were incubated with 4.5 μM PAH in the presence of increasing concentrations of probenecid. Each flask was incubated at 37 ° C for 2 min in a shaking water bath (180 rpm) under 95% O_2/5% CO_2. Assays were run in duplicate at each concentration. At the end of each assay the total IRPT sample in each flask was analyzed for tubular PAH accumulation. Probenecid concentrations used were 25, 50, 100, 150 or 250 μM. Each point represents mean PAH content (pmol/mg protein) ± SE for n=8 (PAH) or n=4 (+probenecid). Data were analyzed by Nonlinear Regression analysis. The IC_{50} value of probenecid for PAH uptake in IPRTs was calculated from the nonlinear equation (f=a*x/(b+x); r^2=0.97) to be 106.5 μM.

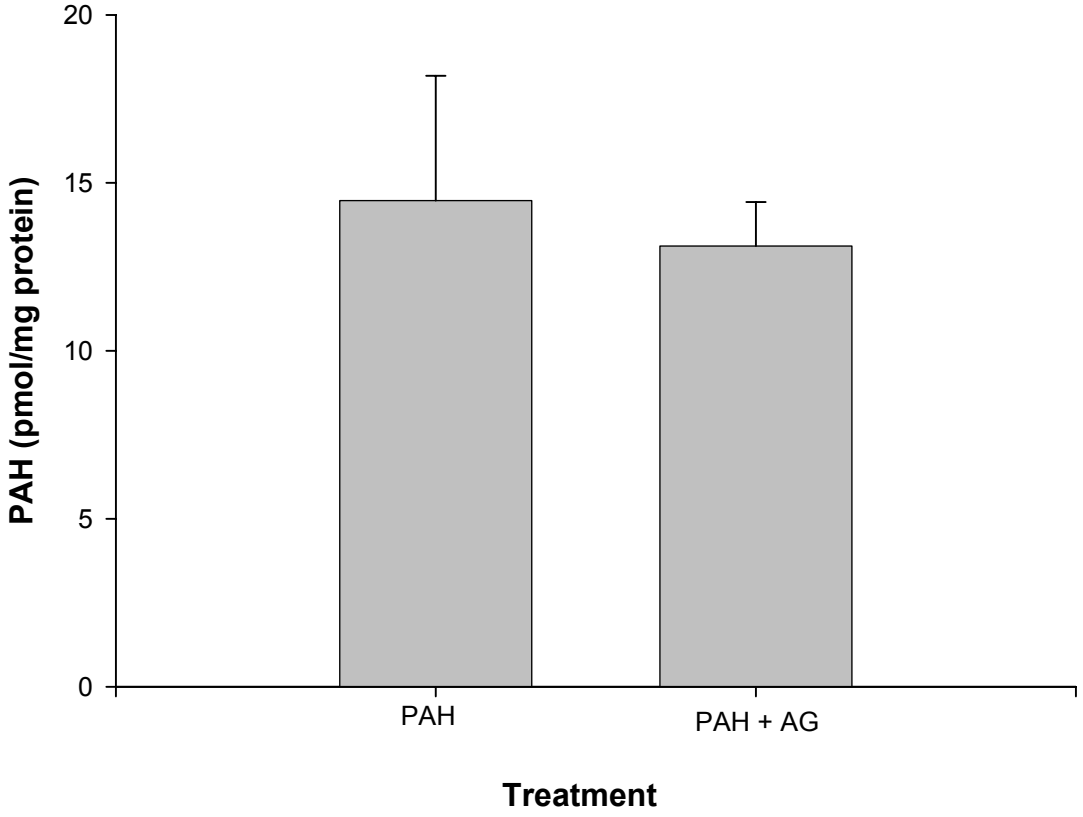

Figure 4.18. Effect of acetamidophenyl glucuronide on PAH accumulation in IRPTs. To determine the effect of AG on PAH accumulation along the basolateral membrane in IRPTs, 3 ml of tubules (at 1 mg protein/ml) were incubated at 37ºC with 2.5 μM ^{14}C-PAH in the presence or absence of 1 mM AG. Each flask containing IRPT suspension was incubated for 30 seconds in a shaking water bath (180 rpm) under 95% O_2/5% CO_2. At the end of the assay, the total IRPT sample in each flask was analyzed for tubular PAH accumulation. All assays were run in duplicate. Bars represent mean PAH content (pmol/mg protein) ± SE for n=4. PAH accumulation was not significantly inhibited by incubation with AG. Data were analyzed by Student's t-test, with a 95% confidence interval.

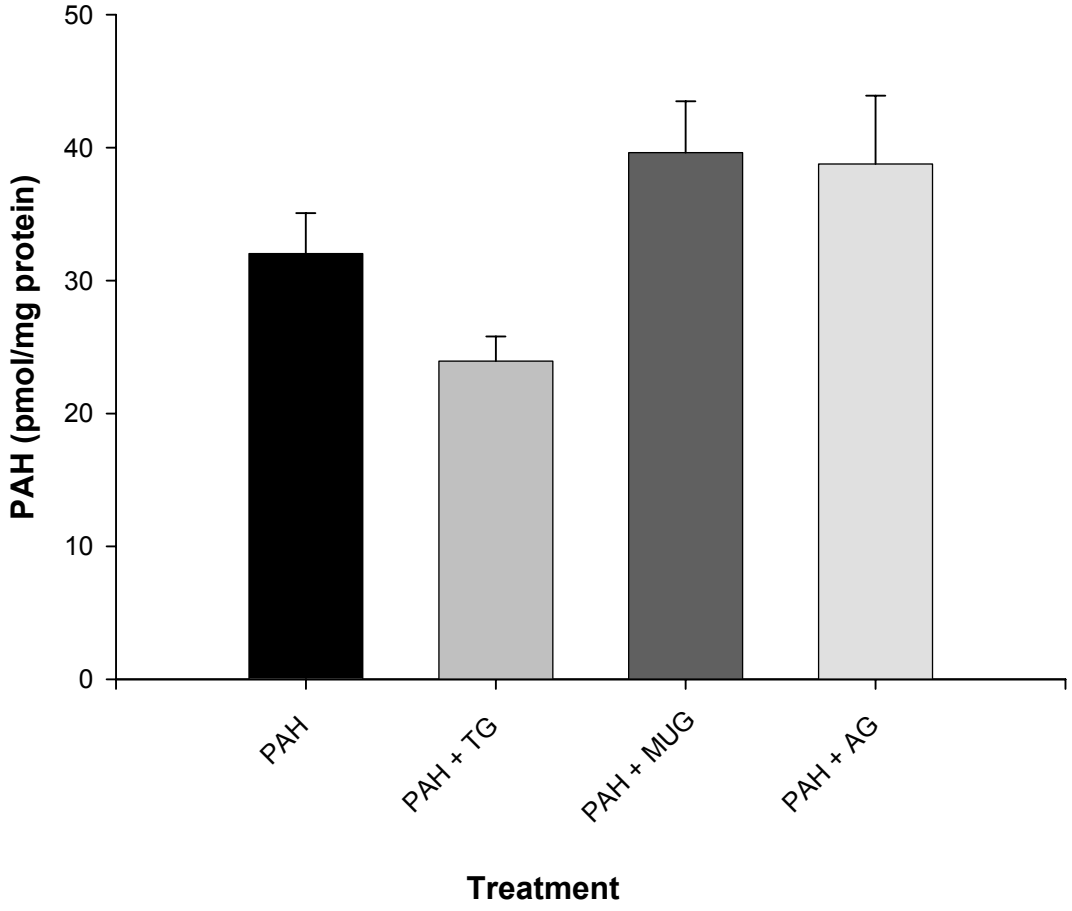

Figure 4.19. Effect of testosterone glucuronide (TG), methylumbelliferyl glucuronide (MUG), and acetamidophenyl glucuronide (AG) on PAH accumulation in IRPTs. To determine the effect of TG, MUG, and AG on PAH accumulation in IRPTs, 3 ml of tubule suspension (1mg protein/ml) were incubated with 4.4μM ^{14}C-PAH in the absence or presence of 500 μM TG, MUG, or AG. Tubules were incubated at 37ºC for 30 seconds in a shaking water bath (180 rpm) under 95% O_2/5% CO_2. At the end of each assay, the total IRPT sample in each flask was analyzed for tubular PAH accumulation. All assays were run in duplicate. Bars represent mean PAH content (pmol/mg protein) ± SE for n=4 (PAH + TG) or n=5 (PAH + MUG, AG). Incubation with PAH in the presence of TG, MUG or AG did not cause significant inhibition of PAH accumulation in IRPTs. Data were analyzed by Repeated Measures ANOVA.

4.1.3.3 Estrone sulfate accumulation in IRPTs.

Estrone sulfate (ES) has been used as the typical substrate of OAT3 in numerous OAT transport studies. Since ES is selective for OAT3 rather than OAT1, it allows for direct study of the interaction of compounds with the OAT3 protein. Therefore, ES was used to characterize the contribution of OAT3 in transport along the basolateral membrane of IRPTs from F344 rat, and to determine also the potential role of OAT3 in glucuronide metabolite uptake.

To characterize OAT3 transport in this IRPT model, it was first necessary to determine whether accumulation of ES in this model was a carrier protein-mediated process. To determine this, temperature dependent uptake of ES was studied. Tubules (1 mg protein/ml) were incubated with ^{3}H-ES in a shaking water bath (180 rpm) at 37 or 4ºC (Fig. 4.20). Incubation at 4ºC significantly inhibited ES uptake in IRPTs by approximately 38%. This temperature dependent inhibition is consistent with the presence of carrier protein-mediated transport.

To further characterize ES transport in this model, probenecid was used as the classical OAT inhibitor to determine whether ES transport in this model was probenecid sensitive. Probenecid sensitivity would give additional supporting evidence for the presence and function of OAT3 in this model. For this study, tubules (1 mg protein/ml) were incubated with 4 pM ^{3}H-ES in the absence or presence of 1 mM probenecid (Fig. 4.21). Incubation with ES in the presence of probenecid caused significant inhibition of ES uptake in IRPTs by approximately 41%. This indicates that OAT transport (as demonstrated by ES accumulation) is in part carried out by OAT3 in this model. These results combined with those found for temperature sensitivity of ES uptake, also suggest that there may be other transporters involved in ES transport in this model, or potentially another transporter involved in the transport of OAT3 substrates.

Self-inhibition of ES accumulation in IRPTs was also used to characterize ES transport and OAT3 function in this model. Self-inhibition, or the inhibition of radiolabeled substrate uptake by addition of excess amounts of unlabeled substrate, is commonly used as an indicator of true carrier-mediated "transport" of a compound vs. other forms of entry into a cell (i.e. diffusion). To determine whether ES is subject to self-inhibition, IRPTs (1 mg protein/ml) were incubated with 4 pM ^{3}H-ES, in the absence or presence of 500 μM unlabeled ES (Fig 4.22). Incubation of IRPTs with ^{3}H-ES in the presence of excess unlabeled ES showed significant inhibition of ES accumulation by approximately 63%. This demonstrates that ES transport in IRPTs from Fischer 344 rat is a carrier-mediated transport process, and also demonstrates the presence and function of OAT3 along the tubular basolateral membrane.

To assess the potential interaction between AG and OAT3, AG was used as a potential inhibitor of uptake of ES, a known OAT3 substrate. In this study IRPTs (1 mg protein/ml) were incubated with 4 pM ^{3}H-ES in the absence or presence of 1 mM AG for 60 seconds (Fig. 4.23). Incubation of IRPTs with ES in the presence of AG did not demonstrate significant inhibition of ES accumulation. This indicates that AG does not interfere with ES transport, further demonstrating that AG either does not interact with OAT3 transporters along the basolateral membrane of the PT, or is such a weak substrate that it can not displace ES (a high-affinity OAT3 substrate) from the protein.

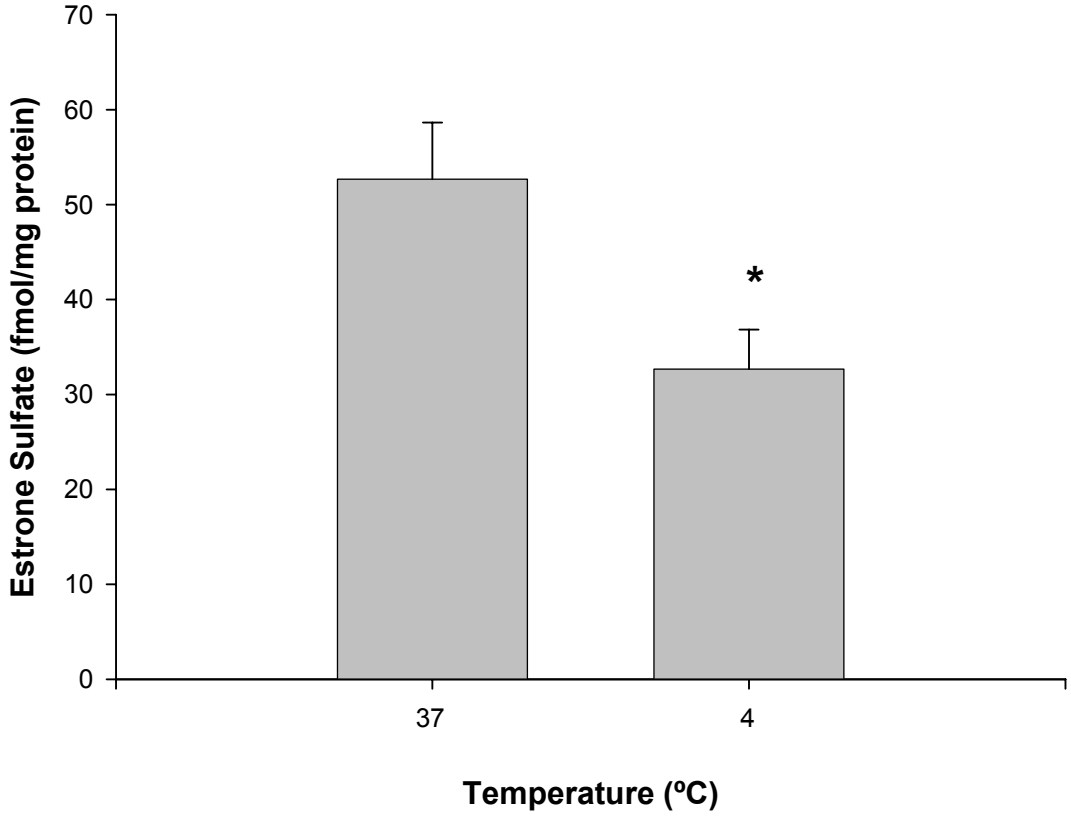

Figure 4.20. The effect of temperature on estrone sulfate accumulation in IRPTs. To determine the effect of temperature on ES uptake in IPRTs, 3 ml of tubules (at 1 mg protein/ml) were incubated at 37ºC or 4ºC in the presence of 4 pM ^{3}H-ES. ES was added to each flask of IRPT suspension and incubated for 60 seconds in a shaking water bath (180 rpm) under 95% O_2/5% CO_2. At the end of each assay, the total IRPT sample in each flask was analyzed for tubular ES accumulation. All assays were run in duplicate. Bars represent mean ES content (fmol/mg protein) ± SE for n=5, * Significantly different from control (37) values ($P<0.05$). Data were analyzed by Student's t-test, with a 95% confidence interval.

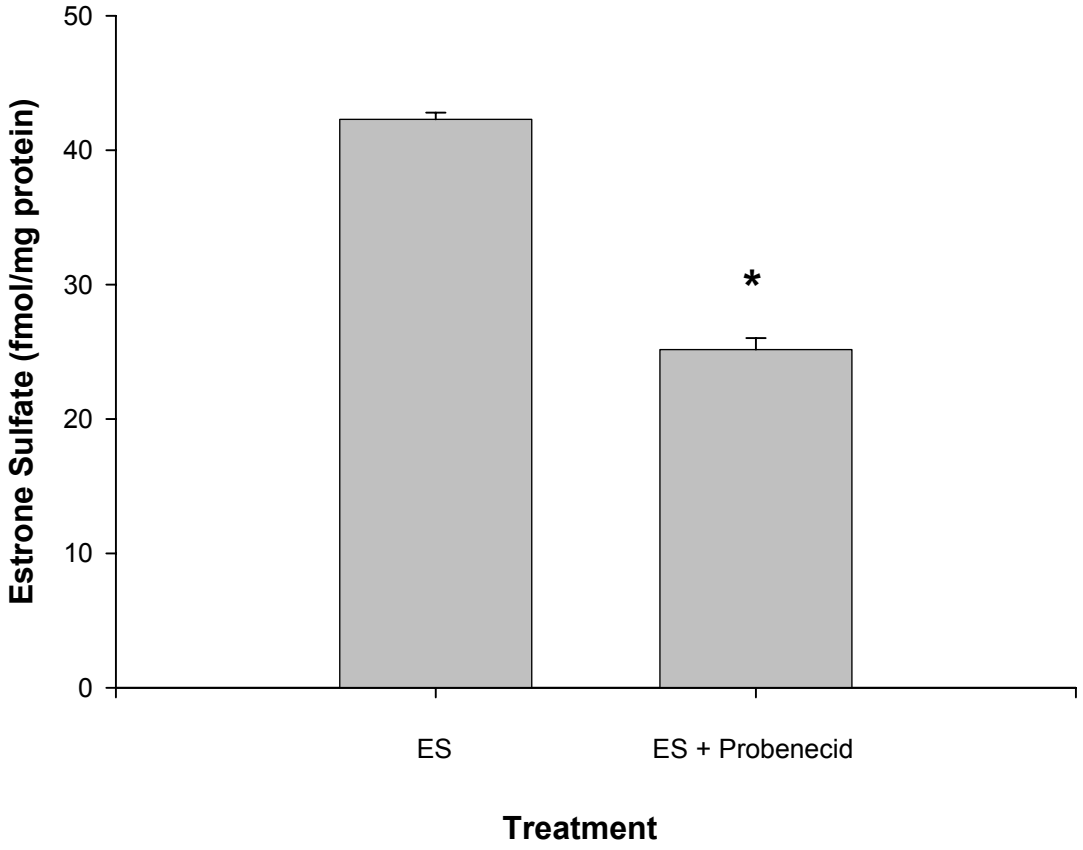

Figure 4.21. The effect of probenecid on ES accumulation in IRPTs.

To determine the effect of probenecid on ES accumulation in IRPTs, 3 ml of tubules (at 1mg protein/ml) were incubated for 30 seconds with 4 pM ^{3}H-ES in the absence or presence of 1 mM probenecid. Each flask was incubated at 37ºC in a shaking water bath (180rpm) under 95% O_2/5% CO_2. At the end of each assay the total IRPT sample in each flask was analyzed for tubular ES accumulation. All assays were run in duplicate. Bars represent mean ES content (fmol/mg protein) ± SE, n=3. * Significantly different from control (ES) values ($P<0.05$). Data were analyzed by Student's t-test, with a 95% confidence interval.

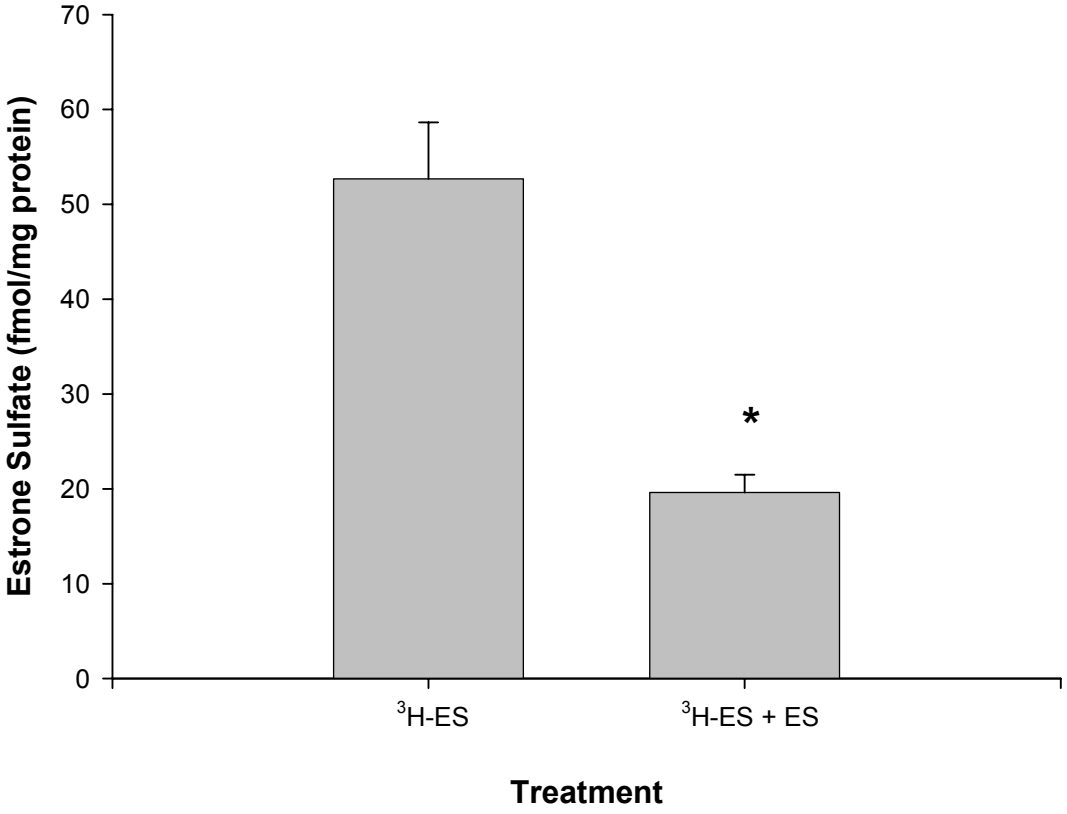

Figure 4.22. The effect of self-inhibition on estrone sulfate accumulation in IRPTs. To determine the effect of self-inhibition on ES uptake in IRPTs, 3 ml tubules (at 1 mg protein/ml) were incubated for 60 seconds with 4 pM ^{3}H-ES in the absence or presence of 500 μM unlabeled ES. Each flask was incubated at 37ºC in a shaking water bath (180rpm) under 95% O_2/5% CO_2. At the end of each assay the total IRPT sample in each flask was analyzed for tubular ES accumulation. All assays were run in duplicate. Bars represent mean ES content (fmol/mg protein) ± SE for n=4. * Significantly different from control (^{3}H-ES) values ($P<0.05$). Data were analyzed by Student's t-test, with a 95% confidence interval.

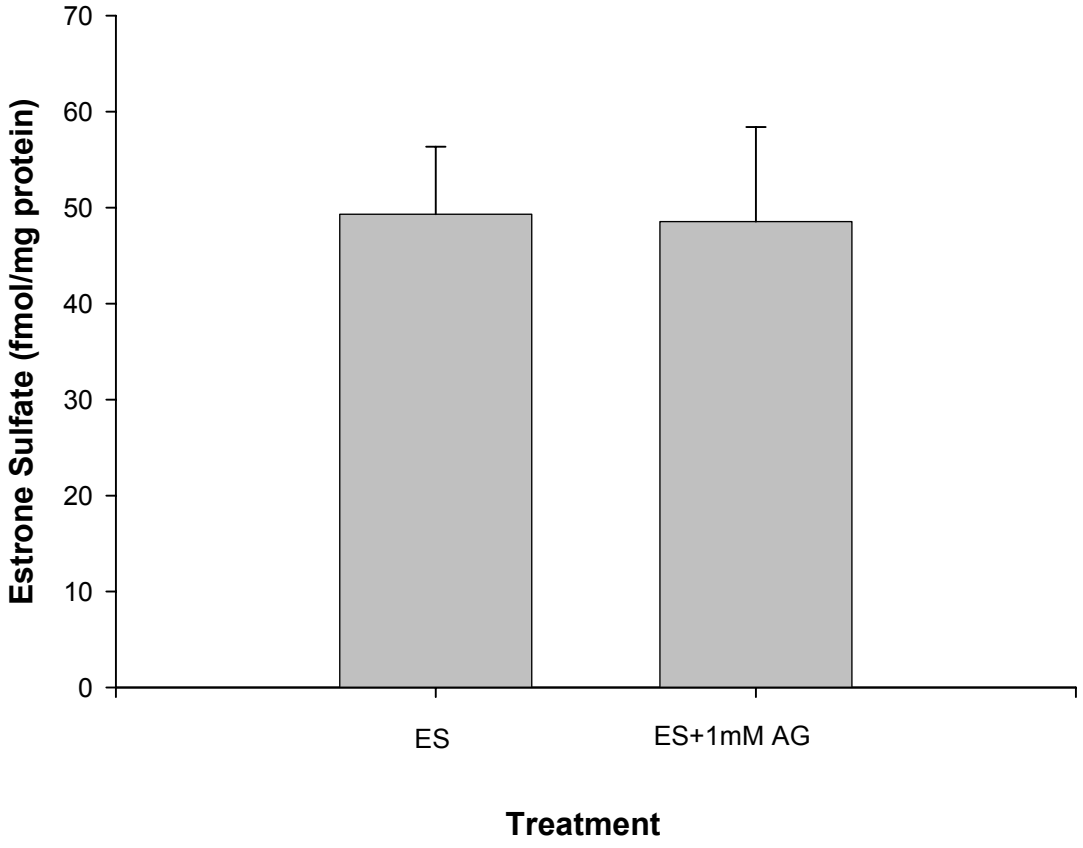

Figure 4.23. The effect of acetamidophenyl glucuronide on estrone sulfate accumulation in IRPTs. To determine the effect of AG on ES accumulation along the basolateral membrane in IRPTs, 3 ml of tubules (at 1 mg protein/ml) were incubated for 60 seconds with 4 pM ^{3}H-ES in the presence or absence of 1 mM AG. Each flask containing IRPT suspension was incubated for 37 ºC in a shaking water bath (180 rpm) under 95% O_2/5% CO_2. At the end of the assay, the total IRPT sample in each flask was analyzed for tubular ES accumulation. All assays were run in duplicate. Bars represent mean ES content (fmol/mg protein) ± SE for n=3. ES accumulation was not significantly inhibited by incubation with AG. Data were analyzed by Student's t-test, with a 95% confidence interval.

4.1.3.4 Acetamidophenyl glucuronide (AG) accumulation in IRPTs

AG was selected as a model glucuronide for the study of glucuronide transport along the basolateral membrane of the renal PT. This compound was available radiolabeled, and previous studies suggest that AG has the ability to be secreted by the kidney (Duggin and Mudge, 1975; Galinsky and Levy, 1981; Watari et al., 1983). To elucidate whether OAT proteins contribute to AG secretion (and possibly glucuronide metabolites in general) across the basolateral membrane of the PT, various aspects of AG accumulation by IRPTs were studied. Temporal studies revealed that when IRPTs are incubated with 4.5 μM AG, AG appears to demonstrate time-dependent accumulation within the tubule fragments (Fig. 4.24). Accumulation appeared gradual over time with AG tubular content doubling between 15 and 300 seconds.

To elucidate further the mechanism of uptake of AG in IRPTs, temperature dependent studies were used to determine whether accumulation of AG appeared to be via a carrier protein-mediated process (such as OAT). IRPTs incubated with 2 μM ^{14}C-AG at either 37ºC or 4ºC did not reveal significant decrease in AG accumulation across the basolateral membrane of IRPTs (Fig. 4.25). Decreased temperature generated only approximately 18% inhibition. These results indicate that AG entry into IRPTs across the basolateral membrane may, in large part, be due to mechanisms other than a carrier protein-mediated pathway.

To determine whether AG interacts with OAT transporters, probenecid was used as the typical OAT transport inhibitor. Since probenecid has been demonstrated to inhibit the uptake of organic anions in this model, if AG accumulation is due in any part to transport by OAT proteins, treatment with probenecid should yield inhibition of AG accumulation. IRPTs pretreated with probenecid or coincubated with probenecid in the presence of 2 μM ^{14}C-AG did

not demonstrate inhibition of AG accumulation (Fig. 4.26). Lack of inhibition of AG accumulation in IRPTs by probenecid demonstrates that AG accumulation may by via a different mechanism than OAT transport.

Since the previous experiments raise question as to whether transport of AG across the basolateral membrane is due to a protein-mediated transport process, self-inhibition studies were used to characterize further the mechanism of AG transport into IRPTs. IRPTs incubated with ^{14}C-AG in the presence of excess unlabeled AG did not demonstrate inhibition of labeled AG accumulation (Fig. 4.27). This provides further evidence that AG entry across the basolateral membrane in this IRPT model may be due to other mechanisms than carrier-mediated transport.

To characterize further whether AG interacts with OAT transporters along the basolateral membrane, potential transport by OAT3 was specifically examined. Since AG is a bulky, charged molecule (as are glucuronides in general), AG is more likely to interact with OAT3 than other OATs should AG have any interaction with OAT proteins along the basolateral membrane of renal PTs. IRPTs incubated with 4.5 μM AG in the presence of 100 μM ES did not demonstrate inhibition of AG accumulation (Fig. 4.28). Since the presence of ES (a high affinity substrate for OAT3) did not interfere with AG accumulation in this model, this finding further supports that AG accumulation into IRPTs is not due to OAT proteins along the basolateral membrane, and more specifically, AG does not appear to interact with OAT3 proteins.

In the previous studies, the mechanism of AG uptake across the basolateral membrane of IRPTs does not appear to be due to a carrier protein-mediated process such as OAT. With concern that these results may have been affected by metabolism of the AG metabolite by β-glucuronidase during incubation, AG accumulation studies were conducted in the presence of D-

saccharic acid 1,4-lactone (SL), a β-glucuronidase inhibitor (Soars et al., 2001). Since deconjugation of AG would have yielded a glucuronic acid moiety, and a labeled acetaminophen (APAP) molecule, it was necessary to determine whether what was documented as AG uptake was due to AG or APAP, since APAP does have the ability to diffuse through the cell membrane. If uptake was due to diffusion of APAP into the IRPTs rather than AG, treatment with SL should completely inhibit accumulation of labeled substrate (AG). IRPTs treated with 4.5 μM AG in the presence of SL demonstrated no inhibition of AG accumulation (Fig. 4.29). This indicates that the demonstrated accumulation of AG in previous studies is in fact due to the AG molecule, and not deconjugation to APAP with subsequent entry of APAP into the tubules.

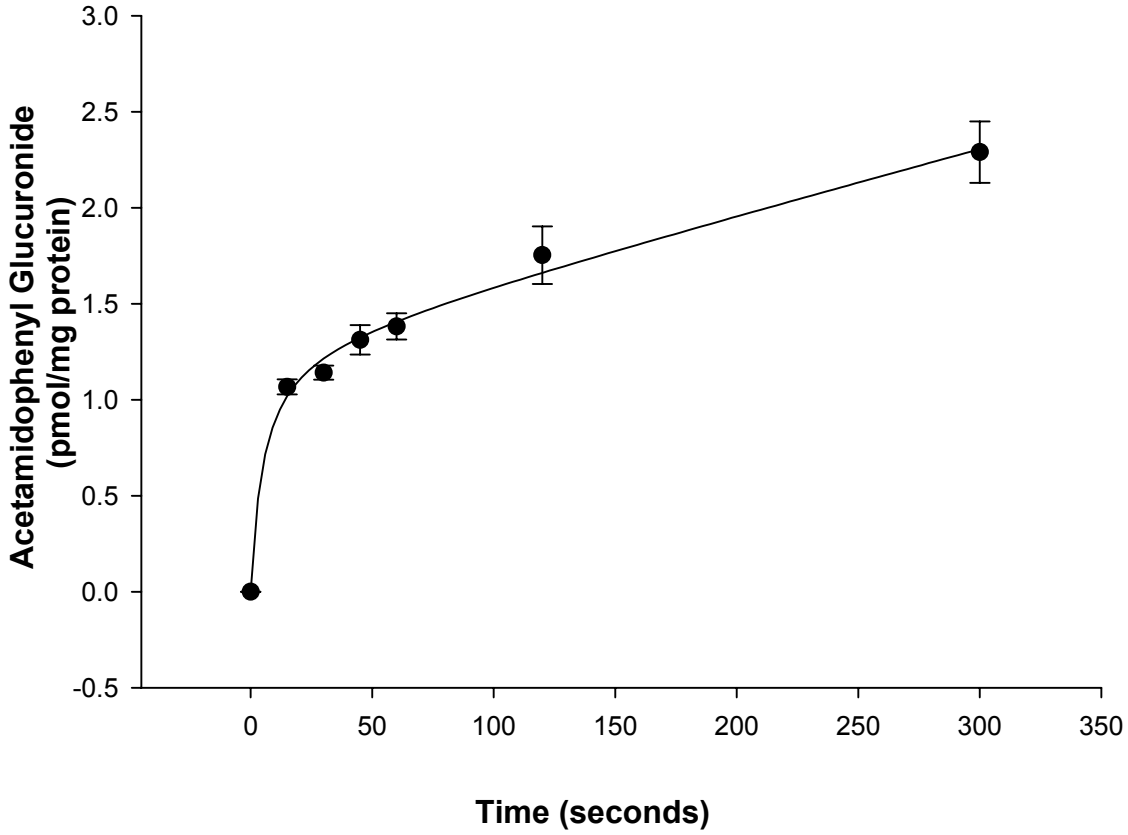

Figure 4.24. Time-dependent accumulation of acetamidophenyl glucuronide in IRPTs. To determine the time-dependent accumulation of AG in IRPTs, 3 ml tubules (at 1 mg protein/ml) were incubated with 4.5 μM ^{14}C-AG for 15, 30, 45, 60,120 or 300 seconds. Tubules were incubated at 37 ºC in a shaking water bath (180 rpm) under 95% O_2/5% CO_2. All assay was run in duplicate. At the end of each time point, the total tubule suspension from each flask was analyzed for tubular AG accumulation. Each point represent mean tubular AG content (pmol/mg protein) ± SE for n=3. Data were analyzed by Nonlinear Regression analysis [(f=a*x/(b+x)+c*x); r^2=0.994].

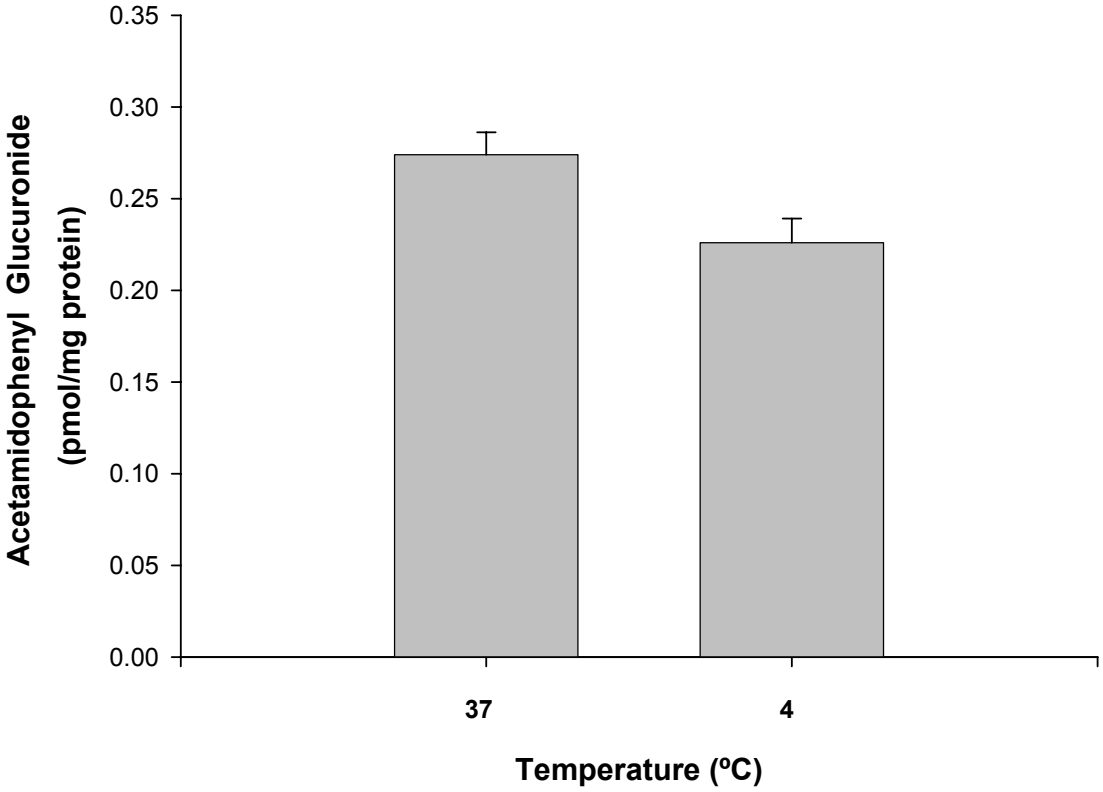

Figure 4.25. The effect of temperature on acetamidophenyl glucuronide accumulation in IRPTs. To determine the effect of temperature on AG uptake in IPRTs, 3 ml of tubules (at 1 mg protein/ml) were incubated at 37ºC or 4ºC in the presence of 2 μM ^{14}C-AG. AG was added to each flask of IRPT suspension and incubated for 30 seconds in a shaking water bath (180 rpm) under 95% O_2/5% CO_2. At the end of each assay, the total IRPT sample in each flask was analyzed for tubular AG accumulation. All assays were run in duplicate. Bars represent mean AG content (pmol/mg protein) ± SE for n=4, AG accumulation was not significantly inhibited by incubation at 4ºC. Data were analyzed by Student's t-test, with a 95% confidence interval.

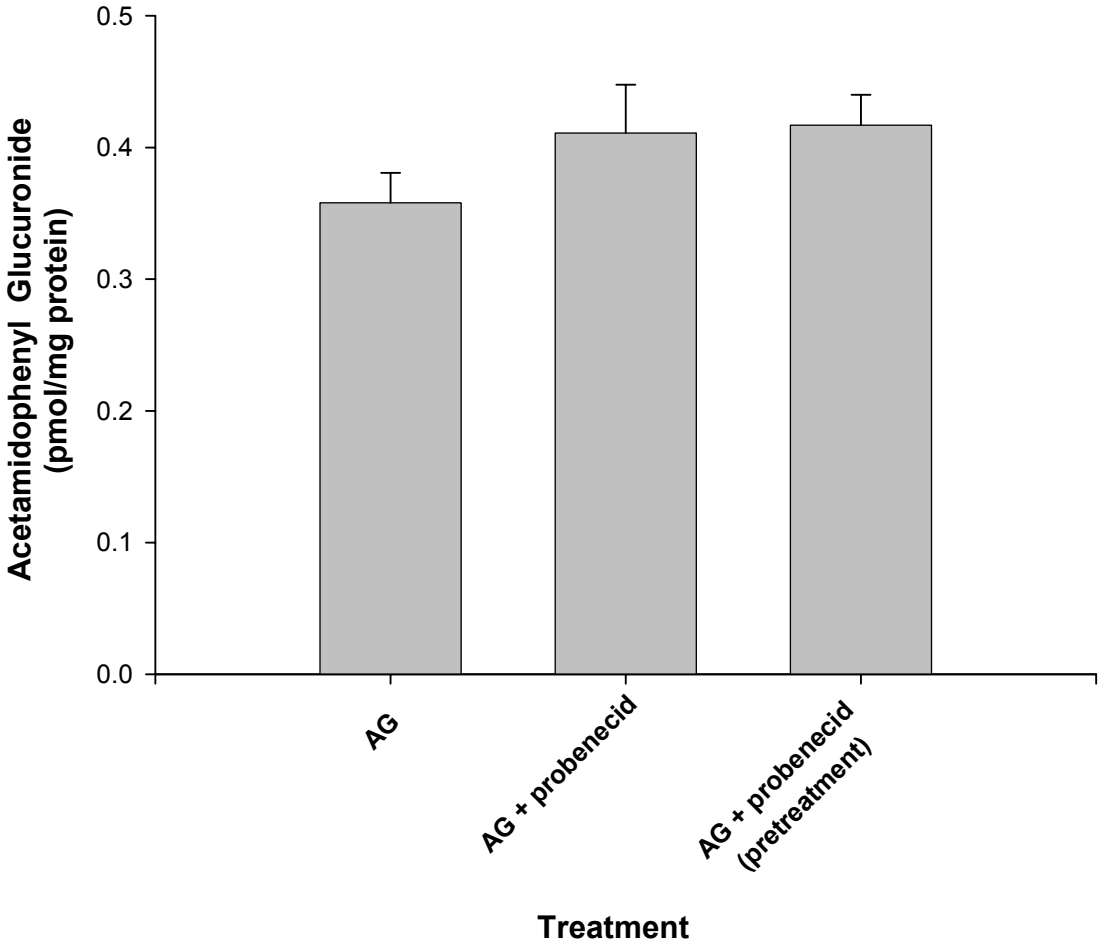

Figure 4.26. The effect of probenecid on acetamidophenyl glucuronide accumulation in IRPTs. To determine the effect of probenecid on AG accumulation in IRPTs, 3 ml of tubules (at 1mg protein/ml) were either incubated for 30 seconds with 2 μM ^{14}C-AG in the absence or presence of 1 mM probenecid or preincubated with 1mM probenecid before the addition of 2 μM ^{14}C-AG. Each flask was incubated at 37ºC in a shaking water bath (180rpm) under 95% O_2/5% CO_2. At the end of each assay the total IRPT sample in each flask was analyzed for tubular AG accumulation. All assays were run in duplicate. Bars represent mean AG content (pmol/mg protein) ± SE for n=4. Probenecid did not significantly inhibited AG accumulation in IRPTs from Fischer 344 rat. Data were analyzed by Student's t-test, with a 95% confidence interval.

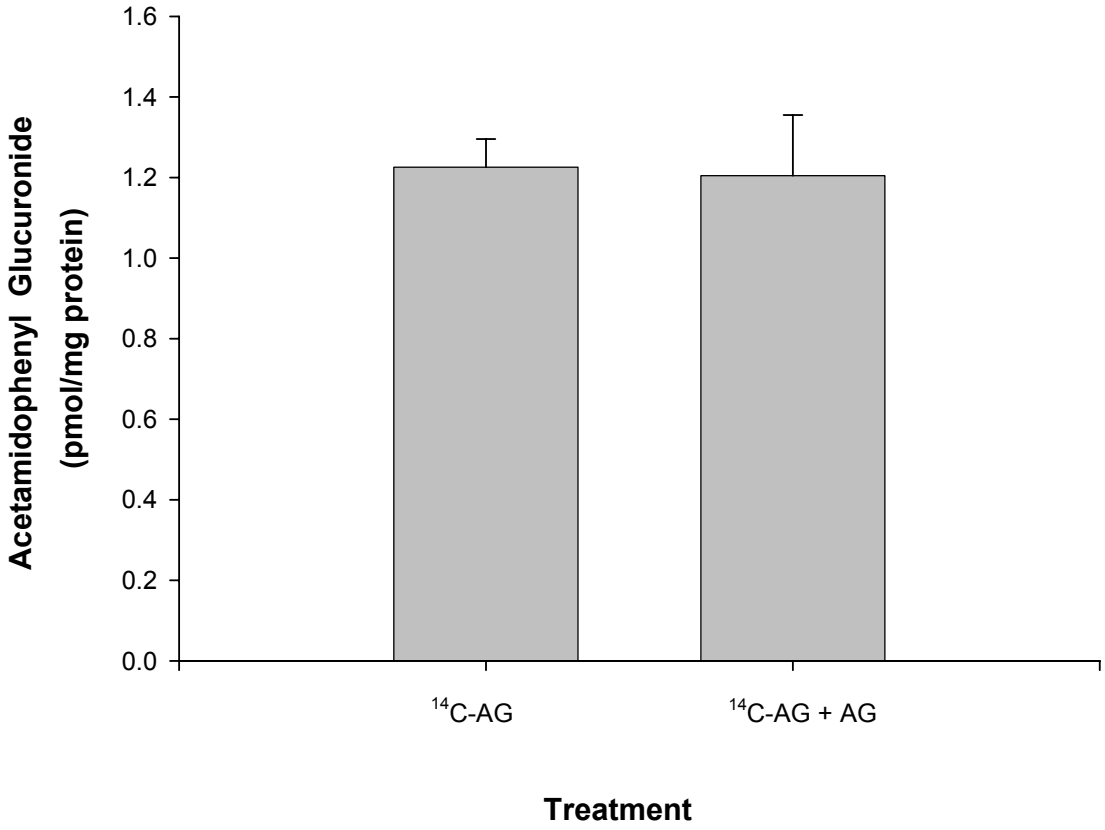

Figure 4.27. The effect of self-inhibition on acetamidophenyl glucuronide accumulation in IRPTs. To determine the effect of self-inhibition on AG uptake in IRPTs, 3 ml tubules (at 1 mg protein/ml) were incubated for 30 seconds with 4.5 μM ^{14}C-AG in the absence or presence of 5 mM unlabeled AG. Each flask was incubated at 37ºC in a shaking water bath (180rpm) under 95% O_2/5% CO_2. At the end of each assay the total IRPT sample in each flask was analyzed for tubular AG accumulation. All assays were run in duplicate. Bars represent mean AG content (pmol/mg protein) ± SE for n=3. The presence of unlabeled AG did not significantly inhibit the accumulation of ^{14}C-AG in IRPTs. Data were analyzed by Student's t-test, with a 95% confidence interval

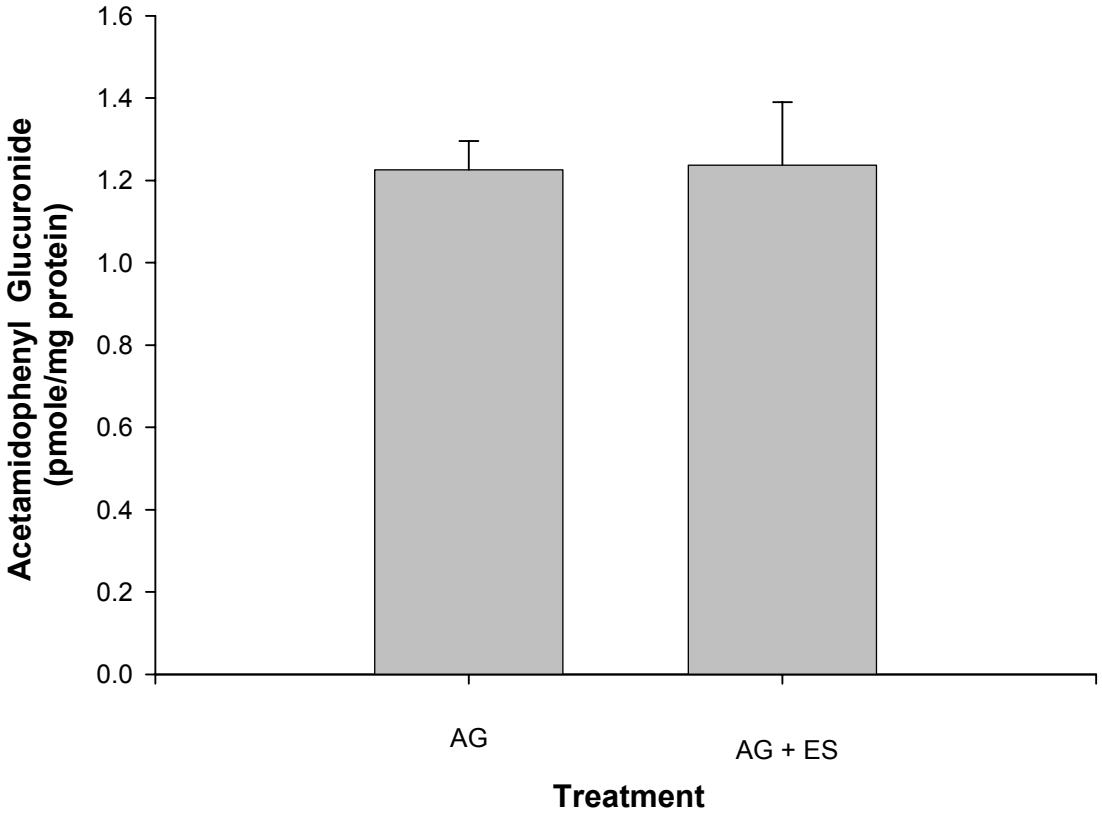

Figure 4.28. The effect of estrone sulfate on acetamidophenyl glucuronide accumulation in IRPTs. To determine the effect of ES on AG accumulation in IRPTs, 3 ml of tubules (at 1mg protein/ml) were incubated for 30 seconds with 4.5 μM ^{14}C-AG in the absence or presence of 100 μM ES. Each flask was incubated at 37ºC in a shaking water bath (180rpm) under 95% O_2/5% CO_2. At the end of each assay the total IRPT sample in each flask was analyzed for tubular AG accumulation. All assays were run in duplicate. Bars represent mean AG content (pMole/mg protein) ± SE for n=3. Incubation with ES did not significantly inhibited AG accumulation in IRPTs. Data were analyzed by Student's t-test, with a 95% confidence interval.

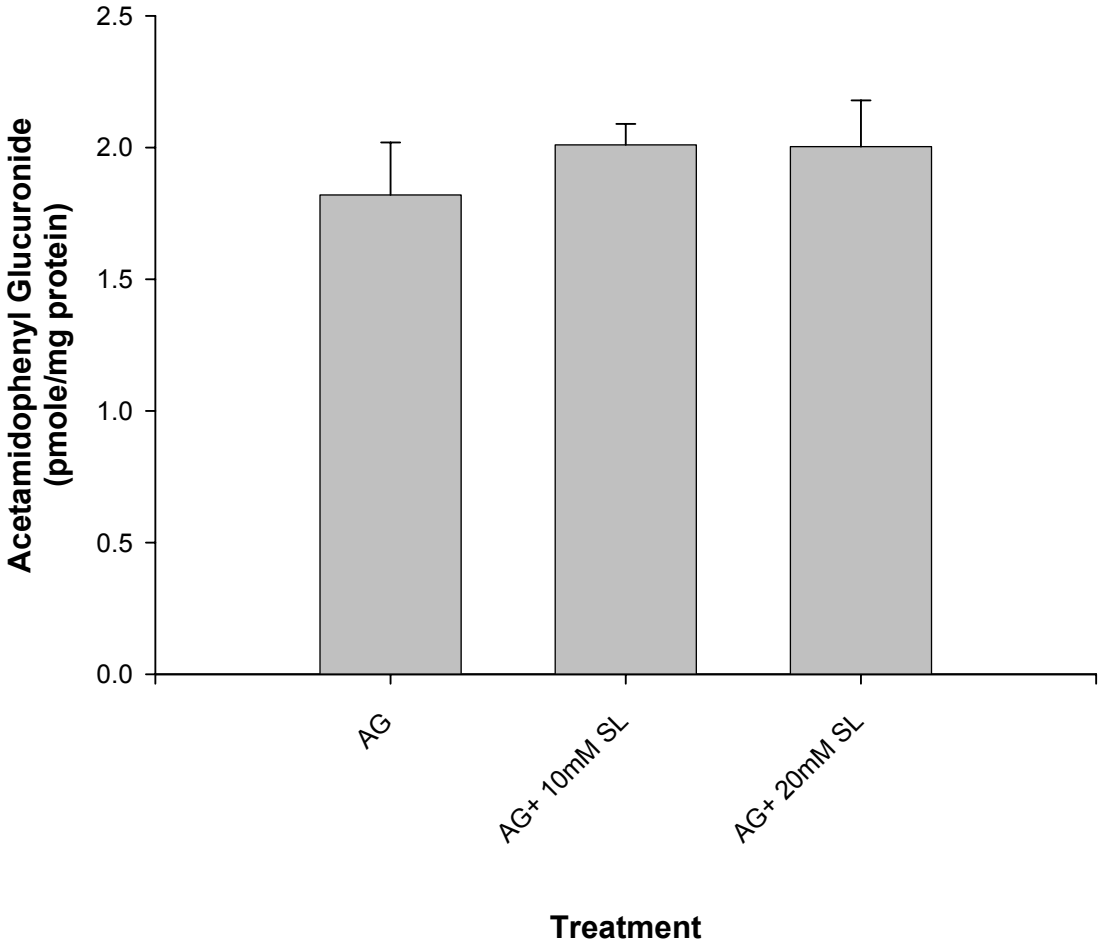

Figure 4.29. The effect of D-saccharic acid 1,4-lactone on acetamidophenyl glucuronide accumulation in IRPTs. To determine the effect of SL on AG accumulation in IRPTs, 3 ml of tubules (at 1mg protein/ml) were incubated for two min with 4.5 μM ^{14}C-AG in the absence or presence of either 10mM or 20 mM SL following 5 min preincubation with SL. Each flask was incubated at 37ºC in a shaking water bath (180rpm) under 95% O_2/5% CO_2. At the end of each assay the total IRPT sample in each flask was analyzed for tubular AG accumulation. All assays were run in duplicate. Bars represent mean AG content (pMole/mg protein) ± SE for n=3. Incubation with SL at either concentration did not significantly inhibited AG accumulation in IRPTs. Data were analyzed by Repeated Measures ANOVA, with a 95% confidence interval.

4.1.3.5 Western Blot Analysis of OAT1 and OAT3 in Fischer 344 IRPTs

Western blot analysis of the organic anion transporters, OAT1 and OAT3, was performed using crude membrane fractions isolated from Fischer 344 rat IRPTs (Fig. 4.30). IRPTs were isolated as described in the Methods chapter and western blot analysis was carried out by Eliza Robertson. Molecular weight is given for protein bands larger than 50 kD, as smaller bands are thought to be due to either incompletely formed proteins or breakdown products. Antibodies synthesized against peptides homologus to the amino-terminus were used and would therefore bind whole and partial proteins. The OAT1 band demonstrated for Fisher 344 IRPTs at 75 kD is comparable to the 77 kD band reported by Ji et al (2002) for OAT1, where the 61.3 kD band is likely the nonglycosylated protein form. Faint bands for OAT3 were detected at 54 and 63 kD which is comparable to the 54 and 65 kD, bands reported by Hasegawa et al. (2002) for rOAT3. Heavier darker bands may potential represent breakdown products. While western blot analysis can not show whether OAT1 and OAT3 are functional, it demonstrates that OAT1 appears to be present while raising question as to the presence of OAT3 in F344 IRPTs.

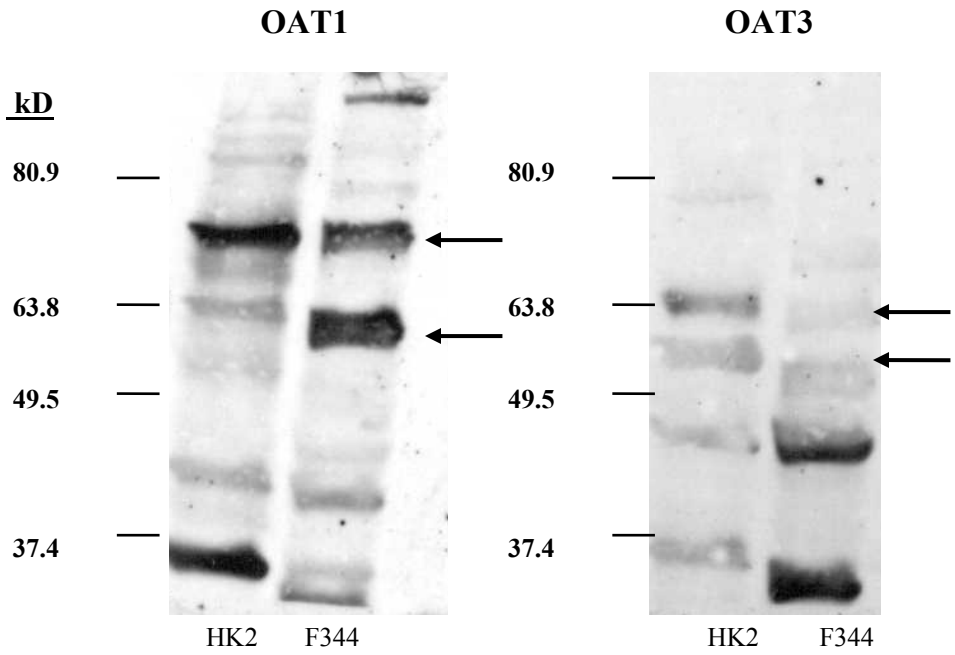

Figure 4.30. Western Blot Analysis for OAT1 and OAT3. Crude membrane fractions (250 µg/lane) isolated from HK-2 cells, passage 29, scraped from T75 flasks and from Fisher 344 (F344) rat IRPTs were separated on a 12% polyacrylamide gel, blotted onto nitrocellulose then exposed to antibodies against OAT1 or OAT3. In freshly isolated F344 IRPTs, bands were detected at 61.3 and 75 kD for OAT1, and faint bands for OAT3 were detected at 54 and 63 kD.

4.2 Studies in Renal Cortical Slices (RCS)

4.2.1 Uptake studies in renal cortical slices (RCSs)

The isolation of renal PTs used in the previously described studies involved the use of collagenase digestion. Collagenase digestion, while providing healthy tubule fragments for uptake studies, may potentially cause partial digestion of some transporters along the basolateral membrane. To determine whether the results for AG uptake in IRPTs are due to partial digestion of the transport mechanisms for the AG molecule (partial digestion of OAT transporters at a critical AG binding site) has occured, additional studies were conducted in renal cortical slices. It is important to note that the IRPT model was able to demonstrate transport of known organic anions such as FL, PAH, and to a certain extent ES. These compounds may have multiple recognition sites within the OAT proteins and transport of these OAs would be less sensitive to partial digestion by collagenase. AG however, if it has extremely low substrate specificity for OAT, may be more susceptible to the effects of partial digestion of the OAT proteins by collagenase digestion. RCSs have the same transport properties as IRPTs, but their isolation does not involve the use of collagenase. Therefore, in the RCS model, OAT proteins along the proximal tubular basolateral membrane should remain fully intact. If digestion of OAT proteins in the IRPT model caused decreased affinity of AG for the transporter proteins, this affinity should be unchanged in the RCS model.

4.2.1.1 Mannitol accumulation in RCSs

Accumulation of ^{3}H-mannitol was used to assess interstitial accumulation in the RCS model. Mannitol does not undergo transport by any portion of the RCS. Therefore, mannitol does not accumulate in RCSs by transport mechanisms but accumulation is due to movement (leak) of MN into interstitial

spaces between cells within the slices. Thus, MN accumulation gives an indication as to the amount of interstitial space where compounds may collect by mechanisms other than cellular transport. RCSs incubated over time in the presence of 176 pM ^{3}H-mannitol demonstrated accumulation of less than 7 fmol/mg protein of mannitol over a 60 min incubation time (Fig. 4.31). Accumulation of mannitol was minimal over the entire time period (10-60 min), indicating that the slices were of good quality (no large interstitial spaces or gaps created during slicing) and could be used for uptake studies.

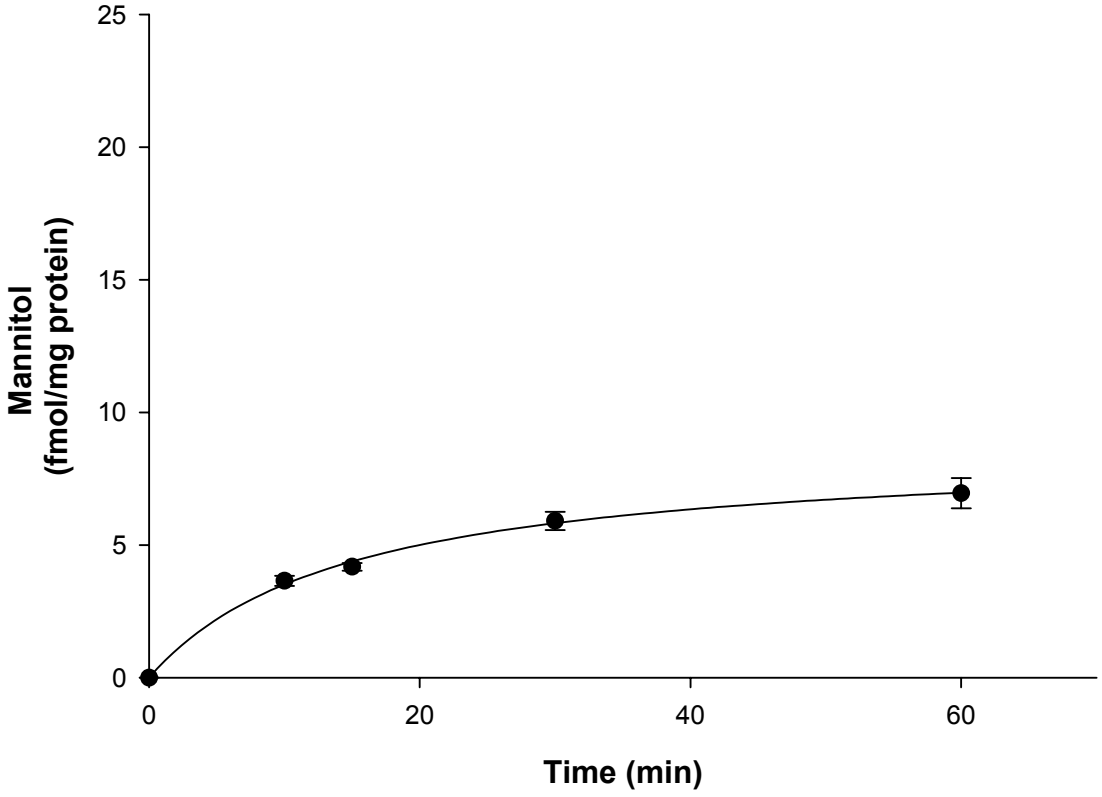

Figure 4.31. Mannitol accumulation in RCSs. To assess the quality of the RCS technique, RCSs (30-60 mg) were incubated for 10, 15, 30, and 60 min in the presence of 176 pM ^{3}H-mannitol. Slices were incubated at 37ºC in a shaking water bath (100 rpm). At the end of each time point, the total slice content of each well was analyzed for mannitol accumulation. Each assay was run in duplicate. Each point represents mean mannitol content (fmol/mg protein) ± SE for n=4. Mannitol accumulation appeared to reach a maximum of less than 7 fmol/mg protein. Data were analyzed by Nonlinear Regression analysis [f=a*x/(b+x); r^2=0.99].

4.2.1.2 PAH accumulation in RCSs

Accumulation of PAH, the typical OAT1/OAT3 substrate, was used to assess the activity of OAT transporters along the basolateral membrane of PTs in the RCS model. Since the tubular lumens collapse in the slice model, the only entry for PAH into the PT cells in RCSs is via tubular OAT transporters along the basolateral membrane.

To characterize best that PAH uptake in the RCS model is mediated by OAT proteins, probenecid, the typical OAT transport inhibitor, was used to demonstrate inhibition of PAH uptake. RCSs incubated with 4.7 μM ^{14}C-PAH in the presence of probenecid showed accumulation of PAH with significant inhibition of PAH accumulation in the presence of 1 mM probenecid (Fig. 4.32). Inhibition of PAH accumulation by probenecid was approximately 80%. This result is similar to that found in IRPTs (86%; Fig. 4.16), indicating that OAT proteins are functional in this model and transport is probenecid sensitive.

To characterize the potential interaction of OAT transport with glucuronide metabolites in the RCS model, TG, MUG, and AG were used to assess their interaction with PAH transport. RCSs incubated with 4.7 μM ^{14}C-PAH in the presence of 500 μM TG, MUG, or AG demonstrated no inhibition of PAH transport (Fig. 4.33). TG, MUG, and AG all failed to inhibit PAH accumulation in RCSs, indicating that these compounds do not interact with the same transport mechanisms as PAH in the RCS model. This finding is also in agreement with that found in the IRPT model (Fig. 4.19).

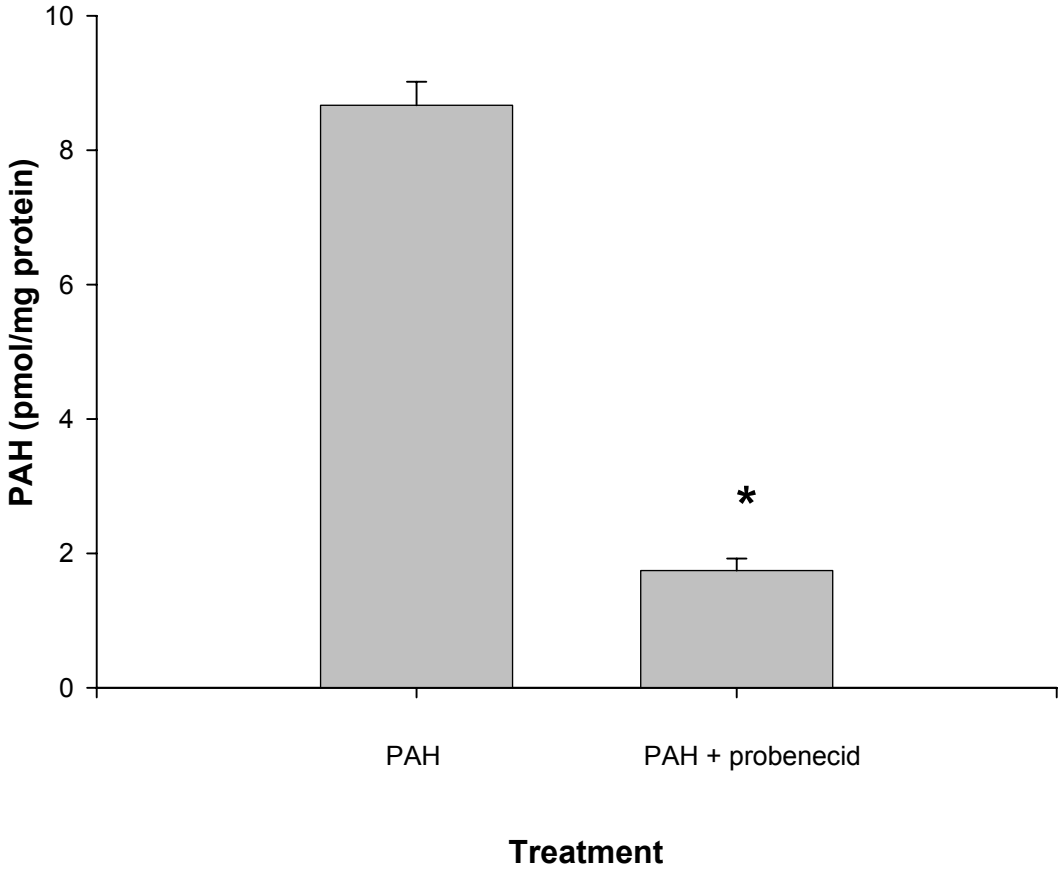

Figure 4.32. The effect of probenecid on PAH accumulation in RCSs. To determine the effect of probenecid on PAH transport in RCS, RCSs (30-60 mg) were incubated for 30 min with 4.7 μM ^{14}C-PAH in the absence or presence of 1mM probenecid. RCSs were incubated at 37ºC in a shaking water bath (100 rpm). At the end of each assay, total slice content of each well was analyzed for PAH accumulation. Each assay was run in duplicate. Bars represent mean PAH content (pmol/mg protein) ± SE for n=4. * Significantly different from control (PAH) values ($P<0.05$). Data were analyzed by Student's t-test with a 95% confidence interval.

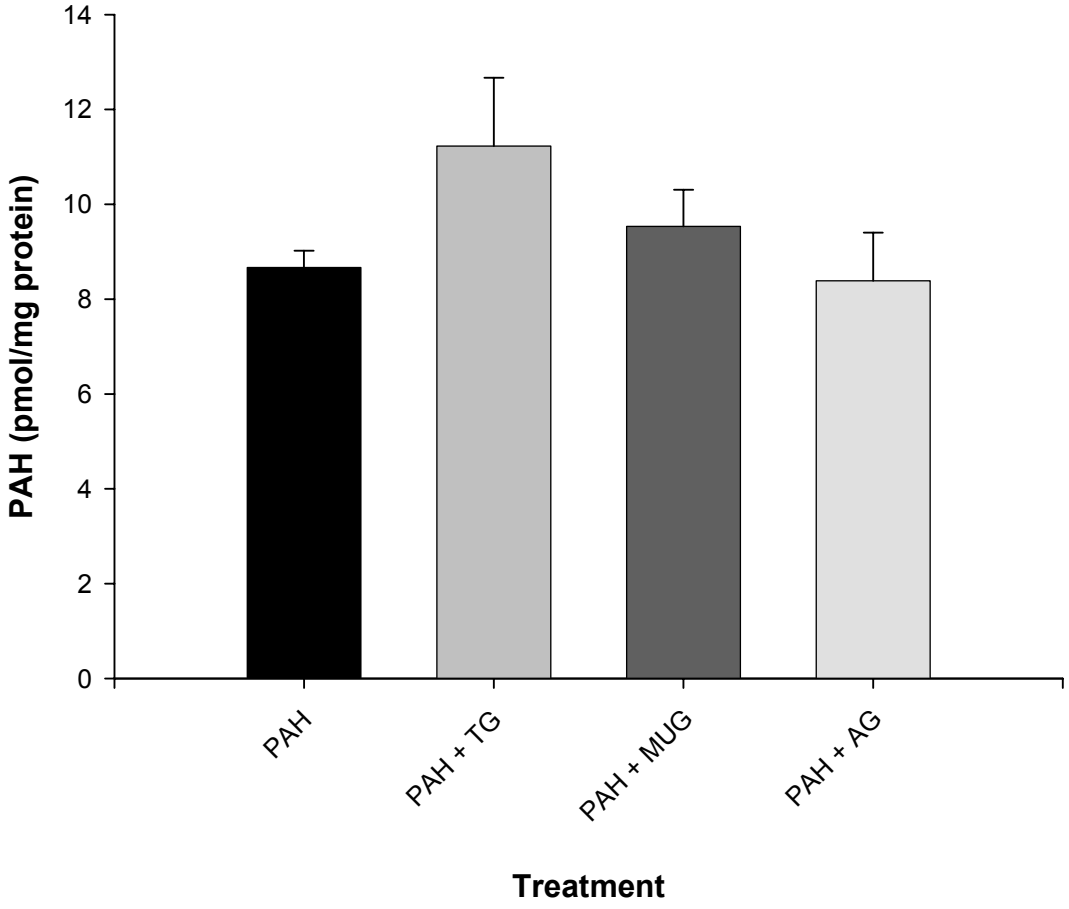

Figure 4.33. The effect of testosterone glucuronide (TG), methylumbelliferyl glucuronide (MUG), and acetamidophenyl glucuronide (AG) on PAH accumulation in RCSs. To determine the effect of TG, MUG and AG on PAH accumulation in RCSs., RCSs (30-60 mg) were incubated for 30 min with 4.7 μM PAH in the absence or presence of 500 μM TG, MUG or AG. Slices were incubated at 37ºC in a shaking water bath (100 rpm). At the end of each assay, total slice content from each well was analyzed for PAH accumulation. Each assay was run in duplicate. Each bar represents mean PAH content (pmol/mg protein) ± SE for n=4. Data were analyzed by One Way Repeated Measures ANOVA.

4.2.1.3 Estrone sulfate accumulation in RCSs.

To evaluate the activity and contribution of OAT3 to organic anion transport in RCSs, estrone sulfate was used as the typical substrate for OAT3. Since OAT3 is most likely responsible for the transport of bulky organic anions (and thus glucuronide conjugates), it was important to determine the presence of active OAT3 function in this model, and determine whether AG appeared to have any interaction at this transporter. Temporal uptake studies in RCSs, show that when treated with 4 pM ^{3}H-ES, RCSs accumulate ES in a time-dependent manner (Fig. 4.34). Accumulation of ES increases steadily until 30 min, and by 60 min uptake appears to be reaching equilibrium.

To characterize further ES transport, and thus OAT3, in the RCS model, the effects of probenecid and temperature on ES accumulation were assessed. Probenecid inhibition would indicate that ES is transported by an OAT protein in this model, and temperature sensitivity would indicate that transport is via a carrier protein-mediated process. RCSs incubated with 4 pM ^{3}H-ES in the presence of 1mM probenecid or at 4ºC demonstrated significantly decreased ES accumulation (Fig. 4.35). Probenecid treatment caused a 33% reduction in ES accumulation, while incubation at 4ºC caused an 80% decrease in ES accumulation. Since low temperature demonstrated a significantly greater decrease in ES accumulation than treatment with probenecid, this indicates that there may be another transport mechanism involved in ES accumulation.

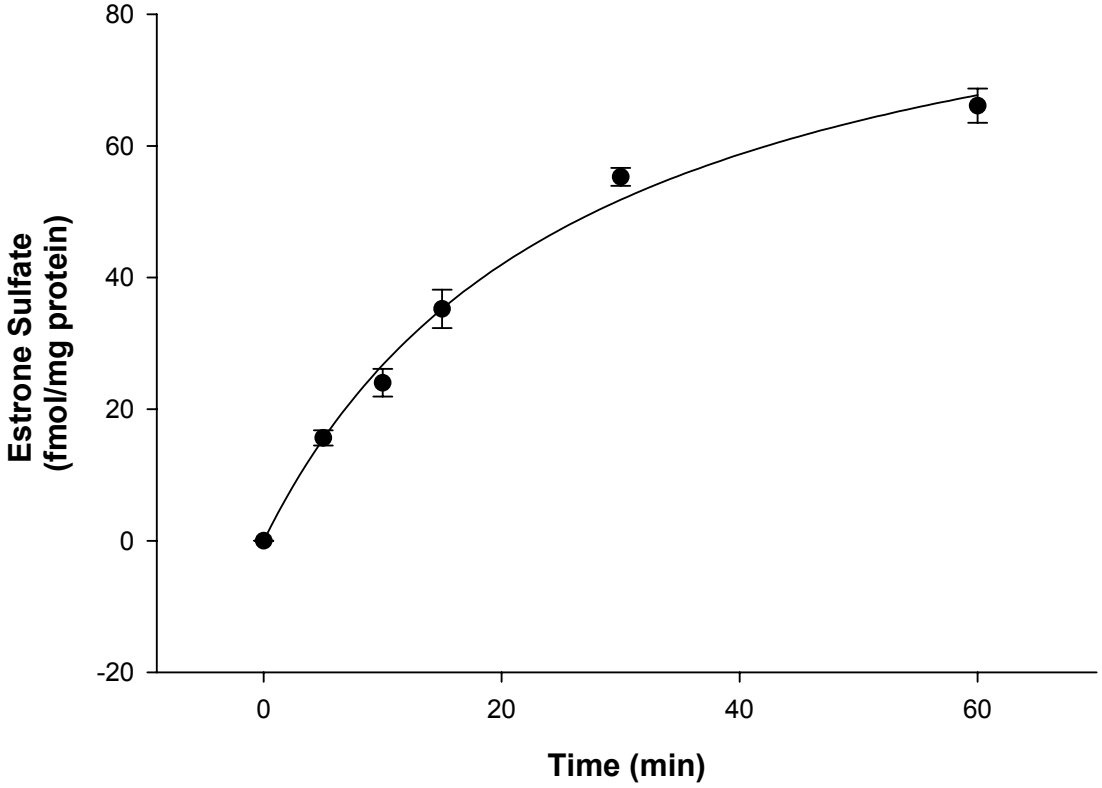

Figure 4.34. Time-dependent accumulation of estrone sulfate in RCSs. RCSs (30-60mg) were incubated for 10, 15, 20, 30 or 60 min in the presence of 4 pM ^{3}H-ES. Slices were incubated at 37ºC in a shaking water bath (100 rpm). At the end of each time point, total slice content of each well was analyzed for ES accumulation. Each assay was run in duplicate. Each point represents mean ES content (fmol/mg protein) ± SE for n=4. Data were analyzed by Nonlinear Regression analysis [f=a*x/(b+x); r^2=0.99].

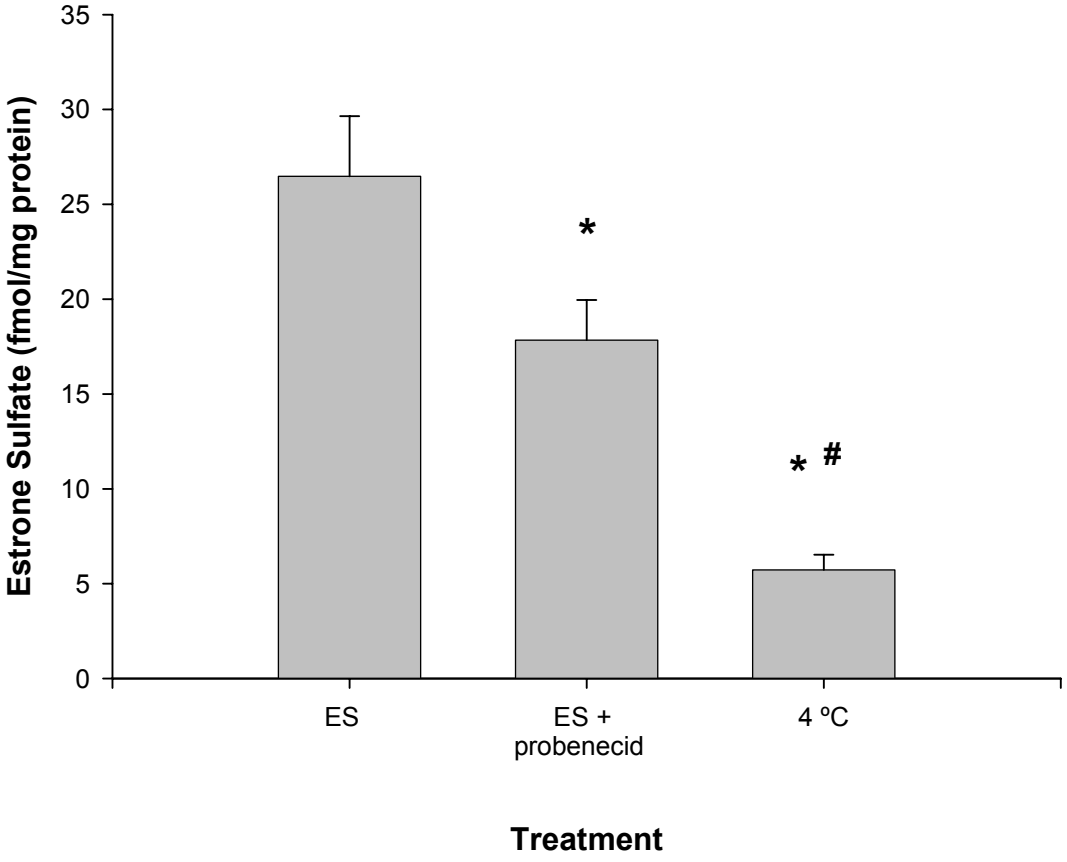

Figure 4.35. Effect of probenecid and temperature on ES accumulation in RCSs. To determine the effect of probenecid and temperature on ES accumulation, RCSs (30-60 mg) were incubated for 10 min with 4 pM ^{3}H-ES in the absence or presence of 1mM probenecid at 37ºC, or with 4 pM ^{3}H-ES alone at 4ºC. At the end of each assay, total slice content from each well was analyzed for ES accumulation. Assays were run in duplicate. Each bar represents mean ES content (fmol/mg protein) ± SE, n=4. * Significanlty different from control (ES) value (P<0.001). # Significantly different from treatment with probenecid (P<0.001). Data were analyzed by One Way Repeated Measures ANOVA, followed by Student-Newman-Keuls analysis with a 95% confidence interval.

4.2.1.4 Acetamidophenyl glucuronide accumulation in RCSs

Accumulation of AG in RCSs was studied in various experiments to determine whether the affinity of AG for OAT transporters may have been affected by the collagenase digestion treatment in the IRPT isolation procedure. If OAT proteins along the basolateral membrane had become partially digested, the tubule fragments may no longer be able to recognize AG as a potential substrate. Accumulation studies in RCS allow for the study of glucuronide transport in a model that does not have enzymatically digested proteins, such as OAT. If enzymatic digestion has destroyed a critical recognition site for glucuronide substrates in IRPTs, this may be a reason why the IRPT model appears to lack the ability to demonstrate AG accumulation via carrier protein-mediated mechanisms. If a critical binding site has been digested in the IRPT model, this site should be functional in the RCS model. Therefore, the RCS model should demonstrate a protein carrier-mediated accumulation mechanism for AG, if AG or other glucuronide metabolites are transported across the basolateral membrane by carrier proteins such as OAT1 or OAT3. To assess whether accumulation of AG in RCS differed from that seen in IRPTs, temporal studies were conducted. RCSs incubated over time in the presence of 4.7 μM ^{14}C-AG demonstrates a slightly biphasic accumulation pattern (Fig. 4.36). AG accumulation in RCS occurs rapidly during the first 5 min, and reaches an apparent equilibrium by 20 min. At 45 min, accumulation appears to begin to increase, however this increase may be due to loss of slice integrity with increased accumulation within interstitial spaces, or increased binding to exposed intracellular proteins.

To determine whether AG accumulation in slices is due to carrier protein-mediated process temperature sensitive studies were conducted. At the same time studies were conducted to determine the effects of probenecid on AG accumulation. Inhibition of AG accumulation by probenecid would give an indication of the role of OAT in AG accumulation in this model. RCS incubated

with 4.7 μM ^{14}C-AG at 4ºC demonstrated a significantly lower accumulation of AG than RCSs incubated at 37ºC (Fig. 4.37). AG accumulation was inhibited at 4ºC by approximately 30%. While this is not a large degree of inhibition, it indicates that there may be some protein-mediated process for AG accumulation in RCS. No inhibition was seen in the IRPT model. When RCSs were incubated with 4.7 μM ^{14}C-AG in the absence or presence of 1mM probenecid, AG accumulation was significantly inihibited (Fig. 4.37). Accumulation of AG was inhibited approximately 22%. This probenecid sensitivity of AG accumulation in RCSs indicates that OAT may play a small role in AG accumulation in this model. It is important to note, however, that there is a large amount of AG accumulation that is not accounted for by either a temperature-dependent, carrier protein-mediated mechanism, or by a probenecid-sensitive (OAT) mechanism (70% and 78%, respectively).

To study further whether AG interacts with OAT proteins along the tubular basolateral membrane in RCS, PAH and ES were used as potential competitive inhibitors of AG accumulation. PAH was used to assess both OAT1 and OAT3, and ES used to assess primarily the OAT3 contribution. RCSs incubated with 4.7 μM ^{14}C-AG in the absence or presence of either 1mM PAH or 500 μM ES did not demonstrate inhibition of AG accumulation in RCSs (Fig 4.38). This finding is similar to that found in IRPTs for ES, and further indicates that OAT1 and OAT3 may not be responsible for AG accumulation in this model.

Since AG accumulation did not appear to be due to OAT transport along the basolateral membrane, self-inhibition studies were conducted to further characterize the presence of a protein carrier-mediated uptake mechanism, as demonstrated by the temperature dependent studies. While uptake does not appear to be via OAT proteins, there may be other protein carriers responsible for AG accumulation in the RCS model. However, RCSs incubated with 4.7 μM ^{14}C-AG in the absence or presence of 500 μM unlabeled AG did not show

inhibition of AG accumulation (Fig. 4.39). This indicates that AG accumulation in the RCS model is not due to a carrier protein-mediated process, supporting the results found in the IRPT model. Accumulation of AG must, therefore, be due to other mechanisms such as non-specific binding.

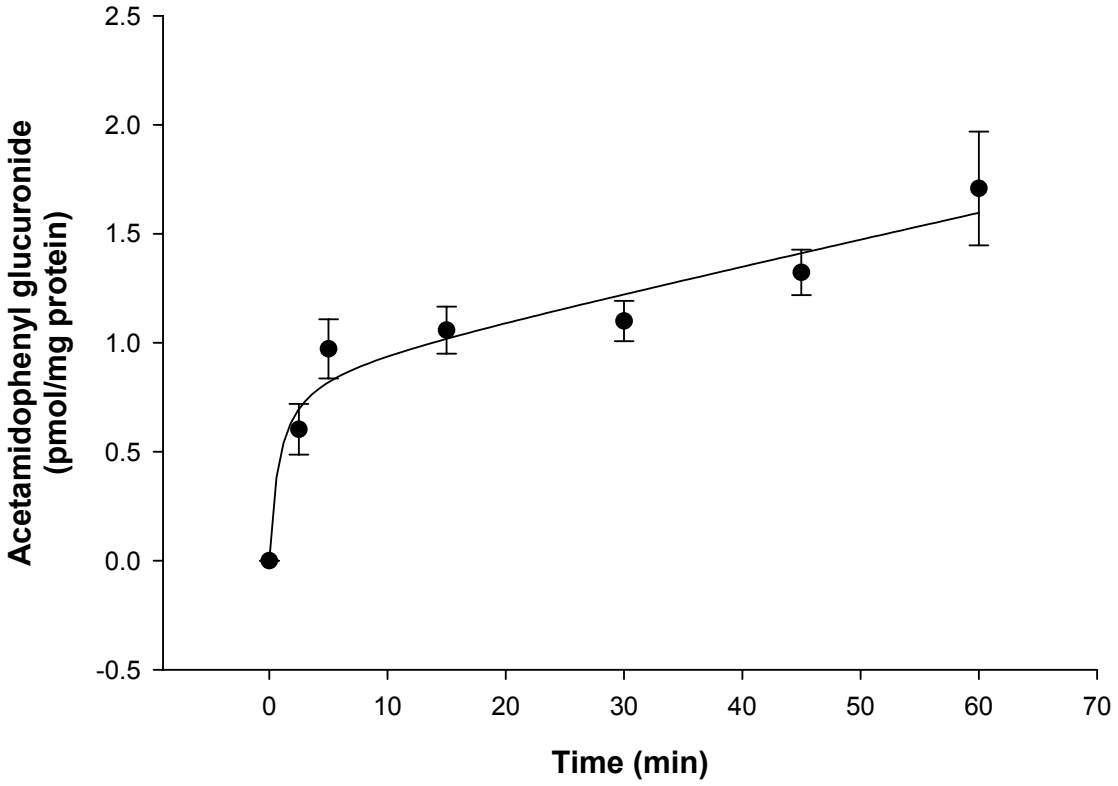

Figure 4.36 Time-dependent accumulation of acetamidophenyl glucuronide in RCSs. RCS (30-60 mg) were incubated for 2.5, 5, 15, 30, 45 or 60 min in the presence of 4.7 μM ^{14}C-AG. Slices were incubated at 37ºC in a shaking water bath (100 rpm). At the end of each time point total slice content of each well was analyzed for AG accumulation. Each assay was run in duplicate. Each point represents mean AG content (pmol/mg protein) ± SE for n=3. Data were analyzed by Nonlinear Regression analysis [(f=a*x/(b+x)+c*x); r^2=0.96].

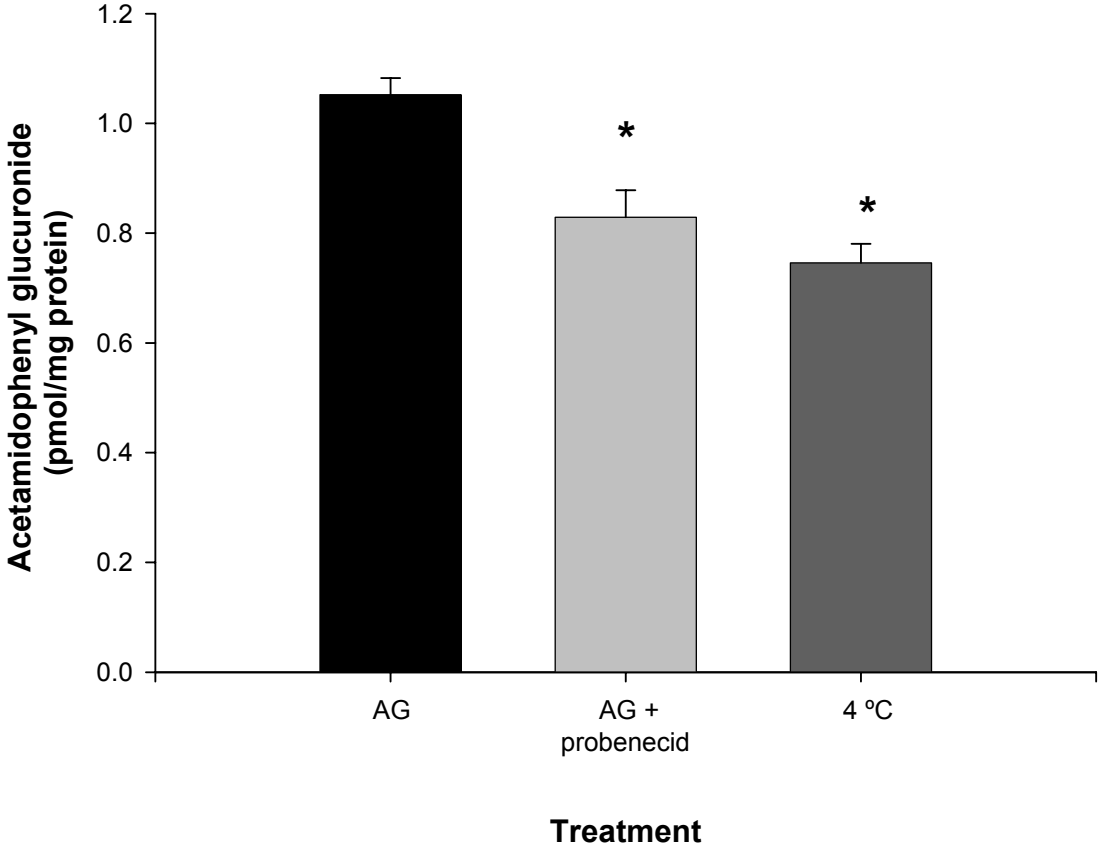

Figure 4.37. The effect of temperature and probenecid on AG accumulation in RCSs. To determine the effects of temperature on AG accumulation, RCSs (30-60 mg) were incubated for 30 min with 4.7 μM ^{14}C-AG at either 37ºC or at 4ºC. To determine the effect of probenecid on AG accumulation, RCSs were incubated for 30 min with 4.7 μM ^{14}C-AG at 37ºC in the absence or presence of 1 mM probenecid. Slices were incubated in a shaking water bath (100 rpm). At the end of each assay, total slice content from each well was analyzed for AG accumulation. Each assay was run in duplicate. Each bar represents mean AG content (pmol/mg protein) ± SE for n=4. * Significantly different from control (AG) values ($P<0.05$). Temperature and probenecid treatments were not significantly different from each other. Data were analyzed by One Way Repeated Measures ANOVA, followed by Student Newman-Keuls analysis at a 95% confidence interval.

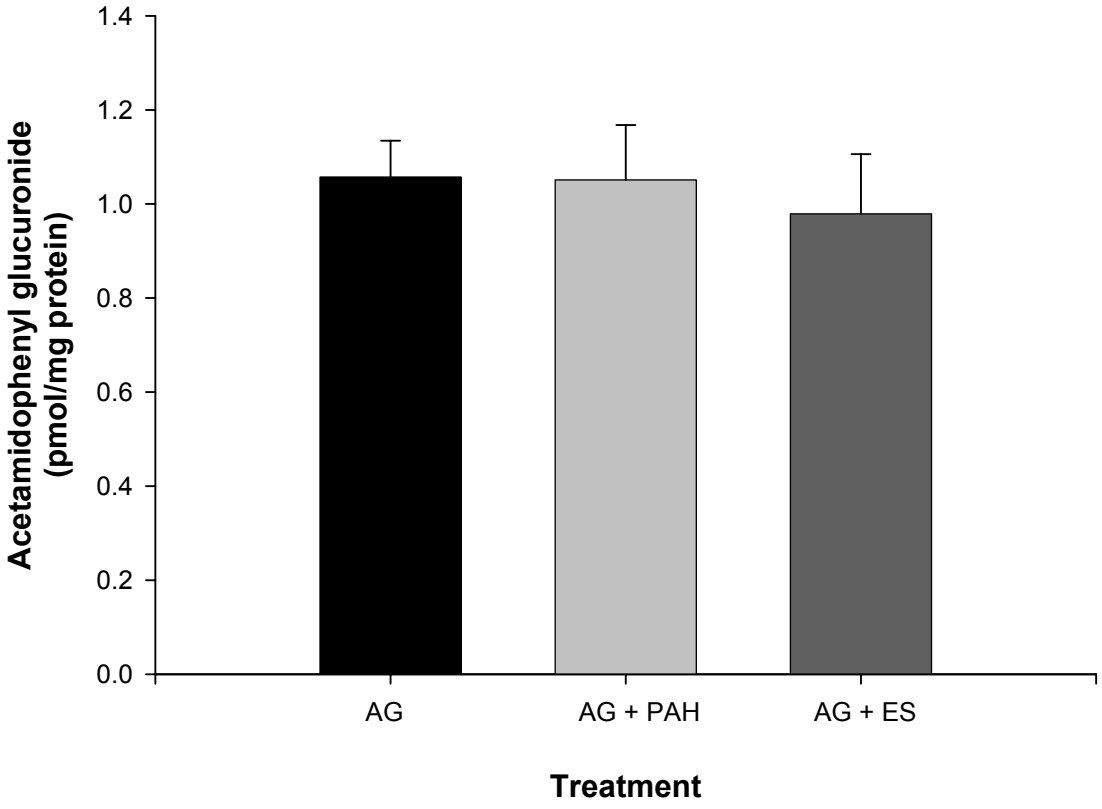

Figure 4.38. The effect of p-aminohippuric acid and estrone sulfate on AG accumulation in RCSs. To determine the effects of PAH and ES on AG accumulation, RCSs (30-60 mg) were incubated for 30 min with 4.7 μM ^{14}C-AG in the absence or presence of either 1 mM PAH or 500 μM ES. Slices were incubated at 37ºC in a shaking water bath (100 rpm). At the end of each assay, total slice content from each well was analyzed for AG accumulation. Each assay was run in duplicate. Each bar represents mean AG content (pmol/mg protein) ± SE for n=5. Incubation with PAH or ES did not significantly inhibit AG accumulation in RCSs. Data were analyzed by One Way Repeated Measures ANOVA.

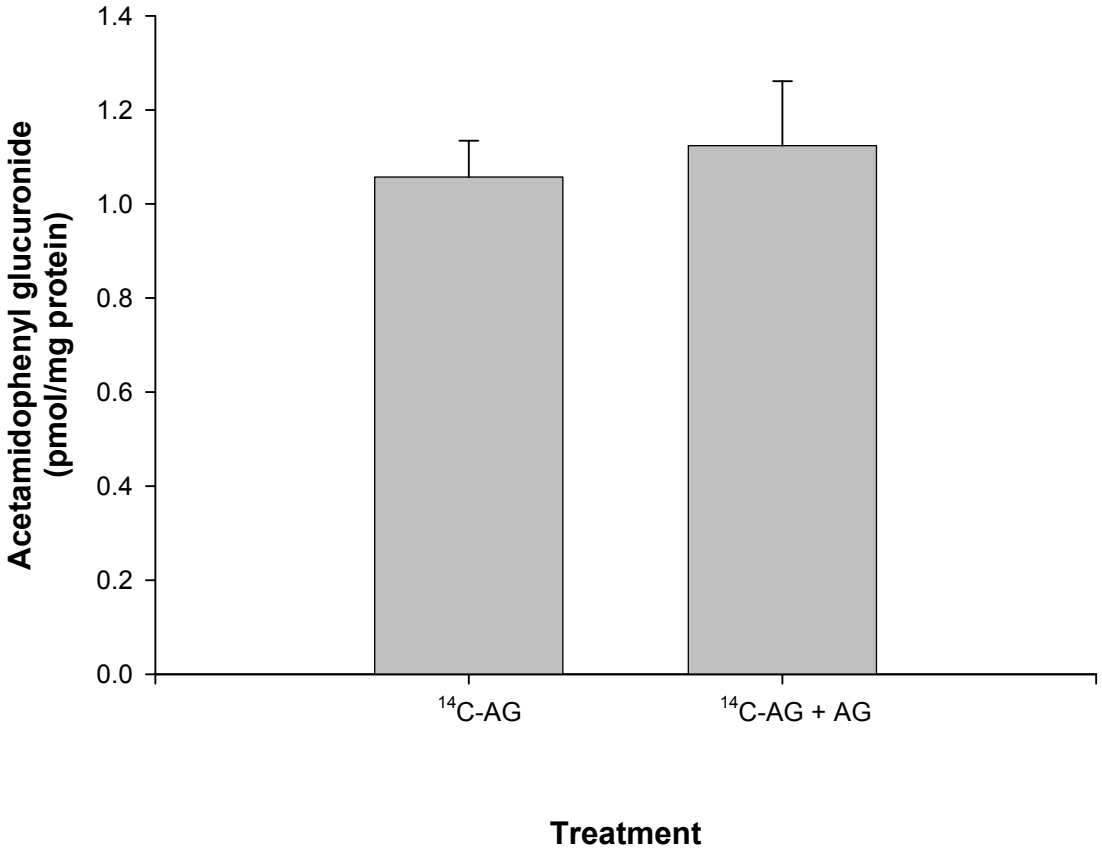

Figure 4.39. The effect of self-inhibition on AG accumulation in RCSs. To determine the effect of self-inhibition on AG accumulation, RCSs (30-60 mg) were incubated for 30 min with 4.7 μM ^{14}C-AG in the absence or presence 500 μM unlabeled AG. Slices were incubated at 37ºC in a shaking water bath (100 rpm). At the end of each assay, total slice content from each well was analyzed for AG accumulation. Each assay was run in duplicate. Each bar represents mean AG content (pmol/mg protein) ± SE for n=5 (^{14}C-AG) or n=4 (^{14}C-AG+AG). Incubation with excess AG did not significantly inhibit AG accumulation in RCSs. Data were analyzed by Student's t-test with a 95% confidence interval.

4.2.1.5 Acetamidophenyl glucuronide accumulation in RCSs from Sprague-Dawley (SD) rat

Studies conducted in IRPTs and RCSs from male F344 rat provided evidence that these models are able to accumulate organic anions such as FL, PAH and ES. Uptake of these molecules was carrier protein-mediated, and determined to be via OAT transport proteins. However, these models did not demonstrate that accumulation of AG was due to a protein-mediated process, and more importantly, accumulation does not appear to be via OAT mechanisms along the basolateral membrane of the PT. Because studies that have indicated renal secretion of AG were conducted in other rat strains (SD; Galinsky and Levy, 1981) (Wistar; Watari et al. 1983), it was necessary to investigate whether studies in a different rat strain would produce different results. Possibly the F344 rat does not have the same renal OAT substrate specificities as other rat strains. To investigate whether AG accumulation can be documented in another rat strain, male SD rats were chosen for this study, and RCS selected as the model (to eliminate collagenase digestion issues).

To determine whether AG accumulation appeared to be via a carrier protein-mediated process, temperature-dependent studies were conducted. Probenecid sensitivity was used to determine whether AG accumulation across the basolateral membrane is an OAT-mediated process. RCSs from male SD rats incubated with 4.3 μM ^{14}C-AG at 4ºC demonstrated significantly reduced AG accumulation (Fig. 4.40). Incubation at 4ºC decreased AG accumulation approximately 29%. This finding is similar to that found in RCS from F344 rats (30%). However, when RCSs were incubated with 4.3 μM ^{14}C-AG in the presence of 1 mM probenecid, no reduction of AG accumulation was found (Fig 4.40). This finding differs from that found in F344 RCSs. Most importantly, this indicates that AG accumulation, while it may have a small protein-mediated component, does not appear to be via OAT in SD RCSs.

To document further any potential interaction of AG with OAT proteins along the basolateral membrane, PAH was selected as a competitive inhibitor of AG accumulation. RCSs incubated with 4.3 μM ^{14}C-AG in the presence of 1 mM PAH showed no inhibition of AG accumulation (Fig. 4.41). This again indicates that AG uptake does not appear to be via OAT proteins along the basolateral membrane of the renal PT.

To verify whether apparent AG accumulation is truly via a carrier protein-mediated process, self-inhibition studies were conducted in RCSs from male Sprague-Dawley rats as had been conducted in Fischer 344 models. RCSs incubated with 4.3 μM ^{14}C-AG in the presence of 500 μM unlabeled AG demonstrated no inhibition of AG accumulation in this model (Fig. 4.42). This result again demonstrates that AG accumulation is via a mechanism(s) other than carrier protein-mediated process.

Together, these findings demonstrate that AG accumulation in SD rat is comparable to that found in models from F344 rat. AG accumulation does not appear to be mediated by a carrier protein mechanism, and cannot be demonstrated to be due to OAT proteins at the basolateral membrane of the PT in either F344 or SD rat strains. Accumulation of AG must, therefore, be due to other mechanisms.

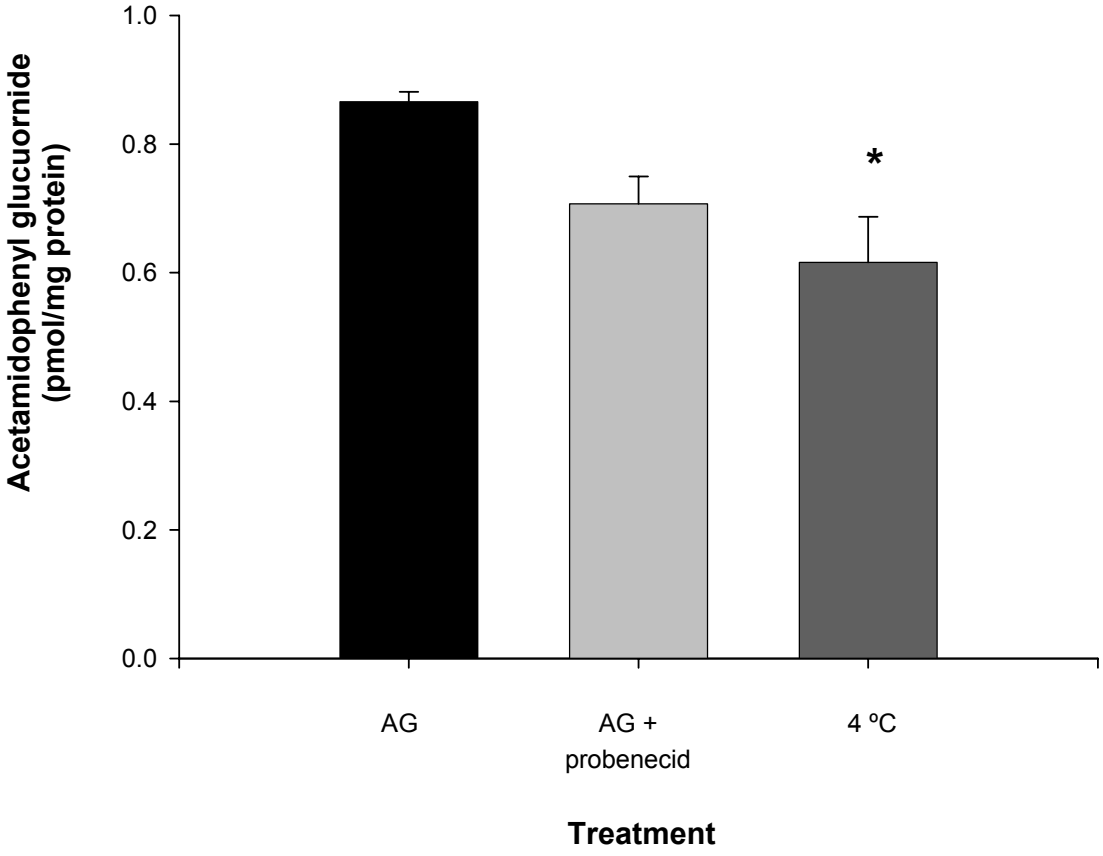

Figure 4.40. The effect of temperature and probenecid on AG accumulation in RCSs from Sprague-Dawley rat. To determine the effects of temperature on AG accumulation, SD RCSs (30-60 mg) were incubated for 30 min with 4.3 μM ^{14}C-AG at either 37ºC or at 4ºC. To determine the effect of probenecid on AG accumulation, RCSs were incubated for 30 min with 4.3 μM ^{14}C-AG at 37ºC in the absence or presence of 1 mM probenecid. Slices were incubated in a shaking water bath (100 rpm). At the end of each assay, total slice content from each well was analyzed for AG accumulation. Each assay was run in duplicate. Each bar represents mean AG content (pmol/mg protein) ± SE for n=4. *Significanlty different from control (AG at 37ºC) values ($P<0.05$). Data were analyzed by One Way Repeated Measures ANOVA, followed by Dunnett's analysis with a 95% confidence interval.

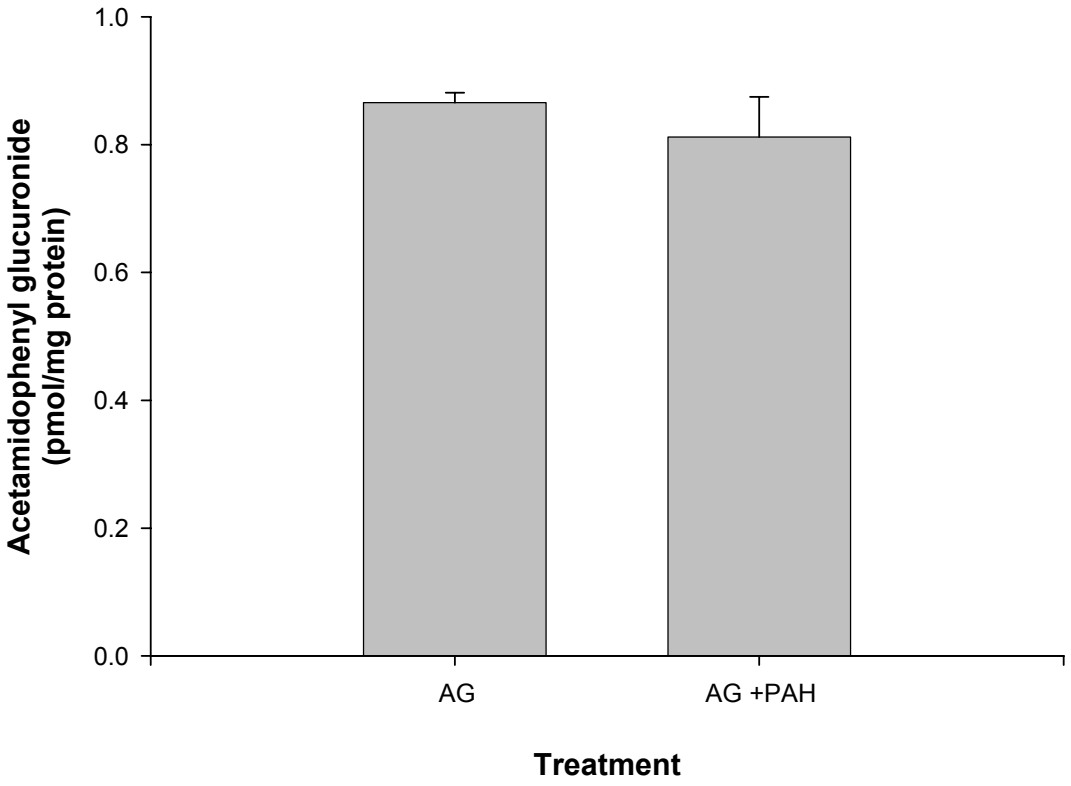

Figure 4.41. The effect of *p*-aminohippuric acid on AG accumulation in RCSs from Sprague-Dawley rat. To determine the effects of PAH on AG accumulation, SD RCSs (30-60 mg) were incubated for 30 min with 4.3 μM ^{14}C-AG in the absence or presence of 1 mM PAH. Slices were incubated at 37ºC in a shaking water bath (100 rpm). At the end of each assay, total slice content from each well was analyzed for AG accumulation. Each assay was run in duplicate. Each bar represents mean AG content (pmol/mg protein) ± SE for n=4. Incubation with PAH did not significantly inhibit AG accumulation in RCSs. Data were analyzed by Student's t-test with a 95% confidence interval.

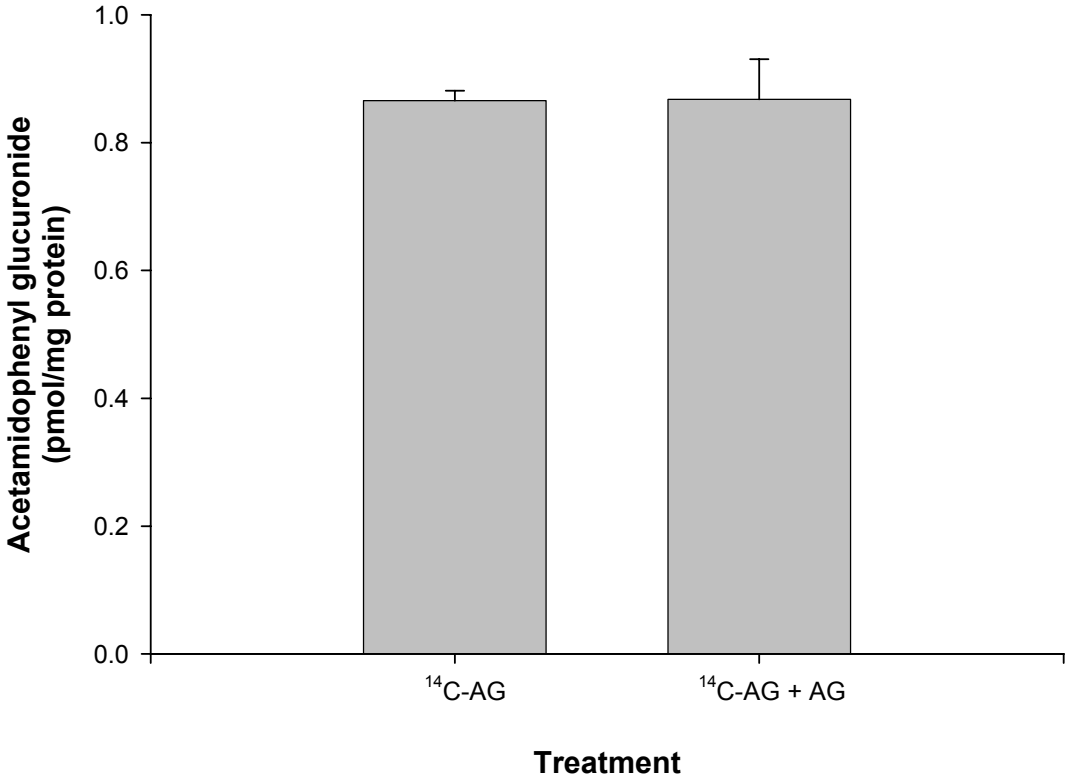

Figure 4.42. The effect of self-inhibition on AG accumulation in RCSs from Sprague-Dawley rat. To determine the effect of self-inhibition on AG accumulation, SD RCSs (30-60 mg) were incubated for 30 min with 4.3 μM ^{14}C-AG in the absence or presence 500 μM unlabeled AG. Slices were incubated at 37ºC in a shaking water bath (100 rpm). At the end of each assay, total slice content from each well was analyzed for AG accumulation. Each assay was run in duplicate. Each bar represents mean AG content (pmol/mg protein) ± SE for n=4. Incubation with excess AG did not significantly inhibit AG accumulation in S-D RCSs. Data were analyzed by Student's t-test with a 95% confidence interval.

CHAPTER V

Discussion

5.1 Characterization of IRPTs

Characterization of IRPTs utilized for organic anion uptake in these studies involved enzymatic analysis and visual assessment. Because the isolation technique for IRPTs from rat has been established previously, only minor characterization was necessary. The main objective of this characterization was to establish that the population of renal tissue isolated from the male F344 kidney was enriched in proximal tubular segments. Hexokinase (HK) and alkaline phosphatase (AP) enzyme assays demonstrated that the tubular samples isolated are of PT origin. Microscopic examination also revealed that the population of tubules isolated was primarily of proximal tubular origin, and there was no glomerular contamination. Viability for IRPTs was found to be approximately 89%, indicating that the tubule fragments were not damaged in the isolation process. Western blot analysis also demonstrated the presence of OAT1 and OAT3 proteins in IRPTs. Enzymatic, microscopic and Western blot analysis demonstrated that IRPTs isolated from male F344 rat are greatly purified, intact, and contain both OAT1 and OAT3 proteins, demonstrating that the IRPTs isolated can be used to study OA transport.

5.2 Toxicity Studies

Toxicity studies utilizing APAP and AG both demonstrated that these compounds are non-toxic in the IRPT model. Both LDH release and nucleotide levels remained at control levels indicating that these compounds do not cause

any type of toxic reactions within the proximal tubular cells at the concentrations and time points studied. This allowed for the study of transport of AG knowing that AG did not interfere with any cellular mechanisms (e.g., ATP production) that may be directly connected to the ability of the cells to transport the compound.

Studies with DC provided important new information on the toxicity of this compound in the IRPT model. Diclofenac had been associated with nephrotic syndrome and acute interstitial nephritis, however, the exact mechanism of DC toxicity in the kidney is not fully understood. Initial studies conducted at 30 min demonstrated that DC was mildly toxic at both concentrations. LDH release was significantly increased over control LDH release values, and ATP and ADP levels were significantly depressed compared to control nucleotide values. To determine whether this toxicity originated with an early toxicity event (e.g., depression of mitochondrial function and thus altered ATP production) or whether toxicity appeared to be a whole cell event, as demonstrated by cellular LDH release, studies were reduced to a 15 min time frame. At 15 min, LDH release was not elevated compared to control values, however, ATP levels showed significant depression over control values. This finding demonstrates that the early events in DC toxicity appear to result in the alteration of mitochondrial production of ATP, or, due to a toxic cellular reaction, the cellular needs for ATP exceed the ability of the cells to produce ATP. This finding is in agreement with those of Bort et al. (1998), demonstrating that acute diclofenac-induced toxicity in hepatocytes was preceded by a decrease in ATP levels. Bort et al. (1998) concluded that the toxic effect of diclofenac on hepatocytes may have been caused by drug-induced mitochondrial impairment. These results appear to be similar to those found in this study in the kidney. Whether this toxic event is due to the diclofenac molecule or another metabolite (such as DC-acyl glucuronide) remains to be clarified.

5.3 OAT1 and OAT3 studies in IRPTs

Because the transport of organic anions across the basolateral membrane of renal PTs from F344 rats has not been studied previously, it was important to demonstrate the transport of known organic anions (FL, PAH, ES) by the IRPT model. In studying transport of organic anions, inhibition of OA uptake by various mechanisms (low temperature, inhibitors, and self-inhibition) helped characterize the function of the transport proteins (primarily demonstrating the presence of OAT1 and OAT3) along the basolateral membrane of the IRPT model. Time and temperature-dependent accumulation of FL demonstrated that FL accumulation is a protein-mediated process. Further studies using competitive inhibition of FL, PAH and ES accumulation also demonstrated that accumulation of these OAs supported a protein-mediated process. Since FL and PAH are the prototypical substrates for OAT1 and OAT3, this indicates that OAT1 and/or OAT3 transporters are present and functional along the basolateral membrane in IRPTs.

Additional evidence of the role of OAT1 and OAT3 in FL transport is the sensitivity of FL accumulation to probenecid, the prototypical OAT inhibitor. Accumulation of PAH and FL has been demonstrated in isolated proximal tubular cells from Wistar rat and additional studies concluded that in isolated cells, accumulation of FL and PAH was mediated by a carrier at the basolateral membrane (Masereeuw et al., 1994). Findings of the present study are in agreement with these findings as accumulation of both FL and PAH appear to be carrier-mediated. Additionally, FL and PAH appear to undergo accumulation via similar or the same transport mechanisms along the basolateral membrane (OAT1 and OAT3). Sensitivity of FL accumulation to ouabain additionally supports uptake of this compound by OAT1. Treatment of IRPTs with ouabain resulted in approximately 51% inhibition of FL accumulation, providing indirect, supportive evidence that OAT1 is partially responsible for FL accumulation in IRPTs. These findings are in agreement with those found in isolated PTs from

rabbit by Sullivan et al. (1990), thus indicating the role for the classical organic anion system in FL accumulation in the IRPT model. FL transport was also sensitive to inhibition by the OAT3 substrates benzylpenicillin (40%) and DHEA sulfate (82%), indicating a role for OAT3 in FL accumulation as well. The degree of inhibition of DHEAs appears to indicate that at high concentrations (1 mM), DHEAs loses its specificity for OAT3 and appears to inhibit OAT1 transport as well. This is supported by the fact that Hasegawa et al. (2003) demonstrated DHEAs inhibition of rOAT1 PAH uptake. Hasegawa et al. (2003) also demonstrated inhibition of PAH accumulation by rOAT1 with benzylpenicillin, however, the concentrations of benzylpenicillin needed to inhibit FL transport appear to be higher to produce comparable inhibition of FL transport by DHEAs.

Because there is overlap with FL and PAH for transport by OAT1 and OAT3, it is difficult to determine the exact contribution of each transporter in total accumulation of FL and PAH. The potential role of other transporters besides OAT1 and OAT3 can also not be ruled out. Accumulation of ES, the prototypical OAT3 substrate, suggests that OAT3 transporters are also present and functional in the IRPT model, and provides a useful substrate to probe the contribution of OAT3 along the basolateral membrane. Probenecid sensitivity for FL, PAH and ES also provided supporting evidence that accumulation of these compounds is via organic anion transport proteins along the basolateral membrane, as probenecid is the prototypical inhibitor of OAT transport.

While the use of ES helped to identify the function of OAT3 in this model, it does not appear to demonstrate the expected inhibition by probenecid and temperature as would be expected with OAT3 transport. Very weak inhibition by probenecid (41%) and treatment at 4ºC (38%) indicates that there may be other mechanisms for ES accumulation in this model, be it via other non-OAT transporters, or nonspecific binding. Sweet et al. (2003) demonstrated nearly complete inhibition of ES via rOAT3 (~88%) in rOAT3 transfected oocytes. Self-inhibition studies of ES accumulation further support that there may be other mechanisms than OAT transport for ES in this model as self-inhibition provided a

greater level of inhibition of ES than either probenecid treatment or reduction in temperature.

It is important to note that recent studies have shown that OAT1 and OAT3 share similar mechanisms of action as dicarboxylate exchangers indirectly coupled to the sodium gradient (Sweet et al., 2003). Since there is a great deal of overlap in substrate specificity with FL and PAH for OAT1 and OAT3, it cannot be definitively stated that both of these transporters are functional in this model based on data obtained for FL, PAH and ES accumulation by IRPTs. Since both OAT1 and OAT3 may function via a similar mechanism (dicarboxylate exchange coupled to the sodium gradient), OAT1 and OAT3 may be sensitive not only to probenecid but also to ouabain as ouabain would affect the ability of the cells to maintain the sodium gradient necessary for transport via. Whether ouabain interferes with OAT3 transport remains to be clarified in this model. Cha et al. (2001) and Kusuhara et al. (1999) demonstrated that hOAT3 and rOAT3 expressed in oocytes were not inhibited by ouabain. This raises the question as to the driving force of OAT3 transport, whether OAT3 is also dependent on the Na^+/K^+ ATPase to maintain the sodium gradient for α-ketoglutarte, thus maintaining the α-ketoglutarte gradient to drive OAT3 transport.

5.4 Acetamidophenyl glucuronide accumulation in IRPTs

OAT proteins, specifically OAT3, have been demonstrated to transport the glucuronide conjugate 17β-estradiol-d-17β-glucuronide. In the IRPT model, OAT1 and OAT3 appear to be functional, transporting the known organic anions PAH (OAT1 and OAT3) and ES (OAT3). Since glucuronide metabolites are organic anions at physiological pH, AG may be a substrate for the OAT transporters along the basolateral membrane of the renal PT. This is the first time that IRPTs have been used to study the renal handling (secretory process) of a non-steroid glucuronide conjugate across the basolateral membrane of the renal PT. While rOAT3 has been shown to transport estradiol glucuronide, it has

not been determined whether transport of estradiol glucuronide relies on the glucuronide moiety, or the steroid structure. Previous studies that have assessed renal secretion of AG have used whole animal studies where the exact nature of the interaction of AG with renal OAT transporters cannot be determined. Use of the IRPT model to study renal AG secretion allows for the assessment of the interaction of the AG molecule directly with the basolateral membrane, and thus, the transport proteins (OAT1 and OAT3 primarily) that are active along that membrane.

The accumulation of AG in IRPTs does not support protein-mediated uptake across the basolateral membrane. While AG accumulation appears to have a time-dependent factor for accumulation, uptake can not be deminished by reduction of temperature to 4ºC. Since uptake is not temperature dependent, it indicates that accumulation is not by a protein-mediated mechanism, and is more likely due to non-specific binding of the AG molecule to proteins along the tubule, or gradual accumulation into interstitial spaces between the proximal tubular cells, as rat PTs in general are noted to be significantly leaky. In addition to not being temperature sensitive, self-inhibition studies using 1000-fold excess unlabeled AG did not show inhibition of AG accumulation as well. This again demonstrates that apparent accumulation of AG is not due to a protein-mediated process.

As it has been shown that AG accumulation does not appear to be a protein-mediated process, more specifically, it does not appear to be mediated by OAT proteins along the basolateral membrane of the IRPTs. Cotreatment with AG was not able to inhibit the accumulation of the known OAs, FL, PAH or ES. In addition, the accumulation of AG was not inhibited by the presence of ES. This demonstrates that AG does not appear to interact with the organic anion transporters OAT1 or OAT3 along the basolateral membrane in this model. In addition, AG accumulation was also not found to be probenecid sensitive, again showing that AG does not appear to interact with OAT proteins in this model. This finding supports the finding by Duggin and Mudge (1975) that AG secretion

did not appear to be probenecid sensitive, while the secretion of the sulfate conjugate was. Additionally, AG accumulation was not found to be influenced by metabolism (deconjugation) during incubation with IRPTs, as inhibition of β-glucuronidase activity had no effect of AG accumulation. The fact that inhibition of glucuronide deconjugation did not affect the results of AG accumulation in IRPTs shows that results obtained in these experiments are due directly to movement of the AG molecule and not deconjugation to the parent compound APAP.

5.5 OAT1 and OAT3 studies in RCSs

To assure that these studies were not compromised by inadequate activity of OAT proteins due to partial enzymatic digestion, a number of studies were also carried out in renal cortical slices. Since AG appears to have extremely limited affinity for OAT transporters, it was necessary to demonstrate that collagenase digestion during the IRPT preparation did not have a detrimental effect on the activity of OAT transporters. If the OAT transporters had become partially digested during the PT isolation procedure, their ability to interact with AG may have been greatly weakened, or collagenase digestion may have left fewer functional OAT transporters along the basolateral membrane of the tubules. Partial digestion of membrane OAT proteins could potentially account for the apparent lack of AG transport by basolateral OAT proteins.

Initial OAT transporting capabilities were tested with PAH and ES. RCS demonstrated probenecid sensitive uptake of both PAH and ES, as well as time and temperature dependent accumulation of ES. Time-dependent accumulation of ES by RCS follows a similar pattern as that determined by Sweet et al. (2003) and Hasegawa et al. (2003), with nearly linear uptake for the first 15 min and approaching steady state during the subsequent 45 min. Additionally, uptake of ES was concentrative. These PAH and ES accumulation studies indicate that the OAT transporters are functional in this model and this model could be used to

study the interactions between OAT transporters and AG. Probenecid inhibition of PAH uptake was approximately 80% which was very similar to inhibition in IRPTs (86%). ES accumulation also appeared to show similar results as those found in IRPTs. Inhibition of ES with probenecid demonstrated a 33% inhibition in RCSs, which is similar to the 41% inhibition found in IRPTs, indicating that the same mechanisms for ES accumulation are in place in both models. Interestingly, Sweet et al. (2003) demonstrated nearly twice the amount of inhibition of ES accumulation by probenecid (66%) in their rat renal cortical slice model. This indicates that in the F344 rat, there may be a lower level of expression of OAT3 compared to other rat strains. This was further supported by Western blot analysis, demonstrating only weak labeling for OAT3 in the F344 kidney.

Temperature-sensitive uptake of ES in RCSs however, appeared quite different than in IRPTs. In RCSs, reduction of temperature to 4ºC caused an 80% reduction in ES accumulation, whereas in IRPTs, it only inhibited ES uptake by 38%. This seems to indicate that there are also mechanisms of ES accumulation other than OAT3 in the RCS model, as in the IRPT model, that may be more sensitive to the effects of collagenase digestion. While non-specific binding appears to be less in the RCS than in the IRPT model, the amount of ES accumulation accounted for by OAT3 (probenecid sensitive) appears to be similar. Since these results in general appear similar to those found in IRPTs, the similarity of results in both RCS and IRPT models indicates that in the IRPT model, the digestion of proteins did not appear to affect OAT transporting capabilities. Additionally, both the RCS and IRPT models appear to show similar capabilities for OAT transport and both are useful models for studying the effects of OAT transport on AG accumulation in the renal PT.

5.6 Acetamidophenyl glucuronide accumulation in RCSs

In renal cortical slices, AG accumulation appears to demonstrate possible protein-mediated transport. Temperature-dependent uptake showed only a 30% decrease in AG accumulation, indicating that while it appears there may be some type of protein-mediated transport, there is still a large amount of AG accumulation that cannot be accounted for by a protein-mediated transport mechanism (e.g., non-specific binding). However, while temperature and probenecid sensitivity can indicate a carrier-mediated OAT mechanism lack of self-inhibiton of AG accumulation is a more accurate determination of whether a carrier-mediated mechanism exists for AG accumulation. Self-inhibition studies did not demonstrate any inhibition of AG accumulation. Lack of self-inhibition in AG accumulation provides a conflicting result to the temperature-dependent study. Since self-inhibition failed to demonstrate inhibition of AG accumulation, this suggests that AG accumulation is actually not a protein-mediated process in this model and provides additional new in vitro data that may help to clarify in vivo results found by other investigators.

OAT proteins in RCSs do not appear to play a major role in AG accumulation at the basolateral membrane. AG accumulation in RCSs was only weakly inhibited (22%) by treatment with probenecid, indicating a very weak interaction at OAT proteins. More importantly, however, is the finding that cotreatment of AG with PAH or ES was not able to inhibit the accumulation of AG in RCSs. This strongly suggests that AG does not interact with OAT1 and OAT3 along the basolateral membrane. These findings are similar to those found in IRPTs.

To assure that the results found in male F344 rats were not a strain-dependent phenomenon (i.e., this strain may show a lower expression of OAT transporters than another strain), AG accumulation was also studied in RCSs from male SD rats. AG has been suggested to undergo renal secretion in SD rats (Galinsky and Levy, 1981) as well as Wistar rats (Watari et al. 1983).

Findings in SD rats, however, did not support the findings of Galinsky and Levy (1981), and rather supported those found in this lab in F344 rats. Decreasing the incubation temperature inhibited AG accumulation by only 29%, similar to that found in RCSs from F344 rats. Self-inhibition studies however, did not demonstrate any inhibition of AG accumulation. This finding is also the same as the findings in F344 rat and reconfirms that AG accumulation is not via a protein-mediated process. AG accumulation in RCSs from SD rats was also not probenecid sensitive, indicating that AG accumulation is not via OAT proteins. The finding that AG is not transported by OATs was further verified by the fact that AG accumulation was not inhibited by the presence of PAH, a known OAT substrate. These findings demonstrate that the results found in F344 rats are not a rat strain-dependent phenomenon, and AG accumulation does not appear to undergo protein-mediated transport, and more specifically does not interact with OAT transporters along the basolateral membrane of the renal PT in rat models.

While AG does not appear to undergo transport in this model, it does appear to accumulate via some mechanism. It is possible that this accumulation is actually by non-specific binding. The studies that examined mannitol uptake actually further suggest that AG accumulation may be due to protein binding, as AG accumulation is much greater than mannitol accumulation, as can be seen by the time-dependent accumulation of each compound. Mannitol uptake, which measures the amount of substrate accumulation into water filled spaces is much smaller than that of AG, indicating that while AG may also accumulate in spaces between the cells in both IRPTs and RCSs, there appers to be another factor to AG accumulation that is not accounted for by transport or accumulation into spaces. This mechanism is quite possibly via protein binding within the tissue, or intercalation of the APAP portion of the AG molecule into the surface of the IRPT or RCS, since APAP is lipid soluble and can undergo diffusion through membranes.

5.7 Interaction of glucuronide metabolites with OAT1 and OAT3 in IRPTs and RCSs

While studies using AG have indicated that this glucuronide metabolite does not interact with OAT1 or OAT3 transporters along the basolateral membrane, it was important to determine whether other glucuronide metabolites may interact with transporters along the PT basolateral membrane. To study the potential interaction of other glucuronide metabolites with OAT, PAH was used as the prototypical substrate to determine whether testosterone glucuronide (TG) or methylumbelliferyl glucuronide (MUG) demonstrated any interaction with the transport of PAH (OAT1 and OAT3). Since TG is a steroid, studies with TG may potentially help to elucidate the role of the steroid portion of the molecule in transport across the basolateral membrane vs. the glucuronide portion of the moiety, helping determine whether there is a difference in transport of steroid glucuronides and non-steroid glucuronides. MUG is a non-steroid glucuronide metabolite of a similar molecular weight as AG (352.3 and 349.3, respectively). Studies conducted in both IRPTs and RCSs from F344 rats showed that these glucuronide metabolites do not appear to inhibit the accumulation of PAH along the basolateral membrane. In these studies AG was also used as a secondary control for the effects of TG and MUG. Treatment with TG and MUG were not statistically different from AG treatment, suggesting that TG and MUG may possibly interact along the basolateral membrane in a similar manner as AG. The fact that TG and MUG do not interfere with PAH accumulation suggests that these glucuronide metabolites do not interact with OAT proteins along the basolateral membrane of rat PTs, and may be transported or enter the proximal tubular cells by other mechanisms.

5.8 Conclusion

The present study provides some of the first characterization of organic anion transport in the F344 rat. Several studies have been conducted in SD and Wistar rats, but to date, information in the F344 model is lacking. With the vast amounts of toxicity data for various compounds available in the F344 rat, it is important to more fully understand the function of transport mechanisms for potentially toxic compounds in the F344 rat model. With the information gained in this study, it can help to better understand the mechanisms of cellular entry of potentially toxic compounds. Uptake of organic anions appears to follow similar patterns in both IRPT and RCS from Fisher 344 rats. In the IRPT model, collagenase digestion does not appear to have a negative impact on the ability of this model to demonstrate OA transport, as compared to the RCS model. In general, the RCS model has some benefits over the IRPT model, mainly in technical simplicity. While the isolation procedure for IRPTs is time consuming, the IRPT model offers a highly purified population of PT fragments that are useful for studying the impact of OAT transport in the proximal tubules handling of xenobiotics without the interference of other cell populations.

In terms of glucuronide transport, studies in IRPTs and RCSs from both F344 and SD rats suggest that glucuronide metabolites are not transported by the OAT proteins along the basolateral membrane of rat PTs. While glucuronides are organic anions at physiological pH, it appears that the specificity of these compounds for OAT is extremely low, and if they have the ability to cross the basolateral membrane, it is via another mechanism. It is also important to note that the findings presented in these studies do not support the findings found in the literature. The findings of Duggin and Mudge (dog; 1975), Galinsky and Levy (SD rat; 1981), and Watari et al. (Wistar rat; 1983) have all suggested that the kidneys possess the ability to secrete glucuronide metabolites, and demonstrate renal secretion with AG. The conflicting findings with those of Duggin and Mudge (1975) may be accounted for by species

differences in transporters along the basolateral membrane of the renal PT (rat vs. dog). However, similar results were expected in these studies as those found by Galinsky and Levy (1981) and Watari et al. (1983), who suggested renal secretion of AG in rat models.

Upon thorough study of the findings in these papers, there were a number of mechanistic discrepancies that may account for the conflicting results between their studies and those found in this present study. During studies on the renal clearance of AG in SD rats conducted by Galinsky and Levy (1981), control rats for renal CL_{CR} were not the same rats used for studying AG clearance. Since AG clearance values and CL_{CR} values were not conducted in the same rats at the same time, the actual CL_{CR} values determined do not reflect any potential effects that AG itself may have on renal clearance, and therefore CL_{CR} values. Therefore, the clearance of AG may have appeared to be higher than control renal creatinine clearance, thus indicating secretion. To accurately determine the true AG clearance in the model, AG treatment and clearance should have been conducted on the same rats at the same time, and control values should not have been determined in a separate group of rats. A similar discrepancy also occurs with the study conducted in Wistar rats by Watari et al. (1983). In the study conducted by Watari et al. (1983) control CL_{CR} values used for comparison with AG clearance values were those determined by Galinsky and Levy (1981) in SD rats. Thus, the same control issues exist. CL_{CR} values and AG clearance values in the study by Watari et al. (1983) were not only measured in separate rats at a separate time, but data was collected in a different rat strain as well. Making the comparison between CL_{CR} in SD rats from one experiment to AG clearance in Wistar rats in a separate experiment, under likely different laboratory conditions, compromises the validity of the results. Therefore, what Watari et al.(1983) demonstrate as secretion of AG, based on AG clearance values in Wistar rats being higher than CL_{CR} in SD rats, cannot be accurate.

The current findings in the literature on the renal secretion of glucuronide metabolites remain limited. AG has been used in a number of studies as it is a

common, renally excreted metabolite of acetaminophen. While the studies mentioned above suggest that the kidney can secrete AG, other conflicting studies suggest that it is not secreted but rather is excreted in the urine solely via glomerular filtration (Heckman et al. 1986). The findings in the present study support the role for glomerular filtration rather than secretion of this glucuronide metabolite (AG) along the basolateral membrane of the PT. Specifically, AG does not appear to be a substrate for renal basolateral membrane OAT proteins in the F344 model. The overall contribution of OAT in the basolateral membrane transport of AG (and potentially other glucuronide metabolites, as suggested by OAT inhibition studies with TG and MUG), is also minimal in the F344 rat. Furthermore, while there appears to be tubular accumulation of AG, the accumulation of AG does not appear to be due to a non-OAT, protein carrier-mediated mechanism along the basolateral membrane. Thus, rat renal basolateral proximal tubular cells do not appear to facilitate the transport of glucuronide conjugates, and thus do not appear to contribute to the renal secretion of glucuronide conjugates by transport mechanisms along the basolateral membrane. If uptake with subsequent secretion is occurring across the basolateral membrane, it is by a mechanism other than a protein-mediated or OAT transport and other mechanisms of flux of AG across the basolateral membrane need to be evaluated.

5.9 Future Directions

To gain a more complete picture of the renal secretion of AG, and potentially other glucuronide metabolites, the other type of information that needs to be gathered is an accurate measurement of the renal secretion of AG in a rat model. Because the papers mentioned in this discussion failed to accurately establish the values of AG clearance, it is difficult to determine whether the data truly reflect AG secretion. Based on the findings of this current study, it is believed that their results do not reflect true AG secretion. Accurate

determination of AG secretion by the rat kidney could be accomplished by repeating data collection for AG clearance in the whole animal with inulin clearance values being measured in the same animals at the same time as APAP or AG clearance. These data would help to clarify the discrepancy between the studies discussed and this one.

As far as determining further the potential role for OAT transporters in the uptake of glucuronide conjugates, particularly AG, the simplest way to accomplish this would be to use rOAT1 and/or rOAT3 transfected cells (i.e., oocytes or LLC-PK_1 cells). Transfected cell models, used frequently in OA uptake studies, would allow for direct contact between the selected transporter without interference from other transport proteins that are present in the basolateral membrane of IRPT and RCS models. By directly treating a cell expressing rOAT1 or rOAT3 with AG, the uptake of AG could be determined, assessing the contribution of each transporter in the renal handling (secretion) of AG.

Another potential for studying further glucuronide transport would be the use of cultured cells. The use of primary cell culture could provide crucial evidence for the renal handling of these conjugates as cells grown on permeable membranes would allow for a dynamic system from which data could be obtained from both the basolateral and luminal membranes of the renal PT. Where this study in IRPT and RCS demonstrated that there did not appear to be a secretory mechanism for AG, it does not address the potential for luminal uptake of the AG compound and potentially other glucuronide conjugates. Primary cultures of renal PTs from F344 rat was the original aim of this study. However, a number of contamination conditions led to the use of IRPTs and RCSs to study the basolateral uptake of AG. Initial characterization of PT cells grown in culture demonstrated that they were of PT origin (based on enzymatic analysis as in the IRPT model) and should, therefore, have been capable of demonstrating OAT-mediated transport. In the right setting, primary cultures would have provided a system similar to the IRPT model (maintenance of cell-to-cell contact and

communication, maintained cellular metabolism and transport) with the benefit of being able to more completely study how the renal PT handles glucuronide conjugates. Again, in addition to the basolateral membrane, the luminal membrane would have also been intact and functional, providing a much more dynamic model for studying the transport of AG.

Another important study that would greatly clarify the findings found in the present study would be to examine the nature of the apparent protein binding of AG. Whether it could be done immunohistochemically or by other means of studying protein binding, it would allow for greater understanding as to the disposition of the AG molecule in the IRPT and RCS model.

Bibliography

Adachi Y, Roy-Chowdhury J, Roy-Chowdhury N, Kinne R, Tran T, Kobayashi H, Arias IM. Hepatic uptake of bilirubin diglucuronide: analysis by using sinusoidal plasma membrane vesicles. *J Biochem*. 107: 749-54. 1990.

Aleo M.D., Wyatt R.D., Schnellmann R.G. Mitochondrial dysfunction is an early event in ochratoxin A but not oosporein toxicity to rat renal proximal tubules. *Tox. Appl Pharm.* 107: 73-80, 1991.

Amos HE, Wilson DV, Taussig MJ, and Carlton SJ. Hypersensitivity reactions to acetylsalicylic acid. *Clin Exp Immuno* 8:563-572, 1971.

Apiwattanakul N, Sekine T, Chiaroungdua A, Kanai Y, Nakajima N, Sophasan S, Endou H. Transport properties of nonsteroidal anti-inflammatory drugs by organic anion transporter 1 expressed in *Xenopus laevis* oocytes. *The Am Soc for Pharmaco and Exp Ther.* 55:847-854. 1999.

Babu E, Takeda M, Narikawa S, Kobayashi Y, Enomoto A, Tojo A, Cha SH, Sekine T, Sakthisekaran D, Endou H. Role of human organic anion transporter 4 in the transport of ochratoxin A. *Biochim Biophys Acta.* 1590(1-3):64-75, 2002.

Bahn A**,** Knabe M, Hagos Y, Rodiger M, Godehardt S, Graber-Neufeld DS, Evans KK, Burckhardt G, Wright SH. Interaction of the metal chelator 2,3-dimercapto-1-propanesulfonate with the rabbit multispecific organic anion transporter 1 (rbOAT1). *Mol Pharmacol*. 62(5):1128-36. 2002.

Bahn A, Hauss A, Appenroth D, Ebbinghaus D, Hagos Y, Steinmetzer P, Burckhardt G, Fleck C. RT-PCR-based evidence for the in vivo stimulation of renal tubular p-aminohippurate (PAH) transport by triiodothyronine (T3) or dexamethasone (DEXA) in kidney tissue of immature and adult rats. *Exp Toxicol Pathol.* 54(5-6):367-73. 2003.

Bakhiya A, Bahn A, Burckhardt G, Wolff N. Human organic anion transporter 3 (hOAT3) can operate as an exchanger and mediate secretory urate flux. *Cell Physiol Biochem*.13(5):249-56. 2003.

Bakke OM, Wardel WM, and Lasagna L. Drug discontinuation in the United Kindom and the United States, 1964-1983: issues of safety. *Clinical and Pharmacological Therapeutics.* 34: 559-567. 1984.

Bergwerk AJ, Shi X, Ford AC, Kanai N, Jacquemin E, Burk RD, Bai S, Novikoff PM, Stieger B, Meier PJ, Schuster VL, Wolkoff AW. Immunologic distribution of an organic anion transport protein in rat liver and kidney. *Am J Physiol.* 271(2 Pt 1): G231-8, 1996.

Bertorello A and Aperia A. Na+-K+-ATPase is an effector protein for protein kinase C in renal proximal tubule cells. *Am J Physiol*. 256(2 Pt 2):F370-3. 1989.

Bessey O.A., Lowry O.H., Brock M.J. A method for the rapid determination of alkaline phosphatase with five cubic millimeters of serum. *J Biol Chem*. 164:321. 1946.

Bort R, Ponsoda X, Jovier R, Gomez-Lechon MJ, Castell JV. Diclofenac toxicity to hepatocytes: a role for drug metabolism in cell toxicity. *J Pharm Exp Ther*. 288:65-72. 1998.

Bradford MM. A rapid and sensitive method for the quantitation of microgram quantities of protein utilizing the principle of protein-dye binding. *Anal Biochem* 72:248-54, 1976.

Braun W, Wittaker VP, Lotspeich WD. Renal excretion of phlorizin and phlorizin glucuronide. *Am J. Physiol*. 190(3):563-9. 1957.

Brendayan R. Renal drug transport- a review. *Pharmacother*. 16: 971-985. 1996.

Buist SC, Cherrington NJ, Choudhuri S, Hartley DP, Klaassen CD. Gender-specific and developmental influences on the expression of rat organic anion transporters. *J Pharmacol Exp Ther*. 301(1):145-51. 2002.

Buist SC, Cherrington NJ, Klaassen CD. Endocrine regulation of rat organic anion transporters. *Drug Metab Dispos.* 31(5):559-64. 2003.

Burckhardt BC, Brai S, Wallis S, Krick W, Wolff N, Burckhardt G. Transport of cimetidine by flounder and human renal organic anion transporter 1. *Am J Physiol Renal Physiol* 284: F503-9, 2003.

Burckhardt BC and Burckhardt G. Transport of organic anions across the basolateral membrane of proximal tubule cells. *Rev Physiol Biochem Pharmacol* 146:95-158, 2003.

Burckhardt G, Pritchard JB. Organic anion and cation antiporters. In: Seldin ED, GiebischG (eds) The Kidney. Physiology and pathophysiology. Lippincott Williams and Wilkins, Philadelphia, pp. 193-222. 2000.

Burckhardt G and Wolff NA. Structure of renal organic anion and cation transporters. *Am J Physiol Renal Physiol* 278:F853-F866, 2000.

Burckhardt G, Bahn A, Wolff N. Molecular physiology of renal p-aminohippurate secretion. *News Physiol Sci* 16:114-118, 2001.

Buttler D, Ebbinghaus C, Hillemann A, Wolff NA, Fuzesi L, Burckhardt G, Bahn A. In vivo studies, cloning and functional characterization of the isoforms of the human organic anion transporter 1 (hOAT1). *Pflungers Arch Eur J Physiol*. 441: R170. 2001.

Cerrutti JA, Brandoni A, Quaglia NB, Torres AM, Sex differences in p-aminohippuric acid transport in rat kidney: role of membrane fluidity and expression of OAT1. *Mol Cell Biochem*. 233(1-2):175-9. 2002.

Cha SH, Sekine T, Kusuhara H, Yu E, Kim JY, Dim DK, Sugiyama Y, Danai Y and Endou H. Molecular cloning and characterization of multispecific organic anion transporter 4 expressed in the placenta. *J Biological Chemistry* 275:4507-4512, 2000.

Cha SH, Sekine T, Fukushima JI, Kanai Y, Kobayashi Y, Goya T and Endou H. Identification and characterization of human organic anion transporter 3 expressing predominantly in the kidney. *Mol Pharmacol* 59(5):1277-86, 2001.

Cihlar T, Lin DC, Pritchard JB, Fuller MD, Mendel DB, Sweet DH. The antiviral nucleotide analogs cidofovir and adefovir are novel substrates for human and rat renal organic anion transporter 1. *Mol Pharmacol* 56(3):570-80, 1999.

Cihlar T and Ho ES. Fluorescence-based assay for the interaction of small molecules with the human renal organic anion transporter 1. *Analy Biochem* 283: 49-55, 2000.

Corre KA and Rothstein RJ. Anaphylactic reaction to Zomepirac. *Ann. Allergy* 48:299-301. 1982

Groves CE, Morales MN. Chlorotrifluoroethylcystein interaction with rabbit proximal tubule cell basolateral membrane organic anion transport and apical membrane amino acid transport. *J Pharm Exp Ther*. 291: 555-561. 1999.

Dantzler, WH. Renal organic anion transport: a comparative and cellular perspective. *Biochim Biophys Acta* 155S6: 169-181, 2002.

Dantzler WH and Wright SH. The molecular and cellular physiology of basolateral organic anion transport in mammalian renal tubules. *Biochim Biophys Acta*. 30:1618(2):185-93. 2003.

Deguchi T, Ohtuki S, Otagiri M, Takanaga H, Asaba H, Mori S, Terasaki T. Major role of organic anion transporter 3 in the transport of indoxyl sulfate in the kidney . *Kidney Int*. 61:1760-1768. 2002.

Diamond and Quebbemann, In vivo quantification of renal sulfate and glucuronide conjugation in the chicken.*Drug Metab Dispos*. 9(5):402-9. 1981.

Dickenson RG. Acyl glucuronide conjugates: Reactive metabolites of non-steroidal anti-inflammatory drugs. *Proc West Pharmacol Soc* 36: 157-162. 1993.

Dresser MJ, Leabman MK, Giacomini KM. Transporters involved in the elimination of drugs in the kidney: organic anion transporters and organic cation transporters*. J. Pharm Sci*. 90(4):397-421. 2000.

Duggin GG and Mudge GH. Renal tubular transport of paracetamol and its conjugates in the dog. *Br J Pharmac* 54:359-366, 1975.

Eckhardt U, Schroeder A, Stieger B, Hochli M, Landmann L, Tynes R, Meier PH, and Hagenbunch B. Polyspecific substrate uptake of the hepatic organic anion transporter Oatp1 in stably transfected CHO cell. *Am J Physiol*. 276: G1037-G1042. 1999

Elbers R, Kampffmeyer HG, Rabes H. Effects and metabolic pathway of 4-dimethylaminophenol during kidney perfusion. *Xenobiotica*. 10(7-8):621-32. 1980.

Emslie KR, Calder IC, Hart SJ, Tange JD, Induction of paracetamol metabolism in the isolated perfused kidney. *Xenobiotica.* 11(9):579-87. 1981.

Enomoto A, Kimura H, Chairoungdua A, Shigeta Y, Jutabha P, Cha SH, Hosoyamada M, Takeda M, Sekine T, Igarashi T, Matsuo H, Kikuchi Y, Oda T, Ichida K, Hosoya T, Shimokata K, Niwa T, Kanai Y, Endou H. Molecular identification of a renal urate-anion exchanger that regulates blood urate levels. *Nature* 417:447-452. 2002.

Enomoto A, Takeda M, Shimoda M, marikawa S, Kobayashi Y, Kobayashi Y, Yamamoto Y, Sekine T, Cha SH, Niwa T, Endou H. Interaction of human organin anion transporters 2 and 4 with organic anion transport inhibitors. J Pharmacol Exp Ther. 301:797-802. 2002b

Evans AM. Membrane transport as a determinant of the hepatic elimination of drugs and metabolites. *Clin Exp Pharmacol Physiol* 23: 970-974. 1996.

Faed EM. Properties of acyl glucuronides: Implications for studies of the pharmacokinetics and metabolism of acidic drugs. *Drug Metab. Reb.* 15: 1213-1249. 1984

Feng B, Dresser MJ, Shu Y, Johns SH, Giacomini KM. Arginine 454 and lysine 370 are essential for the anion specificity of the organic anion transporter rOAT3. *Biochemistry*. 40:5511-5520. 2001.

Galinsky RE and Levy G, Dose- and time-dependent elimination of acetaminophen in rats: pharmacokinetic implications of cosubstrate depletion. *J Pharmacol Exp Ther*. 219(1):14-20. 1981.

Gekle M, Mildenberger S. Sauvant C, Bednarczyk D. Wright SH, Dantzler WH. Inhibition of initial transport rate of basolateral organic anion carrier in renal PT by BK and phenylephrine. *Am J Physiol Renal Physiol*. 277: F251-F256. 1999.

George RL, Wu X, Fei YJ, Leibach FH, Ganapathy V. Molecular cloning and functional characterization of a polyspecific organic anion transporter from Caenorhabditis elgans. *J Pharmacol Exp Ther*. 291: 596-603. 1999.

Gesek FA, Wolff EW, Strandhoy JW. Improved separation method for rat proximal and distal renal tubules. *Am J Physiol* 253: F358-F365, 1987.

Groves CE and Morales MN. Chlorotrifluoroethylcysteine interaction with rabbit proximal tubule cell basolateral membrane organic anion transport and apical membrane amino acid transport. *J Pharm Exp Ther.* 291:555-561, 1999.

Guggino SE, Martin GJ, Aronson PS. Specificity and modes of the anion exchanger in dog renal microvillus membranes. *Am J Physiol*. 244: F612-F621. 1983.

Hagos Y, Bahn A, Asif AR, Krick W, Sendler M, Burckhardt G. Cloning of the pig renal organic anion transporter 1 (pOAT1). *Biochimie*. 84(12):1221-4. 2002.

Halpin PA and Renfro JL. Renal organic anion secretion: evidence for dopaminergic and adrenergic regulation. *Am J Physiol*. 271(5 Pt 2):R1372-9. 1996.

Haque SH., Peterson DD, Nebert DW, Makenzie PI. Isolation, sequence, and developmental expression of rat UGT2B2; the bene encoding a constitutive UDP glucuronosyltransferase that metabolized stiocholanolone and androsterone. *DNA Cell Biol*. 10: 515-24. 1991.

Hart D, Ward M, and Lifschitz MD. Suprofen related nephrotoxicity. *Annals of Internal Medicine*. 106:235-238. 1987.

Hart S. Calder I, Ross B, Tange J. Renal metabolism of paracetamol: studies in isolated perfused rat kidney. *Clin Sci (Lond).* 58(5): 379-84. 1980.

Hartiala K. Metabolism of hormones, drugs and other substances by the gut. *Physiological Reviews*. 53: 496-534. 1973.

Hasegawa M, Kusuhara H, Sugiyama D, Ito K, Ueda S, Endou H, Sugiyama Y. Functional involvement of rat organic anion transporter 3 (rOat3; Slc22a8) in the renal uptake of organic anions. *J Pharmacol Exp Ther* 300(3):746-53. 2002.

Hasegawa M, Kusuhara H, Endou H, Sugiyama Y. Contribution of organic anion transporters to the renal uptake of anionic compounds and nucleoside deriviaties in rat. *J Pharmacol Exp Ther*. 305(3):1087-97. 2003.

Heckman P, Russel FG and vanGinneken CA. Renal transport of the glucuronides of paracetamol and p-nitrophenol in the dog. *Drug Met Dispo* 14(3): 370-371. 1986.

Ho ES, Lin DC, Mendel DB, Cihlar T. Cytotoxicity of antiviral nucleotides adefovir and cidofovir is induced by the expression of human renal organic anion transporter 1. *J Am Soc Nephrol*. 11(3):383-93. 2000.

Hohage H, Lohr M, Querl Y, Greven J. The renal basolateral transport system for organic anions: properties of the regulation mechanism. *J Pharmacol Exp Ther*. 269: 659-664. 1994.

Hosoyamada M, Sekine T, Kanai Y, Endou H. Molecular cloning and functional expression of a multispecific organic anion transporter from human kidney. *Am J Physiol* 276: F122-F128. 1999.

Hyneck ML, Smith PC, Munafo A, McDonagh AF, and Benet LZ. Disposition and irreversible plasma protein binding of tomentin in humans. *Clin Pharmacol Ther*. 44: 107-14. 1988.

Insel PA. Analgesic-antipyretic and anti-inflammatory agents in drugs employed in the treatment of gout. *Goodman and Gilman's The Pharmacological Basis of Therapeutics.* 9th Edition.(Eds. Hardman GJ, Limbird LE). McGraw-Hill, New York; 617-657. 1996.

Isern J, Hagenbuch B, Steiger B, Meier P, Meseguer A. Functional analysis and androgen regulated expression of mouse organic anion transporting polypeptide 1(Oatp1) in the kidney. *Biochemical et Biophysica Acta*. 1518:73-78. 2001.

Islinger F, Gekle M, Wright SH Interaction of 2,3-dimercapto-1-propane sulfonate with the human organic anion transporter hOAT1. *J Pharmacol Exp Ther*. 299(2):741-7. 2001.

Jariyawat S, Sekine T, Takeda M, Apiwattanakul N, Kanai Y, Sophasan S,Endou H. The interaction and transport of β-lactam antibiotics with the cloned rat renal organic anion transporter 1. *J Pharmacol Exp Ther*. 290:672-677. 1999

Jenkins DAS, Harrison DJ, MacDonald MK, and Winney RJ. Mefenamic acid nephropathy: and interstitial and mesangial lesion. *Nephrol Dial Transplant.* 2: 217-220. 1988.

Ji L, Masuda S, Saito H, Inui K. Down-regulation of rat organic cation transporter rOCT2 by 5/6 nephrectomy. *Kidney Int* 62(2):514-24, 2002.

Jones D.P., Sundby G.B., Ormstad K., Orrenius S. Use of isolated kidney cells for study of drug metabolism. *Biochem. Pharmacol*. 28: 929-935, 1979.

Joshi MD and Jagannathan V. Hexokinase. *Methods Enzymol* 9:371-375, 1966.

Jung KY, Takeda M, Kim Dk, Tojo A, Narikawa S, Yoo BS, Hosoyamada M, Cha SH, Sekine T. Characterization of ochratoxin A transport by human organic anion transporters. *Life Sci*. 69:2123-2135. 2001.

Kacew S, Festing MF. Role of rat strain in the differential sensitivity to pharmaceutical agents and naturally occurring substances. *J Toxicol Environ Health*. 47(1):1-30. 1996.

Kahn AM, Branham S, Weinman EJ.Mechanism of urate and p-aminohippurate transport in rat renal microvillus membrane vesicles. *Am J Physiol*. 245(2):F151-8. 1983.

Kahn AM and Aronson PS. Urate transport via anion exchange in dog renal microvillus membrane vesicles. *Am J Physiol*. 244(1):F56-63. 1983.

Kanai N, Lu R, Boa Y, Wolkoff AW, Vore M, Schuster VL. Estradiol 17 beta-glucuronide is a high-affinity substrate for oatp organic anion transporter. *Am J Physiol* 270(2 Pt 2):F326-31, 1996.

Kato Y, Kuge K, Kusuhara H, Meier PJ, Sugiyama Y Gender difference in the urinary excretion of organic anions in rats. *J Pharmacol Exp Ther*. 302(2):483-9. 2002.

Kelly RA and Smith TW. Pharmacological treatment of heart failure. *Goodman and Gilman's The Pharmacological Basis of Therapeutics.* 9th Edition.(Eds. Hardman GJ, Limbird LE). McGraw-Hill, New York; 809-838. 1996.

Keppler K, Leier I, Jedlitschky G. Transport of glutathione conjugates and glucuronides by the multidrug resistance proteins MRP1 and MRP2. *Biol Chem*. 378(8):787-91. 1997.

Khamdang S, Takeda M, Noshiro R, Narikawa S, Enomoto A, Anzai N, Piyachaturawat P, Endou H. Interactions of human organic anion transporters and human organic cation transporters with nonsteroidal anti-inflammatory drugs. *J Pharmacol Exp Ther*. 303(2):534-9. 2002.

Khamdang S, Takeda M, Babu E, Noshiro R, Onozato ML, Tojo A, Enomoto A, Huang XL, Narikawa S, Anzai N, Piyachaturawat P, Endou H. Interaction of human and rat organic anion transporter 2 with various cephalosporin antibiotics. *Eur J Pharmacol*. 28;465(1-2):1-7. 2003.

Kikuchi R, Kusuhara H, Sugiyama D, Sugiyama Y. Contribution of organic anion transporter 3 (Slc22a8) to the elimination of p-aminohippuric acid and benzylpenicillin across the blood-brain barrier. *Pharmacol Exp Ther* 306(1):51-8, 2003.

King AR and Dickinson RG. Studies on the reactivity of acyl glucuronides-IV, Covalent binding of diflunisal to tissues of the rat. *Biochem Pharmacol* 45:1043-7, 1993.

Kobayashi A, Hirokawa N, Ohshiro N, Sekine T, Sasaki T, Tokuyama S, Sekine T, Endou H Yamamoto T. Differential gene expression of organic transporters in male and female rats. *Biochem Biophys Res Commun*. 290:482-487. 2002a.

Kobayashi A, Ohshiro N, Shibusawa A, Sakaki T, Tokuyama S, Sekine T, Endou H Yamamoto T. Isolation, Characteriaztion and differential gene expression of multispecific organic anion transporter 2 in mice. *Mol Pharmacol*. 62:7-14. 2002b.

Koepsell H, and Endou H. The SLC22 drug transporter family. *Pflugers Arch.* 447(5):666-76. 2004.

Kojima R, Sekine T, Kawachi M, Cha SH, Suzuki Y, Endou H. Immunolocalization of multispecific organic anion transporters, OAT1, OAT2, and OAT3, in rat kidney. J *Am Soc Nephrol* 13(4):848-57, 2002.

Konig J, Nies AT, Cui Y, Leier I, Keppler D. Conjugate export pumps of the multidrug resistance protein (MRP) family: localization, substrate specificity, and MRP2 mediated drug resistance. *Biochim Biophys Acta*. 1461:377-394. 1999.

Koster AS, Schirmer G. Bock KW, Immunochemical and functional characterization of UDP-glucuronosyltransferases from rat liver, intestine and kidney. *Biochemical Pharmacology,* 35 (22): 3971-5. 1986.

Kudo N, Katakura M, Sato Y, Kawashima Y. Sex hormone regulated renal transport of perfluorooctanoic acid. *Chemico-Biological Interactions*. 139:301-316. 2002.

Kusuhara H, Sekine T, Utsunomiya-Tate N, Tsuda M, Kojima R, Cha SH, Sugiyama Y, Kanai Y, Endou H. Molecular cloning and characterization of a new multispecific organic anion transporter from rat brain. *Biol Chem.* 274(19):13675-80, 1999.

Lash LH, Tokarz JJ. Isolation of two distinct populations of cells from rat kidney cortex and their use in the study of chemical-induced toxicity. *Anal Biochem*. 182(2):271-9. 1989.

Lash LH, Tokarz JJ, Pegouske DM. Susceptibility of primary cultures of proximal tubular and distal tubular cells from rat kidney to chemically induced toxicity. *Toxicology*. 103: 85-103. 1995.

Leier I, Hummel-Eisenbeiss J, Cui Y, Keppler D. ATP-dependent para-aminohippurate transport by apical multidrug resistance protein MRP2. *Kidney Int.* 57(4): 1636-42, 2000.

Li L, Lee TK, Meier PH, and Ballatory N. Identification of glutathione as a driving force and leukotriene C4 as a substrate for oatp1, the hepatic sinusoidal organic solute transporter. *J Biol Chem*. 273: 16184-16191. 1998.

Li XD, Xia SQ, Lv Y, He P, Han J, Wu MC. Conjugation metabolism of acetaminophen and bilirubin in extrahepatic tissues of rats. *Life Sci*. 74(10):1307-15. 2004.

Lock EA, Reed CJ. Xenobiotic metabolizing enzymes of the kidney. *Toxicol Pathol*. 26(1): 18-25, 1998

Lopez-Nieto CE, You G, Bush KT, Barros EJ, Beier DR, Nigam SK., Molecular cloning and characterization of NKT, a gene product related to the organic cation transporter family that is almost exclusively expressed in the kidney. *J Biol Chem.* 272(10):6471-8, 1997.

Lu R, Chan BS, Schuster VL., Cloning of the human kidney PAH transporter: narrow substrate specificity and regulation by protein kinase C. *Am J Physiol.* 276(2 Pt 2): F295-303, 1999.

Lucier GW, McDaniel OS. Steroid and non-steroid UDP glucuronyltransferase: glucuronidation of synthetic estrogens as steroids. *Journal of Steroid Biochemistry*. 8; 867-72. 1977.

Macdonald JI, Wallace SM, Herman RJ, Verbeeck RK.Effect of probenecid on the formation and elimination kinetics of the sulphate and glucuronide conjugates of diflunisal. *Eur J Clin Pharmacol.* 47(6):519-23.1995.

Makenzie PI, Rodbourn L. Organization of the rat UDP-glucuronosyltransferase, UDPGTr-2, gene and characterization of its promoter. *J Biol Chem.* 265; 11328-32, 1990.

Martinez F, Manganel M, Montrose-Rafizadeh C, Werner D, Roch-Ramel F. Transport of urate and p-aminohippurate in rabbit renal brush-border membranes. *Am J Physiol*. 258(5 Pt 2):F1145-53. 1990.

Masereeuw R, van den Bergh EJ, Bindels RJ, Russel FGCharacterization of fluorescein transport in isolated proximal tubular cells of the rat: evidence for mitochondrial accumulation. *J Pharmacol Exp Ther*. 269(3):1261-7. 1994.

Masuda S, Saito H, Nonoguchi H, Tomita K, Inui K. mRNA distribution and membrane localization of the OAT-K1 organic anion transporter in rat renal tubules. *FEBS Lett.* 407: 127-131, 1997.

Masuda S, Ibaramoto K, Takeuchi A, Saito H, Hashimoto Y, Inui K. Cloning and functional characterization of a new multispecific organic anion transporter, OAT-K2, in rat kidney. *Molec Pharm.* 55:743-752, 1999.

Matern S. Matern H, Farthmann EH, Gerok W. Hepatic and extrahepatic glucuronidation of bile acids in man. Characterization of bile acid uridine 5'-diphosphate-glucuronosyltransferase in hepatic, renal, and intestinal microsomes. *Journal of Clinical Investigation*. 74: 402-10. 1984

McGurk KA, Remmel RP, Hosagrahara V, Tosh D and Burchell B. Reactivity of mefenamic acid 1-o-acyl glucuronide with proteins *in vivo* and *ex vivo*. *Drug Met Dispo* 24(8): 842-849, 1996.

McKinnon GE and Dickinson RG. Covalent binding of diflunisal and probenecid to plasma protein in humans: persistence of the adducts in the circulation. *Research Communications in Chemical Pathology and Pharmacology.* 66: 339-354. 1989.

Miller DS, Protein kinase C regulation of organic anion transport in renal proximal tubule. *Am J Physiol*. 274(1 Pt 2):F156-64.1998.

Miller DS, Prichard JB. Dual Pathways for Organic Anion Secretion in Renal Proximal Tubule. *J Exp Zool.* 279(5):462-70, Dec 1, 1997.

Moller JV, Sheikh MI. Renal organic anion transport system: pharmacological, physiological and biochemical aspects*. Pharmacol Rev*. 34(4): 315-358. 1982.

Moolenaar F, Crancrinus S, Visser J, de Zeeuw D, Meijer DKF. Clearance of indomethacin occurs predominantly by renal glucuronidation. *Pharm Weekly Sci*. 14(4):191-5, 1992.

Morita N, Kusuhara H, Sekine T, Endou H, Sugiyama Y. Functional characterization of rat organic anion transporter 2 in LLC-PK1 cells. *J Pharmacol Exp Ther*. 298:1179-1184. 2001.

Morris ME, Levy G, Renal Clearance and Serum Protein Bidking of Acetaminophen and Its Major Conjugates in Humans. *J Pharm Sci.* 73(8):1038-41, Aug 1984.

Motohashi H, Sakurai Y, Saito H, Masuda S, Urakami Y, Goto M, Fukatsu A, Ogawa O, Inui K. Gene Expression Levels and Immunolocalization of Organic Ion Transporters in the Human Kidney. *J Am Soc Nephrol.* 13(4):866-74, 2002.

Motojima M, Hosokawa A, Yamato H, Muraki T, Yoshioka T Uraemic toxins induce proximal tubular injury via organic anion transporter 1-mediated uptake. *Br J Pharmacol*. 135(2):555-63. 2002.

Mulato AS, Ho ES, Cihlar T. Nonsteroidal anti-inflammatory drugs efficiently reduce the transport and cytotoxicity of adefovir mediated by the human renal organic anion transporter 1. *J Pharmacol Exp Ther*. 295:10-15. 2000.

Mulder GJ, Coughtrie MWH and Burchell B. *Conjugation reactions in drug metabolism*, Chapter 4. Taylor & Francis Ltd, 1990.

Nagai J, Yano I Hasimoto Y, Takano M, Inui KI. Inhibitino of PAH transport by parathyroid hormone in OK cells: involvement of protein kinase C pathway. *Am J Physiol Renal Physiol.* 273:F674-679. 1997.

Nagata Y, Kusuhara H, Endou H, Sugiyama Y. Expression and functional characterization of rat organic anion transporter 3 (rOat3) in the choroid plexus. *Mol Pharmacol.* 61(5):982-8, 2002.

Nakajima N, Sekine T, cha SH, Toho A, Hosoyamada M, Kanai Y, Yan K, Awa S, Endou H. Developmental changes in multispecific organic anion transporter 1 expresion in rat kidney. *Kidney Int*. 57:1608-1616. 2000.

Newton JF, Braselton JR, Kuo CH, Kluwe WM, Gemborys MW, Mudge GH, Hook JB. Metabolism of acetaminophen in the isolated perfused kidney. *J Pharmacol Exp Ther.* 221(1): 76-79, 1982.

Nikiforov A. Stimulation by aminooxyacetate of fluorescein uptake in rat renal tubules in vitro: role of intracellular α-ketoglutarate. *J Pharmacol Exp Ther.* 274:1204-1208. 1985.

O'Brien WM and Bagby GF. In Advances in Inflammation Research (Rainsford KD, Velo GP Eds.) Vol 6. Raven Press, New York, 1984.

Ohoka K, Takano M, Okano T, Maeda S, Inui KI, Hori R. p-Aminohippurate transport in rat renal brush-border sensitive transport system and an anion exchanger. *Biol Pharm Bull*. 16(4):395-401. 1993.

Parquet M, Pessah M, Ascquet E, Salvat C, Reizman A, Infante R. *FEBS Letters*. 189: 183-7. 1985.

Perri D, Ito S, Rowsell V, Shear NH. The kidney--the body's playground for drugs: an overview of renal drug handling with selected clinical correlates. *Can J Clin Pharmacol*. 10(1):17-23. 2003.

Pombrio JM, Giangreco A, Li L, Wempe MF, Anders MW, Sweet DH, Pritchard JB, Ballatori N Mercapturic acids (N-acetylcysteine S-conjugates) as endogenous substrates for the renal organic anion transporter-1. *Mol Pharmacol*. 2001 Nov;60(5):1091-9 2001

Pritchard JB. Coupled transport of p-aminohippurate by rat kidney basolateral membrane vesicles. *Am J Physiol.* 255(4 Pt 2): F597-604, 1988.

Pritchard JB and Miller DS. Renal secretion of organic anions and cations. *Kidney Int.* 49: 1649-54, 1996.

Pritchard JB and Miller DS. Mechanisms mediating renal secretion of organic anions and cations. *Physiol Rev*. 73(4): 765-96. 1993

Race JE, Grassl SM, Williams WJ, Holzman EJ, Molecular Cloning and Characterization of Two Novel Human Renal Organic Anion Transporters (hOAT1 and hOAT3), *Biochem Biophys Res Commun*. 225, 508-514, 1999.

Reid G, Wolff NA, Dautzenberg FM, Burckhardt G. Cloning of a human renal p-aminohippurate transporter, hROAT1. *Kidney Blood Press Res.* 21(2-4):233-7, 1998.

Ross B, Tange J, Emslie K, Hart S, Smail M, Calder I Paracetamol metabolism by the isolated perfused rat kidney. *Kidney Int*. 18(5):562-70. 1980.

Rossi AC and Knapp, DE. Tolmetin-induced anaphylactoid reactions. *N Eng J Med*. 307:499. 1982.

Rover N, Kramer C, Stark U, Gabriels G, Greven J. Basolateral transport of glutarate in proximal S2 segments of rabbit kidney: kinetics of the uptake process and effect of activators of protein kinase A and C. *Pflungers Arch*. 436:243-428. 1998.

Rush GF, Newto JF, Hook JB. Sex differences in the excretion of glucuronide conjugates: the role of intrarenal glucuronidation. *J Pharm Exp Ther*. 227:658-62. 1983.

Saito H, Masuda S, Inui K, Cloning and functional characterization of a novel rat organic anion transporter mediated basolateral uptake of methotrexate in the kidney. *J Biol. Chem*. 271(34): 20719-20725, 1996.

Sallustio BC, Knights KM, Roberts BJ, Zacest R. In vivo covalent binding of clofibric acid to human plasma proteins and rat liver proteins. *Biochem Pharmacol*. 42(7):1421-5. 1991.

Sallustio BC, Sabordo L, Evans AM, Nation RL. Hepatic disposition of electrophilic acyl glucuronide conjugates . *Curr Drug Metab.* 1(2): 163-80, 2000.

Sasaki M, Suzuki H Ito K, Abe T, Sugiyama Y. Transcellular transport of organic anions across a double-transfected Madin-Darby canine kidney II cell monolayer expressing both human organic anion-transporting polypeptide (OATP2/SLC21A6) and Multidrug resistance-associated protein 2 (MRP2/ABCC2). *J Biol Chem.* 277(8):6497-503, 2002.

Sauvant C, Holzinger H, Gekle M, Modulation of the Basolateral and Apical Step of Transepithelial Organic Anion Secretion in Proximal Tubular Opossum Kidney Cells, *J. Biol. Chem*. 276(18); 14695-14703, 2001.

Sauvant C, Hesse D, Holzinger H, Evans KK, Dantzler WH, Gekle M. Action of EGF and PGE2 on basolateral organic anion uptake in rabbit proximal renal tubules and hOAT1 expressed in human kidney epithelial cells*. Am J Physiol Renal Physiol*. 286(4): F774-83. 2004.

Schachter D and Manis JG. Salicylate and salicyl conjugates: fluorimetric estimation, biosynthesis and renal excretion in man. The Journal of Clinical Investigation. (Edd. Bondy PK.). Lancaster Press Inc. Lancaster Pa.: 800-807. 1958.

Schaub TP, Kartenbeck J, Konig J, Vogel O, Witzgall R. Kriz W. Keppler D. Expression of the conjugate export pump encoded by the mrp2 gene in the apical membrane of kidney proximal tubules. *J Am Soc Nephrol*. 8:1213-1221. 1997.

Schaub TP, Kartenbeck J, Konig J, Spring H, Dorsam J. Staehler G, Storkel S, Thon WF, Keppler D. Expression of the MRP2 gene-encoded conjugate export pump in human kidney proximal tubules and in renal cell carcinoma. *J Am Soc Nephrol*. 10:1159-1169. 1999.

Sekine T, Watanabe N, Hosoyamada M, Kanai Y, Endou H. Expression cloning and characterization of a novel multispecific organic anion transporter. *J Biol Chem.* 272: 18526-18529, 1997.

Sekine T, Cha SH, Tsuda M, Apiwattanakul N, Nakajima N, Kanai Y, Endou H. Identification of multispecific organic anion transporter 2 expressed predominantly in the liver. *FEBS Lett.* 429:179-82, 1998a.

Sekine T, Cha SH, Hosoyamada M, Danai Y, Watanabe N, Furuta Y, Fukuda K, Igarashi T, Endou H. Cloning, functional characterization and localization of rat reanl Na+-dicarboxylate transporter. *Am Physiol Soc.* 275:F298-305. 1998b.

Sekine T, Cha SH and Endou H. The multispecific organic anion transporter (OAT) family. *Pflugers Arch - Eur J Physiol* 440:337-350, 2000.

Shimada H, Mowews B, Burckhardt G. Indirect coupling to Na+ of p-aminohippuric acid uptake in to rat renal basolateral membrane vesicles. *Am J Physiol*. 253(5 pt 2): F795-801. 1987.

Shuprisha A, Lynch RM, Wright SH, Dantzler WH. PKC regulation of organic anion secretion in perfused S2 segments of rabbit proximal tubules. *Am J. Physiol. Renal Physiol*. 278:F104-F109. 2000.

Simonson GD, Vincent AC, Roberg KJ, Huang Y, Iwanij, V. Molecular cloning and characterization of a novel liver-specific transport protein. *J Cell Sci.* 107:1065-1072, 1994.

Smith PC, Benet LZ, McDonagh AF. Covalent binding of zomepirac glucuronide to proteins: evidence for a Schiff base mechanism. *Drug Metab Disp*. 18:639-44. 1990.

Smith RL and Williams RT. In *Glucuronic acid, free and combined*. (Dutton GJ ed.) Academic Press. 457-491. 1966.

Smith PC and Liu JH, Covalent binding of suprofen to renal tissue of rat correlates with excretion of its acyl glucuronide. *Xenobiotica*. 25(5):531-540. 1995.

Soars MG, Riley RJ, Findlay KA, Coffey MJ, Burchell B. Evidence for significant differences in microsomal drug glucuronidation by canine and human liver and kidney. *Drug Metab Dispos*. 29(2):121-6. 2001

Somogyi AA, Nation RL, Olweny C., Tsirgiotis P, Curgten J, Milne RW, Cleary JF, Danz C, Bochner F. Plasma concentrations and renal clearance of morphine, morphine-3-glucuronide and morphine-6-glucuronide in cancer patients receiving morphine. *Clin Pharmacokinet.* 24(5): 413-420, 1993

Spahn-Langguth H and Benet LZ. Acyl glucuronides revisited: is the glucuronidation process a toxification as well as a detoxification mechanism? *Drug Metab Rev.* 24:5-48, 1992.

Steffens TG, Holohan PD, Ross CR. Operational modes of the organic anion exchanger in canine renal brush-border membrane vesicles. *Am J Physiol.* 256:F596-609. 1989.

Stogniew M and Fenselau C. Electrophilic reactions of acyl-linked glucuronides: formation of clofibrate mercapturate in humans. *Drub Metab Dispo*. 10(6):609-613. 1982.

Strom BL, West SL, Sim E, and Carson JL. The epidemiology of the acute flank pain syndrome from suprofen. *Clinical Pharmacology and Therapeutics*. 46:693-699. 1989.

Sugiyama D, Kusuhara H, Shitara Y, Abe T, Meier PJ, Sekine T, Endou H, Suzuki H, Sugiyama Y. Characterization of the efflux transport of 17beta-estradiol-D-17beta-glucuronide from the brain across the blood-brain barrier. *J Pharmacol Exp Ther.* 298(1):316-22. 2001.

Sullivan LP, Grantham JA, Rome L, Wallace D. Grantham JJ. Fluorescein transport in isolated proximal tubules in vitro: epifluorometric analysis. *Am J Physiol.* 258:F46-51. 1990.

Sullivan LP and Grantham JJ. Specificity of basolateral organic exchanger in proximal tubule for cellular and extracellular solutes*. J Am Soc Nephrol*. 2(7): 1192-200. 1992.

Sun W, Wu RR, Van Poelje PD and Enrion MD. Isolation of a family of organic anion transporters from human liver and kidney. *Biochem Biophys Res Commun.* 283(2):417-22, 2001.

Sweet DH, Wolff NA and Pritchard JB. Expression cloning and characterization of ROAT1. *J Biol Chem.* 272:30088-30095, 1997.

Sweet DH, Miller DS, Pritchard JB, Fujiwara Y, Beier DR, Nigam SK. Impaired Organic Anion Transport in Kidney and Choroid Plexus of Organic Anion Transporter 3 (O*at3 (Slc22a8))* Knockout Mice. *J Biol Chem.* 277(30): 26934-26943, 2002.

Sweet DH, Chan LM, Walden R, Yang XP, Miller DS, Pritchard JB. Organic anion transporter 3 (Slc22a8) is a dicarboxylate exchanger indirectly coupled to the Na+ gradient. *Am J Physiol Renal Physiol*. 284(4): F763-9, 2003.

Takano M, Nagai J, Yasuhara M, Inui K.Regulation of p-aminohippurate transport by protein kinase C in OK kidney epithelial cells. *Am J Physiol*. 271(2 Pt 2):F469-75. 1996.

Takeda M, Tojo A, Sekine T, Hosoyamada M, Kanai Y, Endou H. Role of organic anion transporter 1 (OAT1) in cephaloridine (CER)-induced nephrotoxicity. *Kidney Int*. 56:2128-2136. 1999.

Takeda M, Sekine T, Endou H. Regulation by protein kinase C of organic anion transport driven by rat organic anion transporter 3 (rOAT3). *Life Sciences.* 67:1087-93, 2000.

Takeda M, Narikawa S, Hosoyamada M, Cha SH, Sekine T, Endou H. Characterization of organic anion transport inhibitors using cells stably expressing human organic anion transporters. *Eur J Pharmacol.* 419:113-120. 2001.

Takeda M, Khamdang S, Narikawa S, Kimura H, Kobayashi Y, Yamamoto T, Cha SH, Sekine T, Endou H. Human organic anion transporters and human organic cation transporters mediate renal antiviral transport. *J Pharmacol Exp Ther.* 300: 918-924, 2002.

Terlouw SA, Tanriseven O, Russel FGM, Masereeuw R. Metabolite anion carriers mediate the uptake of the anionic drug fluorescein in renal cortical mitochondria. *J Pharmacol Exp Ther*. 292(3):968-973. 2000.

Terlouw SA, Masereeuw R, Russel FG. Modulatory effects of hormones, drugs, and toxic events on renal organic anion transport. *Biochem Pharmacol.* 65(9): 1393-405, 2003.

Tojo A, Sekine T, Nakajima N, Hosoyamada M, Kanai Y, Kimura K, Endou H. Immunohistochemical localization of multispecific renal organic anion transporter 1 in rat kidney. *Am Soc Nephrol*. 10(3):464-71, 1999.

Tsuda M, Sekine T, Takeda M, Cha SH, Kanai Y, Kimura M, Endou H. Transport of ochratoxin A by renal multispecific organic anion transporter 1. *J Pharmacol Exp Ther.* 289:1301-1305. 1999.

Tukey RH and Strassburg CP. Human UDP-glucuronosyltransferases: metabolism, expression, and disease. *Annu Rev Pharmacol Toxicol*. 2000;40:581-616 2000

Uchino H, Tamai I, Yamashita K, Minemoto Y., SAai Y, Yabauuchi H, Miyamoto K, Takesa E, Tsuji A. p-Aminohippuric acid transport at renal apical membrane mediated by human inorganic phosphate transporter NPT1. *Biochem Biophys Res Commun.* 2;270(1):254-9, 2000.

Ullrich KJ, Rumrich G, David C, Fritzsch GBisubstrates: substances that interact with both, renal contraluminal organic anion and organic cation transport systems. II. Zwitterionic substrates: dipeptides, cephalosporins, quinolone-carboxylate gyrase inhibitors and phosphamide thiazine carboxylates; nonionizable substrates: steroid hormones and cyclophosphamides. *Pflugers Arch*. 425(3-4):300-12. 1993.

Ullrich KJ, Rumrich G, Burke TR, Shirazi-Beechey SP, Lang H Interaction of Alkyl/Arylphosphonates, phosphonocarboxylates and diphosphonates with different anion transport systems in the proximal renal tubule. *J Pharmacol Exp Ther*. 283(3):1223-9. 1997.

Ullrich KJ and Rumrich G. Luminal transport of Para-aminohippurate (PAH): transport from PAH-loaded proximal tubular cells into the tubular lumen of the rat kidney in vivo. *Pflungers Arch. Eur J Physiol*. 433: 735-743. 1997.

Uwai Y, Okuda M, Takami K, Hashimoto Y, Inui K. Functional characterization of the rat multispecific organic anion transporter OAT1 mediating basolateral uptake of anionic drugs in the kidney. *FEBS Lett*. 438(3):321-4. 1998.

Uwai Y, Saito H, Inui KI. Interaction between metnotrexate and nonsteroidal anti-inflammatory drugs in organic anion transporter. *Euro J of Pharm*. 409:31-36. 2000.

Van Aubel RA, Peters JG, Masereeuw R, Van Os CH, Russel FG. Multidrug resistant protein Mrp2 mediates ATP-dependent transport of the classic renal organic anion *p*-aminohippurate. *Am J Physiol Renal Physiol*. 279:F713-F717, 2000.

Van Breemen RB, Fenselau CC. Reaction of 1-O-acyl glucuronides with 4-(-p-nitrobenzyl)pyridine. *Drug Metab Disp*. 14: 197-201. 1986.

Van Breemen RB, Fenselau CC. Acylation of albumin by 1-O-acyl glucuronides. *Drug Metab Disp*. 13(3):318-320. 1985.

Van Crugten JT, Sallustio BC, Nation RL, Somogyi AA. Renal tubular transport of morphine, Morphine-6-glucuronide and morphine-3-glucuronide in the isolated perfused rat kidney. *Drug Metab Disp*. 19(6):1087-1092. 1991.

Volland C, Sun H, Dammeyer J, and Benet LZ. Stereoselective degradation of fenoprofen acyl glucuronide enantiomers and irreversible binding to plasma protein. *Drug Metab Disp*. 19: 1080-1086. 1991.

Vree TB, Hekster YA, Anderson PG. Contribution of the human kidney to the metabolic clearance of drugs. *Annal. of Pharmacol*. 26: 1421-28. 1992

Vree TB, Van Ewijk-Beneken Kolmer EW, Wuis EW, Hekster YA, Broekman MM. Interindividual variation in the capacity-limited renal glucuronidation of probenecid by humans. *Pharm World Sci*. 15(5):197-202. 1993

Vree TB, Van den Biggelaar-Martea M, Van Ewijk-Beneken Kolmer EW, Hekster YA. Probenecid inhibits the renal clearance and renal glucuronidation of nalidixic acid. A pilot experiment. *Pharm World Sci*. 15(4):165-70. 1993b.

Vree TB, van den Biggelaar-Martea M, Verwey-van Wissen CP, van Ewijk-Beneken Kolmer EW Probenecid inhibits the glucuronidation of indomethacin and O-desmethylindomethacin in humans. A pilot experiment. *Pharm World Sci*. 16(1):22-6. 1994.

Vree TB, Van der Ven AJ. Clinical consequences of the biphasic elimination kinetics for the diuretic effect of furosemide and its acyl glucuronide in humans. *J Pharm Pharmacol*. 51(3) 239-248, 1999.

Wada S, Tsuda M, Sekine T, Cha SH, Kimura M, Kanai Y, Endou H. Rat multispecific organic anion transporter 1 (rOAT1) transports zidovudine, acyclovir and other antiviral nucleoside analogs. *J Pharmacol Exp Ther*. 294:844-849. 2000.

Watari N, Iwai M, Kaneniwa N. Pharmacokinetic study of the fate of acetaminophen and its conjugates in rat. *J Pharmacokinetics and Biopharmaceuticals*. 11(3):245-273. 1983.

Werner D, Martinez F, Roch-Ramel F. Urate and p-aminohippurate transport in the brush border membrane of the pig kidney. *J Pharmacol Exp Ther.* 252(2):792-9. 1990

Williams AM, Worrall S. DeJersey J, and Dickinson RG. Studies on the reactivity of acylglucuornides: glucuronide-derived adducts of valproic acid and plasma proteins and anti-adduct antibodies in humans. *Biochem Pharmacol.* 43:745-755, 1992.

Wolff NA, Werner A, Burkhardt S, Burckhardt G. Expression cloning and characterization of a renal organic anion transporter from winter flounder. *FEBS Lett.* 417:287-291. 1997.

Wolff NA, Theis K, Kuhnke N, Reid G, Friedrich B, Lang F, Burckhardt G. Protein kinase C activation downregulates human organic anion transporter 1-mediated transport through carrier internalization. *J Am Soc Nephrol*. 14(8): 1959-1968. 2003.

Woods KL. Mefenamic acid nephropathy. *Br. Med. J.* 282:1471. 1981

Yuan JJ, Yang DC, Zhang JY, Bible R Jr, Karim A, Findlay JW. Disposition of a specific cyclooxygenase-2 inhibitor, valdecoxib, in human. *Drug Metab Dispos.* 30(9):1013-21. 2002.

You G, Kuze K, Kohanski RH, Amsler K, Henderson S. Regulation of mOAT-mediated organic anion transport of ocadaic acid and protein kinase C in LLC-PK1 cells. *J Biol Chem*. 275:10278-10284. 2000.

Zia-Amirhosseini P, Ojingwa J, Spahn-Langguth H, McDonagh AF, and Benet LZ. Enhanced covalent binding of tolmentin to proteins in humans after multiple dosing. *Clin Pharmacol Ther.* 55: 21-27, 1994.

Appendix

Perfusion Buffer A

pH 7.36

Chemical	Concentration
NaCl	115.0 mM
KCl	5.0 mM
$NaHCO_3$	25.0 mM
NaH_2PO_4	2.0 mM
$MgSO_4 \bullet 7H2O$	1.0 mM
Alanine	1.0 mM
Glucose	5.0 mM
Deferoxamine	0.1 mM
Mannatol	25.0 mM
Lactate	4.0 mM
Dextran	0.6 % (w/v)
Penicillin G	100 units/ml
$CaCl_2$	1.0 mM

bubble with 95% O_2/ 5% CO_2 for 30 min

Perfusion Buffer B

Chemical	Concentration
Collagenase	130 units/ml
SBTI	0.01 % (w/v)

diluted in 25 ml Perfusion buffer A

Incubation Buffer A

pH 7.36

Chemical	Concentration
NaCl	115.0 mM
KCl	5.0 mM
$NaHCO_3$	25.0 mM
NaH_2PO_4	2.0 mM
$MgSO_4 \bullet 7H2O$	1.0 mM
Alanine	1.0 mM
Glucose	5.0 mM
Deferoxamine	0.1 mM
Malic acid	5.0 mM
Butyric acid	2.0 mM
Lactate	5.0 mM
$CaCl_2$	1.0 mM
Penicillin G	100 units/ml

bubble with 95% O_2/ 5% CO_2 for 30 min

Incubation Buffer B

Chemical	Concentration
Collagenase	150 units/ml
SBTI	0.02% (w/v)
BSA	0.2% (w/v)
Dnase	70 units/ml

diluted in 50 ml Incubation buffer A

Krebs-Henseleit Concentrate (KHB) (10x)

Chemical	Concentration
NaCl	118.0 mM
KCl	4.8 mM
$NaHCO_3$	0.12 mM
$MgSO_4 \bullet 7H2O$	25.0 mM
Hepes	25.0 mM

bubble with 95% O_2/ 5% CO_2 for 30 min

Krebs-Henseleit Buffer (1x)

pH 7.36

Chemical	Amount
KHB 10x	20.0 ml
$_dH_2O$	180.0 ml

bubble with 95% O_2/ 5% CO_2 for 30 min

Transport Buffer #1 (tubules)

295 ± 5 mOsm/kg **pH 7.4**

Chemical	Concentration
NaCl	110.0 mM
$NaHCO_3$	25.0 mM
KCl	5.0 mM
NaH_2PO_4	2.0 mM
$MgSO_4 \bullet 7H2O$	1.0 mM
$CaCl_2$	1.8 mM
Sodium acetate	10.0 mM
Glucose	8.3 mM
Alanine	5.0 mM
Glycine	0.9 mM
Lactate	1.5 mM
Malic acid	1.0 mM
Sodium citrate	1.0 mM

bubble with 95% O_2/ 5% CO_2 for 30 min

Transport Buffer #2 (slices)

pH 7.5

Chemical	Concentration
NaCl	120.0 mM
KCl	16.2 mM
$CaCl_2$	1.0 mM
$MgSO_4 \bullet 7H2O$	1.2 mM
NaH_2PO_4	10.0 mM

bubble with 95% O_2/ 5% CO_2 for 30 min

45% Percoll Density Gradient

pH 7.36

Chemical	Amount
KHB 10x	6.0 ml
$_dH_2O$	27.0 ml
Percoll	27.0 ml

bubble with 95% O_2/ 5% CO_2 for 30 min

mixed in exact order

Alkaline Phosphatase Assay

Procedure 104

Stock substrate solution

40 mg capsule 10 ml H_2O

p-Nitrophenol standard solution

0.5 ml p-nitrophenol standard solution

QS to 100 ml with 0.02 N NaOH

0.02 N NaOH

0.8g NaOH 1000 ml H_2O

Hexokinase Assay

Substrate solution (3.24x)

Glucose	0.88 g
$MgCl_2 \bullet 6H_2O$	1.32 g
Na_2EDTA	0.121 g
Tris/HCl	5.1 g

100.0 ml adjust pH to 7.6

$NADP^+$ (3.24x)

8.1 mg/ 5.0 ml H_2O

ATP (3.24x)

0.267 g/ 3.0 ml H_2O

G6PDH (type VII, Sigma)

Stock = 350 units/mg; 332.5 units/ml

Assay:

Chemical	Concentration
Glucose	15.0 mM
$MgCl_2 \bullet 6H_2O$	20.0 mM
Na_2EDTA	10.0 µM
Tris/HCl	0.1 M
NADP+	0.67 mM
ATP	2 units/ml
G6PDH	50 mM

Bradford Reagent

Chemical	Amount
Coomassie Brilliant Blue	100.0 g
95% EtOH	50.0 ml
85% Phosphoric acid	100.0 ml

QS to 1L with H_2O

p-[glycyl-^{14}C]-aminohippuric acid (PAH)

Stock Solution 50 µCi

1. add 375 µl $_dH_2O$ to bottle (+ 2 drops 1 N NaOH)
2. transfer to scintillation vial
3. was bottle 1x with 375 µl H_2O and transfer to scintillation vial

1.25 ml = 50 µCi/1.25 ml= **40 µCi/ml**

Working solution	**20µCi/ml**	**10µCi/ml**
	250 µl stock PAH solution	100 µl stock PAH solution
	250 µl H_2O	300 µl H_2O
	500 µl = **20 µCi/ml**	400 µl = 1**0 µCi/ml**

Stock cold PAH

14 mM

27.188 mg / 10 ml H2O

several drops of 1N NaOH added

70 µM working solution

1.25 ml stock ^{14}C-PAH
1.25 ml stock cold PAH
2.5 ml **7 mM PAH @ 20 µCi/ml**

4-acetamidophenyl-ring-UL^{14}C β-D-glucuronide sodium salt (AG)

Stock Solution	**250 µCi**
1	add 3.95 µl $_{d}H_2O$ to bottle 6.25 ml = 250 µCi/6.25 ml= **40 µCi/ml**

Working solution	**20µCi/ml**	**10µCi/ml**
	250 µl stock AG solution	100 µl stock AG solution
	250 µl $_{d}H_2O$	300 µl $_{d}H_2O$
	500 µl = **20 µCi/ml**	400 µl = 1**0 µCi/ml**

Assay concentration

1:100 dilution of working solution yields 0.1 or 0.2 µCi/ml

D-[1-^{3}H(N)]-mannitol (MN)

Stock Solution **250 µCi**

1 add 0.25 ml $_{d}H_2O$ to vial
2 transfer to scintaillation vial labeled stock
3 wash vial 4x with 0.5 ml dH2O and add to stock

250 µCi/ 2.5 ml = **100 µCi/ml**

Working solution **10µCi/ml**

50 µl stock MN solution
450 µl $_{d}H_2O$
500 µl = 1**0 µCi/ml**

Assay concentration

1:100 dilution of working solution yields 0.1 or 0.2 µCi/ml

[6,7-^{3}H(N)]-estrone sulfate, ammonium salt (ES)

Stock Solution **50 µCi**

1 Stock solution at 50 µCi/ml

Working solution **10µCi/ml**

50 µl stock ES solution
2.450 ml $_{d}H_2O$
3 ml = 15 µCi/ml
***standards of working soln.= actually at 20 µCi/ml

Assay concentration

1:100 dilution of working solution yields 0.2 µCi/ml

Fluorescein 400uM

1.5 mg/ 10 ml H_2O

Probenecid 100mM

28.54 mg / 1.0 ml
add 1 N NaOH dropwise until in solution
QS to 1 ml with H_2O

p-aminohippuric acid (PAH) 100mM

19.42 mg/ 1 ml
add 1 N NaOH dropwise until in solution
QS to 1 ml with H_2O

Ouabain 10mM

1.82 mg/ 250 µl H_2O (warmed)
protected from light

Saccharic acid 1,4-lactone 2M

38.0 mg/ 100 µl H_2O

20 mM :
30µl 2M stock/3 ml

10 mM :
15µl 2M stock/3 ml

4-acetamidophenyl-β-D-glucuronide sodium salt (AG)

500 mM

70 mg/ 400 µl H_2O

100 mM

35 mg/ 1 ml H_2O

50 mM

17.44 mg/ 1 ml H_2O

20 mM

80 µl 50 mM AG + 180 µl H_2O

Estrone Sulfate (ES)

protected from light

40 mM

4.7 mg/ 360 µl 100% EtOH

warmed

25mM

18.6 mg/ 2 ml 100% EtOH

warmed

10 mM

3.7 mg/ 1 ml 100% EtOH

warmed

Testosterone Glucuronide (TG) 16.7 mM

10 mg/ 1230 µl 66% EtOH

Methylumbelliferyl-β-D-glucuronide 50 mM

8.8 mg/ 500 µl 50% EtOH

warmed

Dihydroxyepiandrosterone sulfate (DHEAs) 100 mM

3.9 mg/ 100 µl H_2O

warmed

Diclofenac (DC)

50 mM

15.8 mg/ 1 ml H_2O

20 mM

80 µl 50 mM DC + 180 µl H_2O

4-Acetamidophenol (APAP)

50 mM

7.6 mg/ 1 ml H_2O

20 mM

80 µl 50 mM APAP + 180 µl H_2O

Benzylpenicillin (PG) 100 mM

35.6 mg/ 1 ml H_2O

Pentobarbital Sodium 50 mg protein/ml

500 mg/ 10 ml H2O

Heparin

22.7 mg/ 10 ml 0.9% saline

0.9% Saline

9 g NaCl/ 1L H_2O

3M Perchloric Acid

50 ml 70% perchloric acid
qs 250 ml with H_2O

Potassium Phosphate Buffer (KH_2PO_4)monobasic - HPLC

13.6 g/ 1.0 L H_2O
pH 6.0, filtered

Solutions for Gel Preparation and Western Blot

† Solutions were prepared by Dr. Kelley Kiningham

Cell Fractionization

Homogenization Buffer (25 ml)

20 mM HEPES .....5 ml x 100 mM
5 mM EGTA.....1.25 ml x 0.1M
10 mM 2-mercaptoethanol (2ME)*.....20 ul
1 ug/1 ml pepstatin..... 25 ul of (1 mg/1 ml)
1 ug/1 ml leupeptin..... 20 ul of (1 mg/1 ml)
1 ug/1 ml aprotinin..... 20 ul of (1 mg/1 ml)
1 mM phenylmethylsufonyl fluoride (PMSF).....500 ul x10mM
Diluted to 25 ml with deionized water
* 2ME was not included for nonreduced protein samples.

Gel Preparation

30% Acrylamide, 0.8% Bisacrylamide† (neurotoxic)

60 g acrylamide

1.6 g bisacrylamide

dilute to 200 ml with water

Use 37°C water bath to dissolve solids if necessary; sterile filter into foil wrapped or brown bottle and store at 4°C.

5X Separation Buffer†

56.76 g TRIS

1.25 g sodium dodecyl sulfate (SDS)

pH to 8.8

Diluted to 250 ml with DI water

5X Stacking Buffer†

37.85 g TRIS

2.5 g SDS

pH to 6.8

Diluted to 500 ml with DI water

10% Ammonium Persulfate (APS) (prepared fresh daily)

0.1 g APS in 1 ml deionized water

2X Sample Buffer†

0.76 g TRIS (125 mM)

2 g SDS (13.9 mM or 4%)

10 ml Glycerol (20%)

5 ml 2-mercaptoethanol (2ME)* (10%)

pH to 6.8

Diluted to 50 ml with DI water

Bromophenol blue (1-2 mg) added until deep blue color obtained

Sample Buffer was prepared without 2-ME which was added just before use (1:10). Note: If 2X sample buffer is prepared without 2ME, it can remain at room temperature.

* 2ME was not included for nonreduced protein samples. DI water was substituted for 2ME.

Separation Gel	8 % Gel (ml)	12.5% Gel (ml)
5X Separation Buffer	7.0	7.0
30% Acrylamine, 0.8% Bis	9.3	14.6
H_2O	18.5	13.2
10% Ammonium Persulfate*	0.15	0.15
TEMED	0.025	0.025
Total	35.0 ml	35.0 ml

N-butanol (~2 ml)

Stacking Gel	ml
5X Separation Buffer	3.0
30% Acrylamine, 0.8% Bis	1.5
H_2O	10.5
10% Ammonium Persulfate*	0.075
TEMED	0.015

After rinsing n-butanol from the set separation gel with a large volume of water then carefully drying the mold, Stacking Gel was prepared and poured over the separation gel then left at room temperature for one hour to set.

10X Electrode Buffer† (Dilute 1:10 prior to use)

30.3 g TRIS (250 mM)

144 g Glycine (1.92 M)

10 g SDS (34.68 mM)

pH to 8.3

Diluted to 1 L with deionized water

Solutions Needed for Western Analysis

Transfer Buffer†

12.12 g TRIS

57.6 g glycine

800 ml methanol

3.2 L distilled water

Solution should be precooled for high voltage transfers.

Ponceau S†

g Ponceau S

5 ml acetic acid

diute to 100 ml with deionized water

Solution is stored in a brown bottle and may be reused.

10X TBS† (Dilute 1:10 prior to use)

12.12 g TRIS

87.66 g NaCl

pH to 8.0

Dilute to 1 L with deionized water

1X TBST

Add 500 μl Tween-20 to 1 L 1X TBS

Blocking solution (Blotto A)

5% non-fat dry milk in TBST (2.5 mg to 50 ml)

Prepared fresh daily and refrigerated.

Curriculum Vitae

NAME: Sarah L. Miles

ADDRESS: Department of Pharmacology
Joan C. Edwards School of Medicine
at Marshall University
1542 Spring Valley Drive
Huntington, WV 25704-9388

EMAIL: kittlaus1@marshall.edu

PHONE: (304)429-6755 ext. 2801
(304)736-9542

EDUCATION: B.S., Biology, with Honors (cum laude) - Randolph-Macon Woman's College, Lynchburg, VA - 1998

Ph.D., Biomedical Science, Pharmacology – Joan C. Edwards School of Medicine at Marshall University, Huntington, WV - 2004

POSITIONS HELD:

Graduate Student, Department of Pharmacology, 1998 – present

Teaching/Laboratory Assistant, Department of Biology, Randolph-Macon Woman's College, 1997-1998

Biology Tutor, Randolph-Macon Woman's College. 1996-1998

HONORS:

Departmental Honors in Biology; 1998

Grace Tayor Wiltshire Award in Biology (Senior with highest GPA in Biology) – 1998

Writing Board Prize for Best Long Paper "A Biosystematic Study of Trees in the Genus *Cedrus*"; Honorable Mention – 1998

PUBLICATIONS:

1. G O. Rankin, S K. Hong, D K. Anestis, L H. Lash, S L. Miles. 2001 In vitro nephrotoxicity induced by N-(3,5-dichlorophenyl)succinimide (NDPS) metabolites in isolated renal cortical cells from male and female Fischer 344 rats. Evidence for a nephrotoxic sulfate conjugate metabolite. Toxicology. June 21; 163 (2-3): 73-82

2. Aspirin, Sarah L. Miles, xPharm (2004); Executive Editors: S.J. Enna and David B. Bylund; Publisher, Elsevier, Inc., NY

3. Azapropazone, Sarah L. Miles, xPharm (2004); Executive Editors: S.J. Enna and David B. Bylund; Publisher, Elsevier, Inc., NY

4. Celecoxib, Sarah L. Miles, xPharm (2004); Executive Editors: S.J. Enna and David B. Bylund; Publisher, Elsevier, Inc., NY

5. Etodolac, Sarah L. Miles, xPharm (2004); Executive Editors: S.J. Enna and David B. Bylund; Publisher, Elsevier, Inc., NY

6. Fenoprofen, Sarah L. Miles, xPharm (2004); Executive Editors: S.J. Enna and David B. Bylund; Publisher, Elsevier, Inc., NY

7. Ibuprofen, Sarah L. Miles, xPharm (2004); Executive Editors: S.J. Enna and David B. Bylund; Publisher, Elsevier, Inc., NY

8. Ketoprofen, Sarah L. Miles, xPharm (2004); Executive Editors: S.J. Enna and David B. Bylund; Publisher, Elsevier, Inc., NY

9. Leflunomide, Sarah L. Miles, xPharm (2004); Executive Editors: S.J. Enna and David B. Bylund; Publisher, Elsevier, Inc., NY

10. Meclofenamate, Sarah L. Miles, xPharm (2004); Executive Editors: S.J. Enna and David B. Bylund; Publisher, Elsevier, Inc., NY

11. Methyl Salicylate, Sarah L. Miles, xPharm (2004); Executive Editors: S.J. Enna and David B. Bylund; Publisher, Elsevier, Inc., NY

12. Nabumetone, Sarah L. Miles, xPharm (2004); Executive Editors: S.J. Enna and David B. Bylund; Publisher, Elsevier, Inc., NY

13. Rofecoxib, Sarah L. Miles, xPharm (2004); Executive Editors: S.J. Enna and David B. Bylund; Publisher, Elsevier, Inc., NY

14. G.O. Rankin, S.L. Miles, D.K. Anestis and J.G. Ball. Effect of N-(3,5-dichlorophenyl)succinimide (NDPS) and NDPS metabolites on renal energetics. Toxicol. Lett. (in preparation).

15. S.L. Miles and G.O. Rankin. In Vitro nephrotoxic potential of Diclofenac in isolated renal proximal tubules from male Fischer 344 rats. (in preparation).

16. S.L. Miles and G.O. Rankin. Characteristics of Fluorescein accumulation along the basolateral membrane of isolated renal proximal tubules from male Fischer 344 rats. (in preparation).

17. S.L. Miles and G.O. Rankin. Characteristics of para-aminohippurate (PAH) and estrone sulfate (ES) accumulation in isolated renal proximal tubules and renal cortical slices from male Fischer 344 rats. (in preparation).

18. S.L. Miles and G.O. Rankin. Characterization of acetaminophen glucuronide handling by isolated renal proximal tubules and renal cortical slices from male Fischer 344 and Sprague-Dawley rats; evidence against renal secretion of acetaminophen glucuronide. (in preparation).

ABSTRACTS AND PRESENTATIONS: NATIONAL AND INTERNATIONAL

1. S.L. Miles, S.K. Hong, O. Noe, II, D.K. Anestis, M.A. Valentovic, J.G. Ball, and G.O.Rankin. 2000. Evidence for nephrotoxic sulfate conjugates of N-(3,5-dichlorophenyl)succinimide metabolites. Toxicologist 54(1), 403-404.

2. G.O. Rankin, J.T. Russell, S.L. Miles, and D.K. Anestis. 2000. In Vitro nephrotoxic potential of N-(3,5-dichlorophenyl)succinimide (NDPS) metabolites in isolated renal cortical cells from female Fischer 344 rats. Presented at Contemporary Concepts in Toxicology: Mechanisms of Nephrotoxicity and Nephrocarcinogenicity. April 15-18, 2000, Martha's Vineyard, MA.

3. S.L. Miles, D.K. Anestis, J.G. Ball, M.A. Valentovic, and G.O.Rankin. 2001 Effect of N-(3,5-dichlorophenyl)succinimide (NDPS) metabolites on adenosine nucleotide levels in isolated rat renal cortical epithelial cells. Toxicologist 60(1), 309-310.

4. S.L. Miles and G.O Rankin. 2004. Renal transport of glucuronide metabolites. FASEB J 18(4), A606.

ABSTRACTS AND PRESENTATIONS: REGIONAL

1. S.L. Miles S.K. Hong, O. Noe, II, D.K. Anestis, M.A. Valentovic, J.G. Ball, and G.O.Rankin. 2000. Evidence for nephrotoxic sulfate conjugates of N-(3,5-dichlorophenyl)succinimide metabolites. Presented at the Thirtheenth Annual Marshall University School of Medicine Reserch Conference, March 27-28, 2000, Huntington, WV.

2. J.T. Russell, S.L. Miles, D.K. Anestis, and G.O.Rankin. 2000. In Vitro nephrotoxic potential of N-(3,5-dichlorophenyl)succinimide (NDPS) metabolites in isolated renal cortical cells from female Fischer 344 rats. Presented at the Thirtheenth Annual Marshall University School of Medicine Reserch Conference, March 27-28, 2000, Huntington, WV.

3. S.L. Miles and G.O Rankin. 2003. Renal transport of glucuronide metabolites. Presented at the Ohio Valley Chapter Meeting, Sockety of Toxicology, November 7-8, 2003, Cincinnati, OH.